Characterization of Genes involved In Development and Senescence

By

Marianne Theresa Kaup Hopkins

A thesis
presented to the University of Waterloo
in fulfillment of the
thesis requirement for the degree of
Doctor of Philosophy
in
Biology

Waterloo, Ontario, Canada, 2006

I hereby declare that I am the sole author of this thesis. This is a true copy of the thesis, including any required final revisions, as accepted by my examiners.

I understand that my thesis may be made electronically available to the public.

Abstract

Plant development is complex and highly regulated. Tens of thousands of genes have been sequenced for the model plant *Arabidopsis thaliana,* yet few have been functionally annotated and characterized. This thesis describes the expression analysis and characterization of four genes in *Arabidopsis*. Three of these belong to the eukaryotic translation initiation factor 5A (eIF5A) gene family, and the fourth encodes diacylglycerol acyltransferase 1 (DGAT1). Putative roles for these genes in the development of *Arabidopsis thaliana* are described.

eIF5A is the only known protein to contain the amino acid hypusine. It has been demonstrated previously that eIF5A acts as a shuttle protein, moving specific mRNAs from the nucleus to the cytoplasm for translation. In *Arabidopsis thaliana* (At), there are three isoforms of eIF5A, and it is clear from the present study that they each have a unique temporal and spatial expression pattern. AteIF5A-1 and -2 are up-regulated during natural senescence and wounding/pathogenesis, respectively, and it is proposed that they regulate the onset of programmed cell death during these events. AteIF5A-3 is up-regulated in elongating meristem of the root, and it is proposed that this isoform is involved in cell growth.

Over-expression of the individual *AteIF5A* isoforms *in planta* resulted in pleiotropic phenotypes. When *AteIF5A-1* or *AteIF5A-2* was over-expressed, the phenotypes observed were indicative of their putative roles in the translation of proteins required for programmed cell death. When *AteIF5A-3* was over-expressed, the phenotypes were indicative of a role for this protein in the regulation of cell and tissue elongation.

Lipid analysis of rosette leaves from *Arabidopsis thaliana* revealed an accumulation of triacylglycerol with advancing leaf senescence coincident with an increase in the abundance and size of plastoglobuli. The terminal step in the biosynthesis of triacylglycerol in *Arabidopsis* is catalyzed by DGAT1. When gel blots of RNA isolated from rosette leaves at various stages of development were probed with the *Arabidopsis* EST clone, E6B2T7, which has been annotated as DGAT1, a steep increase in DGAT1 transcript levels was evident in the senescing leaves coincident with the accumulation of triacylglycerol. The

increase in DGAT1 transcript correlated temporally with enhanced levels of DGAT1 protein detected immunologically. Two lines of evidence indicated that the triacylglycerol of senescing leaves is synthesized in chloroplasts and sequesters fatty acids released from the catabolism of thylakoid galactolipids. First, triacylglycerol isolated from senescing leaves proved to be enriched in hexadecatrienoic acid (16:3) and linolenic acid (18:3), which are normally present in thylakoid galactolipids. Second, DGAT1 protein in senescing leaves was found to be associated with chloroplast membranes. These findings collectively indicate that DGAT1 plays a role in senescence by sequestering fatty acids de-esterified from galactolipids into triacylglycerol.

Acknowledgements

I would first like to thank the man who puts the meaning of "super" into the word supervisor, Dr. John Thompson, for his endless enthusiasm and support over the last few years. You have been a great mentor and friend to me. I would also like to thank former members of my committee, Dr. Trish Schulte and Dr. Jack Carlson, for their contributions to the early years of my Ph.D. Also, Dr. Bernard Glick and Dr. Brian Dixon, I thank you for your discussions regarding my thesis and discussions about life in general. I would like to thank Dr. Ray Legge (Department of Chemical Engineering, University of Waterloo) and Dr. Randall Weselake (Department of Agriculture, Food and Nutritional Science, University of Alberta) for their time and meaningful participation in my defence.

Financial support for the duration of my graduate studies was provided in part through an NSERC scholarship and through various University of Waterloo scholarships. Additional support was provided by Dr. Thompson and teaching opportunities in the Department of Biology. I would like to extend my gratitude for all of the funding I have received.

To Lynn Hoyles, for your help and friendship through all of my highs and lows during my graduate studies. Your sincerity and supportive words have helped me through many situations. You are a true friend.

To my great friends Jennifer Czarny, Catherine Taylor, Adrienne Boone and Linda McNamara. Thanks for the coffee-talk! And for sharing important life experiences with me. To all of my other friends and co-workers at the University of Waterloo including all of the present and former JETLAB members.

I would also like to thank my long-time friend Rebekah Main for her friendship and encouragement. You always have the right words of advice.

A special thanks to the plants I worked with and tortured, and the trees sacrificed for the printing of my thesis.

To my parents. Thank-you for pushing me to excel in everything that I do and always expecting more from me. To my mom, for showing me by example what women in

science can achieve and for always wanting to learn more. To my dad, for showing me what compassion is and for teaching me to be able to laugh at myself and have a sense of humour about life. We miss you!

To my brothers and sisters, Helen and Ralph, Katy and Chad, Adam and Candice, and Rosalie and Rob and their families. We've been through a lot, but we'll keep going, and going, and going, and going…Thanks for your love and support.

And finally, to Bruce and Genevieve, for giving me reasons to live my life to the fullest. My dearest Bruce, you know what I want to say here…there just aren't enough words. Genevieve, you light up my life! Don't ever change from the happy, inquisitive girl that you are. I love you both immensely!

I would like to dedicate this thesis to my Dad.

I miss you dearly.

And think of you with every passing day.

-Love your little Tweetie-

Be master of your petty annoyances &

conserve your energies

for the big, worthwhile things.

It isn't the mountain ahead that wears you out –

it's the grain of sand in your shoe.

-Robert Service

Table of Contents

List of Figures

List of Tables

List of Tables of the Appendix

Abbreviations

Ω	Ohms
3`UTR	Three prime untranslated region
5`UTR	Five prime untranslated region
A_{280}	Absorbance of light measured at wavelength 280nm
ABA	Abscisic acid
Ala	Alanine
At	*Arabidopsis thaliana*
A. tumefaciens	*Agrobacterium tumefaciens*
Avr	Avirulent
BIN	Plants containing the empty binary vector T-DNA
BSA	Bovine serum albumin
CFU	Colony forming units
CPU	Central processing unit
DFMO	α-difluoromethylornithine
DGAT	Diacylglycerol acyltransferase
DHH	Deoxyhypusine hydroxylase
DHS	Deoxyhypusine synthase
DNA	Deoxyribonucleic acid
DTT	Dithiothreitol
E. coli	*Escherichia coli*
EDTA	Ethylenediaminetetraacetic acid
EF-P	Elongation factor-P
EGTA	Ethylene glycol bis (2-aminoethyl ether)-N,N,N'N'-tetra acetic acid
eIF5A	Eukaryotic translation initiation factor 5A
EPPS	3-[4-(2-Hydroxyethyl)-1-piperazinyl] propanesulfonic acid
EST	Expressed sequence tag
etr1-1	ethylene response mutant

F	Farad
FITC	Fluorescein isothiocyanate
g	Grams
g	Force of gravity
G1/S	Gap phase 1/ DNA synthesis phase
GA	Gibberellic acid
GC7	N^1-guanyl-1,7-diaminoheptane
GHz	Gigahertz
Gly	Glycine
H	Hour(s)
Hg	Mercury
His	Histidine
HIV	Human immunodeficiency virus
Hs	*Homo sapien*
Hypusine	Hydroxyputrescine and lysine
IFN-α	Interferon-α
IgG	Immunoglobulin G
Kan^r	Kanamycin resistance
kDa	KiloDalton
KLH	Keyhole Limpet Hemocyanin
Le	*Lycopersicon esculentum*
LEA	Late embryogenesis abundant proteins
Lys	Lysine
MBS	*m*-maleimidobenzoyl-*N*-hydroxysuccinimide ester
MCS	Multiple cloning site
MES	2-[*N*-Morpholino] ethanesulfonic acid
Mj	*Methanococcus jannaschii*
µl	Microlitre
mg	Milligram
mL	Millilitre

mm	millimetre
mRNA	Messenger ribonucleic acid
MS	Murashige and Skoog Basal medium
NAD	Nicotinamide adenine dinucleotide
NADH	Nicotinamide adenine dinucleotide, reduced
ng	Nanograms
PBMCs	Peripheral blood mononuclear cells
PBS	Phosphate buffered saline
PCR	Polymerase chain reaction
PHA	Phytohaemagglutinin
PMA	Phorbol 12-myristate 13-acetate
Pst DC3000	*Pseudomonas syringae* pv. *Tomato* DC3000
PVDF	Polyvinyldiene difluoride
rbcS3`	3` end ribulose-1,5-bisphosphate carboxylase small subunit gene
rpm	Rotations per minute
Rubisco	Ribulose-1,5-bisphosphate carboxylase
s	Second(s)
Sc	*Saccharomyces cerevisiae*
SDS	Sodium dodecyl sulphate
SDS-PAGE	SDS Polyacrylamide gel electrophoresis
Ser	Serine
siRNA	Small interfering RNA
snRNA	Small nuclear RNA
SSC	Sodium chloride and sodium citrate buffer
T_0	Plants transformed with *Agrobacterium tumefaciens*
T_1	Plants of the first transformed generation
T_2	Plants of the second transformed generation
T_3	Plants of the third transformed generation
T_4	Plants of the fourth transformed generation

TdT	Terminal deoxynucleotidyl transferase
Tet^r	Tetracycline resistance
TLR-4	Toll-like receptor 4
TNFR1	Tumour necrosis factor receptor 1
Thr	Threonine
Tn	*Tetraodon nigroviridis*
TNF-α	Tumour necrosis factor-α
TUNEL	Terminal deoxynucleotidyl transferase mediated dUTP Nick-End Labeling
TRITC	Tetramethyl Rhodamine Iso-Thiocyanate
UP	Ubiquitin-proteasome
V	Volts
Vir	Virulent
v/v	Volume/volume
WT	Wild type plants; *Arabidopsis thaliana*, ecotype Columbia
w/v	Weight/volume
YT broth	1.6% Tryptone, 1.0% yeast extract, 0.5% NaCl

Chapter 1: *Arabidopsis thaliana*: A Model Plant for Studying Development & Senescence

1.1 Plant development: *Arabidopsis thaliana*

Plant development is quite distinct in comparison to animal development. There are four major features that account for this distinction (Jager *et al.*, 2005). First, plants are sessile organisms with no ability to move about. This impacts significantly on how they respond developmentally to their environment. Factors such as light, temperature and nutrient availability affect the growth rate, and in some cases the pattern of growth, of plants. Second, plant cells are surrounded by a rigid cell wall. This cell wall imposes restrictions on cell behaviour during development limiting in particular their migration, which is a requirement for organ development in animals (Mathur, 2005). The third feature that distinguishes plant development from animal development is the lack of overlap between embryogenesis and organogenesis. Plant embryogenesis is mainly concerned with the production of groups of "stem" cells or meristems (Jager *et al.*, 2005). These stem cells are totipotent cells that become dormant in the seed, the dispersal unit of flowering plants, and are reactivated upon optimal growing conditions during germination. Animal embryogenesis, on the other hand, gives rise to a mature embryo that already possesses the major organ systems of the post-embryonic organism. A final distinguishing feature of plant development in comparison with animal development is that plant meristems can indeterminately produce new organs. Shoot apical meristems primarily give rise to leaves to support photosynthesis, but also construct reproductive structures for seed production to ensure the continuation of the species. Root apical meristems develop new root structures to increase surface area for absorption of water and minerals, thereby nutritionally maintaining the aerial structures as well as firmly anchoring the plant in the substrate. By contrast, animal organogenesis is restricted to certain developmental stages during embryogenesis and cannot continue into adulthood. Notwithstanding these substantial differences between plant and animal development, plant and animal cells share several common cell cycle features.

Arabidopsis thaliana is a small flowering plant of the mustard family Brassicaceae (Bowman, 1994), which includes cultivated species such as canola, cabbage, cauliflower and

radish. *Arabidopsis* is not an agronomic species, but offers many advantages for basic research in genetics and molecular biology. In particular, its small size, short lifecycle and small diploid genome render it well suited to genetic screening techniques. The lifecycle (Figure 1-1) of *Arabidopsis* is approximately 6-8 weeks from germination to seed set, depending on the growing conditions and cultivar (Boyes *et al.*, 2001). During the *Arabidopsis* lifecycle, there is an obvious change from vegetative growth to reproductive growth. Vegetative growth begins at germination. During germination, the seedling emerges from the seed and continues to grow until it is capable of supporting the reproductive structures which produce seed for the next generation. Reproductive growth begins when the leaf meristem gives rise to the flower meristem and ensuing bolting, which is characterized by a significant increase in internode length. Reproductive growth ends with seed set, which results in embryos encased within seeds.

1.1.1 Vegetative growth

1.1.1.1 Germination

The seed is an extremely important stage in the lifecycle of a higher plant, as it ensures the survival of the species through times of unfavourable environmental conditions. Though it is important for a seed to remain dormant during such times, it is also of equal importance that, upon exposure to favourable growing conditions, the seed be capable of growing into a vital seedling. Seedling establishment is critically dependent upon stored nutrient reserves that accumulate in the embryo during seed set and the ability of the embryo to mobilize these nutrients efficiently during germination.

By definition, germination includes the sequential processes of initial water uptake by the seed, known as imbibition, to the point of radicle/primary root emergence (Bentsink and Koornneef, 2002). Though not much has occurred that is visible to the naked eye during this period, germination is one of the most highly co-ordinated events in a plant's lifecycle. A transcriptome study of dry seed and imbibition has demonstrated that more than half of all genes in *Arabidopsis thaliana* are represented in mRNA stored in seeds (Nakabayashi *et al.*, 2005), and that the mRNA profile of seeds imbibed for six hours is dramatically altered.

Figure 1-1: Growth stages during the lifespan of *Arabidopsis thaliana* (ecotype Columbia)

A schematic illustration of the chronological progression of the principal growth stages for *Arabidopsis thaliana*. The timeline and growth stages are defined according to Boyes *et al.* (2001). Some features of the lifespan, such as rosette leaf number and time of transition to reproductive growth, can vary with growth conditions. Events that occur during vegetative growth are indicated by blue bars, and events that occur during reproductive growth are indicated by red bars.

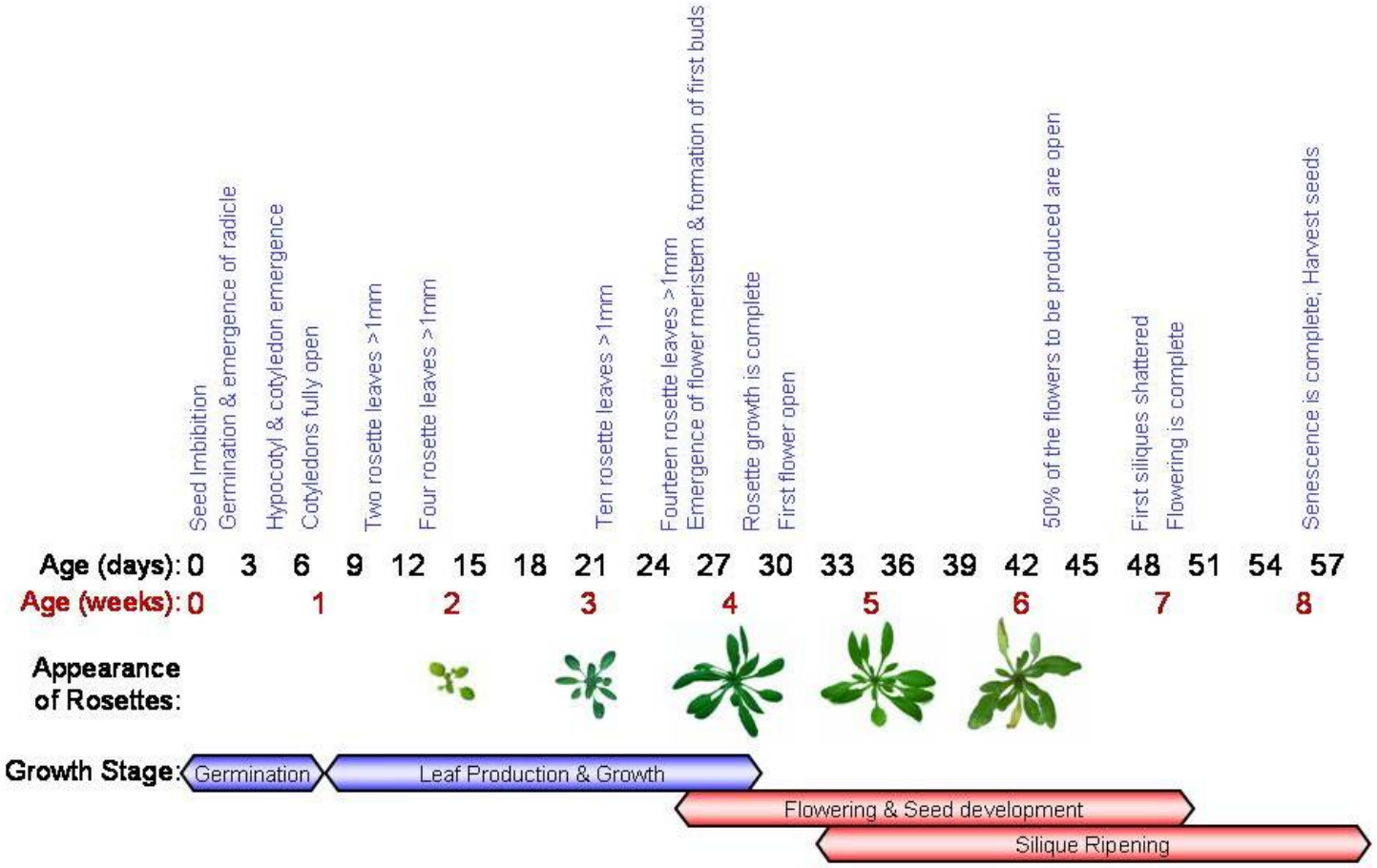
Seed Imbibition
Germination & emergence of radicle
Hypocotyl & cotyledon emergence
Cotyledons fully open
Two rosette leaves >1mm
Four rosette leaves >1mm
Ten rosette leaves >1mm
Fourteen rosette leaves >1mm
Emergence of flower meristem & formation of first buds
Rosette growth is complete
First flower open
50% of the flowers to be produced are open
First siliques shattered
Flowering is complete
Senescence is complete; Harvest seeds
Age (days): 0 3 6 9 12 15 18 21 24 27 30 33 36 39 42 45 48 51 54 57
Age (weeks): 0 1 2 3 4 5 6 7 8
Appearance of Rosettes:
Growth Stage:
Germination
Leaf Production & Growth
Flowering & Seed development
Silique Ripening

Specifically, embryogenic genes were largely down-regulated within six hours of imbibition. During the subsequent six hour period, there was extensive induction of metabolic genes involved in germination.

The mobilization of food reserves during germination is a key element of seedling establishment, and for this to be achieved lipid and carbohydrate catabolizing enzymes must be up-regulated. *Arabidopsis thaliana* is an oil seed as most of its food reserves are stored as lipid (Rylott *et al.*, 2001). In order to mobilize these lipid reserves to provide energy to the growing seedling, lipases and enzymes of the glyoxylate cycle, specifically malate synthase and isocitrate lyase, are up-regulated. The coordination that is involved in the transcription and translation of essential genes during germination is controlled by plant growth regulators.

The principal plant growth regulators that are involved in germination are abscisic acid (ABA), which is an inhibitor of germination, and gibberrellic acid (GA), which promotes germination. It is the balance between ABA and GA rather than their absolute levels in the seed that controls dormancy and germination in *Arabidopsis thaliana* (McCarty, 1995). During imbibition, there is a dilution effect on ABA as the seed takes on water. This dilution, along with *de novo* synthesis of GA, causes dormancy to be broken, and germination proceeds. GA synthesis may be the most critical regulatory factor of germination in species like *Arabidopsis* that have imposed seed dormancy. Other factors that affect germination of *Arabidopsis* include light and temperature. In keeping with the fact that *Arabidopsis* has very small seeds, which are normally dispersed over the soil surface, seed germination is light-dependent in a manner that is primarily mediated by the red and far-red photoreceptor phytochrome (Yamaguchi *et al.*, 1998). More specifically, phytochrome regulates bioactive GA levels during light-dependent seed germination. Temperature is another crucial external cue that controls seed germination. In many winter species, like *Arabidopsis*, exposure of seeds to low temperature (typically between 2-5^{o}C) immediately after imbibition for one or two days promotes germination. This process, called stratification, is widely used in nature and the laboratory to improve the frequency and synchronization of germination. Though it is not clearly understood how temperature

influences germination, there is evidence that the levels of GA are greatly increased in imbibed seeds exposed to lower temperatures (Yamauchi *et al.*, 2004).

Once germination is underway and the nutrient reserves are mobilized, the embryo begins to grow from the tips of each end of its axis, where the root and shoot apical meristems are located. Meristems are organized cellular structures capable of indeterminate growth (Bowman, 1994). Each meristem contains a structured core of undifferentiated "stem" cells which can divide and differentiate to produce adult tissues, whilst maintaining and regenerating the meristem. While germination ends with the emergence of the radicle, this is just the beginning of seedling establishment. The root must grow into a substrate, and the hypocotyl, which becomes the aerial portion of the plant, must fully emerge and begin growing new leafy structures capable of providing the seedling with sugars through photosynthesis, since at this point of seedling establishment the stored reserves in the seed or seedling are nearly exhausted.

1.1.1.2 Leaf formation and growth

Leaves are responsible for providing most of the fixed carbon in a plant and are critical to plant productivity and survival. As such, the health and development of leaves are of paramount importance to agriculture. In spite of this, little is known about the genetic controls that underlie leaf development. However, developmental landmarks have been defined to divide the process of leaf morphogenesis into three stages (Sinha, 1999). Stage 1 is the organogenesis stage where the cells on the flank of the shoot apical meristem are set aside as the founder cells of the initiating leaf. This region is characterized by increased cell division rates and gives rise to the leaf primordium. During Stage 2, the basic morphological domains for the growth and development of leaf parts are delimited. Finally, cellular and tissue differentiation occurs during Stage 3 through coordinated processes of cell division, expansion and differentiation.

Arabidopsis thaliana produces a rosette of leaves. The first leaves formed are juvenile and are bilaterally symmetric and round. They occur in a decussate phyllotaxy. Adult leaves, which are slightly convex, radially symmetric, increasingly spatulate (oval) and situated in a spiral phyllotaxy, are formed subsequently (Bowman, 1994). Rosette plants

have very little internode elongation between successive nodes (points at which the leaves are attached), and the rosettes are formed close to the soil. The transition from juvenile to adult vegetative meristem generally occurs between leaf numbers four and five in *Arabidopsis thaliana* ecotype Columbia (Kerstetter and Poethig, 1998).

Mature *Arabidopsis* leaves are typical of mesophytic dicotyledons. The mesophyll tissues, which are the photosynthetic layers between the upper and lower epidermal layers, consist of an upper layer of elongate palisade cells and a lower spongy mesophyll layer with large intercellular airspaces. The vasculature of *Arabidopsis* leaves is reticulate (net-like) and, consequently, the stomatal apertures are scattered. The stomata are more abundant on the abaxial (lower) epidermis than on the adaxial (upper) epidermis, whereas trichomes or hairs are more abundant on the adaxial surface. Cell expansion results in a large increase in the mesophyll volume and intercellular air space of the leaves, with an accompanying increase in the vascular system. After a leaf primordium has been laid down by the apical meristem, most of the growth of the leaf is due to cell expansion rather than cell division. Differentiation of the cells within these assorted layers occurs at slightly different times; for instance, the epidermal layers differentiate before the mesophyll layers. Also, in contrast to the vascular tissues, the differentiation of the mesophyll starts at the leaf tip and proceeds towards the base of the leaf. This creates a condition where within each developing leaf there are gradients of cells at varying stages of development, and after maturation, there are gradients of cells at varying stages of senescence.

1.1.1.3 Leaf senescence

Senescence is defined as the developmental stage that leads to death of cells, tissues, organs or even whole organisms (Bleecker and Patterson, 1997). It is a type of programmed cell death, but occurs more slowly than other types of programmed cell death in plants, such as the hypersensitive response induced during pathogenesis, which are generally acute and rapid. Senescence is distinct from developmental aging which is initiated, for example, during leaf development at the time of leaf primordial initiation. Specifically, leaf senescence is initiated only after the leaf is fully expanded and mature. To study whole plant senescence is very difficult as the senescence of different parts of the plant may influence the

development or the senescence of other parts. In *Arabidopsis thaliana* there appears to be a strong relationship between age of leaves and the initiation of their senescence. Unlike other monocarpic species (those that die after a single reproductive event), *Arabidopsis* appears to initiate leaf senescence independently of reproductive initiation (Nooden and Penney, 2001). Thus, since leaf senescence in *Arabidopsis* occurs in a reproducible, genetically controlled fashion, leaves of *Arabidopsis* are often used as a model system for senescence.

After leaves of *Arabidopsis thaliana* are fully developed, they photosynthesize for a period of time, and then the cells of the mesophyll begin to senesce. The cellular degeneration process during leaf senescence occurs under tight regulation and usually begins at a subcellular level within the chloroplasts (Matile, 1992). Since leaf senescence requires active gene expression, the nucleus and mitochondria remain intact until the very final stages. As senescence progresses, most (~60-70%) of the nutrients "stored" in the cells are remobilized to the growing parts of the plants including young leaves, developing seeds and fruit (Matile, 1992). This slow, orchestrated remobilization of nutrients is a characteristic that makes senescence distinct from other types of programmed cell death. Consequently, senescence is not only a deterioration phenomenon, it is also crucial for the fitness of plants and is thought to be an evolutionarily acquired genetic process (Nooden, 1988).

The timing and rate of senescence are affected by several growth regulators including, in particular, cytokinin and ethylene, but also methyl jasmonate, brassinosteroids and salicylic acid. Cytokinin is a growth regulator that promotes maintenance of chloroplast structure and, when applied exogenously, delays leaf senescence in *Arabidopsis thaliana* (Lim *et al.*, 2003). Cytokinins can also reverse senescence after it has been initiated. For instance, in transgenic plants expressing the transgene, isopentenyl transferase, a gene involved in cytokinin production, under the control of a senescence-associated promoter, leaf senescence is reversed after it has been initiated through the production of cytokinins triggered by the induction of senescence (Gan and Amasino, 1995; McCabe *et al.*, 2001). Though cytokinin is an antagonist to senescence, there is a point of no return after senescence induction, beyond which the process cannot be reversed (Buchanan-Wollaston, 1997).

Another important growth regulator involved in the timing of senescence initiation is ethylene. Ethylene is a gaseous growth inhibitor that has long been known to influence senescence initiation and increase the rate at which leaf senescence occurs (Grbic and Bleecker, 1995), but only after leaves reach a certain developmental stage. Specifically, ethylene plays a role in coordinating the timely onset of leaf senescence in *Arabdiopsis,* but is not essential for the execution of senescence (Bleecker and Patterson, 1997). For example, disruption of the ethylene-signalling pathway in ethylene-insensitive *etr1-1* (ethylene response) *Arabidopsis* mutants only delays the onset of leaf senescence (Grbic and Bleecker, 1995). Other plants, particularly climacteric plants, are more sensitive to the senescence-inducing influence of ethylene, particularly in respect of ethylene-sensitive organs like flowers (Thompson *et al.*, 1982; Itzhaki *et al.*, 1994; Orzaez *et al.*, 1999).

It is clear from mutational analysis that the growth regulators involved in leaf senescence influence gene expression. Since senescence is a type of programmed cell death, *de novo* gene expression is essential, and the tight regulation of this expression is critical for ensuring that all pertinent steps are timed and executed flawlessly. The signalling and transcriptional networks associated with senescence appear to be coarse regulators that determine when and where senescence begins. The finer control of the actual execution of senescence entails cascades of activation and inactivation that, for the most part, appear to be regulated post-transcriptionally (Thomas *et al.*, 2003). Several factors including both endogenous and exogenous signals such as leaf age, growth regulators and stressors, are involved in the initiation of leaf senescence. In *Arabidopsis,* although the initiation of leaf senescence is thought to be independent of the commencement of reproductive growth, the mobilization of nutrients from senescing leaves appears to be essential for proper seed fill.

1.1.2 Reproductive growth

1.1.2.1 Flowering and seed development

In *Arabidopsis,* like other plants, the shoot apical meristem provides indeterminate organogenesis. Changes in organogenesis occur through phase transitions in the meristem. Following embryogenesis, the shoot apical meristem produces vegetative structures,

characterized first by a juvenile stage and then an adult stage prior to the transition to a floral meristem. Once the transition to flowering occurs, floral primordia initiate from the flanks of the shoot apical meristem, and floral organs develop. Environmental conditions play a major role in the timing of the floral transition. The number of rosette leaves formed prior to the transition to flowering varies with growth conditions, with low temperatures and short days retarding the transition of the apical meristem to a flower meristem (Bowman, 1994). The *Arabidopsis thaliana* terminal flower meristem never develops into a flower itself, but remains indeterminate, forming flowers in a spiral phyllotaxy until the apex eventually senesces.

Sexual reproduction in higher plants, like *Arabidopsis*, occurs in flowers. Floral organ systems develop in four whorls as sepals, petals, stamen and carpels. Pollen is produced in the anthers, which are part of the stamen. Female gametes, the egg cells, are produced within the ovules that are housed within the carpel. The mature flower of *Arabidopsis thaliana* has a simple structure typical of the Brassicaceae. It has four free sepals and four petals, whose positions alternate with those of the sepals. There are two shorter lateral stamens and four longer medial stamens. The superior gynoecium, the pre-fertilization structure housing the female parts, has two leaf-like carpels whose locules are separated by a false septum. Ovules occur on either side of the septum, and after fertilization give rise to seeds.

Fertilization and subsequent embryogenesis is the ultimate goal of sexual reproduction. Unlike most Brassicaceae, *Arabidopsis thaliana* self-crosses at least 95% of the time, which can be desirable in a laboratory setting. Flowering plants experience double fertilization, in which the central cell and the egg cell within the ovule are both fertilized to produce the endosperm and the embryo, respectively. To complete fertilization, the pollen tube enters the ovule through the micropyle and delivers two haploid nuclei, one of which fuses with the nucleus of the egg cell giving rise to the zygote, while the other combines with the central cell. The zygote goes through many complicated cell divisions to form the body of the embryo. The tissue patterns in late-stage embryos are similar to those of seedlings, though cells in most tissues complete differentiation after germination.

The developing embryo undergoes many changes during embryogenesis. Not only is the basic structure of the seedling laid down, but the events leading to seed dormancy are initiated. Seed development from pollination to mature desiccated seeds occurs over 18 to 21 days in *Arabidopsis thaliana*, ecotype Columbia (Koorneef and Karssen, 1994). Lipids and other storage reserves accumulate between 8 and 16 days after flowering, with the maximum accumulation occurring between 9 and 14 days after flowering (Focks and Benning, 1998). During lipid deposition, the embryo undergoes the largest increase in size, mostly due to cell expansion. Continued cell expansion throughout the embryo causes it to fill most of the embryo sac, crushing the endosperm. At maturity with the onset of desiccation, the rate of reserve deposition slows down considerably, and the embryo decreases in size slightly through the loss of water. Desiccation tolerance is typically a maturation-specific characteristic. Maternal tissues and embryonic tissues synthesize ABA to induce seed dormancy. Proteins essential to desiccation tolerance accumulate at this point. Some of these, including LEA proteins (late embryogenesis abundant proteins) and heat shock proteins, are thought to protect membranes during the desiccation process. The seed coat of *Arabidopsis* is formed by lignification of the outer integuments of the ovule and exerts a germination-restrictive action. In *Arabidopsis*, phenolic compounds and their derivatives affect seed coat properties and influence dormancy and germination.

1.1.2.2 Silique ripening

The gynoecium is the pre-fertilization structure that develops into the fruit, commonly known as a silique. The fruit-mediated seed-dispersal mechanism employed by *Arabidopsis thaliana* is such that the seeds are forcibly ejected from the silique as it "shatters". That is, the silique uses mechanical forces that build up as the fruit dries out in a process known as dehiscence. Tissues required for fertilization are completely differentiated in a mature flower when the anthers shed their pollen onto the stigma located at the top of the ovary. Tissues important for fruit dehiscence require signals after fertilization to complete their development.

1.2 Plant development is affected by environmental factors

There is an urgent need to address challenges facing agriculture in the coming years, including pest and disease control, plant stress and yields. Also, the necessary increases in crop production need to be achieved in a way that will avoid environmental degradation. Small improvements in crop plant tolerances to various stresses have been accomplished by traditional plant breeding programs. With the advent of biotechnology, a wide range of possibilities for increasing plant tolerance to environmental stresses is available and, in comparison to breeding programs, easy to employ.

Plants are sessile organisms that respond to their environment through changes in development. During its lifecycle, a plant will encounter several levels of stress. Obviously, a lethal level of stress changes the outcome of the plant's life. However, it is sub-lethal stress that is the most common type of stress a plant encounters, and this type of stress has substantial effects on development. Sub-lethal stress is a low level of stress that may initiate cessation of growth, either vegetative or reproductive, and/or initiate senescence, though usually only for a short period of time until the stress is alleviated and growth continues (black line Figure 1-2). Though one event of sub-lethal stress may have only a modest effect on the plant, it is the culmination of many such events that leads to an overall loss of growth and, in crop plants, a loss in yield. Several studies have been initiated using *Arabidopsis thaliana* as a model system to further understand the effects of sublethal stress and develop methods to decrease its effects on growth and development either by increasing tolerance to the stress (blue line Figure 1-2) (Gilmour *et al.*, 1992; Thomashow, 1999; Xu *et al.*, 2004; Yi *et al.*, 2004) or increasing the growth rate of the plant (green line Figure 1-2) (Hu *et al.*, 2003; Lee *et al.*, 2003; Camp, 2005). Strategies for increasing yield using biotechnology necessitate the identification of target genes for increasing yield as well as how the gene expression should be modulated for the desired trait(s).

In the current study, several genes involved in the development and senescence of *Arabidopsis* have been characterized. First, three regulatory genes, all different isoforms of eukaryotic translation initiation factor 5A (eIF5A), were isolated. Previous studies with yeast and cultured mammalian cells have indicated that eIF5A regulates the translation

Figure 1-2: The effects of sub-lethal stress on plant growth

During plant growth (━), episodes of sublethal stress (indicated by the red arrows) are encountered which result in cessation of growth and/or initiation of senescence, followed by recovery and continuation of growth. The overall effect of this loss of growing time is a decrease in yield. Biotechnology or breeding methods are employed either to: (1) increase tolerance of plants to sublethal stress such that it has no impact on the growth rate (━) or, (2) increase the growth rate (━) of the plant so that, though it is still sensitive to sublethal stress, the overall yield is increased due to faster growth during optimum times.

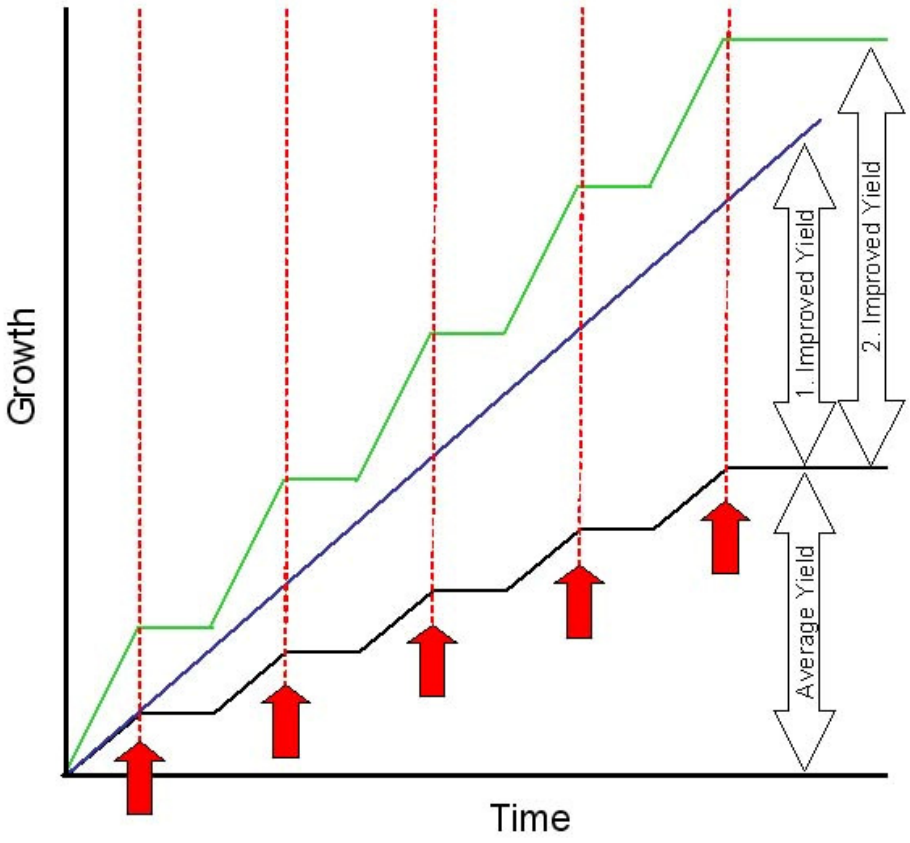
Growth
Time
1. Improved Yield
2. Improved Yield
Average Yield

of mRNAs required for cell division and cell death, although the exact mechanism underlying this regulation has not been elucidated (Caraglia *et al.*, 2003; Xu *et al.*, 2004). eIF5A in plants is largely unexplored. In the present study, three *eIF5A* genes were identified in *Arabidopsis thaliana,* and their putative functions were characterized by analysis of expression patterns and alteration of their expression *in planta*. A proposed role for each of the *eIF5A* isoforms in *Arabidopsis* development is described. Second, the gene encoding diacylglycerol acyltransferase, which mediates the final step of triacylglycerol synthesis, has been shown to play a role in the execution of leaf senescence and perhaps in the maintenance of chloroplast structure.

Chapter 2: The Three Isoforms of Eukaryotic Translation Initiation Factor 5A (eIF5A) in *Arabidopsis thaliana* are Differentially Expressed

2.1 Introduction

Protein synthesis, termed translation, is a central process in all living cells and is the last step in the transmission of genetic information stored in DNA. It occurs on ribosomal particles and consists of three phases: initiation, elongation and termination. Translation appears to be primarily regulated during initiation (Caraglia *et al.*, 2001), and there are indications that translational control may be just as important as transcriptional control, especially in relation to disease states such as cancer (Clemens and Bommer, 1999). One of the proteins known to be involved in the regulation of translation initiation is eukaryotic translation initiation factor 5A (eIF5A). Indeed, studies with yeast and human cell lines have indicated that regulation of translation initiation by eIF5A may be an inherent feature of both cell proliferation (Caraglia *et al.*, 1999; Caraglia *et al.*, 2001; Parker and Gerner, 2002) and cell death (Lee *et al.*, 2002; Li *et al.*, 2004; Taylor *et al.*, 2004).

2.1.1 eIF5A contains the amino acid hypusine

The unusual, strongly basic amino acid hypusine was first isolated in 1971 from extracts of bovine brain by Shiba *et al.* (1971). The structure was determined to be N^{ε}-(4-amino-2-hydroxybutyl)lysine and was named hypusine, a designation derived from the two compounds, hydroxyputrescine and lysine, from which it is formed (Shiba *et al.*, 1971). To date, hypusine has proven to be ubiquitous in animal tissues, both in free form and associated with protein, although it is likely that the detected free hypusine is actually a proteolytic degradation product. Yet it took nearly a decade after identifying hypusine as an amino acid to identify the specific protein that contains this amino acid. Park *et al.* (1981) discovered a single hypusine-containing protein in mammalian cells and later identified it as eukaryotic translation initiation factor 5A, abbreviated to eIF5A (Cooper *et al.*, 1982)[1]. eIF5A was

[1] Prior to 1989 when the nomenclature for translation factors was revised, eIF5A was referred to as eIF4D, but for consistency, eIF5A will be used throughout this study, even when referring to published reports in which the older terminology is used

discovered while studying the role of polyamines as physiological substrates for transglutaminases in normal lymphocytes treated with a mitogen and [^{3}H]-labelled putrescine (Park *et al.*, 1981). Hypusine was shown to be a constituent amino acid of a small acidic protein (M_r~18,000) of lymphocytes, and it was further demonstrated that its 4-amino-2-hydroxybutyl moiety is derived from the butylamine portion of spermidine (Park *et al.*, 1981). The appearance of hypusine, however, appeared to be specific to cells that were mitogen-stimulated in these early studies, and it was barely detectable in resting cells (Cooper *et al.*, 1982). This observation that the rate of hypusine synthesis correlated with growth and cell division became a feature of subsequent eIF5A and hypusine research (Park *et al.*, 1993; Bevec *et al.*, 1994; Byers *et al.*, 1994; Park *et al.*, 1997; Jannsson *et al.*, 2000; Caraglia *et al.*, 2001), although more recently it has been demonstrated that the role of eIF5A in mammalian cells is far more complex than initially envisaged.

The initial identification of eIF5A as a translation initiation factor was through its isolation from ribosomes of rabbit reticulocytes as a protein component that stimulated the initiation phase of eukaryotic translation (Kemper *et al.*, 1976). The connection between eIF5A as a translation factor and the unknown hypusine-containing protein was made through a co-migration experiment by two-dimensional gel electrophoresis of both proteins (Cooper *et al.*, 1983). Unlike other characterized initiation factors, eIF5A is a very abundant protein, largely found in the cytoplasm, with only a small amount associated with the ribosomes. eIF5A was shown not to have an influence on formation of the 80S initiation complex, but was able to stimulate methionyl-puromycin synthesis *in vitro* (Smit-McBride *et al.*, 1989). It is not certain, however, whether eIF5A functions as a translation initiation factor *in vivo* since the deletion of eIF5A in yeast only leads to a 30% decrease in protein synthesis (Kang and Hershey, 1994). In further support of the contention that eIF5A is not required for global protein synthesis, mammalian cells treated with mimosine, an inhibitor of hypusination, have been shown to have only a slight reduction in polysome abundance in comparison with control cells (Hanauske-Abel *et al.*, 1995). Thus, although eIF5A has in fact been shown to be associated with a translating 80S ribosomal complex in mammalian cells and appears to be involved in translation (Jao and Chen, 2005), there is still no conclusive evidence that it is essential for translation initiation *in vivo*.

2.1.2 eIF5A is ubiquitous in eukaryotes and archaebacteria

The hypusine-containing protein, eIF5A, has been found in a variety of mammals (Shiba *et al.*, 1971; Park, 1988; Smit-McBride *et al.*, 1989; Wolff *et al.*, 1992; Chen *et al.*, 1996; Tome and Gerner, 1996), plants (Mehta *et al.*, 1991; Pay *et al.*, 1991; Chamot and Kuhlemeier, 1992; Wang *et al.*, 2001; Chou *et al.*, 2004) and archaebacteria (Bartig *et al.*, 1992), but not in eubacteria (Gordon *et al.*, 1987). Eubacteria lack a hypusine-modified eIF5A equivalent. However, the sequence similarity between archaebacterial eIF5A and eubacterial elongation factor (EF)-P is significant enough to assume that the two are homologous proteins (Kyrpides and Woese, 1998). EF-P is a small acidic protein essential for stimulation of peptide bond synthesis (Glick and Ganoza, 1975). It has been shown to be essential for viability in *Escherichia coli*, and is present in all eubacterial genomes examined so far (Aoki *et al.*, 1997).

Though eIF5A is common to members of such a diverse group as the eukaryotes, it is a highly conserved protein. The hypusine-containing region has interspecies conservation, and a sequence of 12 amino acids containing the hypusine residue has been strictly conserved throughout eukaryotic evolution, from fungi through plants, insects and mammals (Hanauske-Abel *et al.*, 1994). The 12 amino acid sequence surrounding this amino acid residue, Ser-Thr-Ser-Lys-Thr-Gly-Lys*-His-Gly-His-Ala-Lys-[2], is identical in all eukaryotes, suggesting that this sequence is important for recognition by post-translational hypusination enzymes and/or possibly a crucial cellular function (Park *et al.*, 1997).

2.1.2.1 Structural characteristics of eIF5A

X-ray diffraction studies of unhypusinated eIF5A from two Archaea species show that it is composed of two well-defined domains attached by a flexible hinge (Kim *et al.*, 1998; Peat *et al.*, 1998). The flexible hinge between the two domains allows for conformational changes in the protein when it is in the precursor form, the intermediate form or the mature form with the hypusine conversion complete (Joao *et al.*, 1995; Facchiano *et al.*, 2001). The N-terminal domain is folded in a β-roll architecture and bears the hypusine

[2] The "*" designates the lysine that is converted to hypusine

residue in an exposed loop (Kim *et al.*, 1998). The C-terminal domain is organized in a β-barrel structure with five β-strands. The structure of eIF5A, and in particular the structure of the C-terminal domain, suggest that eIF5A may interact with nucleic acids, specifically RNA. This notion is substantiated by several studies (Liu *et al.*, 1997; Xu and Chen, 2001; Xu *et al.*, 2004). Also, hypusine is a 2-fold positively charged amino acid and resembles nucleic acid-binding polyamines.

The discovery of more than one isoform of eIF5A was made first for chicken (Dou and Chen, 1989) then in the yeast species *Saccharomyces cerevisiae* (Schnier *et al.*, 1991). The two eIF5A isoforms detected in chick embryo proved to be two distinct proteins with different polypeptide backbones that exhibited a high degree of identity (Wolff *et al.*, 1992). It was initially believed that other species may only have one isoform, but with the availability of better sequencing, it is now known that there are at least two isoforms of eIF5A in all species, and they are not functionally redundant. The only exception, is the two isoforms found in yeast, which both appear to regulate cell proliferation (Schnier *et al.*, 1991).

eIF5A has a strong propensity for self-polymerization and association with other macromolecules in the absence of reducing agents (Kemper *et al.*, 1976; Park *et al.*, 1986; Chung *et al.*, 1991). Whether the dimeric form of eIF5A is important for its interaction with other members of the protein synthetic system or any of its other activities, is not known. Also, whether various isoforms of eIF5A interact with each other within a given species is unknown.

2.1.2.2 Hypusine is synthesized by deoxyhypusine synthase and deoxyhypusine hydroxylase

It has been established that the biosynthesis of hypusine occurs on eIF5A precursor protein through a two-step post-translational modification involving lysine and spermidine as precursors (Figure 2-1). Several studies proved spermidine to be the specific precursor and not other polyamines (Park *et al.*, 1981; Murphey and Gerner, 1987; Wolff *et al.*, 1990; Chattopadhyay *et al.*, 2003). The exact structural input of lysine and spermidine to hypusine

formation was determined in a series of experiments using specific isotopically labelled precursors (Park *et al.*, 1981; Park *et al.*, 1984; Park *et al.*, 1986). Whether or not the isotope was incorporated into the hypusine indicated which portions of lysine and spermidine participate in hypusine formation. The first step in hypusine formation involves the conversion of a specific lysine on precursor eIF5A protein to deoxyhypusine (Figure 2-1). The identification of deoxyhypusine as an intermediate in hypusine biosynthesis was made in Chinese hamster ovary cells that had been treated with metal chelators (Park *et al.*, 1982). The formation of deoxyhypusine is catalyzed by the enzyme deoxyhypusine synthase (DHS; EC 1.1.1.249). Whether a eukaryote contains two or more isoforms of eIF5A, there is only one way that hypusine is formed on the protein. Furthermore, there is presently only one isoform of DHS known for all species annotated (Joe *et al.*, 1995; Yan *et al.*, 1996).

DHS catalyzes a multistep reaction involving two substrates, spermidine and eIF5A precursor protein, and utilizes the cofactor, nicotinamide adenine dinucleotide (NAD). DHS is highly specific for each substrate and cofactor. The reaction involves an enzyme-imine intermediate formed between the 4-amino-butyl moiety from spermidine and the ε-amino group of Lys329 in the human enzyme (Wolff *et al.*, 1997). This intermediate is essential for the overall reaction. Upon addition of the eIF5A precursor, the butylamine moiety from the enzyme-imine intermediate is transferred to Lys50 of the eIF5A precursor and is reduced to form deoxyhypusine (Wolff *et al.*, 1990; Park *et al.*, 1993; Park *et al.*, 1997; Wolff *et al.*, 1997). The binding of eIF5A to DHS is not affected by truncation of either the N- (9 amino acids) or C-terminal (64 amino acids) half (Thompson *et al.*, 2003), indicating that the interaction is specific to the middle of eIF5A. The native DHS enzyme exists as a tetramer of four identical subunits of 40kDa to 43kDa, depending on the species (Liao *et al.*, 1998), although it binds only one molecule of eIF5A at a time (Lee *et al.*, 1999). There is significant sequence identity across diverse species of annotated DHS, and the enzyme has been shown to be essential for mammalian cell viability (Park *et al.*, 1998). The amino acid sequence of DHS is highly conserved, especially in the C-terminal half, and the enzymes of different species share similar physical and catalytic properties, so much so that the enzymes

Figure 2-1: Post-translational modification of eIF5A

Hypusination of eIF5A occurs post-translationally and involves two enzymatic steps. In the first step, deoxyhypusine synthase catalyzes the NAD-dependent transfer of the butylamine moiety of spermidine to the ε-amino group of a specific lysine residue of the eIF5A precursor to form the intermediate deoxyhypusine. In the second step, mediated by deoxyhypusine hydroxylase, the deoxyhypusine residue is converted to hypusine. Hypusinated eIF5A is believed to be the active form of the protein. Schematic redrawn from Park *et al.* (1993).

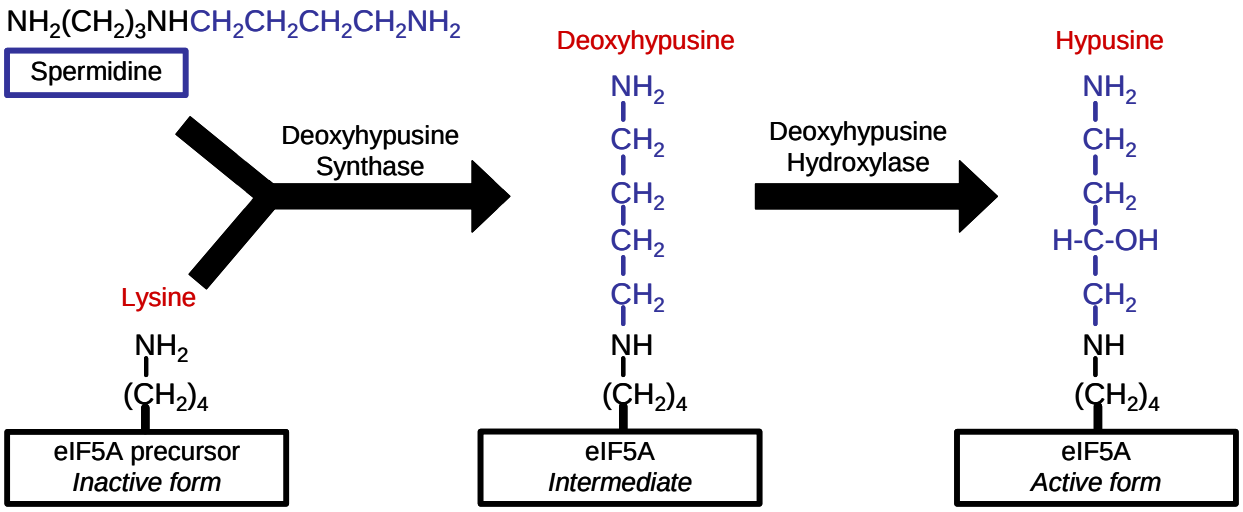
NH2(CH2)3NHCH2CH2CH2CH2NH2
Spermidine
Deoxyhypusine Synthase
Lysine
NH2
(CH2)4
eIF5A precursor
Inactive form
Deoxyhypusine
NH2
CH2
CH2
CH2
CH2
NH
(CH2)4
eIF5A
Intermediate
Deoxyhypusine Hydroxylase
Hypusine
NH2
CH2
CH2
H-C-OH
CH2
NH
(CH2)4
eIF5A
Active form

display cross-species activity with heterologous eIF5A precursors (Park *et al.*, 1998; Wang *et al.*, 2001).

The content of deoxyhypusinated eIF5A is normally very low in cultured mammalian cells, and thus the conversion of this intermediate to hypusinated eIF5A does not appear to be rate-limiting (Beninati *et al.*, 1990). The NADH formed in the first step of the reaction is used for the hydroxylation at carbon 2 of the 4-aminobutyl portion of the deoxyhypusine residue required in the last step (Figure 2-1), which is mediated by deoxyhypusine hydroxylase (DHH; EC 1.14.99.29). The activity of this enzyme was first demonstrated *in vitro* using crude lysates of cells that were grown with metal chelators. Several assays were developed for the hydroxylase (Abbruzzese *et al.*, 1986, 1986), and it was partially purified from rat testis (Abbruzzese *et al.*, 1986). DHH is thought to be related to other hydroxylating enzymes and is effectively inhibited by mimosine. Mimosine and mimosine-like compounds directly interact with the active site of DHH *in vitro* (Hanauske-Abel *et al.*, 1994; McCaffrey *et al.*, 1995), though fast recovery of cellular DHH activity occurs after mimosine removal. The gene encoding DHH has recently been sequenced (Park *et al.*, 2006). Inhibition of DHH by certain metal-chelating compounds suggests a role for a tightly-bound metal at the active site of the enzyme (Beninati *et al.*, 1990; Wolff *et al.*, 1995).

2.1.2.3 Hypusine is an essential amino acid for normal cell function

Hypusine-containing eIF5A is thought to be involved in both cellular proliferation and cell death (Tome and Gerner, 1997; Caraglia *et al.*, 2001; Caraglia *et al.*, 2003). eIF5A is proposed to be responsible for the translation of a subset of proteins that are required for G1/S transition in eukaryotes (Hanauske-Abel *et al.*, 1995; Chan *et al.*, 2002). It is recognized that a large number of growth-related mRNAs are under strict post-transcriptional control, and that even small changes in the expression of a single translation factor can dramatically alter the balance in their production (Hershey and Miyamoto, 2000). Most data concerning eIF5A as a regulator of proliferation have been collected from yeast. Yeast have two isoforms of eIF5A that appear to be functionally redundant (Schwelberger *et al.*, 1993). Double knock-out yeast eIF5A mutants are not able to form viable spores (Schnier *et al.*,

1991); however, as long as one isoform remains functional the yeast grow normally (Schwelberger *et al.*, 1993). Double knock-out eIF5A mutations in yeast can also be rescued by the transient expression of human eIF5A (Schwelberger *et al.*, 1993).

More recently, literature pertaining to eIF5A has shifted into a new light, and its role in apoptosis has come to stage. There are two schools of thought on the involvement of eIF5A in apoptosis. The first is that eIF5A protects cells from apoptosis, and the second is that eIF5A promotes apoptosis. These conflicting data and interpretations are possibly due to differences among experiments in the level of hypusination or perhaps lack of distinction between different isoforms, which may have different functions. In Li *et al.* (2004), eIF5A over-expression induced p53-dependent apoptosis. Further to this, the specific down-regulation of eIF5A by small interfering RNA (siRNA) resulted in a reduced level of p53 protein (Li *et al.*, 2004). Since then, it has been demonstrated that eIF5A is required for the proper expression of p53, a pro-apoptotic protein, in tumour necrosis factor (TNF)-α treated colon cancer cells and that eIF5A is rapidly translocated to the nuclear compartment during apoptosis (Taylor *et al.*, submitted 2006). Indeed, it has been reported that unhypusinated eIF5A is capable of nuclear localization (Jin *et al.*, 2003), and that it is the unmodified eIF5A that accumulates during apoptosis (Tome *et al.*, 1997; Tome and Gerner, 1997; Beninati *et al.*, 1998; Caraglia *et al.*, 2003). Further evidence of eIF5A involvement in apoptosis was demonstrated by the protection effect that siRNA against eIF5A has on TNF-α and camptothecin-induced apoptosis of lamina cribosa cells isolated from human optic nerve heads (Taylor *et al.*, 2004).

Conversely, it has been demonstrated for fibroblast cells that depression of eIF5A activity, through DHS inhibitors, is correlated with induction of apoptosis induced by interferon (IFN)-α (Caraglia *et al.*, 1999; Caraglia *et al.*, 2001). In addition, inhibition of the hypusine modification was found to protect human umbilical vein endothelial cells from serum starvation-induced apoptosis (Lee *et al.*, 2002). When leukemic cells were treated with ubiquitin-proteasome (UP) inhibitors, there was an observed accumulation of unmodified eIF5A (Jin *et al.*, 2003). Also in mammalian cells, excess putrescine accumulation inhibits the formation of hypusine in eIF5A and induces apoptosis (Tome *et*

al., 1997; Tome and Gerner, 1997; Bergeron *et al.*, 1998). It consistently appears that accumulation of the unmodified form of eIF5A through hypusination inhibition is correlated to apoptosis, whereas the specific down-regulation of eIF5A post-transcriptionally, with siRNA, protects the cells from apoptosis. Under normal cell growth conditions, it is the translation of eIF5A mRNA that is probably the rate-limiting step in eIF5A expression. Bevec *et al.* (1994) first demonstrated that eIF5A mRNA in a number of human tissues and in various mammalian cell lines is constitutively expressed. While the uncertainty within the literature as to whether eIF5A actively induces apoptosis continues, it is interesting to note that in plant systems there is a marked up-regulation of eIF5A and DHS during senescence of leaves and fruit (Wang *et al.*, 2001), which is analogous to cell death/apoptosis in mammalian cells.

It was observed fairly early in eIF5A research that blocking hypusine formation greatly altered cellular function. Many studies used inhibitors of polyamine synthesis in addition to inhibitors of DHS or DHH. Several mono-, di-, and polyamines that have structural features similar to spermidine inhibit DHS activity *in vitro* (Jakus *et al.*, 1993). It is well established that polyamines are required for cell growth, not just because of their involvement in the post-translation activation of eIF5A, but also in other more non-specific interactions with nucleic acids (Goyns, 1982; Cohen, 1998; Igarashi and Kashiwagi, 2000). Spermidine is the only polyamine that is required for hypusine formation (Gerner *et al.*, 1986; Wolff *et al.*, 1990; Byers *et al.*, 1993; Chattopadhyay *et al.*, 2003). A common inhibitor of polyamine synthesis, DFMO (α-difluoromethylornithine), has been used to observe the effects of polyamine depletion on cell proliferation as well as hypusination of eIF5A (Gerner *et al.*, 1986; Park and Wolff, 1988; Chen and Chen, 1997; Parker and Gerner, 2002). Depletion of polyamines in the presence of DFMO was shown to inhibit hypusination of eIF5A and, accordingly, disrupt normal cell function (Parker and Gerner, 2002; Nishimura *et al.*, 2005). In addition, DFMO-mediated depletion of cellular polyamines was shown to inhibit cell proliferation in an eIF5A-independent manner (Nishimura *et al.*, 2005).

Mammalian cells treated with inhibitors of DHS or DHH also exhibit inhibition of growth. For example, when Chinese hamster ovary cells or neuroblastoma cells were treated

with DHS inhibitors, cytostasis was induced, but it proved to be reversible with removal of the inhibitors (Park *et al.*, 1994; Chen *et al.*, 1996). DHS inhibitors normally used in these experiments include guanylated diamines such as N^1-guanyl-1,7-diaminoheptane (GC7) and N^1-guanyl-1,8-diaminooctane (Jakus *et al.*, 1993). GC7 is the most common and probably the most effective inhibitor of DHS available. Treatment of cells with GC7, including archaebacteria, induces cell cycle arrest (Lee *et al.*, 1995; Chen *et al.*, 1996; Shi *et al.*, 1996; Kruse *et al.*, 2000; Lu *et al.*, 2000; Lee *et al.*, 2002; Caraglia *et al.*, 2003). Inhibitors of DHH also exert strong antiproliferative effects on various types of mammalian cells, including several human cancer cell lines (Hanauske-Abel *et al.*, 1994; Lee *et al.*, 1995; Csonga *et al.*, 1996; Andrus *et al.*, 1998; Clement *et al.*, 2002), though the efficacy of DHH inhibition varies with cell type, mainly due to uptake differences (Clement *et al.*, 2002). The metal chelator, mimosine, which is an inhibitor of DHH, has been shown to be an antiproliferative agent as well (Hanauske-Abel *et al.*, 1994). However, while mimosine inhibits DHH, it also inhibits other hydroxylases within the cell and may cause other secondary effects (Clement *et al.*, 2002).

2.1.3 eIF5A is a nucleocytoplasmic shuttle protein that has mRNA binding capabilities

Studies with mammalian cells have indicated that most of the cellular eIF5A is localized to the cytoplasm and, therein, is found in two associations, one free and another bound to the endoplasmic reticulum (Shi *et al.*, 1996). It was recently demonstrated through tandem affinity purification and mass spectrometry that eIF5A interacts with translating 80S ribosomal complexes (Jao and Chen, 2005). This interaction is sensitive to RNase and is dependent on the formation of hypusine (Jao and Chen, 2005). Some of the cellular eIF5A interacts with the general nuclear export receptor, CRM1, and is shuttled between the nucleus and the cytoplasm (Rosorius *et al.*, 1999). eIF5A is also involved in protein-protein interactions with exportin-4. The hypusine modification is part of the signal that allows eIF5A to access the exportin-4 pathway (Lipowsky *et al.*, 2000). These findings have raised new possibilities for the function of eIF5A as a nucleocytoplasmic shuttle protein of mRNAs, specifically subsets of mRNAs required for the execution of one or more specific cellular

functions. Of particular note in this context is the finding that eIF5A is far more abundant than other translation initiation factors and is similarly abundant to Ran, a protein involved in nuclear export. This high abundance might explain why higher eukaryotic cells appear to employ a specialized pathway for eIF5A nuclear export. Indeed, eIF5A could act as an adapter molecule between the general mRNA nuclear export pathway and the export of specific mRNAs required for immediate translation to execute rapid cellular responses.

While it is not generally known which mRNAs eIF5A translocates, a few attempts at finding these targets have been made (Liu *et al.*, 1997; Xu and Chen, 2001; Xu *et al.*, 2004). *In vitro* studies have shown that eIF5A binds to Rev response element RNA of HIV and U6 snRNA (Liu *et al.*, 1997), and that hypusine is required for a sequence-specific interaction of eIF5A with mRNA (Xu and Chen, 2001). Xu *et al.* (2004) were successful at cloning some eIF5A mRNA binding targets through differential display PCR from HeLa cells and were able to demonstrate corresponding electrophoretic mobility-shifts. However, most of the clones were not characterized genes and some were not annotated. Another difficulty in finding eIF5A targets is that, unlike DNA-binding proteins, many RNA-binding proteins target structural elements, such as hairpins, bulges and stem-loops, instead of defined sequences (Varani, 1998).

2.1.4 Role of eIF5A in human diseases

It has been reported that the expression of eIF5A is highly correlated to several pathways involved in human diseases. Not only is there a correlation to disease state, but also to inflammation and cell death (Bevec *et al.*, 1994; Bevec *et al.*, 1996; Kruse *et al.*, 2000; Boone *et al.*, 2004; Taylor *et al.*, 2004).

2.1.4.1 HIV

The unexpected finding that eIF5A is a cellular cofactor for the HIV-1 Rev *trans*-activator protein has provided a target for retroviral therapy as well as an interesting opportunity for exploring further the function of eIF5A *in vivo*. Rev is a *trans*-regulator protein of HIV-1 which acts at the post-transcriptional level by mediating the transport of viral mRNAs from the nucleus to the cytoplasm (Bevec and Hauber, 1997). Rev is essential

for the expression of HIV-1 structural proteins and enzymes required for production of progeny virions. Ruhl *et al.* (1993) demonstrated that nuclear export of Rev is dependent on the nucleocytoplasmic shuttling properties of eIF5A. Lymphocytes with mutated eIF5A were not able to replicate HIV-1; though the eIF5A mutant protein was able to bind Rev, it was not able to translocate it out of the nucleus resulting in blockage of replication (Bevec *et al.*, 1996). Moreover, microinjection studies have demonstrated that antibodies directed against eIF5A specifically block the nucleocytoplasmic viral mRNA translocation mediated by HIV-1 Rev (Schatz *et al.*, 1998; Elfgang *et al.*, 1999). Inhibition of hypusination also blocks eIF5A translocation out of the nucleus, and this finding has lead to large-scale testing of inhibitors of DHS (Sommer *et al.*, 2004) and DHH as putative antiretroviral drugs (Andrus *et al.*, 1998). The DHH inhibitor, mimosine, was shown to suppress replication of HIV-1 and, in a concentration-dependent manner, to engender a reduction of polysomal HIV-1 mRNA (Andrus *et al.*, 1998). While DHS and DHH inhibitors could be effective means of inhibiting HIV-1 replication *in vitro,* these compounds are quite toxic to humans, and thus a more specific non-toxic inhibitor of eIF5A would be a better therapy for HIV-1 positive patients.

2.1.4.2 Cancer

The specific role that eIF5A plays in proliferation and apoptosis of cancer cells is somewhat confusing in light of contradictory results and interpretations in the literature. The confusion appears to rest mainly in the lack of a distinction between the isoforms of mammalian eIF5A and their functions. Specifically, since yeast eIF5A isoforms have been demonstrated to be functionally redundant, the same was assumed about mammalian eIF5A isoforms (Schnier *et al.*, 1991). Only recently have the two human eIF5A isoforms been described as functionally distinct (Clement *et al.*, 2003). Indeed, it is now known that the human isoforms, *HseIF5A-1* and *HseIF5A-2*, have unique expression patterns and correlate with different cellular events. It would appear that *HseIF5A-1* is ubiquitously expressed at the mRNA level (Bevec *et al.*, 1994) and is associated with the regulation of apoptosis (Clement *et al.*, 2003), whereas *HseIF5A-2* is associated with the regulation of proliferation and has a role in the development of malignant phenotypes of certain cancers (Clement *et al.*,

2003). Indeed, it has been proposed that *HseIF5A-2* is an oncogene, as it is located at 3q26 within a region frequently amplified in ovarian cancer and over-expressed in a majority of ovarian tumours and ovarian cancer cell lines (Guan *et al.*, 2001). eIF5A expression has also been detected in lung adenocarcinomas. Through immunohistochemical analysis, elevated eIF5A protein expression was detected in tumours showing poor differentiation, although this increase in protein was not correlated with a corresponding increase in eIF5A mRNA (Chen *et al.*, 2003). This suggests that eIF5A may be post-transcriptionally regulated.

The observation that a decrease in cellular hypusine levels inhibits the growth of mammalian cells has lead to the proposal that a potential target for anti-cancer agents is disruption of the post-translational modification of eIF5A. Studies with epidermoid KB cells revealed a reduction in eIF5A, measured by Western blot, when the cells were induced to undergo apoptosis by treatment with IFN-α (Caraglia *et al.*, 2003). Further to this, treatment with the DHS inhibitor, GC7, resulted in growth inhibition of cells treated with IFN-α (Caraglia *et al.*, 2003). These and other observations suggest a critical role for eIF5A in the modulation of cell proliferation and cell death in cancer cells. For example, loss of hypusinated eIF5A in heat-stressed human pancreatic cancer cells (MIA PaCa-2) was implicated as an important factor in the stress-induced death of MIA PaCa-2 cells (Takeuchi *et al.*, 2002).

2.1.4.3 Regulation of the immune system

The immune system requires complex regulation of gene expression for normal function. It has been demonstrated that eIF5A plays a part in the up-regulation of inflammatory cytokines (Boone *et al.*, 2004), is involved in the stimulation of T cells (Park *et al.*, 1981; Cooper *et al.*, 1982; Bevec *et al.*, 1994) and is essential for the maturation of dendritic cells (Kruse *et al.*, 2000). Only low levels of eIF5A mRNA were detectable in unstimulated peripheral blood mononuclear cells (PBMCs) derived from healthy human donors (Bevec *et al.*, 1994), but the levels were high in differentiated human tissue, stimulated PBMCs and PBMCs isolated from HIV patients. Specifically, eIF5A gene induction was easily achieved by stimulation with PHA and PMA as well as with the more T-cell-specific triggers, anti-CD3 mAb, anti-TCR a/b mAb, a combination of anti-CD3 and

anti-CD28 mAbs, and superantigen SEA (Bevec *et al.*, 1994). These data demonstrate that the eIF5A gene is strongly induced in human PBMCs by T-lymphocyte-stimulating agents, and it is hypothesized to be involved in the transport of specific mRNAs encoding proteins required for effective T-cell immune responses or proliferation. Further to this, when eIF5A is down-regulated by siRNA in PBMCs, the up-regulation of TNF-α in response to stimulation with PMA is reduced by at least half (Boone *et al.*, 2004). Also, down-regulation of eIF5A by siRNA in U937 cells results in the down-regulation of toll-like receptor 4 (TLR-4) and TNF receptor 1 (TNFR1) (Boone *et al.*, 2004). TLR-4 and TNFR1 are involved in the induction of proinflammatory cytokines including TNF-α and interleukin-1β.

The expression of eIF5A significantly increases during dendritic cell maturation, and hypusine formation appears to be essential for this process (Kruse *et al.*, 2000). CD83 is a specific marker that is up-regulated at the very end of dendritic cell maturation and cannot be detected on immature dendritic cell precursors. Kruse *et al.* (2000) demonstrated that the up-regulation of CD83 is closely mirrored by the expression pattern for eIF5A, and that the inhibition of hypusine formation by the DHS inhibitor, GC7, resulted in inhibition of CD83 cell surface expression. Interestingly, CD83 mRNA still accumulated within the dendritic cell precursors, but remained within the nucleus. In maturing dendritic cells, where eIF5A is active, CD83 mRNA is localized in the cytoplasm available for translation (Kruse *et al.*, 2000), presumably by reason of the nucleocytoplasmic shuttling properties of eIF5A.

2.1.5 The plant isoforms of eIF5A

A plant protein with a molecular weight of about 18 kDa that proved capable of incorporating radioactivity from spermidine was first identified in tobacco tissue culture (Apelbaum *et al.*, 1988). Almost twenty years later, the role of eIF5A and DHS in plants is still an area that is largely unexplored with only a handful of publications dedicated to this topic. DHS and eIF5A isoforms have been isolated and partially characterized for several plant species including *Senecio vernalis* (Ober *et al.*, 2003), rice (Mehta *et al.*, 1991; Mehta *et al.*, 1994; Chou *et al.*, 2004), tomato (Wang *et al.*, 2001; Wang *et al.*, 2005), *Arabidopsis* (Wang *et al.*, 2001; Wang *et al.*, 2003), tobacco (Chamot and Kuhlemeier, 1992; Ober and

Hartmann, 1999), maize (Dresselhaus *et al.*, 1999), and rubber tree *Hevea brasiliensis* (Chow *et al.*, 2003). The gene for DHH has not yet been characterized in plants.

It has been demonstrated in rice (Chou *et al.*, 2004) and in tomato (Wang *et al.*, 2001) that there are more than two isoforms of eIF5A in plants. It would appear through preliminary experimental data, as well as EST localization data, that plants have an isoform of eIF5A that is specific for cell growth and several isoforms that are specific for different types of cell death. While there are more than two isoforms of eIF5A in plants, there is still only one isoform of DHS in each species examined to date, which presumably services all the isoforms of eIF5A. In fact, when DHS expression is constitutively suppressed by antisense, there are several phenotypes including delayed natural leaf senescence, delayed bolting, increased rosette leaf and root biomass and enhanced seed yield (Wang *et al.*, 2003). It is possible that these pleiotropic effects are due to inhibition of hypusine formation on different isoforms of eIF5A. These pleiotropic effects are reduced when DHS is down-regulated using a leaf specific Rubisco promoter (Jamal, 2004) or when specific eIF5A isoforms are down-regulated (Gatsukovich, 2004; Tshin, 2004).

It is evident that DHS and eIF5A have central roles in development in plants (Dresselhaus *et al.*, 1999; Wang *et al.*, 2003; Chou *et al.*, 2004; Wang *et al.*, 2005). The finding that eIF5A is expressed in senescing tissues, a developmental phase that encompasses programmed cell death, was very interesting as it was established at a point in time when, according to the literature, eIF5A was only implicated in cell proliferation. Further to this, antisense suppression of DHS was shown to inhibit natural leaf senescence in *Arabidopsis thaliana* (Wang *et al.*, 2003). That there is differential expression of genes encoding eIF5A also indicates that in plants the isoforms are not functionally redundant (Chamot and Kuhlemeier, 1992; Wang *et al.*, 2001; Chow *et al.*, 2003; Chou *et al.*, 2004).

Up-regulation of eIF5A occurs in plant tissues undergoing cell proliferation (Dresselhaus *et al.*, 1999), stressed tissues (Wang *et al.*, 2001; Wang *et al.*, 2003; Chou *et al.*, 2004; Han *et al.*, 2004) and senescing tissues (Wang *et al.*, 2001; Wang *et al.*, 2003; Wang *et al.*, 2005). The programmed cell death that occurs prematurely due to stress has been shown to require its own subset of mRNAs, distinct from those required for programmed cell death

accompanying senescence. It is thus plausible that these subsets of mRNA are translocated by different isoforms of eIF5A. This could also be true for subsets of mRNA required for cell proliferation or cell growth. For *Arabidopsis thaliana* (*At*), three isoforms of *eIF5A* have been annotated in GenBank. Wang *et al.* (2001) demonstrated that *AteIF5A-1* is up-regulated during natural leaf senescence, as it was cloned from a senescing leaf library. The results of the present study indicate that the other two isoforms of *AteIF5A* play a role in cell death associated with wounding (*AteIF5A-2*) and cell expansion (*AteIF5A-3*) (Thompson *et al.*, 2004). This information has been gleaned through a detailed analysis of the expression patterns of the isoforms of AteIF5A and also through analysis of the phenotypes obtained by over-expression of *AteIF5A* isoforms *in planta.*

2.2 Materials and Methods

2.2.1 Sequence alignment of eIF5A

Sequences for eIF5A from *Homo sapiens* (Hs; human), *Saccharomyces cerevisiae* (Sc; yeast), *Tetraodon nigroviridis* (Tn; spotted green pufferfish), *Arabidopsis thaliana* (At), *Lycopersicon esculentum* (Le; tomato) and *Methanococcus jannaschii* (Mj) were found through the Entrez Homepage (http://www.ncbi.nlm.nih.gov/gquery/gquery.fcgi). Most, if not all animals have at least two isoforms of eIF5A. Archaebacteria such as Mj only have one isoform. Plants tend to have at least three isoforms of eIF5A. All species however only have one copy of DHS (Joe *et al.*, 1995; Yan *et al.*, 1996). The protein sequences of Hs1 (AAH01832), Hs2 (AAF98810), Sc1 (CAA89575), Sc2 (CAA39693), Tn1 (CAG00705), Tn2 (CAF89591), At1 (AAG53646), At2 (AAL06956), At3 (AAL31161), Le1 (AAG53647), Le2 (AAG53648), Le3 (AAG53649), Le4 (AAG53650), and Mj (AAB99231) were aligned using T-COFFEE at http://www.ch.embnet.org/software/ TCoffee.html. T-COFFEE is a multiple sequence alignment program that combines the information from alignment programs DIALIGN and CLUSTALW to produce a new multiple sequence that has the best agreement within all these methods (Notredame *et al.*, 2000). The resulting sequence alignment was colour coded to indicate which amino acids in the sequence were identical (red), which were conserved substitutions (orange) and which were semi-conserved substitutions (yellow) in all of the aligned sequences. Amino acids that were not highlighted with colour did not exhibit these degrees of conservation in all sequences.

The degree of similarity and identity for all the aligned sequences listed above was determined using the BLAST 2 Sequences tool available at http://www.ncbi.nlm.nih.gov/blast/bl2seq/wblast2.cgi. This tool uses the BLAST engine for local alignment of two given sequences (Tatusova and Madden, 1999). The program that was used was blastp with matrix BLOSUM62 with all the settings at default (open gap 11; extension gap 1; expect 10; word size 3; filter on). The identities and similarities for each pair-wise alignment obtained with these settings are summarized in Table 2-1 in the Results section.

2.2.2 *Arabidopsis thaliana eIF5A* isoforms

The entire genome sequence of *Arabidopsis thaliana* is available on GenBank. The first *Arabidopsis thaliana* (At) eIF5A was sequenced and its hypusination proven experimentally by Wang *et al.* (2001). This *AteIF5A* was isolated from a senescing leaf library, and was similar in sequence to tomato *eIF5A* (*LeeIF5A-4*). Since it was the first of the *AteIF5A*s cloned in our lab, it was named *AteIF5A-1*. The sequence of *AteIF5A-1* was used to BLAST against the *Arabidopsis* genome, and the other two isoforms were thus identified. These were termed *AteIF5A-2* and *AteIF5A-3*. By mapping these sequences onto chromosome 1 using the mapping tool available at http://www.arabidopsis.org/jsp/ChromosomeMap/tool.jsp, it was evident that these *AteIF5A* genes occur in order along the length of the chromosome where *AteIF5A-1* has the locus tag of At1g13950, *AteIF5A-2* has the locus tag of At1g26630, and *AteIF5A-3* has the locus tag of At1g69410. The corresponding genomic, protein, and coding sequences/mRNA were found and aligned for *AteIF5A-1* (AE005172, AAG53646, AY117272), *AteIF5A-2* (T24P13.1, AAL06956, AY084827), and *AteIF5A-3* (AC018364, AAL31161, AY087040).

2.2.3 Protein expression of AteIF5A

2.2.3.1 Antibody production and purification

AteIF5As are highly identical at the amino acid level, especially at the N-terminal region and the central region of the proteins (See Results Figure 2-4). In order to obtain antibodies that are isoform specific, peptides were designed against regions in the isoforms of AteIF5A that appeared to be unique. An additional cysteine residue was added to each peptide at the N-terminus for conjugation with Keyhole Limpet Hemocyanin (KLH; Sigma). The sequences used were: CNDDTLLQQIKS for AteIF5A-1, CTDDGLTAQMRL for AteIF5A-2 and CTDEALLTQLKN for AteIF5A-3. When these sequences were submitted to protein BLAST (short nearly exact sequences; limited by *Arabidopsis thaliana*; expected number 20000; word size 2; Matrix PAM90; Gap cost 91), the significant sequences that were found in the database matched only the respective AteIF5A. The peptides were synthesized at the University of Western Ontario Peptide Synthesis facility.

The carrier protein, Keyhole Limpet Hemocyanin (Sigma; KLH), was conjugated to the N-terminal cysteine of the peptide using *m*-maleimidobenzoyl-*N*-hydroxysuccinimide ester (MBS) according to Drenckhahn *et al.* (1993) and Collawn and Patterson (1999). Dissolved KLH (10mg/mL in water) was mixed dropwise with dissolved MBS (10mg/mL in dimethylformamide) and stirred at room temperature for 30 minutes. The MBS-KLH complex was separated from the free MBS by a Sephadex 25 column. The fractions collected with the activated MBS-KLH, identified as a peak in absorbance at 280nm, were pooled, and the pH was adjusted to 7.4. Approximately 1mg of each of the AteIF5A peptides was added to 1mg of MBS-KLH complex. Under nitrogen, the peptides were allowed to conjugate to the MBS-KLH complex for 3 hours at room temperature with gentle rotation. The resulting AteIF5A peptide-KLH conjugates were dialyzed against phosphate buffered saline (PBS) at 4^{o}C overnight.

The antibodies were raised in rabbits housed in the animal care facility in the Department of Biology according to the University of Waterloo's Animal Care Standard Operating Procedures. The initial immunization was performed with a peptide conjugate emulsion in Freund's complete adjuvant (mixed 1:1; Sigma), and the subsequent injections consisted of peptide conjugate emulsion in Freund's incomplete adjuvant (mixed 1:1; Sigma). The rabbits were injected four times at two-week intervals with the linked peptides. Two weeks after the final injection, the rabbits were exsanguinated, and the antisera were amassed through clotting of the collected blood.

Antibodies were column-purified using SulphoLink Coupling Gel (Pierce) as described by the manufacturer with some changes. The peptides were dissolved in 1mL of equilibration buffer containing 20% DMSO and 4M urea as there were some solvation problems in equilibration buffer alone. Also the A_{280} readings were not very accurate for these particular peptides, as they were very small and contained few amino acids with double bonds. Accordingly, fractions collected from the column were checked by dot blot hybridizations against peptide dotted on nitrocellulose membranes in order to confirm the coupling efficiency of the peptides to the column. For the affinity purification step, the serum collected from the final bleed was added directly (1mL at a time) to the column and

allowed to incubate at room temperature for 1 hour. The purified antibody was eluted by applying 5 column volumes of elution buffer (0.1M glycine, pH 2.8). Fractions of 0.5mL were collected and neutralized by adding 25µL of 1M Tris, pH 9.5. Elution was monitored by A_{280}, and the fractions with a high reading were pooled and dialyzed overnight against 3 litres of PBS. The purified antibodies were aliquoted and stored at -20°C. The titre of the purified antibody was determined using some of the remaining peptide for dot blots, and dilutions were optimized through Western blotting of tissues over-expressing the corresponding *AteIF5A*. The following dilutions were used for Western blotting: AteIF5A-1 (1:100), AteIF5A-2 (1:500), and AteIF5A-3 (1:100). The following dilutions were used for confocal microscopy: AteIF5A-2 (1:50) and AteIF5A-3 (1:25).

2.2.3.2 Plant material

2.2.3.2.1 Plants grown in soil

Seeds of *Arabidopsis thaliana*, ecotype Columbia, were grown in Promix BX soil (Premier Brands, Brampton, ON, Canada) in flats containing 32 cells. Freshly seeded flats were maintained at 4°C for 2 days and then transferred to a growth chamber operating at 22°C with 16-h light/ 8-h dark cycles. Lighting at 150 µmol radiation $m^{-2} \cdot s^{-1}$ was provided by cool-white fluorescent bulbs. Whole rosettes were collected at one week intervals from 2-weeks to 7-weeks of age for Western blotting. Flowers were also collected at various stages defined within the Results section for Western blotting. As well, 3-week-old rosette leaves were collected for genomic DNA isolation for PCR. All tissues were flash-frozen in liquid nitrogen and were either used immediately or stored at -80°C until required.

2.2.3.2.2 Plants grown on MS media plates

Approximately 100mg of *Arabidopsis thaliana*, ecotype Columbia, seed was surface sterilized in 1% (v/v) sodium hypochlorite and 0.1% (v/v) Tween 80 for 10 minutes on a rotator. The seeds were washed 4 times with sterilized water before being plated onto sterile, ½ Murashige and Skoog Basal medium (MS; 2.2g/L) supplemented with 1% (w/v) sucrose, 0.5g/L 2-[*N*-Morpholino] ethanesulfonic acid (MES) and 0.7% (w/v) bacteriological agar (Murashige and Skoog, 1962). The plated seeds were maintained at 4°C for 2 days in

the dark to synchronize germination, and then transferred to a growth chamber operating at 22°C with 16-h light/ 8-h dark cycles. Seedlings were collected 2 to 8 days after germination, flash frozen in liquid nitrogen and stored at -80°C until used for protein extraction for Western blotting.

2.2.3.2.3 Infection of *Arabidopsis thaliana* rosette leaves with *Pseudomonas syringae*

2.2.3.2.3.1 Inoculum preparation

Virulent *Pseudomonas syringae* pv. *Tomato* DC3000 (virulent *Pst* DC3000; containing pVSP61), a kind gift from Dr. Robin Cameron, McMaster University, Hamilton, Ontario, was used to induce a disease response in *Arabidopsis thaliana* plants. Bacterial cultures were grown on a shaker using King's B media (Whalen *et al.*, 1991) containing 50 μg/mL kanamycin at 28°C until the cultures reached mid-log growth (OD_{600}=0.6 to 1.0). The cultures were centrifuged at 2500*g* for 10 minutes in a swinging bucket rotor, and the bacterial pellets were resuspended in 5mL 10mM $MgCl_2$. The inoculum was made by diluting the bacteria to 10^6 colony forming units (CFU)/mL, where, OD_{600}=0.002 of *Pst* DC3000 is 1×10^6 cfu/mL.

2.2.3.2.3.2 Inoculation procedure

Seeds of *Arabidopsis thaliana* ecotype Columbia were sown on Promix BX soil (Premier Brands, Brampton, ON, Canada) in flats containing 32 growth cells. The seeded flats were maintained at 4°C for 2 days and transferred to a growth chamber with a photoperiod of 16h light/8h dark. Rosette leaves of 4-week-old plants were infected with the virulent strain of *Pst* DC3000. The abaxial surface of the rosette leaves was pressure infiltrated with inoculum using a 1mL syringe without a needle until the leaf was water-soaked and the apoplast filled. Plants were given one of two treatments: mock-inoculation with 10mM $MgCl_2$ or virulent *Pst* DC3000 (10^6 CFU/mL in 10mM $MgCl_2$). The inoculated leaves were harvested at 0h, 24h, 48h, and 72h after treatment. Mock infected leaves and leaves infected with virulent *Pst* DC3000 were frozen in liquid nitrogen and stored at -80°C for further analysis or fixed for confocal analysis (see Section 2.2.3.4.1).

2.2.3.2.4 Wounding *Arabidopsis thaliana* plants with a haemostat

Arabidopsis thaliana plants were grown to 3.5-weeks of age under normal growth chamber conditions described above. Rosette leaves were wounded by crushing with a haemostat alongside the midvein (Orozco-Cardenas and Ryan, 1999). The wounded leaves were collected at 0h, 2h, 4h, 5h, 6h, 7h, and 8h after wounding. All tissue was flash-frozen in liquid nitrogen and stored at -80^{o}C until used for protein extraction for Western blotting.

2.2.3.3 Protein fractionation and Western blotting

Tissues were homogenized in buffer (~0.5g/mL; 50mM EPPS, pH 7.4, 0.25M sorbitol, 10mM EDTA, 2mM EGTA, 1mM DTT, 10mM amino-*n*-caproic acid, 1:100 v/v Sigma Protease Inhibitor Cocktail for plant tissues) in an Eppendorf tube with an Eppendorf tube-sized pestle, or in a small mortar with a small pestle. Protein was quantified according to Ghosh *et al.* (1988). SDS-PAGE was performed on Mini protein Dual Slab cells (BioRad, Mississauga, Ontario), and the gels (12% polyacrylamide) were stained with Coomassie brilliant blue R250 (Fairbanks *et al.*, 1971) or transferred to polyvinyldiene difluoride (PVDF) membranes using the semi-dry transfer method (semi-dry transfer cell, Bio-Rad, Hercules, CA) and stained after transfer. The blots were blocked for 30s in 1mg/mL polyvinyl alcohol (Miranda *et al.*, 1993) and for 1 hour in PBS containing 0.1% (v/v) Tween 20 and 5% (w/v) powdered milk. Primary antibody (purified antibody against the corresponding AteIF5A) was diluted in PBS containing 0.1% (v/v) Tween 20 and 1% (w/v) powdered milk. Antigen was visualized using secondary antibody coupled to alkaline phosphatase, made in goat against rabbit IgG (Bioshop, Burlington, Ontario) and the phosphatase substrates, NBT and BCIP (BioRad, Mississauga, ON).

2.2.3.4 Confocal Microscopy

2.2.3.4.1 AteIF5A-2 expression and TUNEL

Discs of leaves that had either been inoculated 24h and 72h previously with virulent *Pst* DC3000 strain and uninfected leaves from line 2-3F (see Section 2.2.6.1) that over-expressed *AteIF5A-2* were stained for DNA fragmentation by Terminal deoxynucleotidyl transferase (TdT)-mediated dUTP Nick-End Labelling (TUNEL) and immunostained for

AteIF5A-2 expression. The tissue discs were cut from the centre portion of the leaves with a cork borer (0.4 cm diameter). The tissue samples were immediately vacuum-infiltrated with fixing buffer (4% paraformaldehyde in PBS) for 10 minutes. Fixed samples were used right away for TUNEL staining and immunolocalization of AteIF5A-2. First, the samples were labelled using the Promega DeadEnd™ Fluorometric TUNEL System. Briefly, the tissue segments were washed in PBS several times at room temperature to remove the paraformaldehyde and permeablized in 1% Triton X in PBS for 15 minutes. The tissue segments were then covered with 100μL of equilibration buffer and allowed to equilibrate for 5-10 minutes. The rTdT reaction mixture was prepared (50 μL per leaf segment). The tissue segments were blotted to remove excess equilibration buffer, covered with the rTdT reaction mixture and placed on slides in a humidified chamber kept at 37^{o}C for 60 minutes to allow the tailing reaction to occur. All steps from this point were light sensitive and were thus performed in the dark. The reaction was terminated by washing the tissue in 2X SSC for 15 minutes. The samples were then washed with PBS twice for 10 minutes at room temperature before incubation with primary antibody against AteIF5A-2 (1:50) in 1% BSA (v/w) in PBS for two hours. The samples were washed three times for 10 minutes each in a relatively large volume of PBS and then incubated with goat anti-rabbit secondary antibody conjugated to TRITC [Sigma; 1:100 in 1% BSA (w/v) in PBS] for one hour. After the secondary antibody incubation, the samples were washed three times for 10 minutes each in PBS and then mounted on slides in 70% glycerol. For optimal visualization by confocal microscopy #1.5 cover slips were used. The samples were observed using a Zeiss LSM 510 confocal laser scanning microscope attached to an axiovert-inverted microscope. This is an optimized protocol, obtained by testing several variations.

2.2.3.4.2 AteIF5A-3 expression

Seedlings germinated under etiolating conditions on sterile filter paper with sterile water were used for observing the expression patterns of AteIF5A-3. The seedlings were fixed by vacuum infiltration of 4% paraformaldehyde for 10 minutes. They were washed 4 times in PBS, labelled with primary (AteIF5A-3) antibody (1:25) and then secondary

antibody conjugated with FITC. Subsequent washes and mounting on slides were as described in section 2.2.3.4.1.

2.2.4 Production of transgenic *Arabidopsis thaliana* plants over-expressing *AteIF5A-1*, *AteIF5A-2* or *AteIF5A-3*

2.2.4.1 Primer design for amplification of the *AteIF5A* isoforms

AteIF5A isoforms are highly similar in the coding region, but have distinct untranslated regions. Plants over-expressing *AteIF5A-1* were produced by Zhongda Liu (J. E. Thompson's laboratory) using the coding region of the cDNA, amplified from a plasmid containing the cDNA cloned by Tzann-Wei Wang (J. E. Thompson's laboratory). Plants over-expressing *AteIF5A-2* and *AteIF5A-3* were created using the entire gene sequence amplified from genomic DNA, from the approximate beginning of the 5`UTR and to the end of the 3`UTR. The 5`UTR and 3`UTR were identified using EST sequence information and genomic sequence information in the GenBank database. Unique restriction sites[3] were added to the ends of the primers for ligation in the sense orientation behind the $35S^2$ promoter in the pKYLX71 binary vector (Figure 2-2). For *AteIF5A-1*, the upstream primer was 5` GAAGCTCGAGGCTGCAACC**ATG**TCC 3`, and the downstream primer was 5` GGGGAGCTCTTGTTAGTC**TCA**CTTGG 3`. For *AteIF5A-2* the upstream primer was 5` CTCGAGTGCTCACTTCTCTCTCTTAGG 3` and the downstream primer was 5` GAGCTCA AGAATAACATCTCATAAGAAAC 3`. The upstream primer for *AteIF5A-3* was 5` CTCGAGCTAAACTCCATTCGCTGACTTCGC 3` and the downstream primer was 5` GAGCTCTAGTAAATATAAGAGTGTCTTGC 3`. The restriction sites that were added to the primers for all *AteIF5A* constructs were *Xho*I and *Sac*I. The PCR fragment from *AteIF5A-1* cDNA was digested and ligated into pKYLX71-$35S^2$ binary vector directly. The PCR fragments of *AteIF5A-2* and *AteIF5A-3* amplified from genomic DNA were first subcloned into pGEM®-T Easy Vector and then into pKYLX71-$35S^2$ binary vector.

[3] The restriction sites are indicated as underlined, and the start and stop codons of *AteIF5A-1* are indicated in bold.

Figure 2-2: Map of binary vector, pKYLX71-35S^2

The binary vector, pKYLX71-35S^2, contains tetracycline resistance (Tet^r) for transformant selection in *E. coli* and *A. tumefaciens*, and kanamycin resistance (Kan^r) for seed transformant selection on MS plates containing kanamycin. The origin of replication (pRK2 ori) permits the plasmid to be maintained in *A. tumefaciens*. The 35S promoter is a strong constitutive promoter isolated from cauliflower mosaic virus; the vector contains 2 consecutive copies (35S^2). The multiple cloning site (MCS) contains several unique restriction enzyme (RE) sites for specific directional ligation of an insert behind the 35S^2 promoter. rbcS3` is the 3` end containing the terminator sequence of ribulose-1,5-bisphosphate carboxylase small subunit gene. The left (T_L) and right (T_R) borders define the T-DNA region that is integrated into the genome during plant transformation.

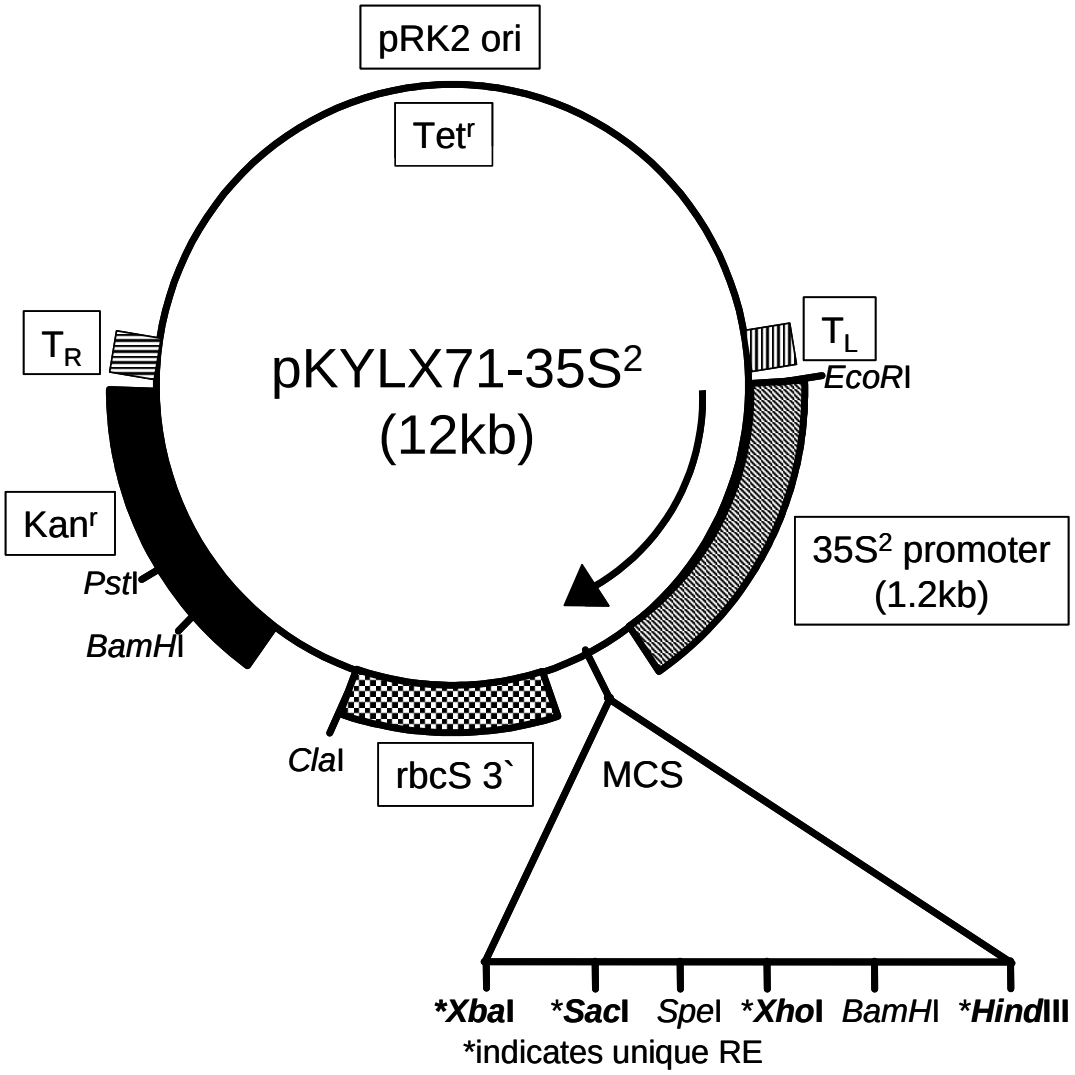
pRK2 ori
Tet^r
T_R
T_L
EcoRI
pKYLX71-35S^2
(12kb)
Kan^r
PstI
BamHI
35S^2 promoter
(1.2kb)
ClaI
rbcS 3`
MCS
*XbaI
*SacI
SpeI
*XhoI
BamHI
*HindIII
*indicates unique RE

2.2.4.2 Isolation of genomic DNA from *Arabidopsis thaliana*

Genomic DNA was isolated from 3-week-old rosette leaf tissue. The tissue was homogenized in extraction buffer (200mM Tris pH 7.5, 250mM NaCl, 25mM EDTA, 0.5% SDS), and the resulting homogenate was vortexed for 15 seconds. The debris was removed by centrifugation in a microcentrifuge at maximum speed for 1 minute. The supernatant was collected and mixed in a 1:1 ratio with isopropanol, vortexed and left at room temperature for 2 minutes. A pellet was collected by centrifugation in a microcentrifuge at maximum speed for 5 minutes, washed with 70% ethanol and vacuum-dried for 2 minutes. The dried pellet was resuspended in water, chloroform (1:1) was added, and the sample was vortexed. After centrifugation in a microcentrifuge at maximum speed for 2 minutes, the top layer was collected and treated with 20μL salt (3M sodium acetate) and 2 volumes of ethanol for precipitation at -20^{o}C for 30 minutes. The purified genomic DNA was then centrifuged at maximum speed for 30 minutes in a microcentrifuge, dried and resuspended gently in water for PCR.

2.2.4.3 Cloning of *AteIF5A-2* or *AteIF5A-3* into pGEM®-T Easy Vector

PCR was performed with the primers described above (Section 2.2.4.1). The PCR reaction mixture contained 1x *Taq* polymerase reaction buffer, 1U *Taq* polymerase, 0.2mM dNTP, 2mM $MgCl_2$, and 15pmols of each specific primer. The reaction was initiated with a hot start at 95^{o}C for 10 minutes, and the first cycle consisted of 1 minute denaturing temperature of 95^{o}C, 1 minute annealing temperature of 55^{o}C, and 1 minute extension temperature of 72^{o}C. The following 29 cycles consisted of the same denaturing, annealing and extension durations and temperatures. The final extension at 72^{o}C was for 10 minutes. The PCR products were separated by 1% agarose gel electrophoresis, cut out and retrieved by Millipore Ultrafree-DNA for DNA Extraction from Agarose spin columns (Millipore Corporation, Bedford, MA) according to manufacturer's directions.

Purified PCR products of *AteIF5A-2* or *AteIF5A-3* were ligated into pGEM®-T Easy Vector according to directions provided by Promega. Briefly, PCR products were mixed in a 3:1 ratio with pGEM®-T Easy Vector and 3 Weiss Units T4 DNA ligase in Rapid Ligation

Buffer [30mM Tris-HCl, 10mM $MgCl_2$, 10mM DTT, 1mM ATP, and 5% polyethylene glycol (MW8000, ACS Grade) pH 7.8] provided in the Promega pGEM®-T Easy Vector System Kit (Promega Corporation, Madison WI). The ligation reaction was incubated overnight at 15°C and transformed into competent *E. coli* DH5-α cell suspension (Kushner, 1978). The transformation mixture was first incubated on ice for 30 minutes, then heat-shocked for 90 seconds at 42°C and allowed to recover at 37°C for 1 hour after the addition of 1mL 2xYT broth. The transformed cells were pelleted, resuspended in a small volume of 2x YT broth and plated on agar plates containing 50μg/mL ampicillin for selection. Only transformants are able to grow on the ampicillin-containing plates as the pGEM®-T Easy Vector provides ampicillin resistance to the cells. Transformants were selected and screened for the PCR product insert ligated into the pGEM®-T Easy Vector.

Colonies that grew on selection media were grown in 5mL 2xYT broth containing 50μg/mL ampicillin overnight at 37°C. The recombinant plasmids from the selected colonies were purified using Wizard Prep DNA Purification Kit (Promega). The plasmid DNA was digested with *EcoR*I for 1hour at 37°C and visualized on a 1% agarose gel for verification that the *AteIF5A-2* or *AteIF5A-3* insert sizes were present. The positive plasmids were then sequenced by the Core Molecular Biology Facility (University of Waterloo, Waterloo, ON) for confirmation.

2.2.4.4 Cloning of *AteIF5A-2* or *AteIF5A-3* into pKYLX71-35S^2

The constructs of pGEM: *AteIF5A-2* and pGEM: *AteIF5A-3* were double-digested with *Xho*I and *Sac*I, and ligated into the binary vector, pKYLX71-35S^2 (Figure 2-2), kindly provided by Dr. B. Moffat, that had also been digested with *Xho*I and *Sac*I (Figure 2-3). These enzyme digestions ensured that *AteIF5A-2* and *AteIF5A-3* would be inserted in the sense orientation in front of the cauliflower mosaic virus double 35S promoter of the binary vector pKYLX71-35S^2 (Schardl *et al.*, 1987). The ligation reaction mixtures comprised 1μg of binary vector and 3μg of the insert in ligation buffer [30mM Tris-HCl, 10mM $MgCl_2$, 10mM DTT, 1mM ATP, and 5% polyethylene glycol (MW8000, ACS Grade) pH 7.8] with 3 Weiss units of T4 DNA Ligase (Fermentas). The ligation mixture was incubated overnight at 15°C and transformed into competent *E. coli* DH5-α cell suspension (Kushner, 1978). The

Figure 2-3: Flowchart illustrating the production and selection of transgenic plants over-expressing *AteIF5A-1*, *AteIF5A-2* or *AteIF5A-3*

The red asterisks denote steps at which the inserts were sequenced for accuracy.

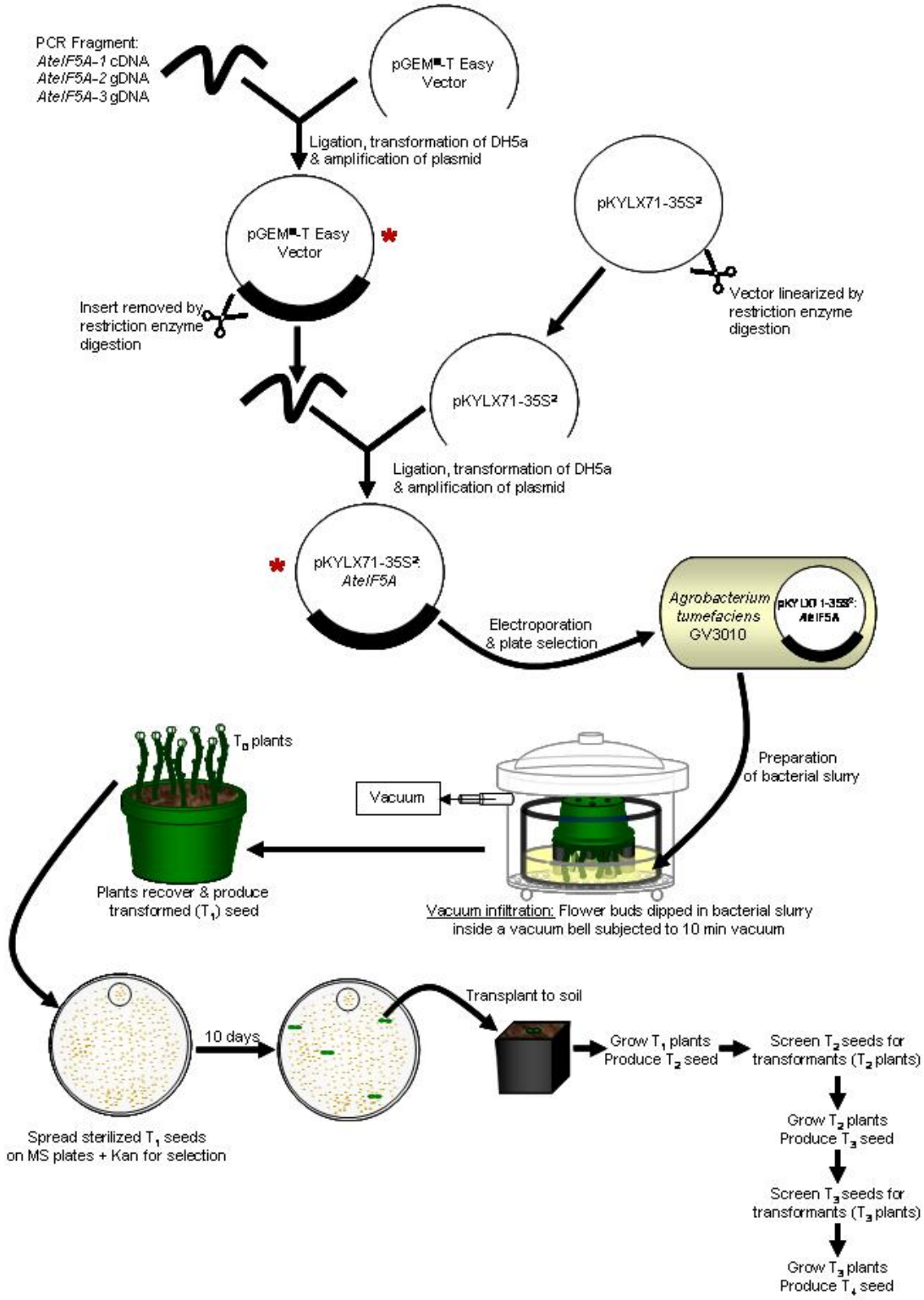
PCR Fragment:
AteIF5A-1 cDNA
AteIF5A-2 gDNA
AteIF5A-3 gDNA
pGEM®-T Easy Vector
Ligation, transformation of DH5a & amplification of plasmid
pGEM®-T Easy Vector
pKYLX71-35S²
Insert removed by restriction enzyme digestion
Vector linearized by restriction enzyme digestion
pKYLX71-35S²
Ligation, transformation of DH5a & amplification of plasmid
pKYLX71-35S²: AteIF5A
Electroporation & plate selection
Agrobacterium tumefaciens GV3010
pKYLX71-35S²: AteIF5A
Preparation of bacterial slurry
T0 plants
Vacuum
Plants recover & produce transformed (T1) seed
Vacuum infiltration: Flower buds dipped in bacterial slurry inside a vacuum bell subjected to 10 min vacuum
10 days
Transplant to soil
Grow T1 plants Produce T2 seed
Screen T2 seeds for transformants (T2 plants)
Grow T2 plants Produce T3 seed
Screen T3 seeds for transformants (T3 plants)
Grow T3 plants Produce T4 seed
Spread sterilized T1 seeds on MS plates + Kan for selection

transformation was performed as described above (Section 2.2.4.3). The transformed cells were pelleted, resuspended in a small volume of 2x YT broth and plated on agar plates containing 50μg/mL tetracycline for selection. Only transformants are able to grow on the tetracycline-containing plates as the binary vector pKYLX71-35S[2] provides tetracycline resistance to bacterial cells. Transformants were screened for the *AteIF5A-2* and *AteIF5A-3* inserts by PCR and by double digestion with *Xho*I and *Sac*I, and the inserts were sequenced by the Core Molecular Biology Facility (University of Waterloo, Waterloo, ON) for sequence accuracy.

2.2.4.5 *Agrobacterium tumefaciens* electroporation and selection

The constructs pKYLX71: *AteIF5A-2* and pKYLX71: *AteIF5A-3* were electroporated into competent *Agrobacterium tumefaciens* GV3010 (Figure 2-3). The preparation of competent *Agrobacterium* cells was obtained by inoculating a single colony in 5mL of 2xYT broth containing 50μg/mL of rifampicin, and 50μg/mL gentamycin and growing the suspension overnight at 28^{o}C on a Forma Scientific Orbital Shaker (Fisher Scientific) at 280rpm. This overnight culture was used to inoculate 30mL cultures of 2xYT containing 50μg/mL of rifampicin, and 50μg/mL gentamycin, and the newly inoculated cultures were grown until the OD_{600} was between 0.5 and 0.8, cooled and centrifuged in an SS-34 rotor (Sorvall) at 2000 *g* for 15 minutes. The pellets were resuspended in 50mL of ice-cold water and centrifuged at 2000 *g* for 15 minutes. This washing procedure was repeated for a total of four times to remove salts and dead cells. The final pellet was resuspended in 40mL ice cold 10% (v/v) glycerol in water and centrifuged at 2000 *g* for 15 minutes, and this procedure of resuspension in glycerol and centrifugation was repeated. The final pellet was resuspended in 100μL ice-cold 10% glycerol, mixed well, divided into aliquots of 100μl and stored on ice.

For electroporation of the DNA constructs into competent *Agrobacterium* cells, the 100μL aliquots were each mixed well with 500ng of DNA construct. The bacteria:vector mixture was then transferred to a pre-cooled electroporation cuvette and placed in the Gene Pulser (Biorad) adjusted to the following settings: 2.5kV, 25μF, and 200Ω. After electroporation, 1mL 2xYT broth was added, and the suspension was transferred to a culture

tube. The electroporated cultures were incubated at 28°C, 280rpm, for 3 hours to allow them to recover, and then 2mL 2x YT broth was added as well as 50µg/mL of rifampicin and 50µg/mL gentamycin. After 2 days of growing in culture, the electroporated cells were plated on tetracycline, gentamycin and rifampicin (all at 50µg/mL) and grown for an additional 2 days. The resulting colonies were screened for pKYLX71: *AteIF5A-2* or pKYLX71: *AteIF5A-3* by PCR and by double digestion with *Sac*I and *Xho*I. The inserts were visualized by separation on a 1% agarose gel.

2.2.4.6 Plant transformation

Agrobacterium tumefaciens GV3010 containing either pKYLX71: *AteIF5A-2* or pKYLX71: *AteIF5A-3* was used for transformation of 4-week-old wild type *Arabidopsis thaliana* plants (ecotype Columbia) (Figure 2-3). To prepare the bacterial slurry used for plant transformation, a single colony of transformed *A. tumefaciens* was inoculated into 5mL of 2x YT broth containing 50µg/mL of tetracycline, 50µg/mL of rifampicin, and 50µg/mL gentamycin. After 2 days of growth at 28°C in a Forma Scientific Orbital Shaker (Fisher Scientific) at 280rpm, the resultant culture was used to inoculate 35mL (total) of 2xYT containing 50µg/mL of rifampicin, and 50µg/mL gentamycin. The 35mL culture was grown overnight at 28°C, 280rpm, and used to inoculate 500mL of 2xYT with 50µg/mL of rifampicin and 50µg/mL gentamycin. Again the culture was grown overnight at 28°C, 280rpm, to an OD_{600} of about 2.0.

These cultures were then transferred to two 250mL tubes before centrifugation for 15 minutes at 1945 *g* at 4°C in a GSA rotor (Sorvall). The pellets were resuspended in 500mL of infiltration media [1.1g MS salts, 25g sucrose, 0.25g MES, pH5.7 with KOH, 100ng/mL benzylaminopurine and 50µl Vac-In-Stuff (Silwet L-77; Lehle Seeds)] and placed in a large plastic dish in a vacuum desiccator with 4 large rubber stoppers. Five pots containing 8 plants each at the right stage of development were used sequentially for infiltration. Each pot was first inverted over a trash can to remove any loose soil, then was placed (still inverted) into a plastic container in the glass desiccator so that the 4 large rubber stoppers acted as stand for the inverted pot, thus allowing the bolts, but not the rosettes, to dip into the bacterial slurry. The plants were then subjected to a vacuum (400mm Hg) in this

inverted state for 10 minutes. The vacuum-infiltrated plants were then allowed to recover and grown to maturity. New flower buds were removed daily to increase seed screening efficiency. After several weeks when the siliques were dry and seed matured, the seeds were collected from each pot and pooled.

2.2.4.7 Selecting plant transformants and segregation analysis

To identify primary transformants, T_1 seeds from the vacuum-infiltrated T_0 plants were surface sterilized in a solution of 1% (v/v) sodium hypochlorite and 0.1% (v/v) Tween 80 for 20 minutes on a rotator, rinsed four times with sterile water, and resuspended in sterile 0.8% agar. The resuspended seeds were then planted onto sterile, half-strength Murashige and Skoog (MS) medium (2.2g/L) supplemented with 1% (w/v) sucrose, 0.5g/L MES, 0.7% (w/v) bacteriological agar and 40 to 50 μg/mL kanamycin (Murashige and Skoog, 1962). Only transformants are able to grow on the kanamycin-containing plates since the binary vector provides the kanamycin resistance gene to the transformant seedlings (Figure 2-3). Seedlings that do not harbour the binary vector become yellow and die, as there is no kanamycin resistance gene. Wild-type (WT) seed as well as seed from a homozygous line containing empty pKYLX71-35S^2 vector (BIN) were used as controls, and were plated onto MS medium without kanamycin and kanamycin-containing plates, respectively. The BIN control is useful in demonstrating the effect kanamycin has on growth of the seedlings as well as the effect of random integration of the binary vector into the genome of *Arabidopsis thaliana.* A small amount of wild type seed was plated onto a small area of each kanamycin plate as well in order to make sure the medium contained enough kanamycin for selection of transformants.

The seeded plates were kept at 4^{o}C for 2 days to synchronize germination. After 2 days, the plates were transferred to growth chambers where they grew for an additional 7 days under 16-h light/ 8-h dark cycles at 20±2^{o}C. Lighting was maintained at 150μmol radiation $m^{-2}{\cdot}s^{-1}$ and was provided by cool-white fluorescent bulbs. The efficiency of transformation of *Arabidopsis thaliana* plants with pKYLX71: *AteIF5A-1*, pKYLX71: *AteIF5A-2* and pKYLX71: *AteIF5A-3* was determined.

2.2.5 Phenotypic analysis of *AteIF5A-1* over-expressing transgenic plants

2.2.5.1 Selection and naming of lines over-expressing *AteIF5A-1*

When T_1 seedlings over-expressing *AteIF5A-1* were 10 days-old, they were transplanted to Promix BX soil (Premier Brands, Brampton, Ontario) in flats containing 32 cells. Green tags were used to label the *AteIF5A-1* over-expressing plants. Corresponding wild type (WT) seedlings in MS plates without kanamycin and empty binary vector (BIN) seedling in MS plates with kanamycin were transplanted into soil at the same time. White tags were used to label the WT plants and yellow tags were used to label the BIN plants. These transplanted T_1 generation plants were then transferred into a growth chamber operating at 22^{o}C with 16-h light/ 8-h dark cycles. Lighting at 150 μmol radiation $m^{-2} \cdot s^{-1}$ was provided by cool-white fluorescent bulbs.

There were 48 *AteIF5A-1* over-expressing T_1 plants transplanted from MS plates to soil, and they were named 1-1, 1-2, 1-3 etc., where the first number denotes the *AteIF5A* isoform and the second number indicates the T_1 plant line number. All of the seeds from the T_1 plants were collected as they became available. Some of the plants exhibited different development timelines, and thus the seeds matured at different times. The T_2 seeds collected from the T_1 plants were quantified by measurement of volume in a 1mL glass syringe that had 10μL markings and also by weight. Several lines were chosen for T_2 analysis based on phenotypic characteristics. Seed from these lines was sterilized and plated on selective MS plates, and 8 sister lines were carried through for each mother line selected. The sister lines were labelled with a letter, for example 1-4A. Again, the first number indicates the isoform of *AteIF5A* over-expressed, the second number indicates the mother line from the T_1 generation, and the letter indicates the sister line of the T_2 generation. Age-matched WT and BIN seeds were used as controls.

2.2.5.2 Photographic record of *AteIF5A-1* over-expressing plants

As the T_1 generation plants over-expressing *AteIF5A-1* grew to maturity, photographic and written records were maintained. Photographs were taken when the plants were 10 days, 3-weeks, 4-weeks, 5-weeks and 6-weeks of age. During growth of the T_2

generation of plants over-expressing *AteIF5A-1*, photographs were taken at 10 days, 3.5-weeks, 4-weeks, 5-weeks, 6-weeks and 7-weeks of age. Plants were observed daily for phenotype and watering needs.

2.2.6 Phenotypic analysis of *AteIF5A-2* over-expressing transgenic plants

2.2.6.1 Selection and naming of the lines over-expressing *AteIF5A-2*

T_1 seedlings over-expressing *AteIF5A-2* were transplanted at 10 days of age from MS plates to soil and grown to maturity. The *AteIF5A-2* over-expressing plants were labelled with pink tags, and corresponding WT and BIN plants were labelled with white and yellow tags, respectively. A total of 14 T_1 transformants over-expressing *AteIF5A-2* were maintained. The lines were named by number, for example 2-1, 2-2, 2-3 etc., where the first number denotes the *AteIF5A* isoform over-expressed and the second number indicates the T_1 plant line number. Only 9 of the 14 T_1 plants proved capable of growing to maturity and producing seed. These seeds were collected and quantified by volume and weight. All of the lines that produced seed were carried through to the T_2 generation. Eight sister lines were carried through for each T_1 mother line and were designated by letter, for example, 2-1A up to 2-1H, where the first number denotes the *AteIF5A* isoform over-expressed, the second number indicates the mother line from the T_1 generation and the letter indicates the line established in the T_2 generation. The T_1 line, 2-12, only produced about 30 T_2 seeds, and from these only one was capable of growing on kanamycin MS plates yielding a single T_2 line called 2-12A. Corresponding age- matched WT and BIN seeds were grown alongside the T_2 plants over-expressing *AteIF5A-2*. The first cauline leaf was harvested at 4-weeks of age for Western blot analysis of all T_2 plants over-expressing *AteIF5A-2*. Only 2-3F and 2-9A were brought to T_3 as they were used for an infection experiment with the virulent strain of *Pst* DC3000 and TUNEL analysis.

2.2.6.2 Photographic record of over-expressing *AteIF5A-2* plants

Photographic and written observations were maintained throughout the lifecycle of the T_1 and T_2 over-expressing *AteIF5A-2* plants. Photographs of T_1 plants were taken at 3-weeks, 4-weeks, 5-weeks, and 6-weeks of age. Photographs of T_2 plants were taken at 10

days, 2-weeks, 3-weeks, 4-weeks, 5-weeks, 6-weeks, and 7-weeks of age. Plants were observed daily for phenotype and watering needs.

2.2.7 Phenotypic analysis of *AteIF5A-3* over-expressing transgenic plants

2.2.7.1 Selection and naming of the lines over-expressing *AteIF5A-3*

T_1 seedlings over-expressing *AteIF5A-3* were transplanted at 10 days of age from MS plates to soil. The *AteIF5A-3* over-expressing plants were labelled with blue tags, whereas corresponding WT and BIN plants were labelled with white tags and yellow tags, respectively. A total of 16 T_1 transformants over-expressing *AteIF5A-3* were maintained. The lines were named by number, for example 3-1, 3-2, 3-3 etc., where the first number indicates the *AteIF5A* isoform over-expressed and the second number indicates the T_1 mother line. The selection of T_2 generation transformants was achieved by scoring germination on kanamycin MS plates. The T_1 line, 3-12, produced no transformants on the selectable media and was not included in any further work. For each of lines 3-1 through 3-16 (minus line 3-12) of the *AteIF5A-3* over-expressing plants, 8 sister lines were carried through to the T_2 generation. These were named A through H so that, for example, for the T_1 line 1, the T_2 generation plants were named 3-1A, 3-1B, 3-1C, etc.

The first cauline leaf from each sister line of *AteIF5A-3* over-expressing T_2 plants was collected for protein analysis. Total extracted protein was fractionated by 12% SDS-PAGE and transferred to a PVDF membrane. The blot was probed with antibodies against AteIF5A-3 at a 1:50 dilution. Control total protein was extracted from the first cauline leaf of wild type and empty binary vector control plants. These Western blots as well as phenotypic observations were used to select lines to be carried through to T_3 generation. The levels of AteIF5A-3 expression in the *AteIF5A-3* over-expression plants were categorized as: high-level expression, medium-level expression, low-level expression, and no expression (presumably due to co-suppression). Two lines were chosen for each of the levels of expression, and 12 plants from each line were transplanted. The actual T_2 lines selected were: 3-1A, 3-2D, 3-4D, 3-8D, 3-9H, 3-11C, 3-15A, and 3-16C, and they were all carried

through to T_3. For T_3 nomenclature, a number was inserted following the letter denoting the T_2 line.

2.2.7.2 Photographic record of plants over-expressing *AteIF5A-3*

Morphological phenotypes of the *AteIF5A-3* over-expression lines and corresponding WT and BIN controls were recorded photographically during segregation. Photographs for the T_1 *AteIF5A-3* over-expressing plants were taken at 10 days, 3-weeks, 4-weeks, and 5-weeks of age. Photographs for the T_2 *AteIF5A-3* over-expressing plants were taken at 10 days, 3-weeks, 4-weeks, 5-weeks and 6-weeks of age. Photographs for the T_3 *AteIF5A-3* over-expressing plants were taken 10 days, 3-weeks, 4-weeks, 5-weeks, 6-weeks, 7-weeks and 8-weeks of age. Plants were observed daily for phenotype and watering needs.

2.2.7.3 Seed measurements

T_3 seeds collected from T_2 plants over-expressing *AteIF5A-3* were quantified, and seed size (length and width) was measured. Total seed yield by weight was measured using a Sartorius analytical digitized balance, and seed volume was determined using a glass 1mL syringe that was graduated every 10μL. To determine seed size, the seeds were placed on a slide containing a micrometer and viewed on an Olympus BX51 Microscope. Photographs of the seeds on the micrometer were taken with a Spot Insight Color Camera (Diagnostic Instruments Inc.) attached to a Compaq Evo D500 (Compaq Company Corporation; Intel® Pentium 4 CPU 1.7GHz, 262 MG RAM, running Windows 2000). Using Image-Pro Express Version 4.0 for Windows™, measurements of 10 seeds for each sister line were made using the micrometer in the image for size calibration. The measurements were imported into Microsoft Excel, and measurements of seed length and width were determined. Seed volume was calculated using the equation for volume of an ellipsoid ($4/3\pi a^2 b$), where a is the minor axis length and b is the major axis length (Kiyosue *et al.*, 1999).

2.3 Results

2.3.1 eIF5A is a highly conserved protein across Kingdoms

Sequences of eIF5A were obtained from GenBank for eukaryotic Kingdoms and the Archaea Kingdom. The sequences were aligned using COFFEE-T, and the similarities of aligned amino acids indicated by colour coding (Figure 2-4). Identical amino acids are indicated in red, residues that are conserved are indicated in orange, and semi-conserved amino acid substitutions are indicated in yellow. A high degree of sequence identity and similarity occurs in the N-terminus portion of the protein, especially in the vicinity of the lysine residue that undergoes modification to hypusine. This lysine residue is indicated by an asterisk in Figure 2-4. Even in regions of non-identity, the amino acid changes are often conserved in the N-terminus. The N-terminus and the C-terminus of eIF5A are attached by a flexible hinge region (Kim *et al.*, 1998), where a conserved proline residue is present and is indicated by the number sign (#) in Figure 2-4. The C-terminus lacks conservation across the Kingdoms, though is more similar within the eukaryotic species than between the eukaryotes and Archaea species. The C-terminus is thought to bind mRNA, and it is likely that the specificity of the binding is dependent on the variations in the eIF5A protein sequences, especially in the central portion of the C-terminus (Figure 2-4).

The sequences aligned in Figure 2-4 were subjected to BLAST 2 Sequences at http://www.ncbi.nlm.nih.gov/blast/bl2seq/wblast2.cgi using the blastp program, BLOSUM62 matrix, with the default settings. A table was created to summarize the identities and similarities between respective sequences retrieved using these defaults (Table 2-1). It was determined that eIF5A is a highly conserved protein, and that the sequences are at least 53% similar, even across these very diverse Kingdoms. The lowest degree of identity between species was 31%, and this occurred in the comparison between *Methanococcus jannaschii* (Mj) and *Arabidopsis thaliana* (At) eIF5As. However, these proteins were still 54% similar to each other (Table 2-1). Interestingly, some of the identities for eIF5A isoforms within a species calculated by BLAST 2 Sequences were less than the identities calculated between species (Table 2-1). For example, the sequences for *Tetraodon nigroviridis* (Tn; spotted

Figure 2-4: Alignment of eIF5A proteins for six species

Protein alignment of eIF5A isoforms for *Homo sapiens* (Hs; human), *Saccharomyces cerevisiae* (Sc; yeast), *Tetraodon nigroviridis* (Tn; spotted green pufferfish), *Arabidopsis thaliana* (At), *Lycopersicon esculentum* (Le; tomato) and *Methanococcus jannaschii* (Mj) are illustrated. The conserved lysine residue that is converted to hypusine through post-translational modification is indicated by an asterisk (*). The conserved proline residue within the hinge region is indicated by the number sign (#). The identical amino acids in all the sequences are coloured red, the conserved amino acids in all the sequences are coloured orange and the semi-conserved amino acids in all the sequences are coloured yellow.

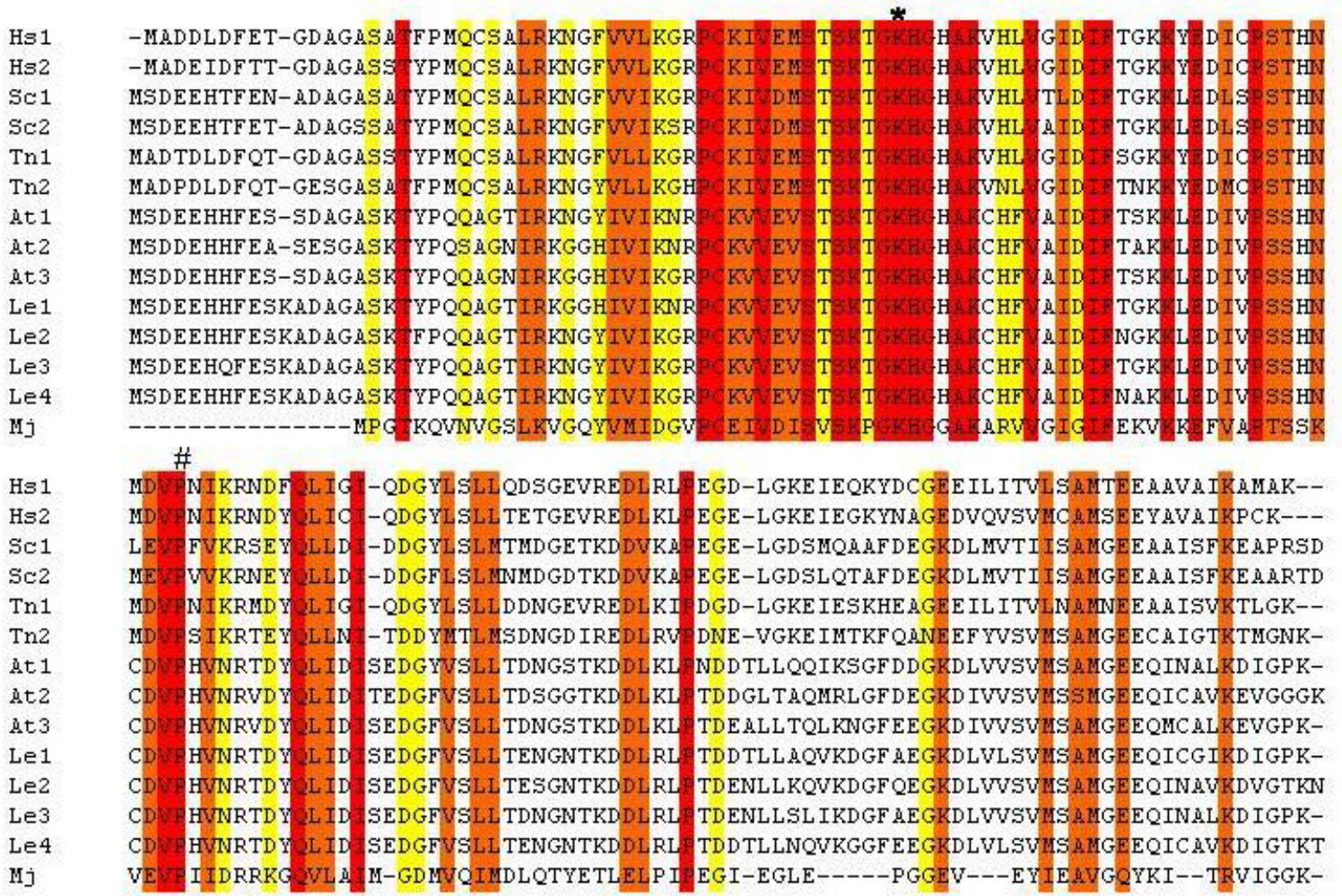
*
#
Hs1
Hs2
Sc1
Sc2
Tn1
Tn2
At1
At2
At3
Le1
Le2
Le3
Le4
Mj

Table 2-1: Identities and similarities between isoforms of eIF5A for six species

*I = identity; S= similarity

Hs= *Homo sapiens* (Human); Sc=*Saccharomyces cerevisiae* (yeast); Tn=*Tetraodon nigroviridis* (spotted green puffer fish); At=*Arabidopsis thaliana*; Le=*Lycopersicon esculentum* (tomato); Mj=*Methanococcus jannaschii*

I/S*	Hs2													
Hs1	-	Hs2												
Hs2	84/94	-	Sc1											
Sc1	65/85	64/82	-	Sc2										
Sc2	64/84	64/82	90/95	-	Tn1									
Tn1	83/93	80/91	62/84	61/84	-	Tn2								
Tn2	69/85	68/85	56/79	58/79	70/87	-	At1							
At1	57/77	58/74	60/80	59/79	54/77	50/74	-	At2						
At2	53/73	54/71	57/75	57/76	50/73	47/70	82/92	-	At3					
At3	54/76	58/73	59/78	59/77	53/76	47/72	86/94	86/94	-	Le1				
Le1	55/74	58/73	58/76	59/77	50/72	47/72	88/94	82/92	84/93	-	Le2			
Le2	57/78	60/76	60/78	60/78	52/77	50/73	86/94	80/90	83/93	89/93	-	Le3		
Le3	55/76	61/75	61/79	61/79	53/75	50/72	89/92	78/89	85/93	91/95	92/95	-	Le4	
Le4	55/76	59/75	58/79	58/78	52/74	50/75	88/94	80/91	84/94	93/94	93/96	90/93	-	Mj1
Mj1	34/54	34/54	35/56	35/57	32/53	36/55	31/54	31/54	34/55	38/60	33/53	35/54	34/54	-

green pufferfish) and human (Hs) were only 70% identical to each other and 84% identical to each other, respectively (Table 2-1). Similarly, *Arabidopsis thaliana* (At) isoforms were also 82-86% identical to each other. Tomato (*Lycopersicon esculentum*; Le) exhibited the highest levels of identity, 89-93%, between its isoforms (Table 2-1).

2.3.2 *Arabidopsis thaliana* has three isoforms of *eIF5A*

The entire genome of *Arabidopsis thaliana* is sequenced and available on public domain databases. Thus through BLAST searches of ESTs and genomic BAC sequences, it was determined that there are three sequences of *eIF5A* in *Arabidopsis* and that they are all located on the first chromosome (Figure 2-5A). They were numbered according to their order when mapped along the first chromosome, where the first one cloned from senescing tissue by Wang *et al.* (2001) coincidently happened to be located closest to the top of chromosome 1 at gene locus At1g13950 and was dubbed *AteIF5A-1*. The other two isoforms that followed in order along chromosome 1 are *AteIF5A-2* and *AteIF5A-3,* which are found at loci At1g26630 and At1g69410, respectively. The inferred amino acid sequences of AteIF5A isoforms are very similar to each other with up to 94% similarity (Figure 2-5B). There are, however, some differences in sequence in the C-termini of the isoforms, and in keeping with this synthetic peptides from these regions were used to make isoform-specific antibodies (Figure 2-5B).

The nucleotide sequence for *AteIF5A-1* is 79% identical to that for *AteIF5A-2* and 81% identical to that for *AteIF5A-3* (Figure 2-6). It has been demonstrated through large scale analysis of the *Arabidopsis thaliana* genome that the region containing *AteIF5A-2* was duplicated into the region containing *AteIF5A-3* (Blanc *et al.*, 2000). Thus it is likely that *AteIF5A-3* originated from *AteIF5A-2*. This duplication does, however, appear to be ancient as the lengths and number of introns differ between these two genes. Indeed, the introns for *AteIF5A-1*, *AteIF5A-2* and *AteIF5A-3* do not show any major similarities except where the splice sites are located.

Figure 2-5: Chromosomal mapping of *AteIF5A* genes and alignment of the amino acid sequences of their cognate proteins

A. Spatial distribution of *AteIF5A* genes mapped along chromosome 1 of *Arabidopsis thaliana* by the map viewer at http://www.arabidopsis.org/servlets/mapper. The top of the chromosome is oriented to the left. *AteIF5A-1* has the locus tag At1g13950, *AteIF5A-2* has the locus tag At1g26630, and *AteIF5A-3* has the locus tag At1g69410. **B.** The amino acid alignment of AteIF5A isoforms. Identical amino acids are highlighted in green. The peptide sequences used as antigens to make isoform-specific antibodies are delineated by a pink box.

A.

B.

```
1 MSDEEHHFESSDAGASKTYPQQAGTIRKNGYIVIKNRPCKVVEVSTSKTGKHGHAKCHFV
2 MSDDEHHFEASESGASKTYPQSAGNIRKGGHIVIKNRPCKVVEVSTSKTGKHGHAKCHFV
3 MSDDEHHFESSDAGASKTYPQQAGNIRKGGHIVIKGRPCKVVEVSTSKTGKHGHAKCHFV

1 AIDIFTSKKLEDIVPSSHNCDVPHVNRTDYQLIDISEDGYVSLLTDNGSTKDDLKLPNDD
2 AIDIFTAKKLEDIVPSSHNCDVPHVNRVDYQLIDITEDGFVSLLTDSGGTKDDLKLPTDD
3 AIDIFTSKKLEDIVPSSHNCDVPHVNRVDYQLIDISEDGFVSLLTDNGSTKDDLKLPTDE

1 TLLQQIKSGFDDGKDLVVSVMSAMGEEQINALKDIGPK
2 GLTAQMRLGFDEGKDIVVSVMSSMGEEQICAVKEVGGGK
3 ALLTQLKNGFEEGKDIVVSVMSAMGEEQMCALKEVGPK
```

Figure 2-6: Alignment of the coding regions of *AteIF5A* gene family members

The isoforms are indicated as 1, 2, and 3 for *AteIF5A-1*, *AteIF5A-2* and *AteIF5A-3,* respectively. Identical nucleotides in all three sequences are indicated in red.

```
1 atgtccgacgaggagcatcactttgagtccagtgacgccggagcgtccaaaacctaccctcaacaagctggaaccatcc
2 atgtctgacgacgagcaccactttgaggccagcgaatccggagcttccaagacctatcctcaatcagccggtaacatcc
3 atgtcagacgacgagcatcacttcgaatccagcgacgccggagcttctaagacttatcctcaacaagccggtaacattc

1 gtaagaatggttacatcgtcatcaaaaatcgtccctgcaaggttgttgaggttcaacctcgaagactggcaagcatgg
2 gtaaaggtggtcacatcgtcatcaaaaaccgtccctgcaaggttgttgaggttcgacttccaaaactggcaagcacgg
3 gtaaaggtggtcacatcgtcatcaagggacgtccctgcaaggtggttgaggtatcgacttcgaagactgggaagcatgg

1 tcatgctaaaatgtcatttgtagctattgatatcttcaccagcaagaaactcgaagatattgttccttcttcccacaat
2 tcacgccaaaatgtcactttgttgctattgatatcttcactgctaagaagcttgaagatattgttccatcttcccacaat
3 tcacgccaagtgtcactttgttgccattgatatcttcttacttctaagaagcttgaagatatcgttccttcttcccacaat

1 tgtgatgttcctcatgtcaaccgtactgattatcagctgattgacatttctgaagatggatatgtcagtttgttgactg
2 tgtgatgttccacatgtgaaccgtgttgattaccagttgattgatatcactgaggatggcttcgtgagccttctcactg
3 tgtgatgttccacatgtgaatcgtgttgattatcagttgattgatatctctgaagatggctttgttagtcttcttactg

1 ataacggtagtaccaaggatgaccttaagctccctaatgatgacactctgctccaacagatcaagagtgggtttgatga
2 acagtggtggcaccaaggatgatctcaagcttcccaccgatgatggtctcaccgcccagatgaggcttggattcgatga
3 ataatggtagcactaaggatgatctgaagctgccaacagatgaagctttactcacacagctcaagaatggatttgagga

1 tggaaaagatctagtggtgagtgtgatgtcagctatgggagaggaacagatcaatgctcttaaggacatcggtcccaag
2 gggaaaggatattgtggtgtctgtcatgtcttccatgggagaggagcagatctgtgccgtcaaggaagttggtggtggc
3 gggtaaggatattgttgtgtctgtcatgtctgcaatgggagaggagcagatgtgtgctctcaaggaagttggtcccaag

1 ---tga
2 aagtaa
3 ---taa
```

2.3.3 AteIF5A isoforms are differentially expressed spatially and temporally

2.3.3.1 Expression of AteIF5A isoforms in rosette leaves

The expression patterns of AteIF5A isoforms in rosette leaves were determined by Western blotting. Rosette leaves were collected from wild type *Arabidopsis thaliana* plants, and total protein was extracted and fractionated for Western blotting. The only isoform expressed during normal development and senescence of *Arabidopsis thaliana* rosette leaves detectable by Western blotting proved to be AteIF5A-1 (Figure 2-7). The expression of AteIF5A-1 is discernible starting at 3-weeks of age of the rosette leaves. The expression of AteIF5A-1 increases at 5-weeks of age when leaf senescence is engaged and is maintained at high levels of expression through 6 and 7-weeks of age.

2.3.3.2 Expression of AteIF5A isoforms in seedlings

Since leaf senescence has often been compared to cotyledon senescence, it was of interest to see if AteIF5A-1 is also expressed during cotyledon senescence after germination. Seedlings were grown on MS plates and collected two to eight days after germination. The proteins from these seedlings were fractionated for Western blotting and probed with AteIF5A isoform-specific antibodies. The Western analysis indicated that all three isoforms of AteIF5A are up-regulated during germination of *Arabidopsis thaliana* seedlings on MS plates, though each isoform displayed a unique expression pattern. Specifically AteIF5A-1 was up-regulated from two days after germination to five days after germination, which is coincident with post germinative cotyledon senescence (Figure 2-8). The primary leaves of the seedling emerge at or around five days after germination, and from this point onwards the seedling becomes dependent on photosynthesis as the lipid stores within the seedling are all but exhausted (Bentsink and Koornneef, 2002).

AteIF5A-2 is expressed throughout seedling development, but the levels of expression are faint and variable (Figure 2-8). Gatsukovich (2004) and this thesis describe AteIF5A-2 as the isoform that is responsive to wounding and pathogenesis. That AteIF5A-2 is not expressed at detectable levels during development and senescence of rosette leaves was determined by Western blotting (Figure 2-7). Moreover, constitutive down-regulation of

Figure 2-7: Western blot illustrating the expression of AteIF5A isoforms during development and senescence of *Arabidopsis thaliana* rosette leaves

A. Western blot of AteIF5A isoforms in total protein (10μg/lane) isolated from the rosette leaves of 2- through 7-week-old *Arabidopsis* plants. The blots were probed with antibodies raised against isoform-specific peptides. AteIF5A is detected at approximately 17kDa. **B.** SDS-PAGE stained with Coomassie Brilliant Blue corresponding to the AteIF5A-1 blot. The molecular masses of the marker are indicated on the left. Loading controls for AteIF5A-2 and AteIF5A-3 blots were similar.

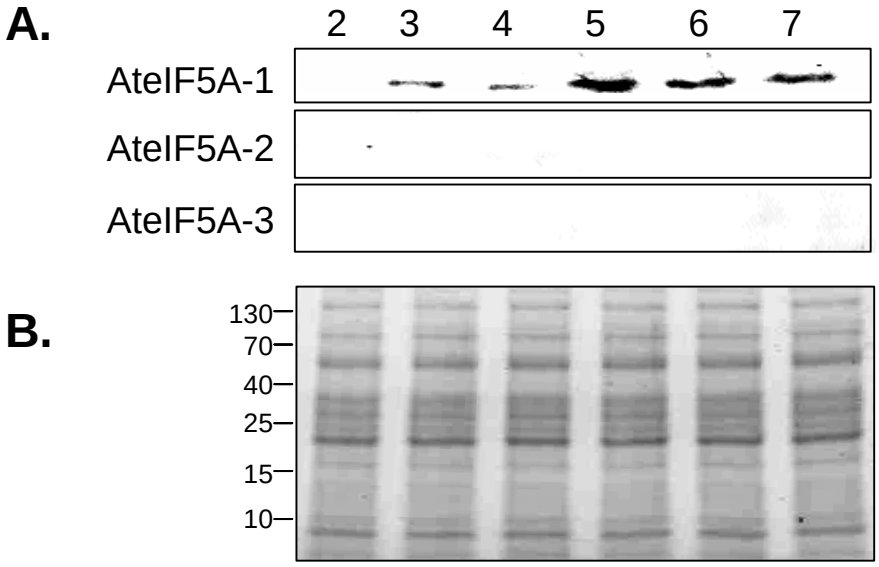
A.
2
3
4
5
6
7
AteIF5A-1
AteIF5A-2
AteIF5A-3
B.
130
70
40
25
15
10

Figure 2-8: Western blots of AteIF5A isoforms in developing seedlings

A. Photographs of the seedlings 2 through to 8 days after germination. **B.** Western blots of AteIF5A isoforms (indicated to the left) in total protein (10μg/lane) isolated from the developing seedlings. The lanes correspond to the images of the seedlings above them. The blots were probed with antibody raised against isoform specific peptides and visualized by a colorimetric reaction. AteIF5A is detected at approximately 17kDa. **C.** SDS-PAGE stained with Coomassie Brilliant Blue corresponding to the AteIF5A-1 blot. The molecular masses of the marker are indicated on the left. Loading controls for AteIF5A-2 and AteIF5A-3 blots were similar.

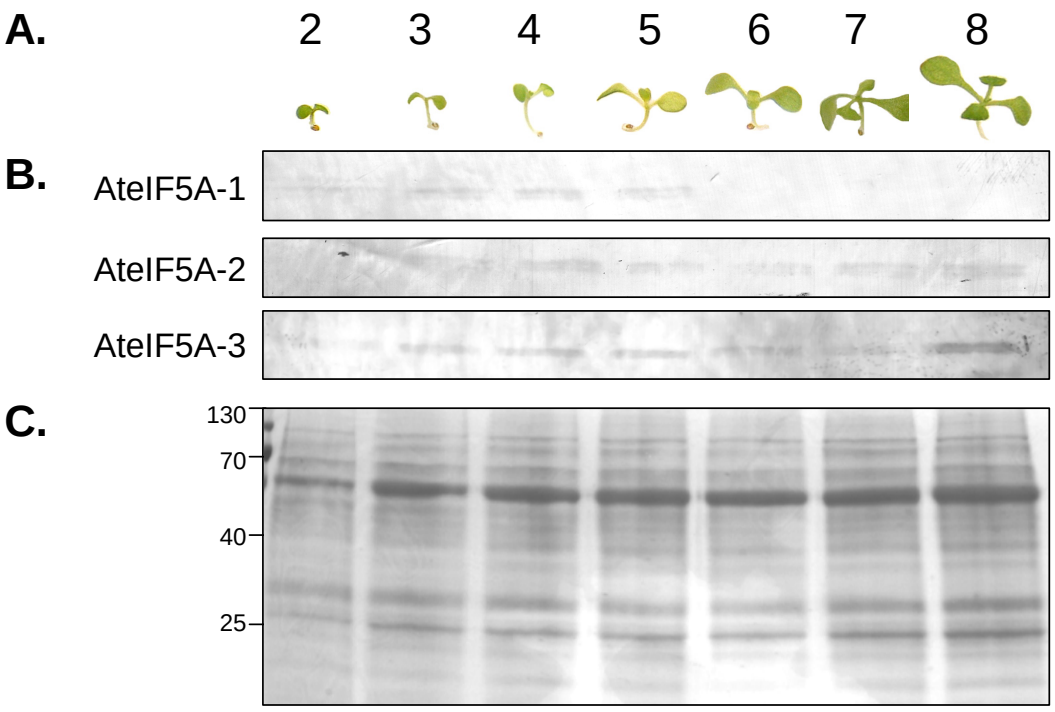
A.
2
3
4
5
6
7
8
B.
AteIF5A-1
AteIF5A-2
AteIF5A-3
C.
130
70
40
25

AteIF5A-2 does not have any obvious developmental effects (Gatsukovich, 2004). These observations are consistent with the view that *AteIF5A-2* is not involved in vegetative development *per se*. Thus, the up-regulation of AteIF5A-2 during germination and seedling establishment on MS plates (Figure 2-8) may be due to wounding of the roots during growth through an unnatural medium such as MS media or wounding incurred during collection.

The expression of AteIF5A-3 increases during seedling growth and establishment. The other dominant feature of germination and seedling establishment, aside from cotyledon senescence, is growth. That there are two isoforms of eIF5A in mammalian cells, one regulating cell death and the other cell division, is well documented and widely accepted (Caraglia *et al.*, 2003; Clement *et al.*, 2003; Thompson *et al.*, 2004). It has recently been proposed that in plants there are two or three, depending on the species, death isoforms of eIF5A and one growth isoform (Thompson *et al.*, 2004). That AteIF5A-1 and AteIF5A-2 are involved in regulation of cell death during senescence and wounding, respectively, has been demonstrated (Duguay, 2004; Gatsukovich, 2004; Tshin, 2004; Liu *et al.*, submitted 2006). The function of AteIF5A-3 has not been clearly established to date, although evidence presented later in this dissertation indicates that it is involved in root elongation. This contention is consistent with the finding that it is up-regulated during seedling development and establishment (Figure 2-8).

2.3.3.3 Expression of AteIF5A isoforms in flowers and fruit

To investigate the expression patterns of the AteIF5A isoforms during flower and fruit formation, a Western blot of total protein extracts from *Arabidopsis thaliana* flowers and fruit was performed using isoform-specific antibodies (Figure 2-9). The flowers were harvested at the bud stage, when they were completely closed, through to the point where the siliques began to ripen and turn yellow (Figure 2-9A). All three isoforms of AteIF5A were up-regulated during this stage of development, but each displayed unique expression patterns (Figure 2-9B).

AteIF5A-1 was detectable during flowering and fruit development by Western blotting (Figure 2-9B). Expression of this isoform increases during pollen senescence (first lane; Figure 2-9B), petal senescence (third lane; Figure 2-9B) and silique senescence (lanes 7

Figure 2-9: Western blots of AteIF5A isoforms in developing flowers and fruit

A. Photographs of the flower buds, flowers and silique development. **B.** Western blots of AteIF5A isoforms (indicated to the left) in total protein (10μg/lane) isolated from the developing flowers and fruit. The lanes correspond to the images of the flowers and fruit above them. The blots were probed with antibody raised against isoform specific peptides. AteIF5A is detected at approximately 17kDa. **C.** SDS-PAGE stained with Coomassie Brilliant Blue corresponding to the AteIF5A-1 blot. The final lane containing protein from the most mature silique has a different profile than the other lanes, but is similarly loaded as determined by densitometry. The molecular masses of the marker are indicated on the left. Loading controls for AteIF5A-1 and AteIF5A-2 blots were similar.

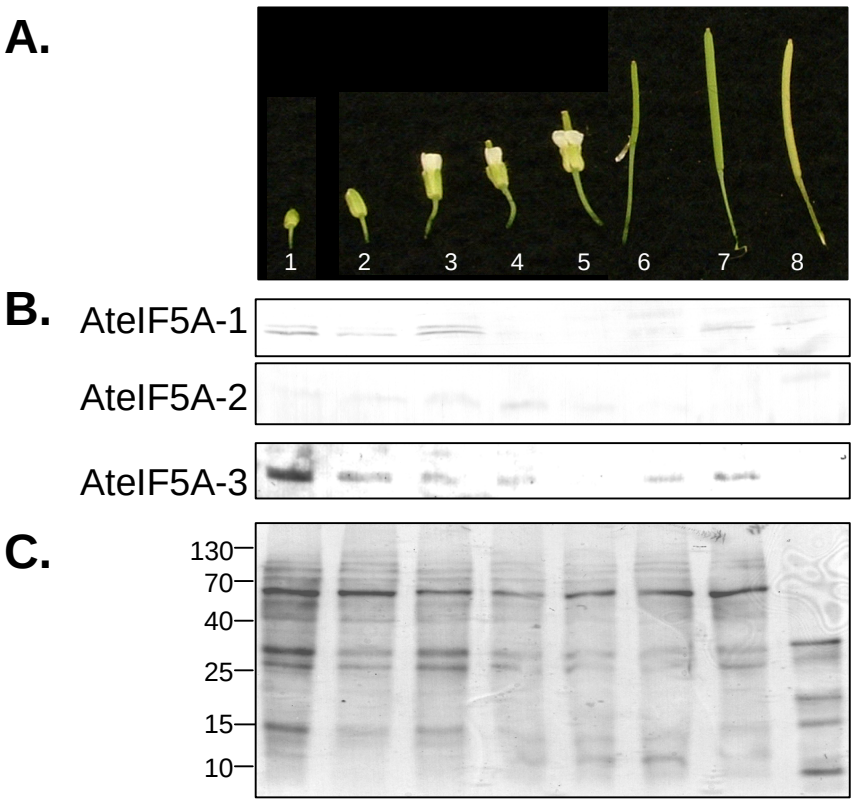
A.
1
2
3
4
5
6
7
8
B.
AteIF5A-1
AteIF5A-2
AteIF5A-3
C.
130
70
40
25
15
10

and 8; Figure 2-9B). The double band that is present in this Western and others throughout this dissertation may be due to phosphorylation. eIF5A is known to be phosphorylated in vivo in yeast (Kang *et al.*, 1993).

AteIF5A-2 was up-regulated very slightly just as the petals began to emerge (third lane, Figure 2-9B), which corresponds with fertilization (Bowman, 1994). Fertilization requires the growth of a pollen tube, which penetrates the maternal tissues causing a wounding effect (Lantin *et al.*, 1999). Thus, it is possible that the expression of AteIF5A-2 does occur developmentally and has a role in developmentally-prompted wounding such as fertilization and root growth through medium.

AteIF5A-3 protein is up-regulated during the bud stage, as the flower tissues are elongating and remains detectable until the silique begins to emerge from the top of the petals (lanes 1 to 4, Figure 2-9B). AteIF5A-3 is not detectable during the transition from flower to silique, but is once again up-regulated near the end of silique maturation (lanes 6 and 7, Figure 2-9B). This corresponds with the time during development when the embryos are elongating and the seeds are filling with storage reserves (Ruuska *et al.*, 2002). As the siliques senesce and the seeds are matured, AteIF5A-3 is not detectable (lane 8, Figure 2-9B).

2.3.4 AteIF5A-1 and AteIF5A-2 are regulators of programmed cell death in development and disease

To observe the effects of these putative regulators of programmed cell death in development and disease, they were constitutively over-expressed *in planta* using the cDNA of *AteIF5A-1* and the genomic version of the *AteIF5A-2* gene driven by the cauliflower mosaic virus double 35S promoter.

2.3.4.1 Plants over-expressing *AteIF5A-1* exhibit four main phenotypes

Plants over-expressing *AteIF5A-1* cDNA were produced by Zhongda Liu (J. E. Thompson's laboratory) using the sequence aligned in Figure 2-10. Over-expressing *AteIF5A-1* seeds (T_1 generation) were plated on MS plates containing the selective antibiotic,

Figure 2-10: Alignment of the *AteIF5A-1* coding sequence and amino acid sequence of its cognate protein

The coding sequence of *AteIF5A-1* is underlined. The primers used for amplification for production of the *AteIF5A-1* cDNA for over-expression in plants are indicated in red. The stop codon is indicated in blue, and the peptide used for the production of isoform-specific antibodies is indicated in green.

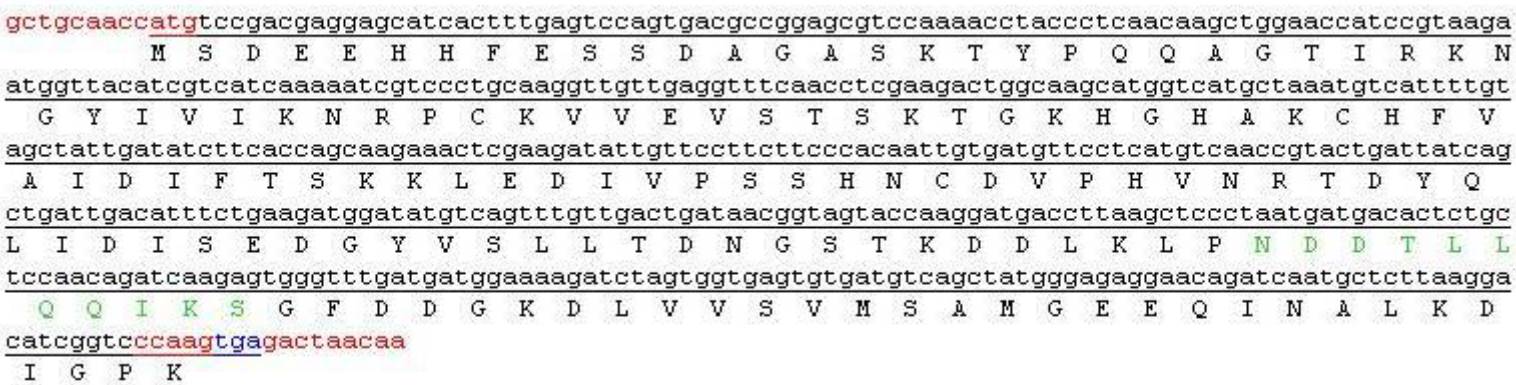
gctgcaaccatgtccgacgaggagcatcactttgagtccagtgacgccggagcgtccaaaacctaccctcaacaagctggaaccatccgtaaga
M S D E E H H F E S S D A G A S K T Y P Q Q A G T I R K N
atggttacatcgtcatcaaaaatcgtccctgcaaggttgttgaggtttcaacctcgaagactggcaagcatggtcatgctaaatgtcattttgt
G Y I V I K N R P C K V V E V S T S K T G K H G H A K C H F V
agctattgatatcttcaccagcaagaaactcgaagatattgttccttcttcccacaattgtgatgttcctcatgtcaaccgtactgattatcag
A I D I F T S K K L E D I V P S S H N C D V P H V N R T D Y Q
ctgattgacatttctgaagatggatatgtcagtttgttgactgataacggtagtaccaaggatgaccttaagctccctaatgatgacactctgc
L I D I S E D G Y V S L L T D N G S T K D D L K L P N D D T L L
tccaacagatcaagagtgggtttgatgatggaaaagatctagtggtgagtgtgatgtcagctatgggagaggaacagatcaatgctcttaagga
Q Q I K S G F D D G K D L V V S V M S A M G E E Q I N A L K D
catcggtcccaagtgagactaacaa
I G P K

kanamycin. The seeds that contained the *AteIF5A-1* insertion were capable of growing on the selection medium. The transformation efficiency of the T_1 seeds was 0.58%. There were 48 seedlings resistant to the kanamycin selection, and they were all transplanted onto soil at 10 days of age. The four main phenotypes that were observed included plants with small rosettes and thin spindly bolts (Figure 2-11), plants with long thin rosette leaves or petioles (Figure 2-12), plants that displayed early leaf senescence (Figure 2-13) and plants that had delayed growth (Figure 2-14). The lines illustrated in Figures 2-11 to 2-14 were carried through to the T_2 generation.

The T_1 plants over-expressing *AteIF5A-1* that had small rosettes and thin spindly bolts (1-4, 1-12, 1-39) all started out with very small rosette leaves (Figure 2-11A). Bolting times of these lines were essentially the same as for control plants (Figure 2-11B), though the bolts were spindly, shorter and fell over easily (Figure 2-11C). When these lines were taken to T_2, and eight sister lines were observed from each mother line, most of them lost the small and spindly phenotype. The sister lines of 1-4 developed an early leaf senescence phenotype. Most of the T_2 sister lines of 1-12 (6 out of 8) lost the spindly phenotype and were comparable to the WT and BIN controls. The sister lines of 1-39 developed a new phenotype where the leaves were more serrated than control leaves and yellowish in colour. In fact, the pattern of yellowing of the rosette leaves, cauline leaves and sepals in the T_2 sister lines of 1-39 was similar to the early leaf senescence phenotype described in this chapter.

The second phenotype of *AteIF5A-1* over-expressing plants, long thin rosette leaves or petioles coincident with a loss of leaf phyllotaxy is illustrated in Figure 2-12. *Arabidopsis thaliana* adult leaves are arranged in a spiral phyllotaxy. These lines exhibited opposite phyllotaxy, similar to that of the juvenile leaves. These T_1 lines also exhibited delayed bolting and leaf senescence (Figures 2-12A and B). In addition, Line 1-21 exhibited unusual flower morphology where the stigmatic papillae were elongated (Figure 2-12C). While line 1-48 did not exhibit the same flower morphology, several of the inflorescence stems were fused together (Figure 2-12D). Thus, it would appear that both the vegetative meristem and the reproductive meristem are affected by over-expression of *AteIF5A-1*. The T_2 seeds of line 1-21 were severely affected in that most of them did not germinate. This may reflect the

Figure 2-11: T_1 plants over-expressing *AteIF5A-1* cDNA: Small rosettes and thin bolts phenotype

A. Lines 1-4, 1-12 and 1-39 at 3-weeks of age compared to control wild type (WT) and empty binary vector (BIN) plants. The rosettes are highlighted by green circles. **B.** The rosettes of the same lines as in A at 5-weeks of age. **C.** Side view of plants at 5-weeks of age.

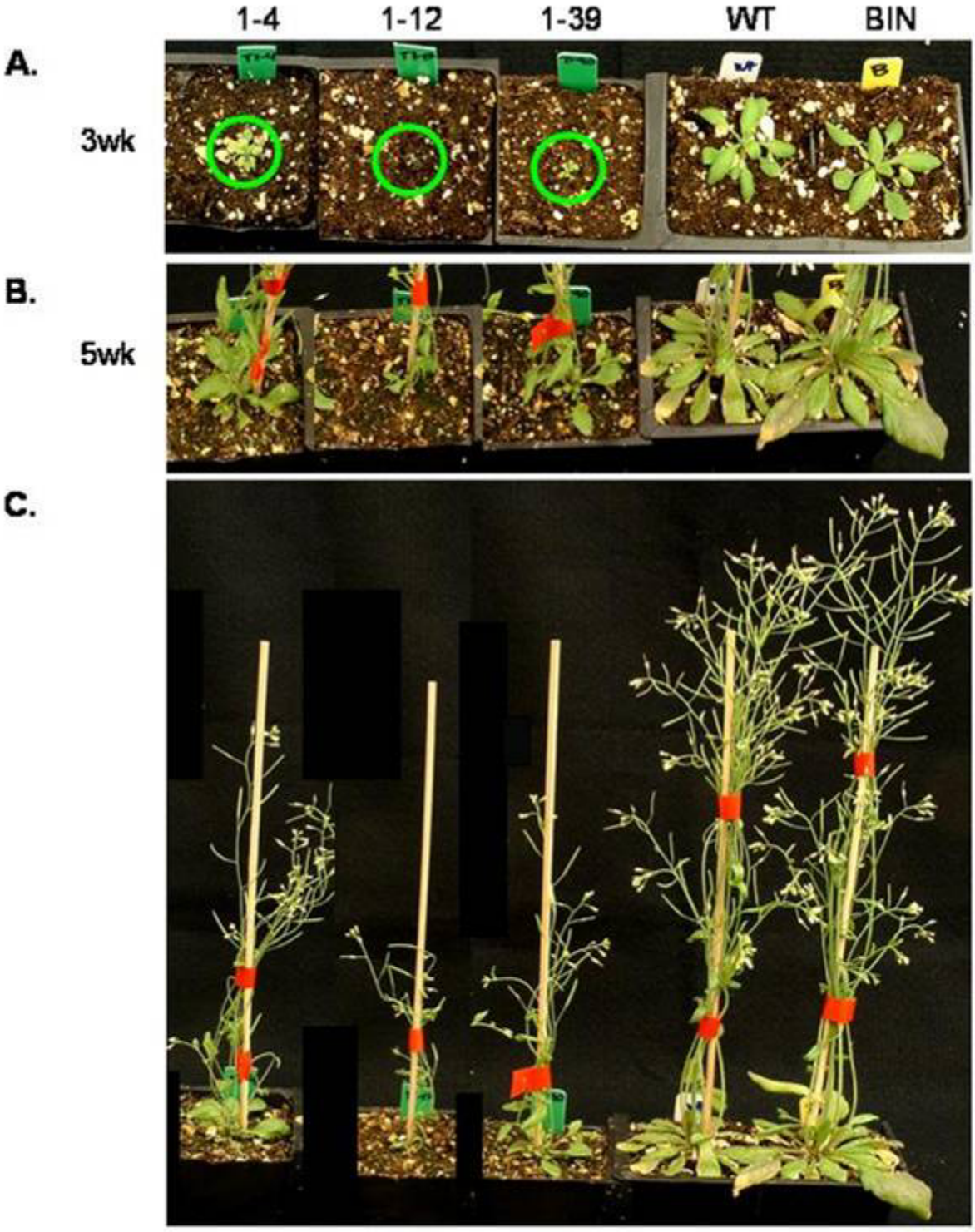
1-4
1-12
1-39
WT
BIN
A.
3wk
B.
5wk
C.

Figure 2-12: T_1 plants over-expressing *AteIF5A-1* cDNA: Long thin leaves and/or petioles phenotype

A. Lines 1-21 and 1-48 at 4-weeks of age compared to the control wild type (WT) and empty binary vector (BIN) plants. Elongated leaf blades (white arrows) and/or elongated petioles (yellow arrows) in comparison with control plants are evident in the rosette leaves. **B.** Lines 1-21 and 1-48 compared to the WT and BIN control plants at 6-weeks of age are less senescent. **C.** Line 1-21 exhibited elongated stigmatic papillae (red arrow) at the top of the style compared to WT control plants. **D.** Line 1-48 (4-weeks of age) had several inflorescences fused together (white bracket).

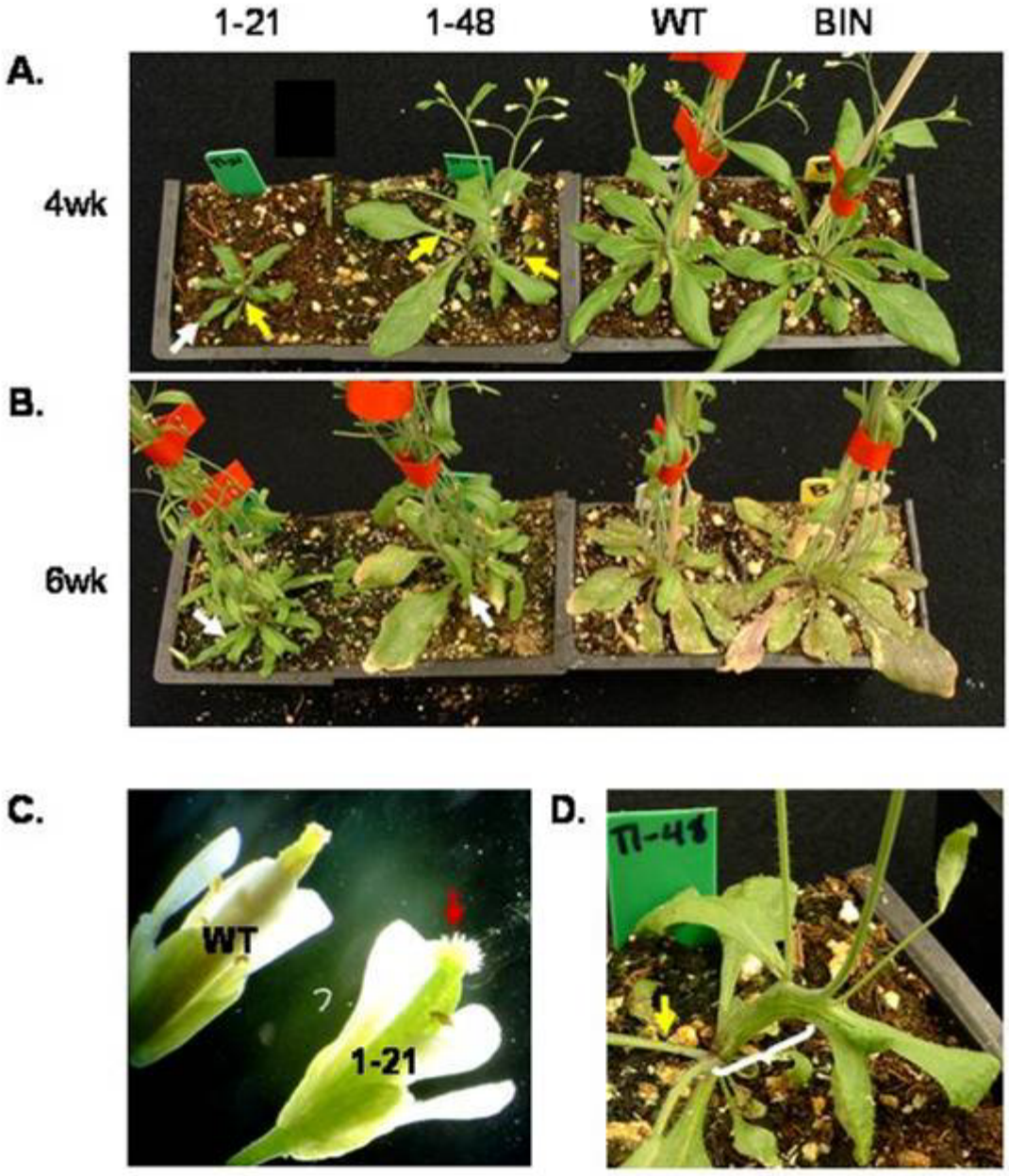
1-21
1-48
WT
BIN
A.
4wk
B.
6wk
C.
WT
1-21
D.
T1-48

Figure 2-13: T_1 plants over-expressing *AteIF5A-1* cDNA: Early leaf senescence phenotype

A. Line 1-37 at 3-weeks of age compared to control wild type (WT) and empty binary vector (BIN) plants. **B.** Line 1-37 at 4-weeks of age compared to WT and BIN plants. The leaves and sepals exhibiting early senescence are indicated by white arrows.

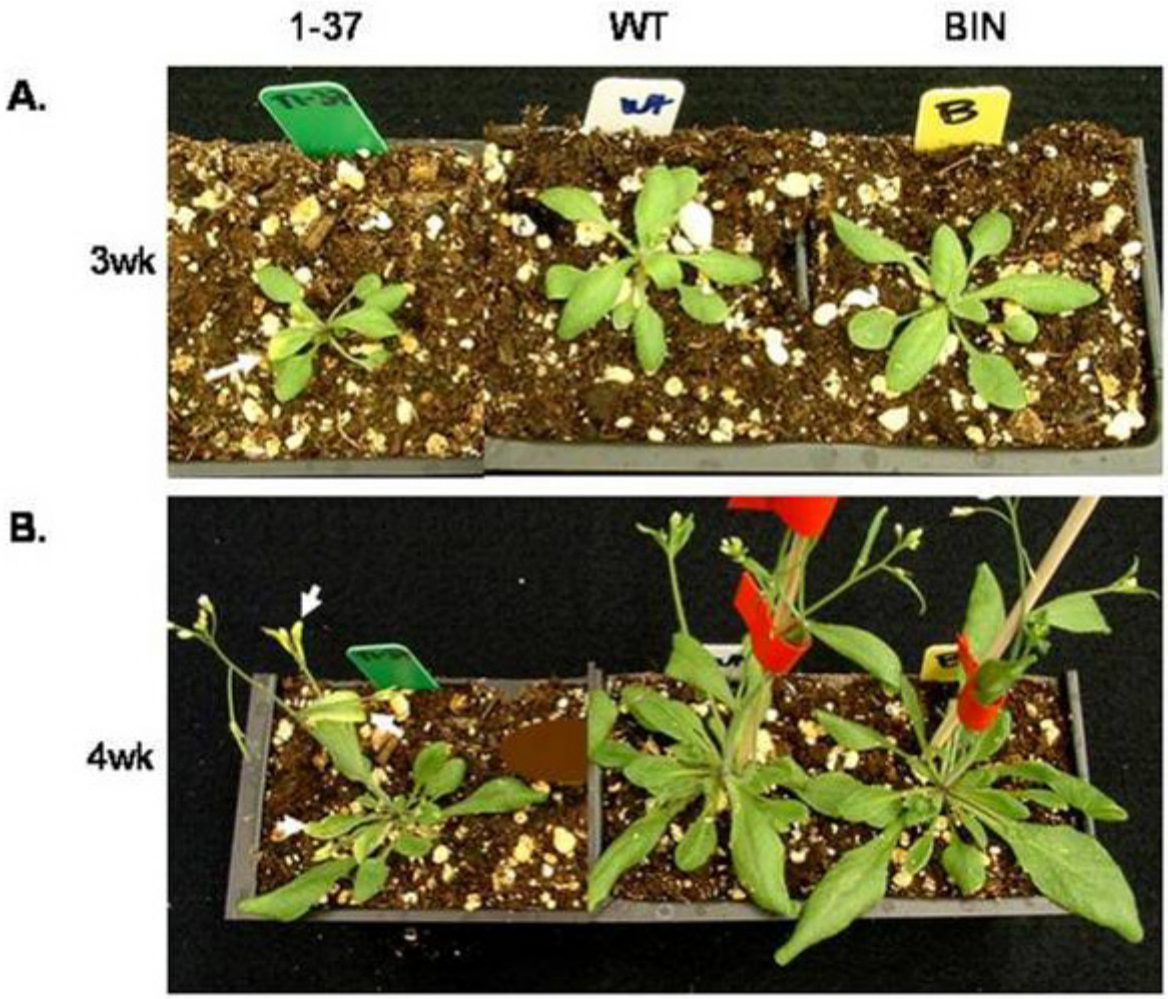
1-37
WT
BIN
A.
3wk
B.
4wk

Figure 2-14: T_1 plants over-expressing *AteIF5A-1* cDNA: Delayed growth phenotype

A. Lines 1-11 and 1-46 (within green circle) and control wild type (WT) and empty binary vector (BIN) plants at 3-weeks of age. **B.** Lines 1-11 and 1-46 rosettes compared to control WT and BIN rosettes at 6-weeks of age. **C.** Lines 1-11 and 1-46 compared to control WT and BIN plants at 6-weeks of age, showing the whole plant.

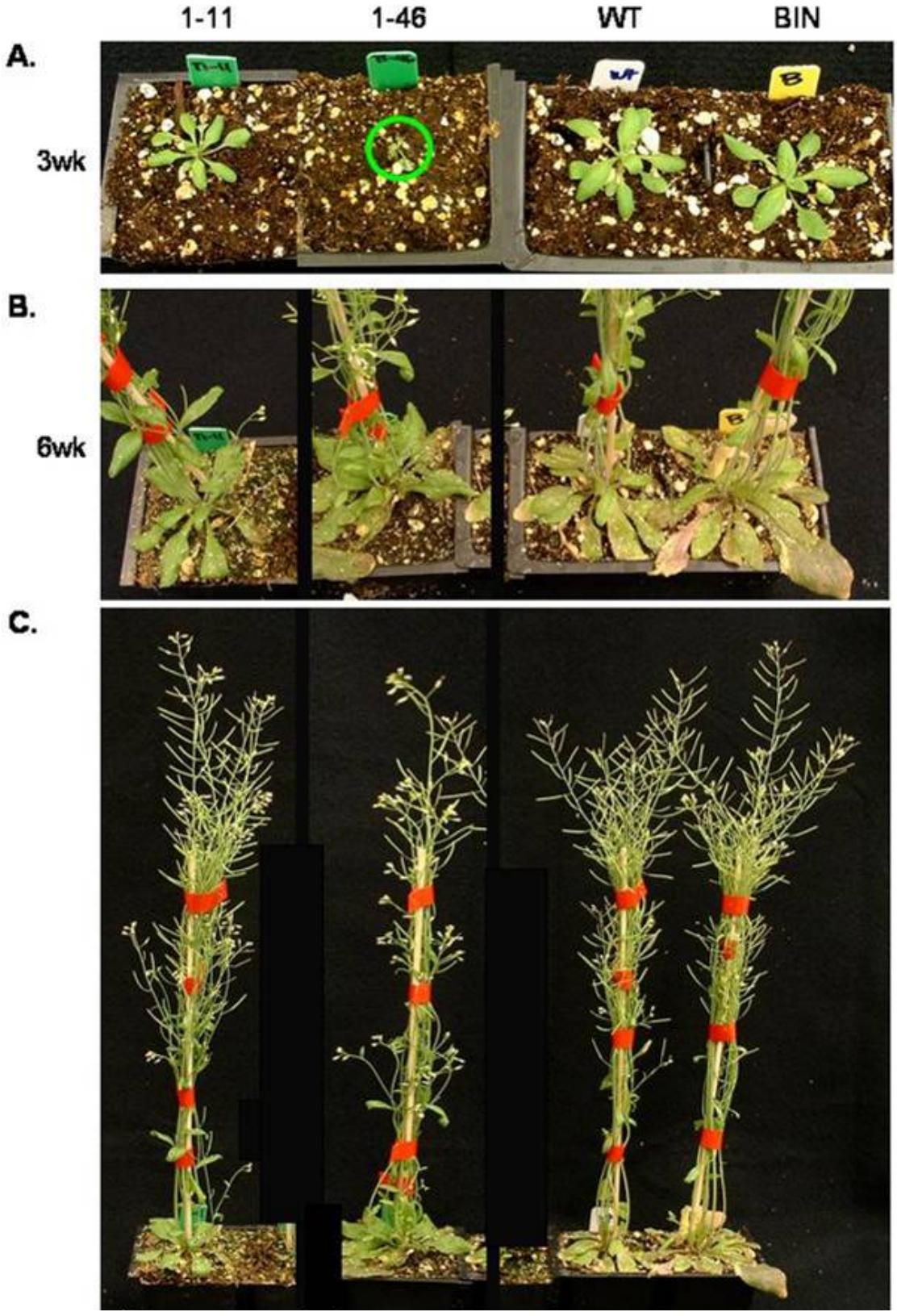
1-11
1-46
WT
BIN
A.
3wk
B.
6wk
C.

fact that the elongated stigmatic papillae interfered with fertilization. Line 1-48 acquired a leaf morphology even more similar to that of juvenile leaves in that the leaf blades were more rounded and the petioles elongated.

The third phenotype observed for plants over-expressing *AteIF5A-1* was characterized by early leaf senescence (Figure 2-13). It was demonstrated by Western blotting that the AteIF5A-1 protein is up-regulated during leaf (Figure 2-7) and cotyledon (Figure 2-8) senescence. Line 1-37, even at 3-weeks of age, exhibited signs of chlorosis in younger leaves of the rosette (Figure 2-13A). Senescence of rosette leaves in *Arabidopsis thaliana* is thought to be mainly due to aging signals (Nooden and Penney, 2001; Lim *et al.*, 2003). The over-expression of *AteIF5A-1* may be a sufficient signal to initiate leaf senescence, indicative of its regulatory function. The T_2 sister lines of 1-37 still displayed early senescence, but only in the cauline leaves and the sepals of the flower, not in the rosette leaves (Figure 2-13B). Interestingly, early cauline leaf senescence is apparent in mutations that affect the growth of the shoot meristem (Nooden and Penney, 2001). That growth and senescence are antagonistic is a common theme in the literature.

The final phenotype of *AteIF5A-1* over-expressing plants that was observed is delayed growth. Most of the T_1 plants, 18 out of 48, over-expressing *AteIF5A-1* exhibited this phenotype. There were varying degrees to which growth was delayed, and it was evaluated by size comparison of the rosettes and differences in bolting times. Interestingly, some of the lines exhibiting delayed growth in comparison with control plants early in development showed increased growth during the later stages of development and caught up to the control plants and in some instances surpassed them in size. For example, lines 1-11 and 1-46 started out small compared to the WT and BIN controls (Figure 2-14A). However, by the time they were 6-weeks-old they were similar to WT and BIN plants in size, rosette area and bolt height (Figure 2-14B). The main difference at this stage of development is the delay in senescence of the rosettes (Figure 2-14B) and flowers (Figure 2-14C). It would seem that the entire lifecycle of these plants is delayed. The T_2 sister lines of 1-11 and 1-46 lost this phenotype of delayed growth. The T_2 sister lines derived from line 1-46 looked

similar to wild type throughout development and the T_2 sister lines derived from 1-11 gained the long leaf and petiole phenotype.

2.3.4.2 AteIF5A-2 is up-regulated coincident with TUNEL labelling

Specific post-transcriptional up-regulation of AteIF5A-2 during wounding and pathogenesis has been demonstrated (Gatsukovich, 2004). To determine whether AteIF5A-2 is associated with programmed cell death, its expression following pathogen ingression was examined by confocal microscopy. Programmed cell death was detected by TUNEL staining, and AteIF5A-2 protein was detected with a TRITC–conjugated secondary antibody against the rabbit-produced AteIF5A-2 –specific antibody (Figure 2-15). The TUNEL technique has often been used to identify apoptotic mammalian cells by detecting *in situ* nuclei containing fragmented DNA (Gorczyca *et al.*, 1994), and it has been adapted for the detection of programmed cell death in plants (Wang *et al.*, 1996). Leaves of wild type *Arabidopsis thaliana* plants were infected by syringe-inoculation with virulent *Pst* DC3000. At 24 hours and 72 hours after inoculation, leaf sections were stained for AteIF5A-2 protein and TUNEL. Examination of these sections by confocal microscopy indicated that the up-regulation of AteIF5A-2 protein following infection and measurable cell death by TUNEL labelling are concurrent (Figure 2-15). There was a positive correlation between the length of time post-inoculation of the virulent strain of *Pst* DC3000 and the extent of TUNEL label. The earlier time points had fewer TUNEL-stained nuclei indicating less cell death (Figure 2-15). Interestingly, especially noticeable at the 24 hour time point is the overlapping labelling of AteIF5A-2 with the TUNEL label. It is apparent, therefore, that up-regulation of AteIF5A-2 following infection correlates with the onset of programmed cell death.

2.3.4.2.1 Analysis of plants over-expressing *AteIF5A-2*

Plants over-expressing *AteIF5A-2* were created by vacuum infiltration of *Agrobacterium* containing the construct pKYLX71: *AteIF5A-2* using the floral dip method (Clough and Bent, 1998). The nucleotide sequence that was used for over-expression is aligned with its cognate protein sequence in Figure 2-16. The T_1 seeds collected from the

Figure 2-15: AteIF5A-2 expression and TUNEL labelling in *Arabidopsis* leaf tissue 24 and 72 hours post-infection with virulent *Pst* DC3000

Confocal images at time points 24 hours post-inoculation and 72 hours post-inoculation with virulent *Pst* DC3000. The 24 hour time points do not have the chlorophyll autofluorescence (Auto) shown for the 24 hour time point as it interferes with the detection of AteIF5A-2: TRITC and TUNEL (FITC). At 72 hours, there is less chlorophyll autofluorescence (Auto) as the leaf tissue is dying and massive chlorosis has set in. There are more nuclei labelled with TUNEL in the 72 hour sample. The merged images are located to the far right. White size bars = 50μm.

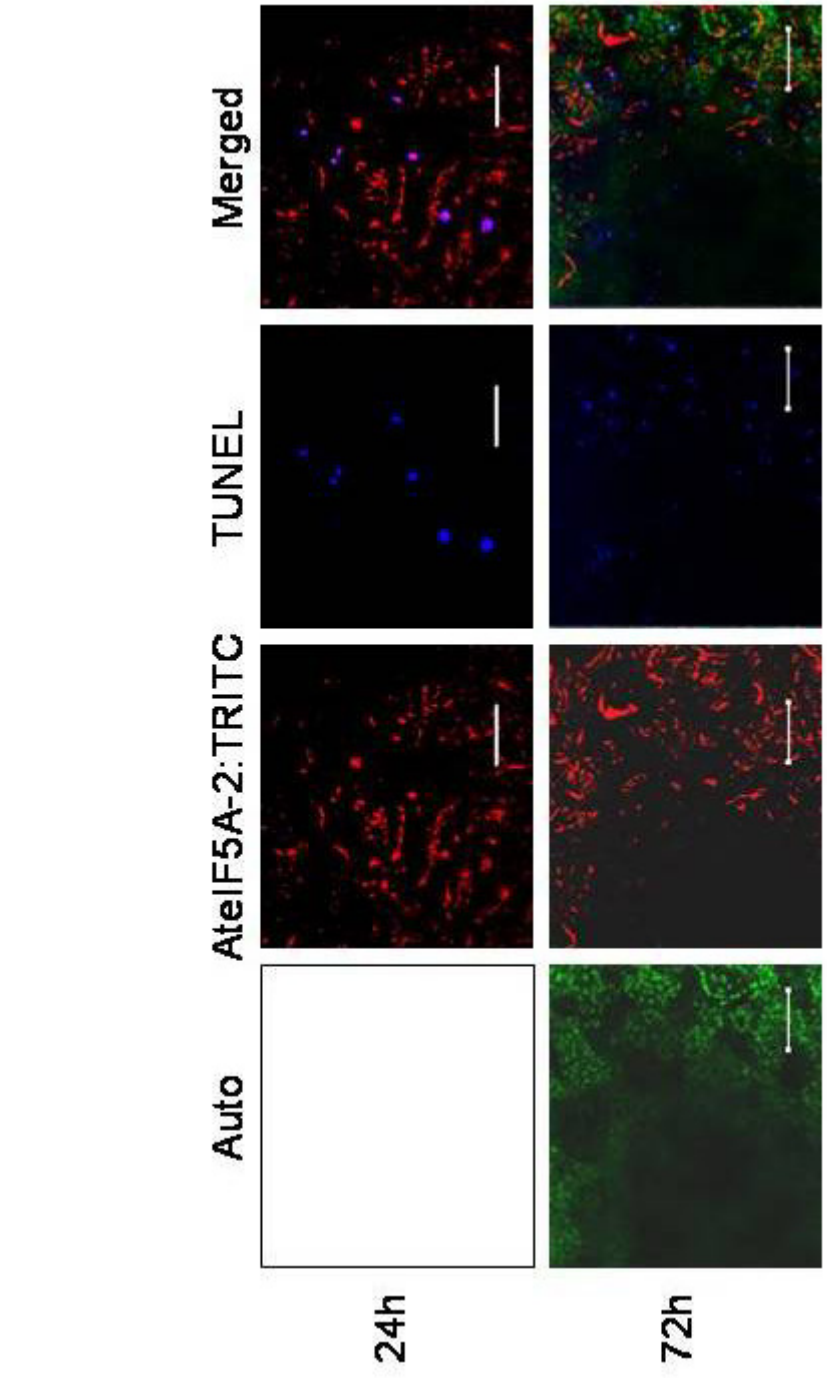
Auto
AteIF5A-2:TRITC
TUNEL
Merged
24h
72h

Figure 2-16: Alignment of the *AteIF5A-2* gene sequence with its cognate protein sequence

The entire gene sequence of *AteIF5A-2* is aligned with its cognate protein sequence. The primers that were used for amplification for the production of the *AteIF5A-2* over-expressing plants are indicated in red. The exons of the *AteIF5A-2* gene are underlined, and the 4 introns within are unformatted. The stop codon is indicated in blue, and the peptide used for the production of isoform-specific antibodies is indicated in green.

```
aggataataatacagtaaccctagaaaggtttcctccaccttcctcttcccctcctatataaaaaaaaatcgacatcgcttttgctcacttctct
ctcttaggttttttttcccttctcccaatctcatcttctccgaaaaccttttcttctctcaaatttctgtgaaaacatgtctgacgacgagcacc
                                                                                  M  S  D  D  E  H  H
actttgaggccagcgaatccggagcttccaagacctatcctcaatcagccggtaacatccgtaaaggtggtcacatcgtcatcaaaaaccgtcc
  F  E  A  S  E  S  G  A  S  K  T  Y  P  Q  S  A  G  N  I  R  K  G  G  H  I  V  I  K  N  R  P
ctgcaaggtctgatttctatttcatcatcaaacatcgttctcgatctcttttttcctgattctagatctcgtctctgtatagtagctccttgatt
 C  K
ttgttttatcctcggatttgacctggttctgtttagtttgaatttttcttatagatcgctacttagatgaatatgatgaatcttatcctgttta
ttttgatggtggtacctctctagattcgtggaattttgggaaatgaaaatgaaaaatggatagaaatcaagcaatatcagacgacgccttttgt
gattttgaatctaagtagtctattgattgatttgatttaaacgtttatggagaacatagatttgattttgatattttggttttgattaggttgt
                                                                                        V  V
tgaggtttcgacttccaaaactggcaagcacggtcacgccaaatgtcactttgttgctattgatatcttcactgctaagaagcttgaagatatt
 E  V  S  T  S  K  T  G  K  H  G  H  A  K  C  H  F  V  A  I  D  I  F  T  A  K  K  L  E  D  I
gttccatcttcccacaattgtgatgtaagttactacacaaactatgtagattcattttcacagtatttgatatgattgtgtgatctgactcaaa
V  P  S  S  H  N  C  D
tattgttccttttctctttttttctcaggttccacatgtgaaccgtgttgattaccagttgattgatatcactgaggatggcttcgtatgttttt
                        V  P  H  V  N  R  V  D  Y  Q  L  I  D  I  T  E  D  G  F
ctttatactcactttcctcatcactccagctttatttatctattcttgccataacttttgtacttgtttacattataggtgagccttctcactg
                                                                              V  S  L  L  T  D
acagtggtggcaccaaggatgatctcaagcttcccaccgatgatggtctcaccgcccaggttattttcttgtcttttcatactcgcacacaaat
  S  G  G  T  K  D  D  L  K  L  P  T  D  D  G  L  T  A  Q
gacttgactttgtattcatctctcgaattgtgatattgaaaacagttgttgtgttttgttaatgcagatgaggcttggattcgatgagggaaag
                                                                  M  R  L  G  F  D  E  G  K
gatattgtggtgtctgtcatgtcttccatgggagaggagcagatctgtgccgtcaaggaagttggtggtggcaagtaaacaagtatcattcgat
D  I  V  V  S  V  M  S  S  M  G  E  E  Q  I  C  A  V  K  E  V  G  G  G  K
atattattaccagtttgacaacggacgtcaatgttataagaaccaaaagatgtttttctttttcctaatttagacccttgtgtgtgtttcttg
ttgcaagacaaccatatctattggttttggattgttggaaaagtttgtgttgaaacattcaaagtttcttatgagatgttattcttaaaaccac
tttttgtttgttcactggatatgtttgttcatgaagcttgttttaagcaactctttacatga
```

vacuum-infiltrated plants (T_0) were spread on MS plates containing kanamycin for selection of transformants. The transformation efficiency for plants over-expressing *AteIF5A-2* was 0.56%. There were 14 transformants that were transplanted to soil alongside the control wild type (WT) and empty binary vector transformed seedlings (BIN). A common phenotype among these 14 T_1 generation plants was stunted growth (Figure 2-17A). Severely stunted plants were scored as being less than 50% the size of WT or BIN controls, moderately stunted lines were scored as being 50-75% the size of WT or BIN controls and plants that were classified as similar to WT or BIN controls were at least 75% the size of the controls. Lines 2-1, 2-4, 2-6, 2-8, 2-10, 2-11, 2-12, 2-13 and 2-14 were severely stunted (Figure 2-17B), and of these lines 2-6, 2-8, 2-10, 2-13, and 2-14 did not produce any seed. Lines 2-2 and 2-3 were moderately stunted, whereas lines 2-5, 2-7 and 2-9 grew similarly to the WT or BIN control plants (Figure 2-17). The stunted plants also exhibited yellow leaves, purple cotyledons, curled up leaves and changes in flower morphology. It is interesting to note that the seedlings did not look any different from each other or the control plants on the selection media plates. The stunted growth phenotype was only observable after a few weeks of growth in soil after transplanting. It is possible that during transplant the roots were damaged slightly, a consequence of transplanting that is unavoidable, and the plants were not able to recover. Damage as a result of transplanting would be a type of wounding. AteIF5A-2 is up-regulated in leaves 4 hours after wounding with a haemostat (Figure 2-18) and during pathogen ingress (Gatsukovich, 2004). If AteIF5A-2 is involved in regulation of cell death that results from wounding, the constitutive over-expression of *AteIF5A-2* could result in constitutive up-regulation of cell death and impair the plant's inability to recover from transplanting. The cell death as a result of a wound effect would counteract the plant's ability to grow. This phenotype was also observed in T_2 generation plants and hence heritable. The T_2 generation included 8 sister lines from mother lines 2-1, 2-2, 2-3, 2-4, 2-5, 2-7, 2-8 and 2-11. The other T_1 plants died and did not produce seed. Also T_2 seed from 2-12 only amounted to less than 10µl, and only one T_2 plant germinated and grew on the selection media.

There were 65 lines in the T_2 generation, and lines 2-3H and 2-4G died after a few

Figure 2-17: T_1 plants over-expressing *AteIF5A-2*

A. Lines 2-1 through to 2-14 of the T_1 plants, 4-weeks of age, over-expressing *AteIF5A-2* compared to corresponding control wild type (WT) and empty binary vector (BIN) transformed plants. **B.** Detail of lines that were severely stunted at 4-weeks of age. Rosettes are located within the pink circles. Only line 2-12 of these severely stunted plants bolted and produced a few seeds.

A.

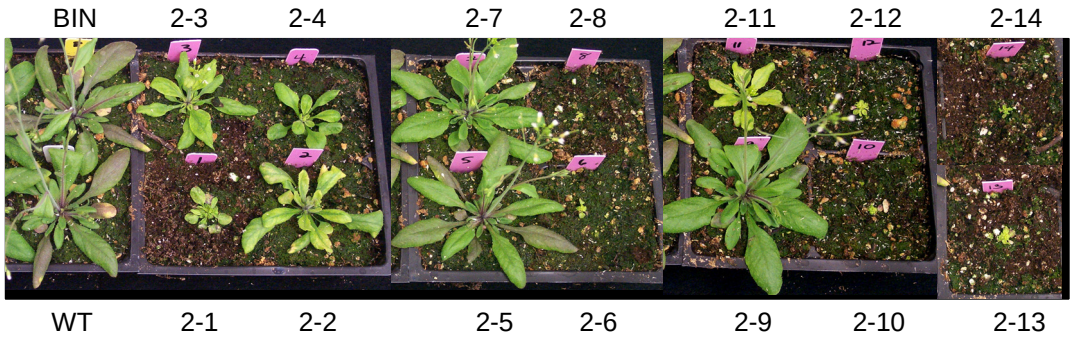

B.

Figure 2-18: Western blot analysis of AteIF5A-2 in 3.5-week-old haemostat-wounded rosette leaves

A. Western blot probed with isoform-specific antibodies against AteIF5A-2. Lanes correspond to hours after wounding. AteIF5A-2 is detected at approximately 17kDa. **B.** Corresponding SDS-PAGE. Each lane contained 10μg of protein, and the gel was stained with Coomassie Brilliant Blue. The approximate molecular weights are indicated on the left.

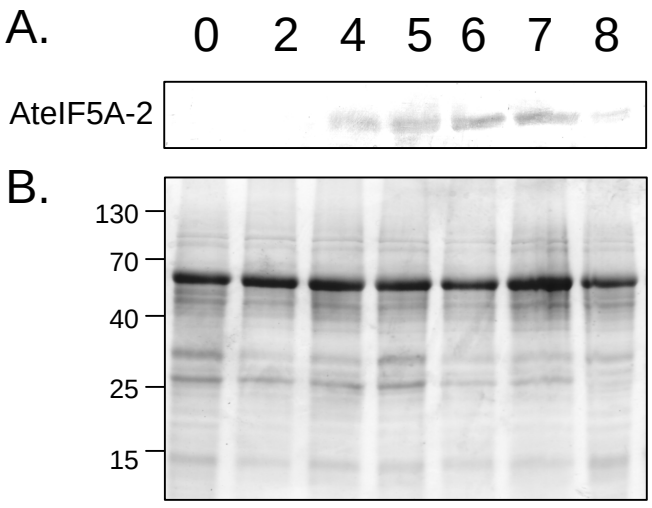
A.
0 2 4 5 6 7 8
AteIF5A-2
B.
130
70
40
25
15

weeks in soil. Most of the T_2 generation plants displayed some phenotype. Indeed, only 6 out of 63 were not distinguishable from the wild type (WT) or empty binary vector control (BIN) plants. The first phenotype that was noticeable was that some of the seed for several lines did not germinate (Figure 2-19A). Lines exhibiting this phenotype included 2-1, 2-2, 2-3, 2-4 and 2-12. It was not determined why these seeds were not able to germinate, but it is possible that the over-expression of *AteIF5A-2* either caused ovule abortion or inhibited embryo growth. High levels of AteIF5A-2 expression would be similar to a constitutive wounding effect. *Arabidopsis* plants that are under high levels of stress experience high levels of ovule abortion, creating empty seeds that are not able to germinate (Sun *et al.*, 2004). Several phenotypes were observed in the rosettes of T_2 generation plants over-expressing *AteIF5A-2* including curved up leaves (Figure 2-19B), severe stunting (Figure 2-19C) and chlorosis and spontaneous lesion formation (Figure 2-19D). These are all phenotypes that reflect an effect on the vegetative meristem and differentiated mesophyll cells. The curved up leaves and the severe stunting of the rosette are a direct result of decreased cell growth (Charrier *et al.*, 2002). Chlorosis and spontaneous lesion formation, which are also observed during pathogen ingress (Katagiri *et al.*, 2002), reflect death of mesophyll cells (Greenberg, 1997).

Phenotypes of the inflorescence of T_2 *AteIF5A-2* over-expressing plants include an increase in basal branches (Figure 2-19E), early bolting (Figure 2-19F) and small stunted siliques (Figure 2-19G). One way in which plants respond to pathogen ingress as well as other stresses is to accelerate the transition to reproduction (Martinex-Zapater *et al.*, 1994; Tienderen *et al.*, 1996; Bradley *et al.*, 1997; Pigliucci and Schmitt, 1999). Thus early bolting as well as changes in branch architecture, for example, an increase in basal branches, likely reflect stress induced by over-expression of *AteIF5A-2*. The small stunted silique phenotype may be a direct consequence of increased cell death within the reproductive tissues brought on by the over-expression of *AteIF5A-2*. To investigate whether precocious cell death occurred in transgenic plants over-expressing *AteIF5A-2*, leaves of 3-week-old plants were excised and immediately fixed in paraformaldehyde. Great care was taken not to damage the tissue in any way. After fixation, the leaves were TUNEL-labelled and also labelled for

Figure 2-19: Phenotypes of T_2 plants over-expressing *AteIF5A-2*

A. Example of compromised germination exhibited in T_2 generation plants over-expressing *AteIF5A-2* derived from line 2-1 at 10 days of age. The arrows indicate seeds (brownish spots) that did not germinate. **B.** Line 2-4C at 3-weeks of age illustrating the curled leaf phenotype. **C.** Line 2-3D at 5-weeks of age illustrating the severely stunted phenotype. **D.** Line 2-2B at 3-weeks of age illustrating necrotic lesions (indicated by white arrows) and premature chlorosis. **E.** Line 2-7C at 5-weeks of age illustrating enhanced basal inflorescence branches compared to wild type (WT) and empty binary vector (BIN) plants. **F.** Line 2-5C shown here at 3-weeks of age, bolted almost an entire week earlier than the WT and BIN control plants. **G.** Line 2-4H at 7-weeks of age illustrating short, stunted siliques that contained few seeds compared to WT and BIN control siliques. Size bars = 1cm.

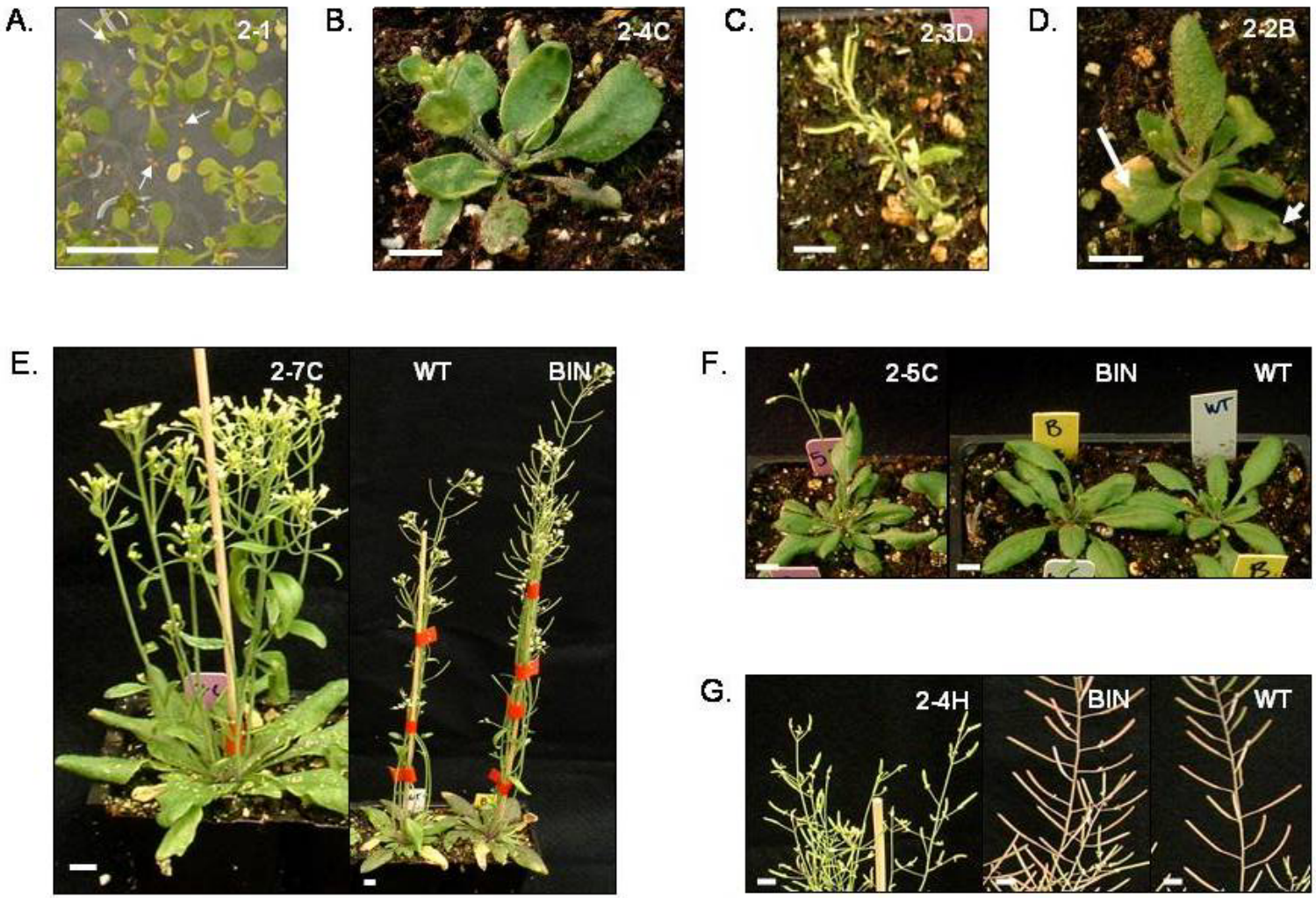
A.
2-1
B.
2-4C
C.
2-3D
D.
2-2B
E.
2-7C
WT
BIN
F.
2-5C
BIN
WT
G.
2-4H
BIN
WT

AteIF5A-2 expression using secondary antibody conjugated to TRITC. TUNEL labelling reflecting programmed cell death was evident in the leaves of line 2-3F (Figure 2-20). The over-expression of *AteIF5A-2* resulted in strong labelling of AteIF5A-2 *in situ*. TUNEL labelling of nuclei within line 2-3F occurred in groups of cells, indicating that neighbouring cells adjacent to ones undergoing programmed cell death are also affected possibly due to intercellular communication.

There was a correlation between the level of AteIF5A-2 expression in the *AteIF5A-2* over-expressing plant and their physical stature (Figure 2-21). Specifically, higher levels of over-expression, as demonstrated by Western blotting, resulted in more severely stunted growth. There was also an observed influence of AteIF5A-2 over-expression on seed yield. Plants with high levels of AteIF5A-2 expression had severely compromised fecundity (Figure 2-21). Gatsukovich (2004) demonstrated that the expression of AteIF5A-2 is post-transcriptionally regulated. That is, AteIF5A-2 mRNA proved to be constitutively expressed in wild-type plants, and protein was not expressed until the plants were either wounded or infected with a pathogen. Of interest is the finding in the present study that this post-transcriptional regulation of AteIF5A-2 translation is overcome in *AteIF5A-2* over-expressing transgenic plants. Indeed, AteIF5A-2 protein was clearly detectable in the transgenic plants by Western blotting in the absence of wounding or pathogen inoculation (Figure 2-21 and Figure 2-22A). Moreover, the level of AteIF5A-2 expression in lines 2-3F and 2-9A when infected with virulent *Pst* DC3000 for 72 hours was comparable to WT AteIF5A-2 expression, being 90 and 120%, respectively, of the WT level as measured by densitometry (Figure 2-22B).

2.3.5 AteIF5A-3 is a regulator of cell growth

2.3.5.1 Over-expression of *AteIF5A-3* in transgenic plants

To investigate the role of AteIF5A-3, transgenic plants over-expressing *AteIF5A-3* were generated and analyzed. The sequence of the *AteIF5A-3* gene with the sequence of its cognate protein is illustrated in Figure 2-23. T_1 generation seeds were grown on selection media plates, and 16 transformants grew. The transformation efficiency was 0.56%.

Figure 2-20: AteIF5A-2 expression and TUNEL labelling in leaves of *Arabidopsis* plants over-expressing *AteIF5A-2*

Confocal images of TUNEL labelled nuclei and AteIF5A-2: TRITC in a leaf of a 3-week-old plant over-expressing *AteIF5A-2* (line 2-3F). Size bar= 50μm.

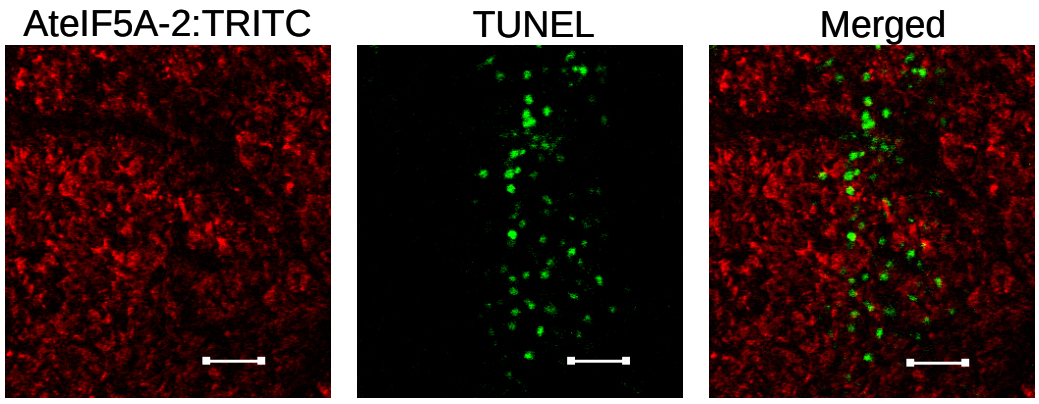
AteIF5A-2:TRITC
TUNEL
Merged

Figure 2-21: T_2 generation plants over-expressing *AteIF5A-2* are extremely stunted

A. Photographs of plants over-expressing *AteIF5A-2*. Plants are ordered from the most stunted to the least stunted, with the wild type (WT) and binary vector (BIN) control to the far right. **B.** Western blot of 5μg total protein isolated from cauline leaves corresponding to the lines above. The blot was probed with AteIF5A-2-specific antibody. AteIF5A-2 is detected at approximately 17kDa. **C.** Seed yield obtained from each line expressed as weight in mg. Standard errors of the means are shown for WT and BIN plants; n=10.

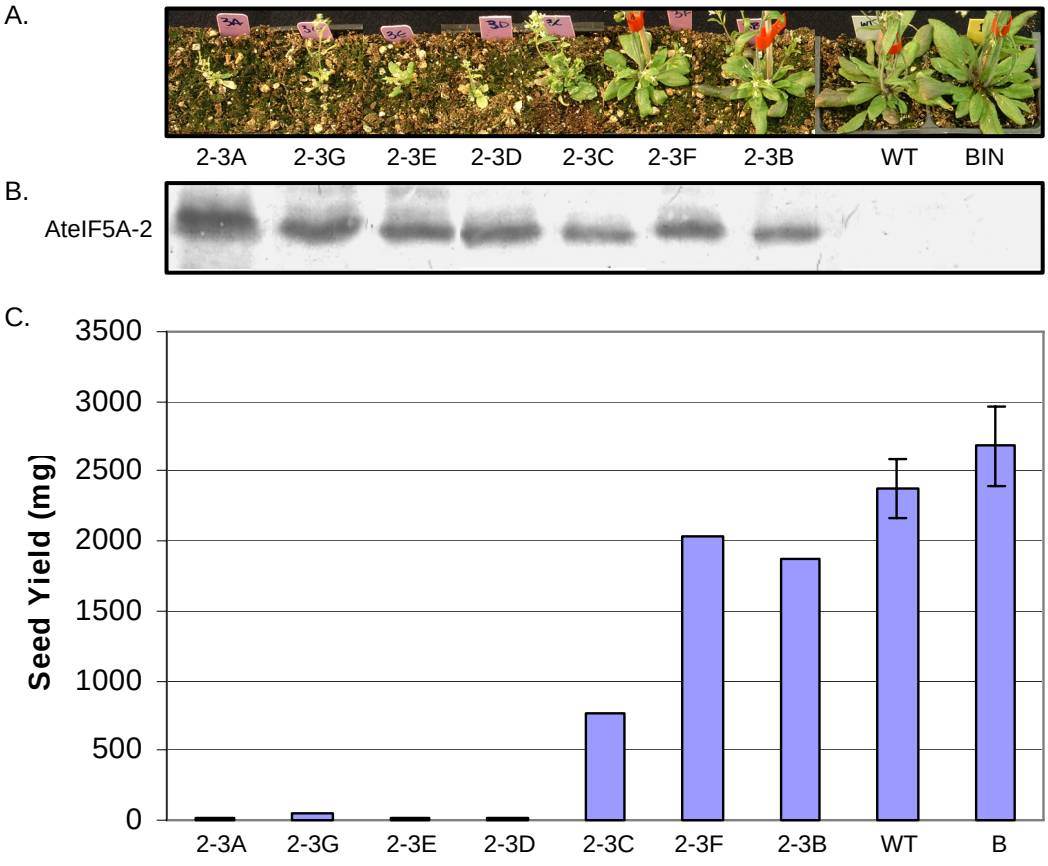
A.
2-3A
2-3G
2-3E
2-3D
2-3C
2-3F
2-3B
WT
BIN
B.
AteIF5A-2
C.
Seed Yield (mg)
3500
3000
2500
2000
1500
1000
500
0
2-3A
2-3G
2-3E
2-3D
2-3C
2-3F
2-3B
WT
B

Figure 2-22: Expression levels of AteIF5A-2 in virulent *Pst* DC3000-infected and uninfected leaves of T_2 plants over-expressing *AteIF5A-2*

A. Western blot showing AteIF5A-2 protein expression in uninfected leaves of wild-type (WT) plants and plants over-expressing *AteIF5A-2* (Lines 2-3F and 2-9A). AteIF5A-2 is detected at approximately 17kDa. The corresponding SDS-PAGE stained with Coomassie Brilliant Blue is illustrated. **B.** Western blot showing AteIF5A-2 protein expression in leaves of wild-type (WT) plants and plants over-expressing *AteIF5A-2* (Lines 2-3F and 2-9A) before infection (0h) and 72 hours (72h) after infection with virulent *Pst* DC3000. AteIF5A-2 is detected at approximately 17kDa. The corresponding SDS-PAGE stained with Coomassie Brilliant Blue is illustrated with the approximate molecular weights shown on the left. [These infections were performed by Yulia Gatsukovich].

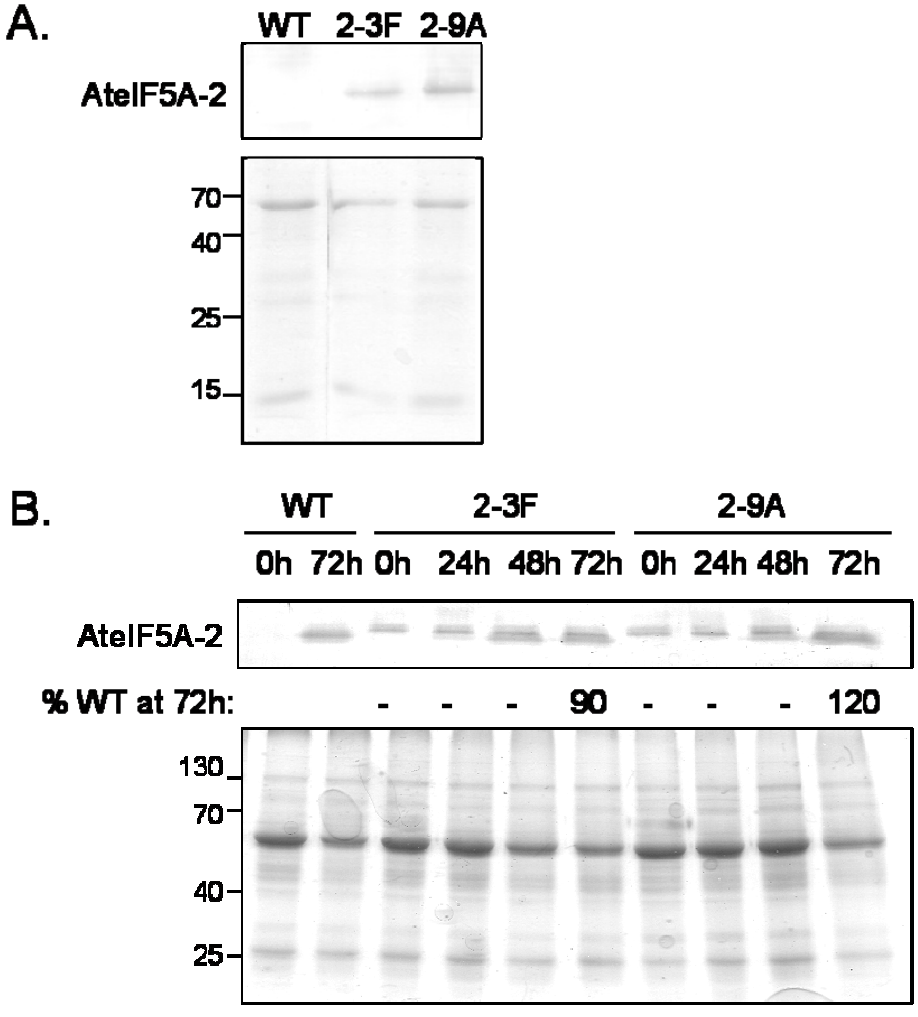
A.
WT
2-3F
2-9A
AteIF5A-2
70
40
25
15
B.
WT
2-3F
2-9A
0h
72h
0h
24h
48h
72h
0h
24h
48h
72h
AteIF5A-2
% WT at 72h:
-
-
-
90
-
-
-
120
130
70
40
25

Figure 2-23: Alignment of the nucleotide sequence of *AteIF5A-3* and the amino acid sequence of its cognate protein

The entire gene sequence of *AteIF5A-3* is aligned with its cognate protein sequence. The primers that were used for amplification for the production of *AteIF5A-3* over-expressing plants are indicated in red. The exons of the *AteIF5A-3* gene are underlined, and the 3 introns are unformatted. The stop codon is indicated in blue, and the peptide used for the production of isoform-specific antibodies is indicated in green.

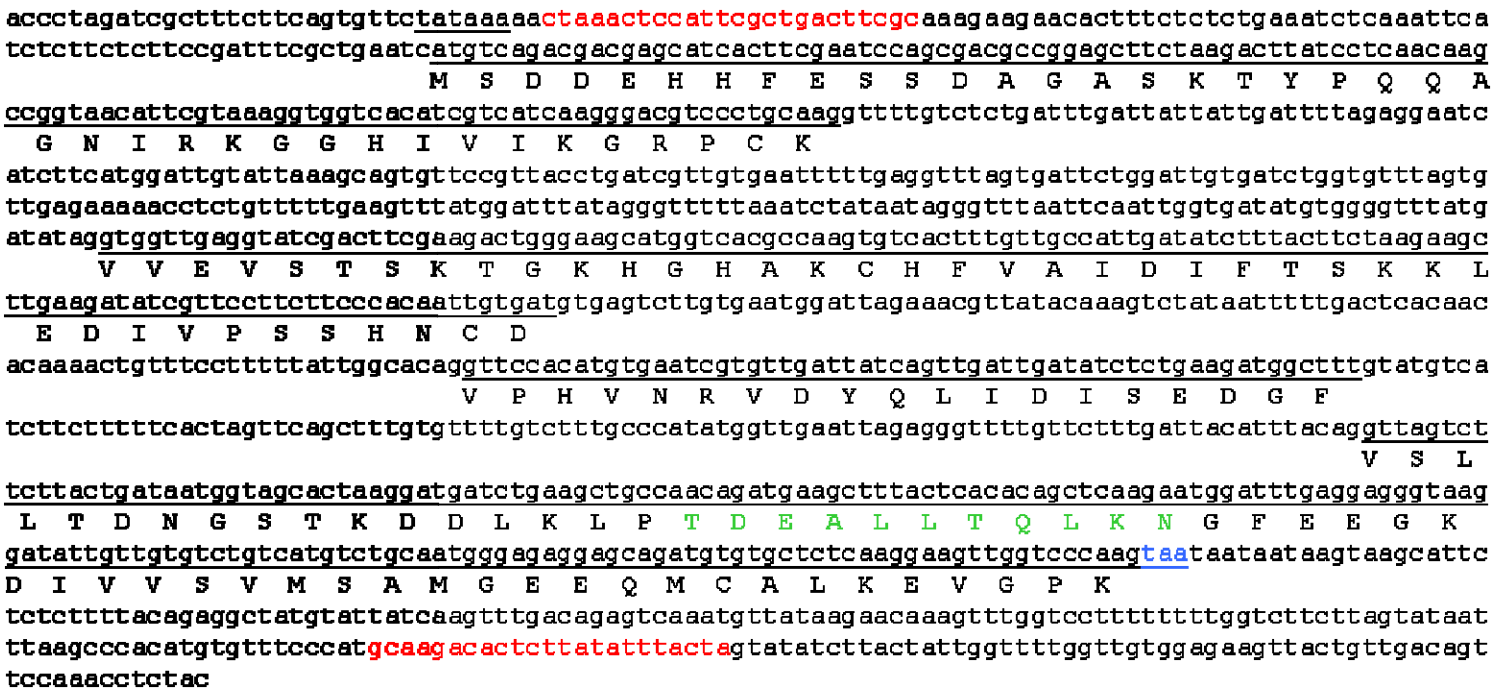
accctagatcgctttcttcagtgttctataaaaactaaactccattcgctgacttcgcaaagaagaacactttctctctgaaatctcaaattca
tctcttctcttccgatttcgctgaatcatgtcagacgacgagcatcacttcgaatccagcgacgccggagcttctaagacttatcctcaacaag
M S D D E H H F E S S D A G A S K T Y P Q Q A
ccggtaacattcgtaaaggtggtcacatcgtcatcaagggacgtccctgcaaggttttgtctctgatttgattattattgattttagaggaatc
G N I R K G G H I V I K G R P C K
atcttcatggattgtattaaagcagtgttccgttacctgatcgttgtgaatttttgaggtttagtgattctggattgtgatctggtgtttagtg
ttgagaaaaacctctgtttttgaagtttatggatttatagggtttttaaatctataatagggtttaattcaattggtgatatgtggggtttatg
atataggtggttgaggtatcgacttcgaagactgggaagcatggtcacgccaagtgtcactttgttgccattgatatctttacttctaagaagc
V V E V S T S K T G K H G H A K C H F V A I D I F T S K K L
ttgaagatatcgttccttcttcccacaattgtgatgtgagtcttgtgaatggattagaaacgttatacaaagtctataattttgactcacaac
E D I V P S S H N C D
acaaaactgtttccttttattggcacaggttccacatgtgaatcgtgttgattatcagttgattgatatctctgaagatggctttgtatgtca
V P H V N R V D Y Q L I D I S E D G F
tcttctttttcactagttcagctttgtgttttgtctttgcccatatggttgaattagagggttttgttctttgattacatttacaggttagtct
V S L
tcttactgataatggtagcactaaggatgatctgaagctgccaacagatgaagctttactcacacagctcaagaatggatttgaggagggtaag
L T D N G S T K D D L K L P T D E A L L T Q L K N G F E E G K
gatattgttgtgtctgtcatgtctgcaatgggagaggagcagatgtgtgctctcaaggaagttggtcccaagtaataataataagtaagcattc
D I V V S V M S A M G E E Q M C A L K E V G P K
tctcttttacagaggctatgtattatcaagtttgacagagtcaaatgttataagaacaaagtttggtccttttttttggtcttcttagtataat
ttaagcccacatgtgtttcccatgcaagacactcttatatttactagtatatcttactattggttttggttgtggagaagttactgttgacagt
tccaaacctctac

The phenotypes for T_1 are illustrated in Figure 2-24, and ranged from very similar to wild type (WT) or binary vector (BIN) controls (Lines 3-1, 3-3, 3-5, 3-6, 3-7, 3-8, 3-10, 3-11, 3-12, 3-13, 3-14, 3-15 and 3-16) to being moderately stunted (Lines 3-2, 3-4, 3-9). All 16 lines were carried through to T_2 generation, with each mother line giving rise to 8 sister lines designated A to H. Line 12 did not produce any transformants in the T_2 generation as determined by the kanamycin screen and was likely a null line. Line 12 was not used for any further analysis.

The T_2 generation plants over-expressing *AteIF5A-3* had more exaggerated phenotypes than was evident for T_1 plants. The plants were grouped based on the level of AteIF5A-3 expression in cauline leaves determined by Western blotting (Figure 2-25). Since most of the sister lines (A-H) demonstrated similar phenotypes and similar protein expression within a mother line, the Western blot depicted in Figure 2-25 was performed with protein only from sister line A to get a general comparison of AteIF5A-3 expression. The relative level of expression observed in these sister lines can be categorized as high (lines derived from 3-1, 3-2, 3-3, 3-10, 3-13), medium (lines derived from 3-4, 3-5, 3- 6, 3-15), low (lines derived from 3-7, 3-8, 3-9, 3-14) or none (lines derived from derived from 3-11, 3-16, and WT/BIN controls). A summary of all the phenotypes observed in the T_2 lines is presented in Table 2-2. The two most consistent features of the plants over-expressing *AteIF5A-3* with detectable AteIF5A-3 protein are an increase in seed size and rounder leaf morphology (Table 2-2). Plants over-expressing *AteIF5A-3* that showed co-suppression, as demonstrated by Western blotting, also had a seed phenotype, specifically seeds that were smaller than those for WT and BIN controls (Table 2-2). The sister lines from the T_2 generation that were brought through to the T_3 generation were chosen based on phenotype as well as the level of expression of AteIF5A-3 and are indicated by coloured ovals in Figure 2-25.

T_2 lines 3-1A and 3-2A exhibited high levels of AteIF5A-3 expression in cauline leaves. Lines 3-1A to 3-1H were very uniform in their phenotype (Figure 2-26A showing lines 3-1A to 3-1D only). All of the T2 sister lines from mother line 3-1 had large round leaves that were darker green than those of WT and BIN controls (Figure 2-26A). They also exhibited a delay in bolting and rosette senescence (Figure 2-26A). Lines 3-2A to 3-2H also

Figure 2-24: Photographs of T_1 plants over-expressing *AteIF5A-3*

Transgenic lines 3-1 through 3-16 over-expressing *AteIF5A-3* are compared to control wild type (WT) and empty binary vector (BIN) transformed plants.


WT
BIN
3-1
3-2
3-3
3-4
3-5
3-6
3-7
3-8
3-9
3-10
3-11
3-13
3-14
3-15
3-16

Figure 2-25: Western blot analysis of leaves from T_2 plants over-expressing *AteIF5A-3*

A. Western blot probed with isoform-specific antibodies against AteIF5A-3. Lanes correspond to the lines indicated above. AteIF5A-3 is detected at approximately 17kDa. Lines for which phenotypes are described in the text are indicated by coloured ovals. The black ovals indicate lines that exhibit high levels of AteIF5A-3 over-expression. The dark-blue ovals indicate lines that exhibit medium levels of AteIF5A-3 over-expression. The light-blue ovals indicate lines that exhibit low levels of AteIF5A-3 over-expression. The white outlined ovals indicate lines that exhibit co-suppression of *AteIF5A-3*. **B.** Corresponding SDS-PAGE gels. Each lane contained 20μg of protein, and the gel was stained with Coomassie Brilliant Blue. The approximate molecular weights are indicated on the left.

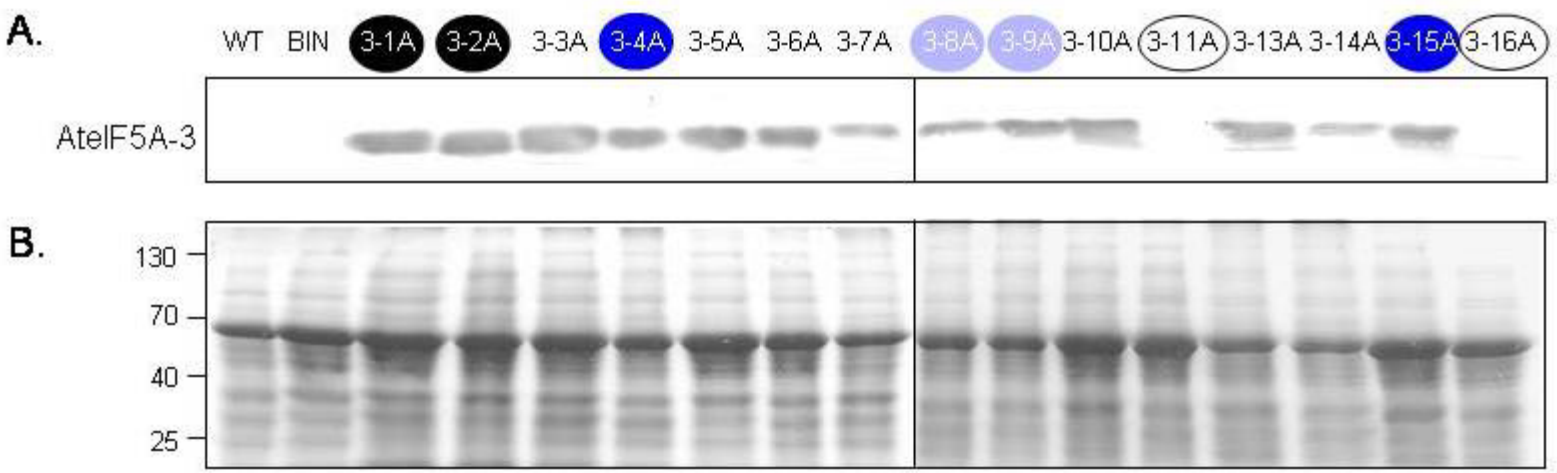
A.
WT
BIN
3-1A
3-2A
3-3A
3-4A
3-5A
3-6A
3-7A
3-8A
3-9A
3-10A
3-11A
3-13A
3-14A
3-15A
3-16A
AtelF5A-3
B.
130
70
40
25

Table 2-2: Summary of phenotypes exhibited by T_2 plants over-expressing *AteIF5A-3*

Rosette Size/Bolt Size: N= normal; S= small; L=large; VL=very large

Seed Size: N= normal; SM= small; SL=slightly larger; L= large; VL=very large

Seed Yield: L=low; N=normal; H=high

Leaf Morphology: N= normal; S= small; R= round; C=curled; L=elongated; B=bilobed

Colour: DG= dark green; G=green (normal); LG= light green

Lines:	**3-1**	**3-2**	**3-3**	**3-10**	**3-13**	**3-4**	**3-5**	**3-6**	**3-15**	**3-7**	**3-8**	**3-9**	**3-14**	**3-11**	**3-16**
Expression Level	High					Medium				Low				None	
Rosette Size	N	S	N	N	N	N	N-L	N-L	L	L	L	S	L	L	VL
Bolt Size	S-N	S	N	N	N	N	N-L	N-L	N-L	N-L	N-L	S	L	N-L	VL
Seed Size	SM-N	VL	SL	SL	SL	L	SL	SL	SL-L	SL-L	SL-L	L	SL-L	SM-N	SM-N
Seed Yield	L	L-N	N	N-H	N-H	H	N	N	N	N-H	N	L	N	L-N	L
Leaf Morphology	N	BSR	N	N	N	N	N	N	N-R	N	R	RC	R	R	L
Colour	DG	LG	G	G	G	G	G	G	LG	G	G	LG	G	G	G

Figure 2-26: Photographs of T_2 plants with high levels of AteIF5A-3 over-expression

A. T_2 lines 3-1A through 3-1D are indicated by blue tags and exhibit the phenotypes of large dark green leaves and delayed bolting and senescence. The wild type (WT) and binary control (BIN) plants are indicated by white and yellow tags, respectively. **B.** T_2 lines 3-2A through 3-2D are indicated by blue tags and exhibit the phenotypes of small round leaves that were light green in colour, delayed bolting and senescence and very large seeds. The wild type (WT) and binary control (BIN) plants are indicated by white and yellow tags, respectively.

A.

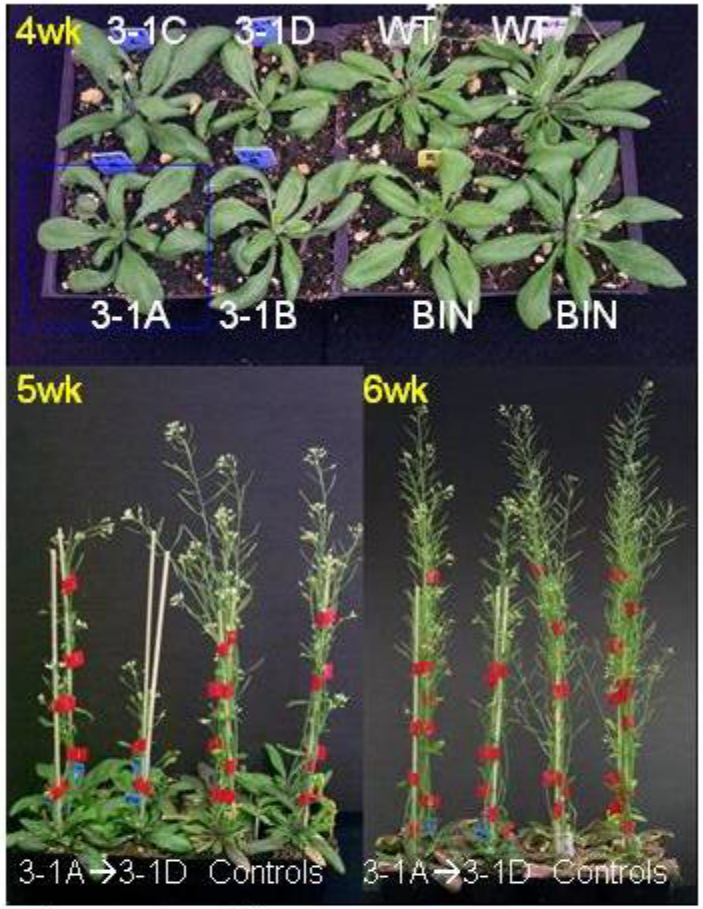

- Large round leaves
- Dark green
- Delayed bolting & senescence

B.

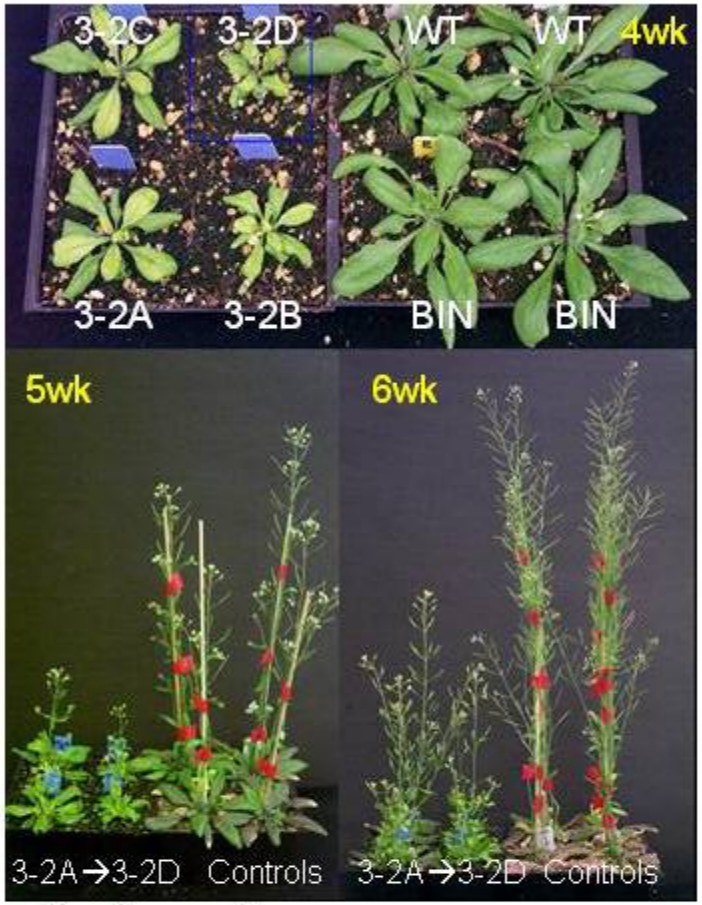

- Small round leaves
- Light green
- Delayed bolting & senescence
- Very large seeds

exhibited a delay in bolting and rosette leaf senescence (Figure 2-26B showing lines 3-2A to 3-2D only). These plants also had very large seeds.

Of the lines exhibiting medium levels of AteIF5A-3 expression, lines 3-4A to 3-4H were similar in stature to wild type plants, but displayed delayed rosette leaf senescence and had very bushy bolts (Figure 2-27A). These bushy bolts resulted in seed yield that was higher than that for WT or BIN controls, and in the case of line 3-4C the seed yield was 2.2-fold more than that for WT or BIN. A second set of transgenic lines with a medium level of AteIF5A-3 expression, lines 3-15A through to 3-15H, are illustrated in Figure 2-27B. These plants were also very similar to wild type plants, but the area that the rosette occupied was larger than for the WT and BIN controls. The leaves of the rosette were also rounder at the tips than were the control leaves.

T_2 lines 3-8A through 3-8H had low levels of AteIF5A-3 expression. These plants had very large leaves and large rosettes compared to the control WT and BIN plants (Figure 2-28A). The leaves also appeared to be wider and rounder than the leaves of the control plants. These lines, like all lines that were not co-suppressed, produced seeds that were larger than those of WT and BIN control plants, and the seeds of these lines had the highest seed weight: seed size ratio. Another set of lines with low levels of AteIF5A-3 expression, lines 3-9A to 3-9H, are illustrated in Figure 2-28B. These lines exhibited an initial delay in growth, but eventually surpassed the WT and BIN controls in stature. The rosette leaves were initially small and round, but expanded into large rosette leaves that exhibited delayed senescence. Bolting too was delayed, and the bolts remained shorter than those of control plants (Figure 2-28B).

T_2 lines 3-11A and 3-16A of the *AteIF5A-3* over-expressing plants have no up-regulated expression of AteIF5A-3 in their cauline leaves. This presumably reflects co-suppression which would also result in silencing of the corresponding endogenous gene. That the transgene is present is evident from the fact that seedlings grew on kanamycin-containing MS plates. Plants of these lines proved to have a similar stature to that of control plants (Figure 29A and Figure 29B), but their distinguishing feature is small seed size (Table 2-2). Seed size is a phenotype of all the over-expressing *AteIF5A-3* lines, where plants

Figure 2-27: Photographs of T_2 plants with medium levels of AteIF5A-3 over-expression

A. T_2 lines 3-4A through 3-4D are indicated with blue tags and exhibit the phenotypes of large leaves, delayed senescence, bushy bolts and high seed yield. The wild type (WT) and binary control (BIN) plants are indicated by white and yellow tags, respectively. **B.** T_2 lines 3-15A through to 3-15D are indicated with blue tags and exhibit the phenotypes of large round leaves and delayed bolting. The wild type (WT) and binary control (BIN) plants are indicated by white and yellow tags, respectively.

A.

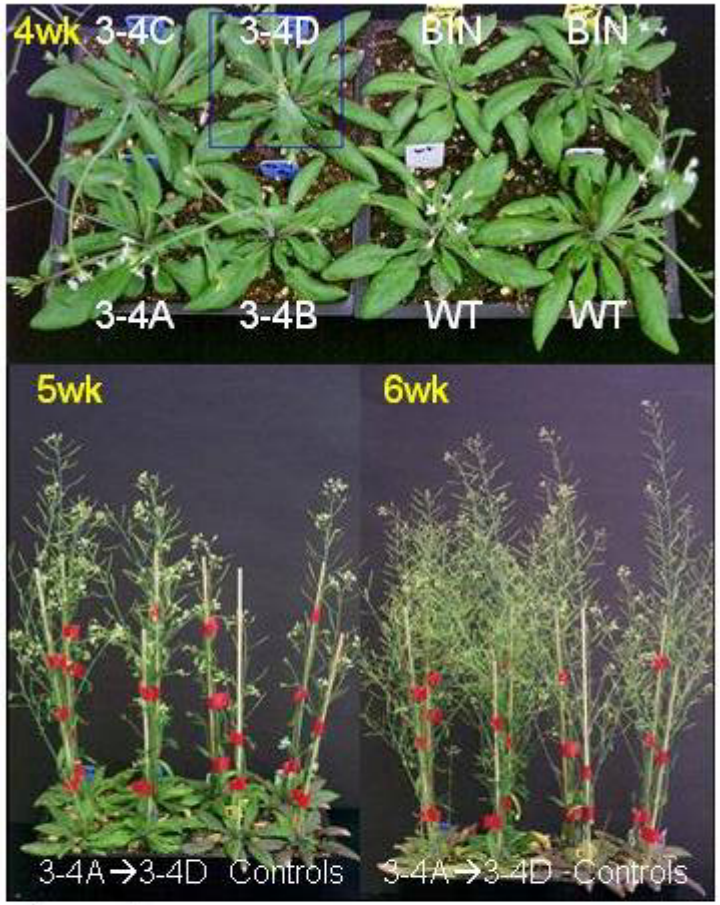

- Large leaves
- Delayed senescence
- Bushy bolts
- Highest seed yield (weight & volume)

B.

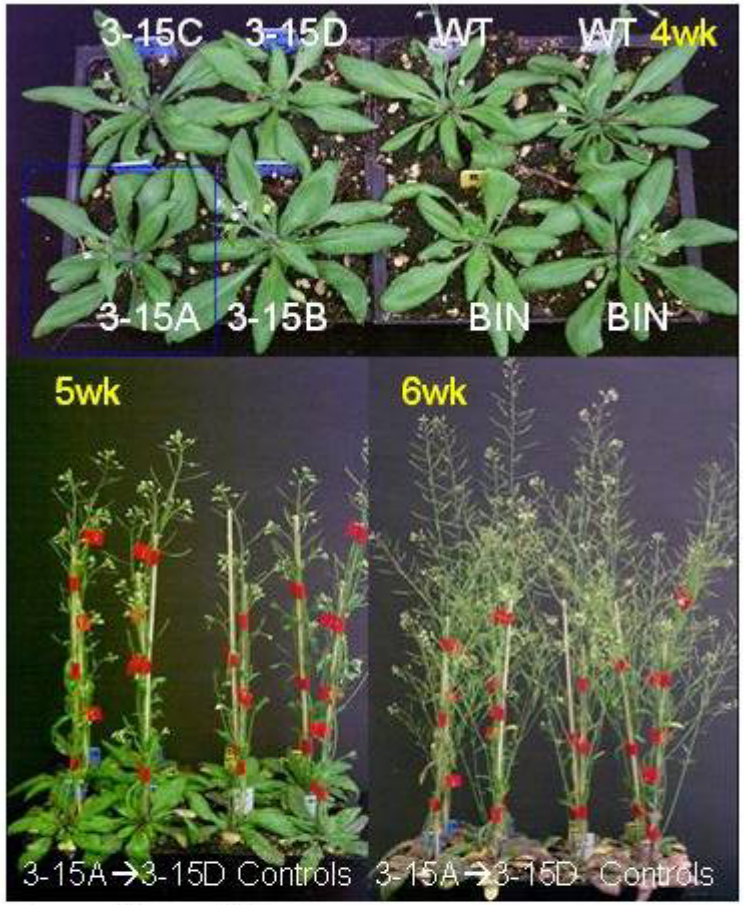

- Large (round) leaves
- Delayed bolting

Figure 2-28: Photographs of T_2 plants with low levels of AteIF5A-3 over-expression

A. T_2 lines 3-8A through 3-8D are indicated with blue tags and exhibit the phenotypes of large round leaves and very dense seeds (high weight: size ratio). The wild type (WT) and binary control (BIN) plants are indicated by white and yellow tags respectively. **B.** T_2 lines 3-9E through to 3-9H are indicated with blue tags and exhibit the phenotypes of delayed growth of the rosette leaves, round rosette leaves, delayed bolting and delayed senescence. The wild type (WT) and binary control (BIN) plants are indicated by white and yellow tags, respectively.

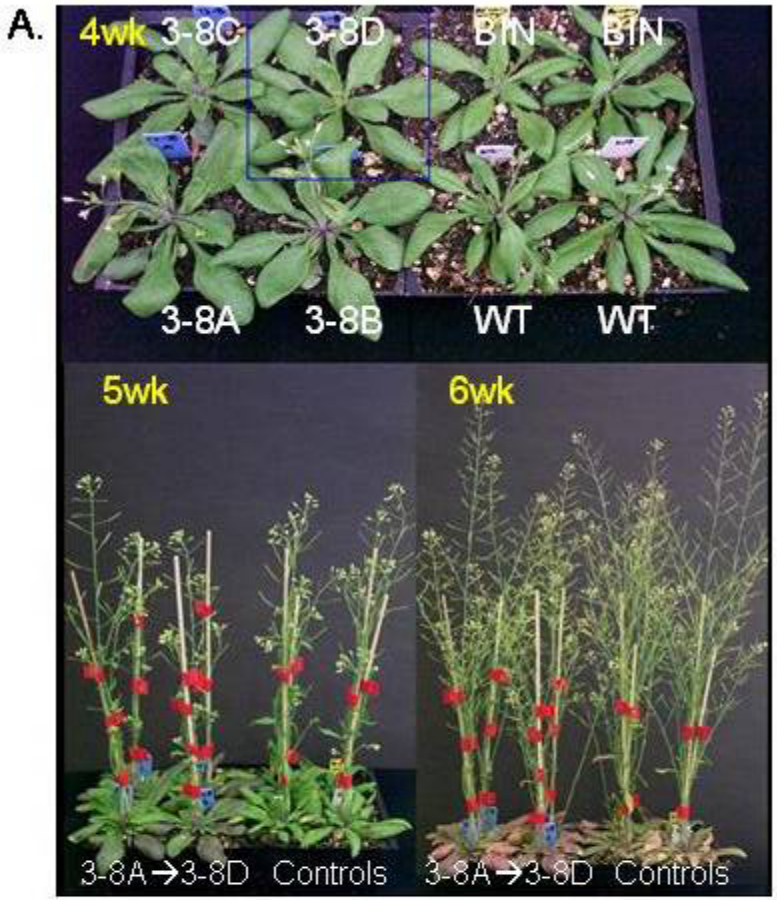

- Large round leaves
- Very dense seeds (high weight: size ratio)

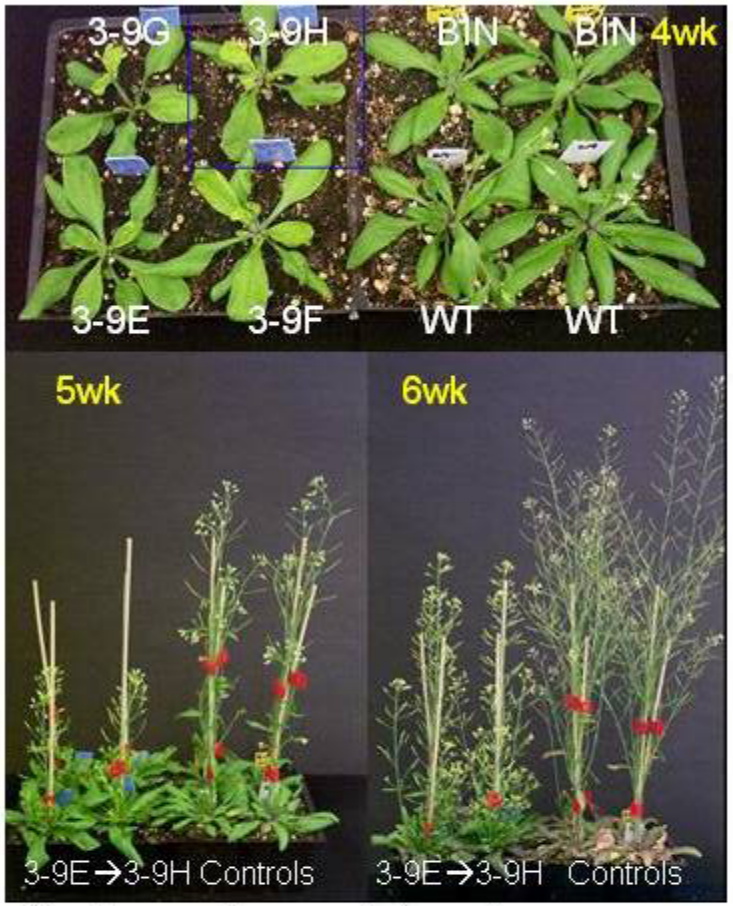

- Small round leaves at 3 weeks
- Leaves become larger than control
- Light green leaves
- Delayed bolting and senescence

Figure 2-29: Photographs of T_2 plants with co-suppression of AteIF5A-3 expression

A. T_2 lines 3-11A through 3-11D are indicated with blue tags and looked very similar to the wild type (WT) and binary control (BIN) plants indicated by white and yellow tags respectively, though they also had very small seeds. **B.** T_2 lines 3-16A through 3-16D are indicated with blue tags and exhibit the small seed phenotype as well as large leaves and large bolts. The wild type (WT) and binary control (BIN) plants are indicated by white and yellow tags, respectively.

A.

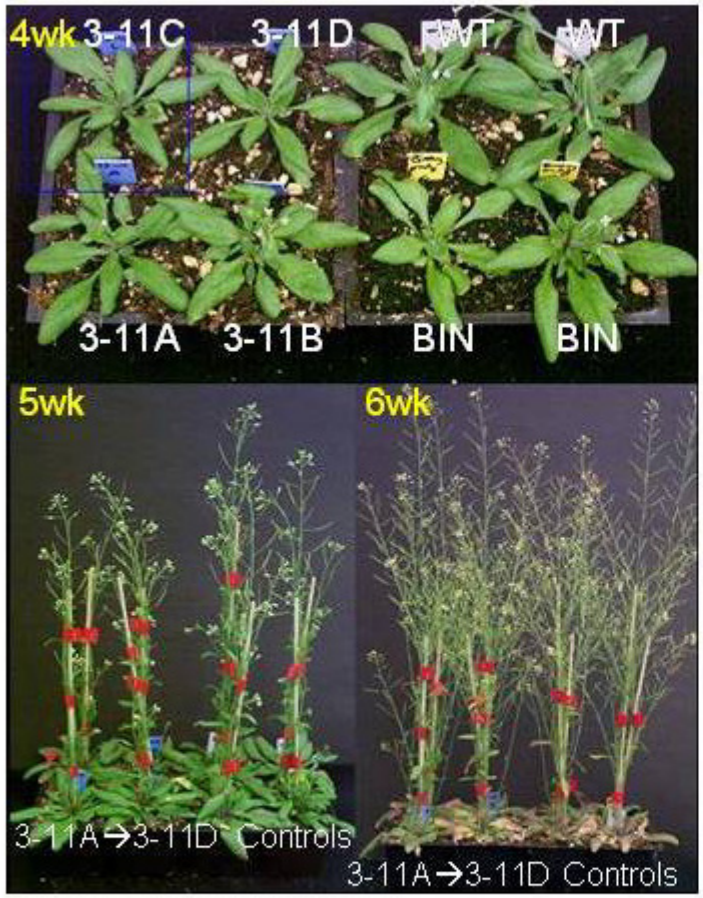

- Look similar to controls
- Very small seeds

B.

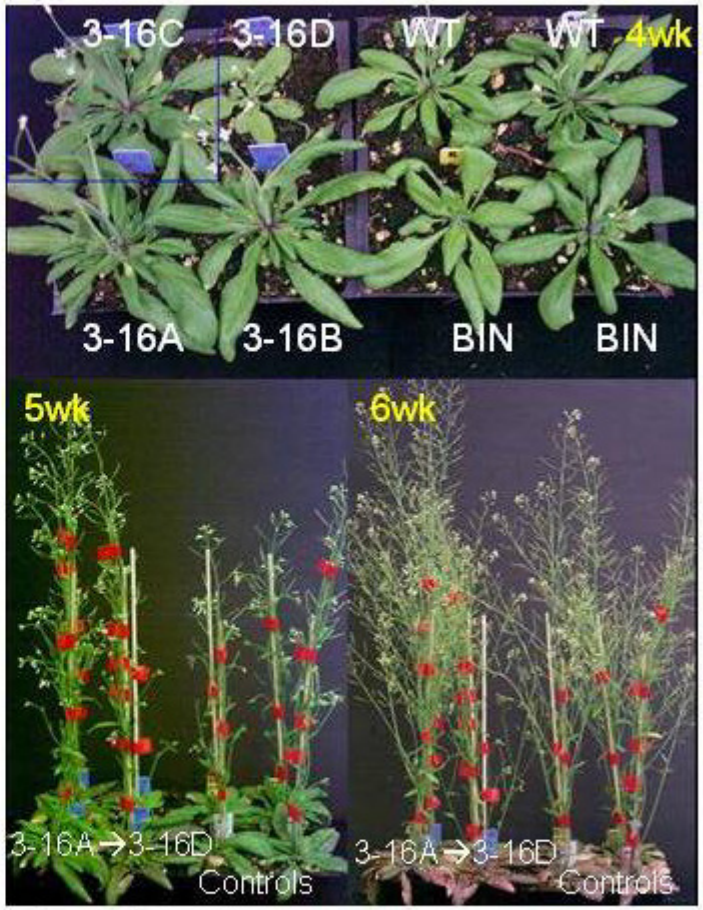

- Large leaves
- Very large bolts
- Small seeds

that display some level of AteIF5A-3 expression have significantly larger seeds than the control WT or BIN plants. The lines with suspected co-suppression have smaller seeds than the WT or BIN control plants.

The sizes of T_3 seeds produced by the T_2 plants characterized above were measured. Photographs were taken of the seeds for each line (the largest and the smallest seeds measured are shown in Figure 2-30), and measurements were made on the photographs *in silico* using Image-Pro Express Version 4.0 for Windows™. For each line and for the WT and BIN controls, ten seeds were measured and the volumes calculated according to Kiyosue *et al.* (1999). It was found that the high expression lines 3-2A to 3-2H (Figure 2-30C and Figure 2-31) had seeds that were up to 3 times larger than those of WT and BIN control plants (Figure 2-30A and Figure 2-31). By contrast, lines with the lowest AteIF5A-3 expression (Lines 3-11A to 3-11H and 3-16A to 3-16H) produced seeds that were only 86-88% of the size of WT or BIN control seeds (Figure 2-30B and Figure 2-31). The average seed size for each line was expressed as nm^3 (Figure 2-32) and was calculated using an equation for the volume of an ellipsoid since seeds from *Arabidopsis thaliana* are approximately ellipsoid (Kiyosue *et al.*, 1999). The measured size of the control seeds (Figure 2-31) is within the published *Arabidopsis* seed size range (Boyes *et al.*, 2001). Seed size is controlled by the growing embryo, the endosperm and/or the maternal tissues (Riefler *et al.*, 2006). These findings are consistent with the notion that seed size is maternally controlled and that the level of AteIF5A-3 expression in these tissues may regulate this phenomenon. Furthermore, not only were the seeds of high expressing lines affected, but fruit development, which is controlled solely by gene expression of maternal tissues (Dinneny and Yanofsky, 2004), was also affected. Normally, *Arabidopsis* siliques are composed of 2 valves or locules that are separated by a false septum or partition. T_3 plants derived from the high AteIF5A-3-expressing T_2 lines, 3-2A to 3-2H, had 4 valves on their siliques and 3 partitions, likely the result of 4 fused carpels rather than 2 as in the WT (Figure 2-30D).

Figure 2-30: Analysis of seed and siliques from transgenic plants over-expressing *AteIF5A-3*

A. Seeds from control wild type (WT) and empty binary vector transformed (BIN) plants. **B.** T_3 seeds from lines producing the smallest seeds. **C.** T_3 seeds from lines producing the largest seeds. **D.** Siliques of T_3 plants and wild type (WT) control plants.

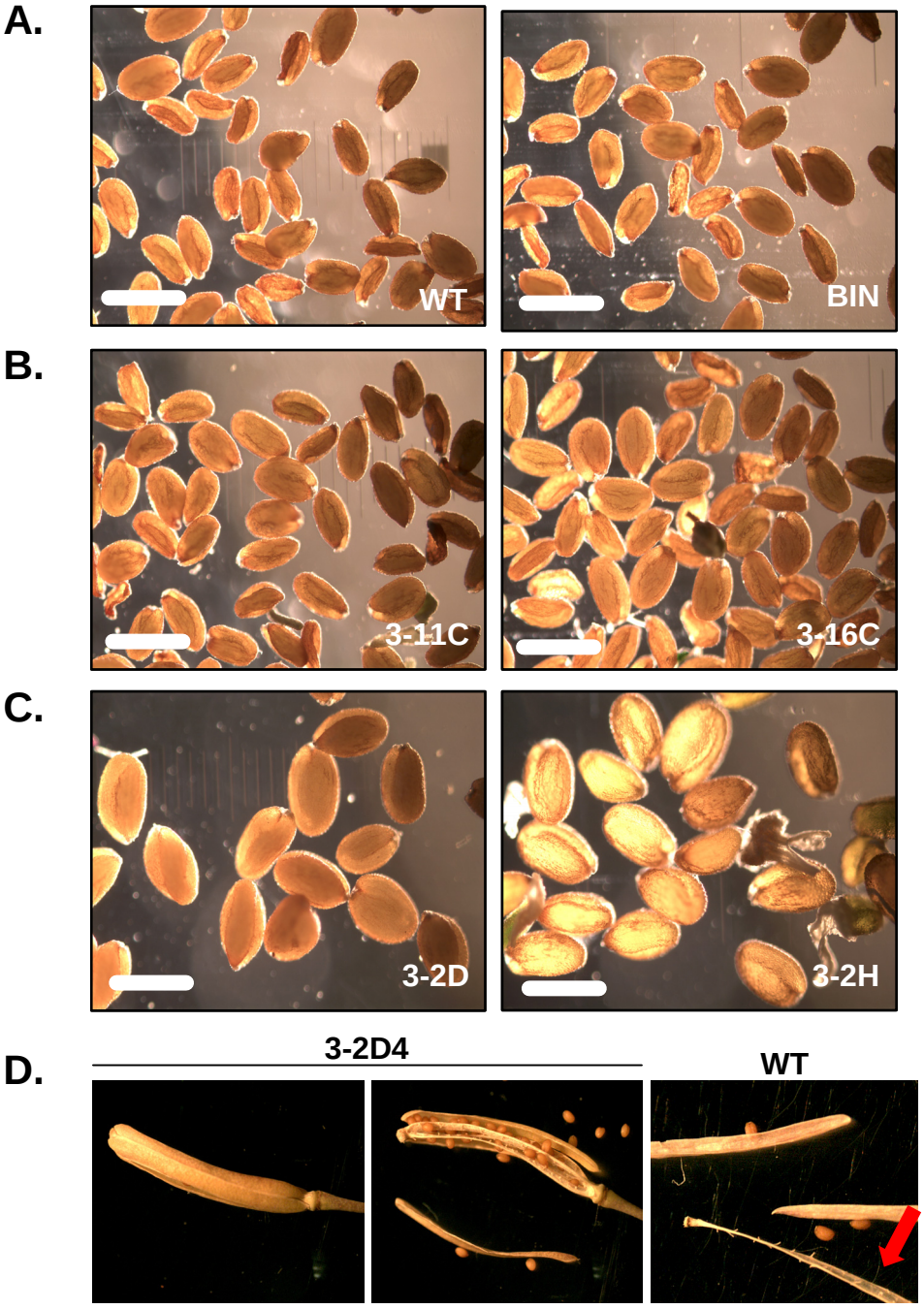
A.
WT
BIN
B.
3-11C
3-16C
C.
3-2D
3-2H
D.
3-2D4
WT

Figure 2-31: Size of T_3 seeds from T_2 plants over-expressing *AteIF5A-3*

A total of 10 seeds were measured for each line. The transgenic lines over-expressing *AteIF5A-3* are indicated in blue. The empty binary vector (BIN) and wild type (WT) control plants are indicated in yellow and white, respectively.

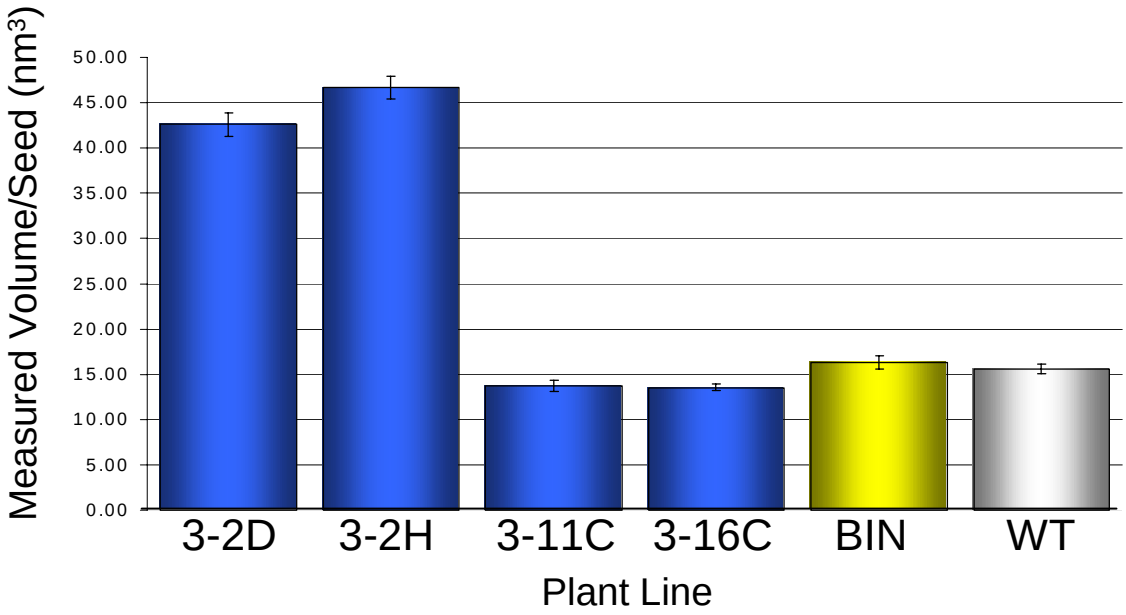
Measured Volume/Seed (nm³)
50.00
45.00
40.00
35.00
30.00
25.00
20.00
15.00
10.00
5.00
0.00
3-2D
3-2H
3-11C
3-16C
BIN
WT
Plant Line

To examine phenotype heritability for *AteIF5A-3* over-expressing lines in more detail, T_3 seeds from mother lines 3-1A, 3-2D, 3-4D, 3-15A, 3-8D, 3-9H, 3-11C and 3-16C were screened on kanamycin plates and the resultant seedlings transplanted to soil. Several other T_3 sister lines over-expressing *AteIF5A-3* did not germinate, including 3-1B, 3-1D, 3-1E, 3-1F, 3-1G, 3-2H, 3-14B. Many of the phenotypes that were described for the T_2 generation were not as apparent in the T_3 generation. However, a phenotype that was observed in many T_3 lines was an increase in petal number (Figure 2-32A). There were also instances of bilobed leaves (Figure 2-32B) similar to what was observed in T_2 plants, and several lines produced more than one leaf at each node (Figure 2-32B). These phenotypes are reflective of interrupted cell division within the meristems during organogenesis (Hu *et al.*, 2003). Fused bolts (Figure 2-32B) is also indicative of interrupted cell division, specifically cell separation, in the inflorescence meristem (Ohno *et al.*, 2003)

2.3.5.2 Localization of *AteIF5A-3* expression

Since very little is known about expression of the endogenous *AteIF5A-3* gene, the localization of its cognate protein was examined by confocal microscopy. By subjecting the 2kb region upstream of *AteIF5A-3* gene to PLACE (http://www.dna.affrc.go.jp/PLACE/index.html), several interesting tissue-specific promoter elements were identified. Specifically, some seed storage and ABA responsive elements were identified, as well as pollen and root specific motifs. Furthermore Birnbaum *et al.* (2003) used cell sorting to sort the different tissues of *Arabidopsis* root expressing tissue-specific GFP and then subjected the mRNA from these sorted cells to microarray analysis. From the raw data (Birnbaum *et al.*, 2003), it is apparent that *AteIF5A-3* transcript is present in root tissues, specifically within the zone of elongation and the area in which cells differentiate, but not in the apical meristem region.

That AteIF5A-3 is expressed in developing seedlings was demonstrated by Western blotting (Figures 2-8). To confirm this, confocal microscopy was performed using purified AteIF5A-3 antiserum and goat-anti-rabbit IgG secondary antibody conjugated to FITC (Figure 2-33). It was found that expression of AteIF5A-3 was detectable in the developing roots of emerging seedlings, specifically in the root cap, the zone of elongation and

Figure 2-32: Photographs illustrating some phenotypes of T_3 plants over-expressing *AteIF5A-3*

A. Several lines of T_3 plants over-expressing *AteIF5A-3* had extra flower petals (indicated by red arrows). **B.** T_3 plants also exhibited bilobed leaves (line 3-2D7) and multiple leaves per node (line 3-9H6) (indicated by white arrow). There were also instances of fused bolts and strange bolt morphology (indicated by a blue arrow).

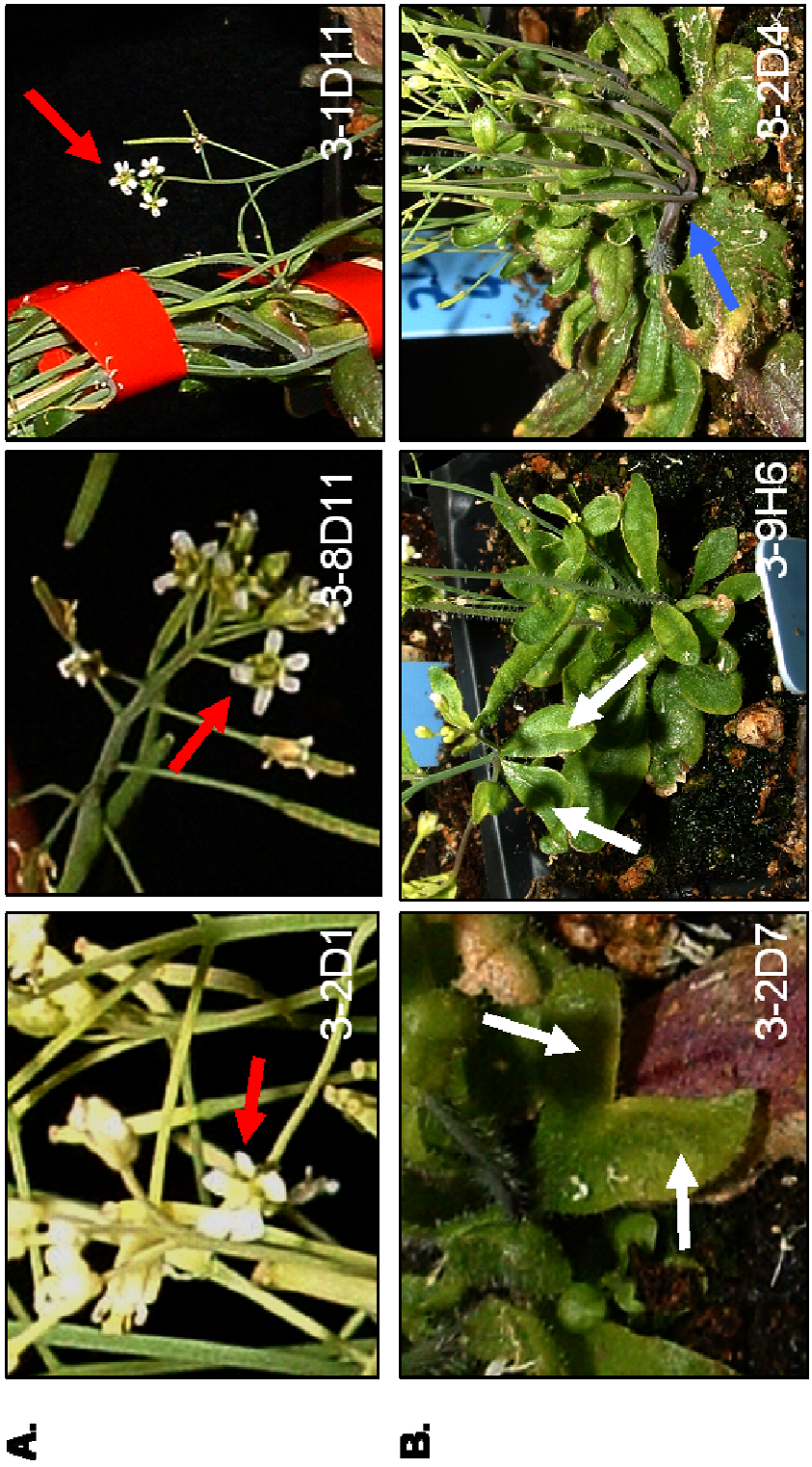
A.
B.
3-1D11
3-8D11
3-2D1
3-2D4
3-9H6
3-2D7

Figure 2-33: Confocal microscopy images of AteIF5A-3 expression in seedlings and flowers

A. Expression of AteIF5A-3 detected by FITC labelling in an emerging root from a wild-type seed. The image is a composite of 20 optical slices. **B.** Expression of AteIF5A-3 detected by FITC labelling in a 4 day old wild-type seedling. This image is a composite of 17 optical slices. **C.** Expression of AteIF5A-3 detected by FITC labelling in the root tip of an 8 day old wild-type seedling. The image is a composite of 17 optical slices. **D.** Expression of AteIF5A-3 detected by FITC labelling in pollen associated with the stigma of a 35 day-old wild-type plant. The image is a composite of 13 optical slices. Size bars = 100μm

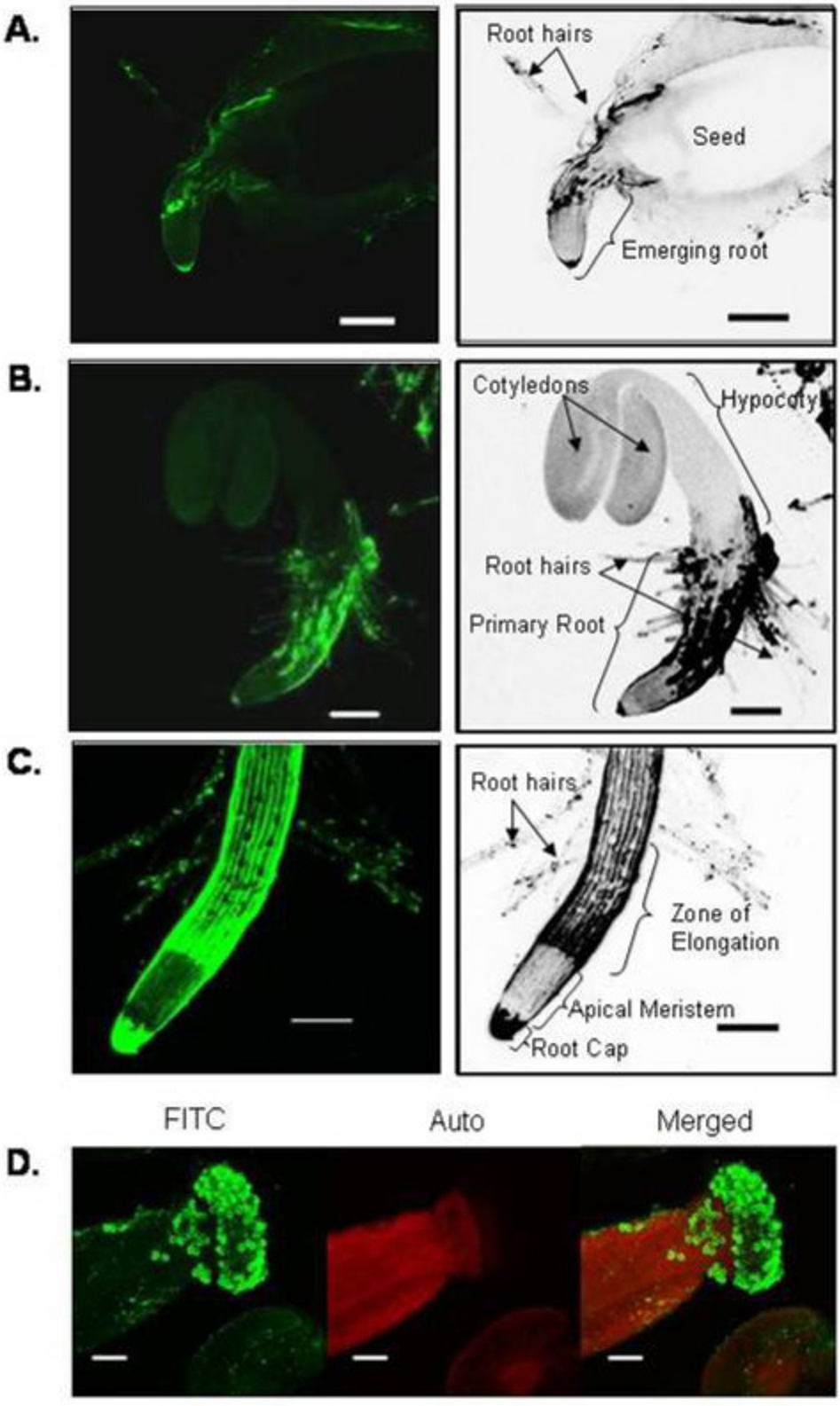
A.
Root hairs
Seed
Emerging root
B.
Cotyledons
Hypocotyl
Root hairs
Primary Root
C.
Root hairs
Zone of Elongation
Apical Meristem
Root Cap
FITC
Auto
Merged
D.

elongating root hairs (Figure 2-33A to C). For 4-day-old seedlings, the expression of AteIF5A-3 was observed in all tissue layers, but was highest in the epidermis and lateral root cap. There was no obvious expression in the shoot of the seedling (Figure 2-33B). The expression pattern in the root was even more brilliant in 8 day old seedlings (Figure 2-33C). That the expression of AteIF5A-3 is not evident in the meristem region indicates that it is probably not involved in cell division directly, but rather is involved in the elongation and differentiation of cells in the zone of elongation and during maturation of roots. These findings are consistent with the microarray data found in Birnbaum *et al.* (2003). Even though there was no detectable expression in the shoots of these seedlings, this does not preclude the possibility that AteIF5A-3 is normally expressed in shoots, as the seedlings used in these experiments were grown under conditions of etiolation.

That there is up-regulation of AteIF5A-3 during flower development was determined by Western blotting (Figure 2-9). This was confirmed by confocal microscopy after labelling of flowers with purified AteIF5A-3 antibody and FITC conjugated secondary antibody (Figure 2-33D). AteIF5A-3 was detectable in pollen grains associated with the stigma, and only pollen associated with the stigma (Figure 2-33D). This is consistent with the proposed function of AteIF5A-3 in cell elongation, as pollen associated with the stigma grows a pollen tube that penetrates the maternal tissues to fertilize the eggs stored within (Edlund *et al.*, 2004). It is not clear from these experiments whether AteIF5A-3 is also expressed in unfertilized eggs, but there is a report of stored eIF5A transcripts in unfertilized eggs of maize (Dresselhaus *et al.*, 1999).

The expression of AteIF5A-3 in the roots of transgenic lines over-expressing *AteIF5A-3* was also visualized by confocal microscopy. Plant roots for line 3-2D, which has high levels of AteIF5A-3 expression, labelled very intensely throughout the root tip, with the exception of the quiescent centre just above the root cap (Figure 2-34B). The quiescent centre is a metabolically inactive area of the root tip (Birnbaum *et al.*, 2003). By contrast, the intensity of the AteIF5A-3 labelling in the roots of co-suppressed transgenic plants was much reduced in comparison with wild-type plants (Figure 2-34C and Figure 2-34D). Furthermore, these roots either lacked root caps, or had very small root caps, and the minimal

Figure 2-34: Confocal microscopy images of AteIF5A-3 expression in seedling roots of wild type and transgenic plants

A. Expression of AteIF5A-3 detected by FITC labelling in an 8 day old wild-type (WT) seedling. The image is a composite of 17 optical slices. **B.** Expression of AteIF5A-3 detected by FITC labelling in the root of an 8 day old seedling of T_3 transgenic plant derived from line 3-2D. This image is one optical section. **C.** Expression of AteIF5A-3 detected by FITC labelling in the root of an 8 day old seedling of T_3 transgenic plant derived from line 3-11C. This image is one optical section. **D.** Expression of AteIF5A-3 detected by FITC labelling in the root of an 8 day old seedling of T_3 transgenic plant derived from line 3-16C. This image is one optical section. Size bars = 100μm.

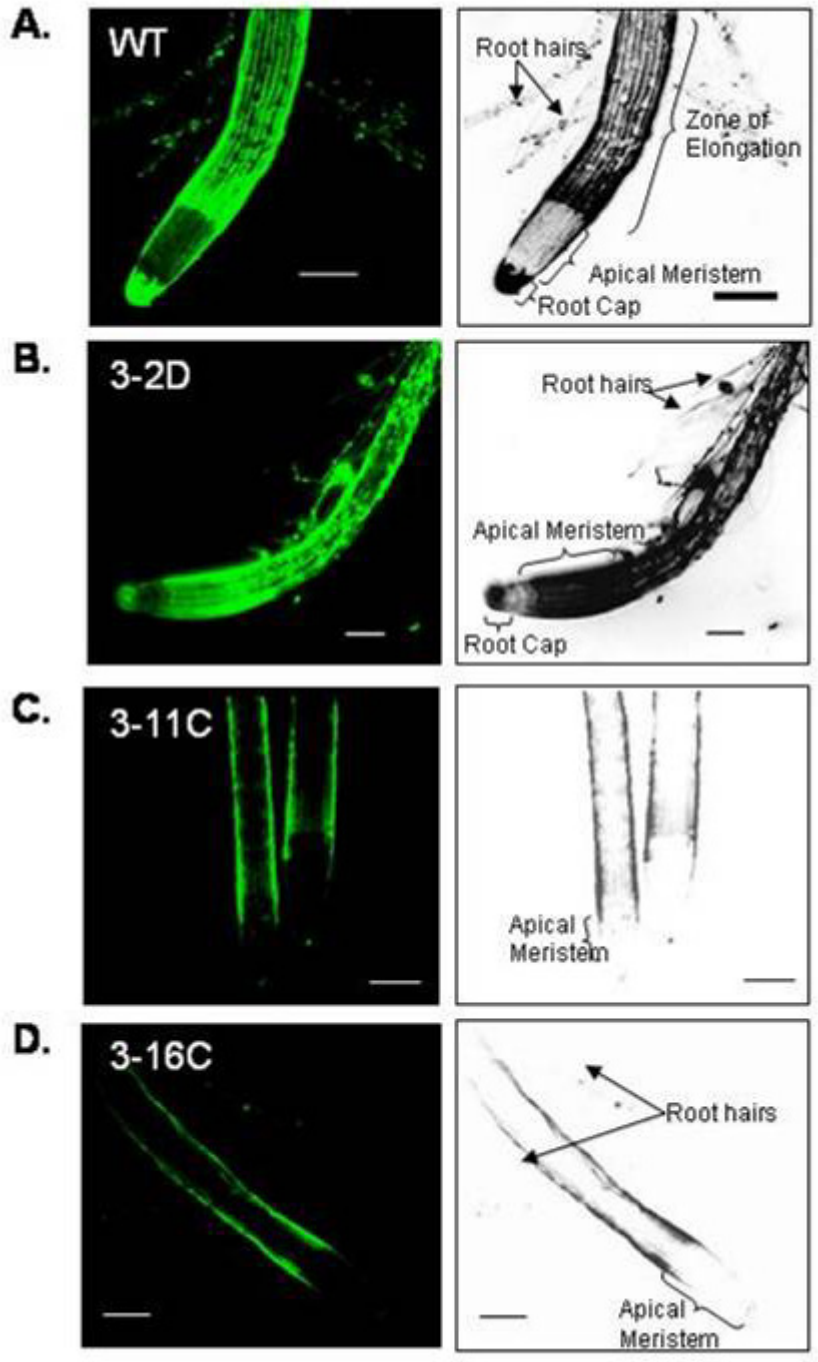
A.
WT
Root hairs
Zone of Elongation
Apical Meristem
Root Cap
B.
3-2D
Root hairs
Apical Meristem
Root Cap
C.
3-11C
Apical Meristem
D.
3-16C
Root hairs
Apical Meristem

expression of AteIF5A-3 that was detectable was mainly in the epidermis (Figure 2-34C and Figure 2-34D). It is known that the epidermal layer controls the extent to which roots elongate (Scheres *et al.*, 2002), and it is likely that the detected AteIF5A-3 is from the endogenous gene. Co-suppression normally results in systemic gene down-regulation. That the co-suppression plants have AteIF5A-3 expression in the epidermis of the root presumably reflects lack of transfer of small interfering RNA from the phloem to the epidermis. This tissue is largely isolated from the rest of the plant as it contains only small simple plasmodesmata, does not have the large branched plasmodesmata required for small interfering RNA translocation and is relatively symplastically isolated from the rest of the root (Duckett *et al.*, 1994).

The subcellular localization of AteIF5A-3 expression was also assessed by confocal microscopy. AteIF5A-3 was clearly evident in the cytoplasm and in the nuclei of cortical cells of the zone of elongation (Figure 2-35). eIF5A is known to act as a nucleocytoplasmic shuttle in mammalian systems (Rosorius *et al.*, 1999; Jao and Chen, 2002). Thus, the expression of AteIF5A-3 in the nuclei and cytoplasm of cortical cells within the zone of elongation of the root implies that it may act as a nucleocytoplasmic shuttle in plants as well.

Figure 2-35: Confocal microscopy images of AteIF5A-3 subcellular localization in root cortical cells

Expression of AteIF5A-3 detected by FITC labelling in the cortex of an 8 day old wild type (WT) seedling root (leftmost image). Differential interference contrast (DIC) image is in the center, and the merged image of DIC and FITC is to the far right. Images are single optical slices. Size bars = 10μm.

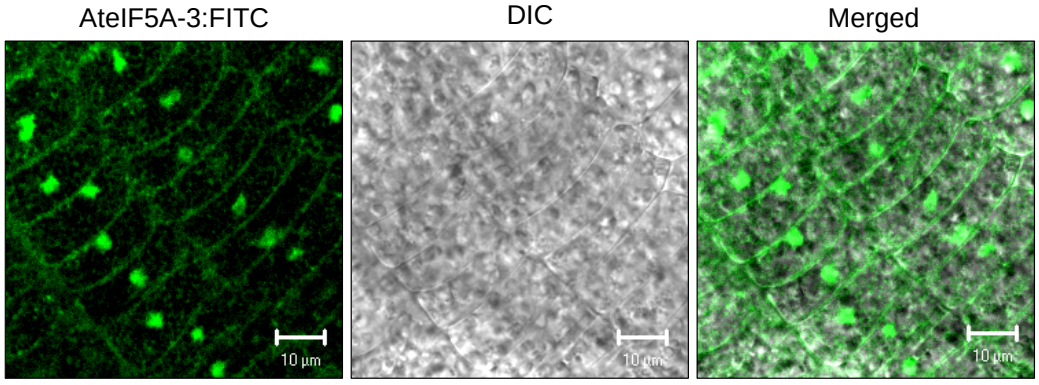
AteIF5A-3:FITC
DIC
Merged
10 µm
10 µm
10 µm

2.4 Discussion

Cells have many means by which they regulate gene expression. In addition to transcription, several such mechanisms involve RNA-protein interactions. RNA processing, translation and degradation are also very potent methods of gene regulation. Recent reports have implicated RNA-binding proteins in the regulation of hormone signalling (Razem *et al.*, 2006) and circadian rhythms in plants (Fedoroff, 2002; Mussgnug *et al.*, 2005). RNA-binding proteins commonly have more than one function and can often link two separate processes, such as intracellular localization and translation (Fedoroff, 2002). Not only do RNA-binding proteins bind to nucleic acids, they also mediate protein-protein interactions. For example, eIF5A, which is thought to be a nucleocytoplasmic shuttle, facilitating the movement of specific subsets of mRNAs from the nucleus into the cytoplasm for translation (Henderson and Percipalle, 1997; Shi *et al.*, 1997; Rosorius *et al.*, 1999), has been shown to have specific interactions with RNA (Bartig *et al.*, 1992; Campbell *et al.*, 1994; Xu *et al.*, 2004) and with proteins (Kang *et al.*, 1993; Ruhl *et al.*, 1993; Valentini *et al.*, 2002). RNA-protein interactions tend to be more difficult to observe than transcription factor-DNA interactions, as they are not usually sequence-specific, but rather entail three dimensional interactions (Varani, 1998). Attempts to discover the mRNA binding partners of eIF5A have not been very fruitful (Liu *et al.*, 1997; Xu and Chen, 2001; Xu *et al.*, 2004), though downstream effects of down-regulation of the expression of eIF5A or its activation by hypusination have been observed (Kruse *et al.*, 2000; Boone *et al.*, 2004; Li *et al.*, 2004; Taylor *et al.*, 2004).

Development in plants and animals requires a balance between cell growth and cell death. In mammalian cells, eIF5A has been shown to be involved in both of these disparate events in an isoform-specific manor (Cracchiolo *et al.*, 2004), and thus eIF5A has been called the translational switch between cell growth and cell death (Jin *et al.*, 2003; Thompson *et al.*, 2004). That the protein sequences of eIF5A in plants are highly similar to mammalian and yeast eIF5A, suggests that the protein has similar functions in plants and mammals.

Arabidopsis thaliana has three isoforms of *eIF5A*, all of which are found on chromosome 1. Each of these isoforms displays a unique expression pattern and unique

phenotypes when over-expressed *in planta*. Wang *et al.* (2001) first identified and functionally annotated an *eIF5A* sequence in *Arabidopsis* (*AteIF5A-1*). The cDNA for *AteIF5A-1* was isolated from a library created from mRNA expressed in senescing leaves and proved to be similar to tomato *LeeIF5A-4*. The sequence for *AteIF5A-1* corresponds to the At1g13950 gene locus on chromosome 1 in *Arabidopsis thaliana*. When this sequence was used to BLAST the *Arabidopsis* genome, two additional eIF5A sequences, also on chromosome 1, were identified and were denoted as *AteIF5A-2* (At1g26630) and *AteIF5A-3* (At1g69410).

At the time the experiments reported in this thesis were initiated, not much was known about the isoforms of *eIF5A* in *Arabidopsis*. In fact, they were only annotated as being similar to tomato *LeeIF5A-4* or as an unknown protein. There was very limited EST information, and it was not known where the isoforms were expressed. It has since been determined through the work of this thesis as well as of others in our laboratory that *AteIF5A-1* is the senescence associated isoform, *AteIF5A-2* is the wounding and pathogenesis associated isoform and *AteIF5A-3* is the growth associated isoform. The temporal and spatial expression patterns for the AteIF5A isoforms documented herein were determined using isoform-specific antibodies, and it is proposed that since their expression patterns are unique, they transport different subsets of mRNA from the nucleus to the cytoplasm for translation.

While *AteIF5A-1* seems to have a regulatory role in leaf senescence (Figure 2-7), it also has a known function in xylogenesis (Duguay, 2004; Tshin, 2004; Liu *et al.*, submitted 2006). Duguay (2004) determined the expression pattern of *AteIF5A-1* transcript using the reporter gene, GUS, driven by the *AteIF5A-1* promoter. His work as well as that of Tshin (2004) and Liu *et al.* (submitted 2006) demonstrated that AteIF5A-1 is important for the formation of xylem. Xylogenesis is a form of programmed cell death (Greenberg, 1996; Richberg *et al.*, 1998). When differentiating tracheary elements in the *Zinnia* model system were treated with actinomycin D or cyclihexamide, maturation by programmed cell death was blocked (Fukuda and Komamine, 1983). This suggests that cell death required for the maturation of tracheary elements of the xylem requires protein synthesis. *AteIF5A-1* was cloned from senescing tissues by Wang *et al.* (2001) and, as demonstrated in this thesis, is

up-regulated in senescing rosette leaves, senescing cotyledons and senescing reproductive organs. These expression patterns are consistent with the GUS expression analysis performed by Duguay (2004) of the *AteIF5A-1* promoter. Given that *AteIF5A-1* and its cognate protein are up-regulated during both senescence and xylogenesis, it is reasonable to hypothesize that AteIF5A-1 is involved in different types of programmed cell death associated with development.

The induction of senescence and programmed cell death during xylogenesis appears to be regulated by the hypusinated form of AteIF5A-1. This is apparent from the finding that deoxyhypusine synthase (AtDHS) is up-regulated in parallel with AteIF5A-1 during leaf and cotyledon senescence (Wang *et al.*, 2003; Duguay, 2004). The constitutive down-regulation of DHS resulted in many phenotypes, including pollen sterility (Wang *et al.*, 2005). However, the down-regulation of DHS specifically in leaves, regulated by a leaf-specific RbsS2 promoter, resulted in delayed leaf senescence by approximately one week (Jamal, 2004). This delay in the onset of senescence was attributed to the delay in activation of the AteIF5A-1 isoform regulating senescence. The over-expression of *AteIF5A-1* resulted in phenotypes attributable to increased cell death, namely delayed growth and premature senescence.

To investigate further the possible role of AteIF5A-1 in programmed cell death, *Arabidopsis* plants over-expressing *AteIF5A-1* cDNA were generated by Zhongda Liu of Dr. J. E. Thompson's laboratory. Liu *et al.* (submitted 2006) observed that these transgenic plants had increased levels of xylem. Moreover, corresponding transgenic plants with suppressed AteIF5A-1 exhibited decreased xylem development in comparison with control plants. Thus, it seems clear that the amount of xylem formed correlates with the level of AteIF5A-1 expression. In the present study, additional phenotypes of the plants over-expressing *AteIF5A-1* were identified and characterized. The main phenotypes that were observed included small rosettes and spindly bolts, long thin rosette leaves or petioles, early rosette leaf senescence and delayed growth. This array of phenotypes indicates that AteIF5A-1 has a broad influence on plant development. The delayed growth phenotype was particularly prominent and is illustrative of the antagonistic relationship between growth and

senescence. In fact, it has been demonstrated that there is a direct relationship between the differentiation of xylem tracheary elements and inhibition of cell expansion (Lee and Roberts, 2004) . Furthermore, death repressing proteins have been shown to promote growth and development of plants (Yang *et al.*, 2006). The finding in the present study that AteIF5A-1, which promotes cell death, appears to repress growth and development when over-expressed in transgenic plants is consistent with these earlier observations.

Evidence obtained in the present study has indicated that AteIF5A-2 is also involved in cell death, specifically premature cell death induced by pathogen ingression or wounding. Plant-pathogen interactions are either compatible or incompatible. During the incompatible interaction, the plant's defence system is activated, and the cells within the region of infection undergo programmed cell death known as the hypersensitive response (HR). HR leads to systemic acquired resistance (SAR), though it is now thought that the programmed cell death that occurs during HR is not necessary for SAR and may be a second layer of defence if a certain threshold of defence stress signals is reached (Pozo *et al.*, 2004). Depending on their lifestyle, whether biotrophic or necrotrophic, pathogens suppress or promote programmed cell death to induce disease susceptibility. Facultative necrotrophic pathogens, such as *Pseudomonas syringae* pv. *Tomato* DC3000 (*Pst* DC3000), start off as biotrophs, living on the nutrients available within the apoplast, but subsequently become necrotrophic by inducing host programmed cell death and the ensuing release of host cell nutrients. Experimental evidence suggests that the timing of host programmed cell death is crucial in determining the outcome of the disease state (Pozo *et al.*, 2004). Early HR-based programmed cell death in the host leads to resistance by isolating the pathogen to the apoplast with no chance of receiving more nutrients from the host; thus the induction of disease is averted. The later-onset of disease-associated cell death is normally suppressed by the pathogen initially, but once infection is established the pathogen initiates host cell death (Katagiri *et al.*, 2002). Recent evidence has demonstrated that the cell death accompanying development of the disease state includes programmed cell death (Abramovitch and Martin, 2004; Pozo *et al.*, 2004).

Gatsukovich (2004) determined the time-course of AteIF5A-2 expression during compatible and incompatible interactions of virulent *Pst* DC3000 and avirulent *Pst* DC3000, respectively, with *Arabidopsis thaliana*. When wild type *Arabidopsis* plants were infected with virulent *Pst* DC3000, AteIF5A-2 expression increased at 24 hours and peaked at 72 hours post inoculation. When wild type *Arabidopsis* plants were infected with avirulent *Pst* DC3000, AteIF5A-2 expression increased at 24 hours, but by 72 hours had diminished to background levels. Thus, the timing of the up-regulation of AteIF5A-2 following treatment with either avirulent or virulent bacteria coincides with host cell death (Katagiri *et al.*, 2002). Moreover, down-regulation of AteIF5A-2 abrogates the development of virulent *Pst* DC3000 disease symptoms (Gatsukovich, 2004). That AteIF5A-2 regulates the occurrence of cell death during pathogenesis was demonstrated by constitutive down-regulation using the 3` UTR (Gatsukovich, 2004) and the constitutive over-expression of *AteIF5A-2* in this thesis. eIF5A is known to be a regulator of apoptosis in mammalian cells (Caraglia *et al.*, 2001; Li *et al.*, 2004; Taylor *et al.*, 2004; Taylor *et al.*, submitted 2006), and is likely a regulator of programmed cell death in plants cells too. Specifically, AteIF5A-2 appears to be a regulator of programmed cell death during compatible and incompatible interactions with *Pst* DC3000.

It is generally recognized that development of the disease state following necrotrophic infection reflects the progressive onset of programmed cell death. (Beers and McDowell, 2001; Greenberg and Yao, 2004; Pozo *et al.*, 2004). In the present study, evidence indicating that AteIF5A-2 is involved in the induction of this programmed cell death was obtained by confocal microscopy. Leaves of *Arabidopsis* plants infected with virulent *Pst* DC3000 were TUNEL labelled and also labelled with TRITC-conjugated secondary antibodies against AteIF5A-2 primary antibodies. At 24 hours after inoculation, there was no visible chlorosis associated with disease in the infected leaves, but at the microscopic level there was detectable AteIF5A-2 coincident with TUNEL labelling. The latter depicts DNA fragmentation associated with programmed cell death (Ning *et al.*, 2002). By 72 hours after infection with virulent *Pst* DC3000, the typical disease symptoms of necrotic lesions surrounded by diffuse chlorosis were clearly evident, and there was strong up-regulation of AteIF5A-2 coincident with TUNEL labelling. That AteIF5A-2 antibody and TUNEL were labelling the same cells in the infected leaves at 24 and 72 hours post-

inoculation indicates that AteIF5A-2 is involved in the regulation of cell death during pathogenesis. The TUNEL-positive reaction is considered as a better index of death by programmed cell death than other cell death markers such as fluorescein diacetate and Evan's Blue (Ning *et al.*, 2002). Furthermore, there was an overlap of the TUNEL-positive nuclei and AteIF5A-2 protein detected with TRITC, which is consistent with the contention that eIF5A functions as a shuttle protein, recruiting specific subsets of mRNA from the nucleus. This finding is also consistent with reports that there is an accumulation of eIF5A within the nuclei of mammalian cells undergoing apoptosis (Tome *et al.*, 1997; Tome and Gerner, 1997; Beninati *et al.*, 1998; Caraglia *et al.*, 2003; Jin *et al.*, 2003).

Wounding and pathogenesis both result in massive programmed cell death. Wounding is a common stress in plants engendered by weather or insect feeding (Cheong *et al.*, 2002). Damaged plant tissues provide entrance points for pathogen invasion, and thus wounding and pathogen responses share common components in their signalling pathways (Maleck and Dietrich, 1999). For example, certain phytohormones, including jasmonic acid, are involved in both phenomena (Lantin *et al.*, 1999; Orozco-Cardenas and Ryan, 1999; Cheong *et al.*, 2002). The mRNA levels change by approximately 8% in the event of wounding, and a large number of these encode signalling molecules (Cheong *et al.*, 2002). Both wounding and pathogen ingress induce expression of a large number of genes encoding transcription factors including AP2 (Cheong *et al.*, 2002), WRKY (Yu *et al.*, 2001) and MYB (Urao *et al.*, 1993) families. Through the up-regulation of defence genes, the area in which the wound has occurred becomes resistant to pathogen ingress. Further to this, the cells around the wound site undergo programmed cell death, and SAR is initiated.

The finding in the present study that AteIF5A-2 is strongly up-regulated within 4 hours post-wounding suggests that it plays a role in programmed cell death associated with wounding. Moreover, AteIF5A-2 expression increases more quickly in the event of wounding than following *Pst* DC3000 ingression. This presumably reflects the time it takes for *Pst* DC3000 to colonize the apoplast and generate an association with a plant cell. It is possible that the pili puncturing cellular membranes are the signals for AteIF5A-2 up-regulation in both the compatible and incompatible interactions.

AteIF5A-2 appears to be post-transcriptionally regulated in that its mRNA is constitutively expressed, whereas the protein is only up-regulated post- infection or after wounding (Gatsukovich, 2004). It is clear from the present study that this post-transcriptional control is overcome in plants over-expressing *AteIF5A-2*. One possible interpretation of this finding is that translation is triggered by a threshold level of *AteIF5A-2* transcript, a threshold that is exceeded in the event of constitutive over-expression. There may also be an upper threshold for the expression of AteIF5A-2 protein as was demonstrated by time-course Western blots of plants over-expressing *AteIF5A-2* infected with virulent *Pst* DC3000. At 72 hours post- infection with virulent *Pst* DC3000, the level of AteIF5A-2 expression obtained was 90 to 120% of that for wild type plants similarly infected. It would appear, therefore, that the upper level of expression obtained in the over-expression lines infected with virulent *Pst* DC3000 is similar to the peak level of expression in wild type plants.

In the T_1 plants over-expressing *AteIF5A-2*, over a third of the plants died before bolting and did not produce any seeds. The T_2 plants, however, did not exhibit this lethal phenotype. Rather, they exhibited a phenotype similar to that observed for spontaneous cell death mutants (Dietrich *et al.*, 1994; Pilloff *et al.*, 2002). These lines also exhibited spontaneous cell death envisaged by TUNEL labelling. However, the AteIF5A-2 over-expressing plants are not resistant to the development of disease induced by virulent *Pseudomonas syringae* infection in the way that some spontaneous cell death mutants are (Dietrich *et al.*, 1994; Pilloff *et al.*, 2002; Senda and Ogawa, 2004; Gatsukovich *et al.*, submitted 2006). Instead, the phenotype of the AteIF5A-2 over-expressing plants appears to reflect increased programmed cell death rather than enhancement of the signalling pathway for HR. There is obviously some overlap in the resistance and cell death pathways (Heath, 2000), but it would appear that AteIF5A-2 is not involved in the resistance pathway but rather is solely involved in promoting programmed cell death induced by interactions with pathogens.

Decreased fecundity, early bolting, severe stunting, spontaneous necrotic lesions, and increased basal inflorescence branching were phenotypes of T_2 plants over-expressing

AteIF5A-2. These are also the developmental phenotypes documented previously for plants that are chronically infected with *Pseudomonas syringae* (Korves and Bergelson, 2003). Flowering in *Arabidopsis* is stress-induced; indeed, precocious flowering enables life-cycle completion under conditions that are unfavourable for survival (Simpson *et al.*, 1999). The short and thin siliques seen in the over-expressing *AteIF5A-2* lines can be likened to reduced fruit size and ovule abortion observed in the event of salt stress (Sun *et al.*, 2004), suggesting that over-expression of AteIF5A-2 may simulate the effects of stress. Of particular interest is the finding that the level of AteIF5A-2 over-expression correlated very closely with the degree of stunted growth. Specifically, the lines that were the most stunted had the highest level of expression, whereas the lines that were less stunted had lower levels of expression. The more stunted plants also produced much less seed than the plants that were less stunted. These are phenotypes of plants with severely compromised growth. These phenotypic effects have also been observed in plants with high pathogen load (Korves and Bergelson, 2003).

It is clear from the results presented in this thesis and from other studies conducted in Thompson's lab that AteIF5A-1 and AteIF5A-2 both regulate programmed cell death. Just as plant growth was inhibited by over-expression of *AteIF5A-2*, it was also inhibited by over-expression of *AteIF5A-1*, though the effects were not as extreme as for the *AteIF5A-2* over-expressing plants. The proposed function of AteIF5A-1 is to facilitate the translation of mRNAs involved in cell death during natural senescence and xylogenesis (Liu *et al.*, submitted 2006). The formation of these transcripts is developmentally regulated, and if the mRNAs recognized by AteIF5A-1 are not present within the cells over-expressing the protein, the phenotypic effect of up-regulated AteIF5A-1 would not be apparent. The proposed function of AteIF5A-2 is to facilitate the translation of mRNAs involved in cell death during wounding or pathogen ingress. All cells in a plant, though some better than others, are capable of mounting a wound or pathogenesis response. Moreover, *AteIF5A-2* transcript, but not protein, is constitutively expressed. Thus up-regulation of AteIF5A-2 is likely to have a more pronounced effect than is up-regulation of AteIF5A-1, and one of these effects is clearly suppression of growth. This is in keeping with the fact that growth ceases

coincident with the induction of senescence whether it occurs naturally or prematurely in response to stress (Sun *et al.*, 2004; Thompson *et al.*, 2004; Camp, 2005).

Plant tissues are formed by coordinated cell division and cell expansion. Plant cells are circumscribed by a rigid cell wall matrix. A new wall is deposited during cell division, locking the orientation and position of the daughter cells. The final form of a tissue or organ is due to different patterns of cell proliferation and cell expansion. Thus, the term 'growth' in plants encompasses both cell division and cell expansion. In yeast and certain mammalian cells, eIF5A has been shown to play a role in the cell cycle and to be required for cell proliferation (Park *et al.*, 1993; Park *et al.*, 1997; Chan *et al.*, 2002; Nishimura *et al.*, 2005). That AteIF5A-3 was found to be up-regulated during seedling growth and during the growth phases of flower development in this thesis suggests that this isoform of eIF5A in *Arabidopsis* is involved in growth.

To further investigate this hypothesis, plants over-expressing *AteIF5A-3* were created and analyzed. T_1 plants over-expressing *AteIF5A-3* did not exhibit growth patterns that were significantly different from those of corresponding control plants. However, T_2 plants over-expressing *AteIF5A-3* did have a phenotype and were easily scored into four phenotypic categories that correlated with the level of AteIF5A-3 over-expression detected by immunoblotting. The most predominant phenotypes were a change in leaf and flower morphology and an increase in seed size, and these phenotypes were inherited by T_3 plants.

The phenotypes of *AteIF5A-3* over-expressing plants appear to at least in part reflect an effect of the protein on the vegetative and flower meristems. This is evident from the fact that several of these transgenic lines developed leaves with different shape (round or bilobed) or flowers with increased petal numbers. Whether these phenotypes are exaggerations of wild type phenotypes or induced by precocious translation of mRNAs involved in development remains to be elucidated, though the latter is more likely. Growth in plants requires coordinated control of cell division and cell expansion. The constitutive over-expression of AteIF5A-3 may have caused an imbalance in these two processes required for proper two-dimensional control of leaf shape and three-dimensional control of body form. In support of this, it has been noted previously that plants with mutations affecting leaf

elongation exhibit rounded leaves (Tsukaya, 2002), much like the phenotype of *AteIF5A-3* over-expressing plants.

Two patterns of plant cell expansion are recognized. One is diffuse growth in which the process of growth is dispersed over a large area of the cell. This growth pattern is, for example, exhibited by epidermal cells (Mathur, 2005). The second pattern of cell expansion is termed tip growth, where the growth process is limited to a small region that extends to form a tubular structure (Mathur, 2005). Through examination of microarray data in public domains, it was found that *AteIF5A-3* is greatly up-regulated in the zone of elongation in roots (Birnbaum *et al.*, 2003). Furthermore, analysis of the promoter of *AteIF5A-3* by PLACE (http://www.dna.affrc.go.jp/PLACE/index.html) revealed that there are several pollen-specific motifs within the *AteIF5A-3* promoter. Pollen and root tips exhibit tip growth, and the finding that the *AteIF5A-3* promoter contains pollen-specific elements suggests that its cognate protein is involved in fertilization.

That *AteIF5A-3* transcript abundance has been shown to increase in growing root tips (Birnbaum *et al.,* 2003) together with the fact that its promoter contains pollen-specific elements were used as starting points for expression analysis of AteIF5A-3 in the present study. Confocal microscopy provided evidence for the presence of AteIF5A-3 protein in roots and pollen. In roots, the protein was discernible in the zone of elongation, in the region of maturation and in the epidermis and cortical layers. That AteIF5A-3 was also expressed in the tips of root hairs is consistent with the finding that it is also present in pollen associated with the stigma. Tip growing structures have similar gene expression and are regulated by similar means (Bucher *et al.*, 2002; Xu *et al.*, 2005). Tip growing structures such as root hairs and pollen tubes are also dependent on cytoskeleton components for directional growth. Recently, it was demonstrated that eIF5A is essential for establishing actin polarity during bud formation in *Saccharomyces cerevisiae* (Zanelli and Valentini, 2005). Furthermore, yeast eIF5A mutants exhibited a cell shape change similar to that induced by defects in cell wall integrity pathways (Chatterjee *et al.*, 2006). That eIF5A in yeast is essential for cell size and growth is consistent with the proposed function of AteIF5A-3 in root hairs and pollen of *Arabidopsis*.

When DHS is highly suppressed in tomato plants the pollen grains are severely affected and are sterile (Wang *et al.*, 2005). This is presumably due to the decreased hypusination of the growth isoform in the tomato pollen. The growth isoform, AteIF5A-3, in *Arabidopsis* is expressed in pollen, and only in pollen associated with the stigma and not in pollen within the anther. Pollen associated with the stigma undergoes rapid cell elongation to produce a pollen tube. Growth of the pollen tube is essential for fertilization. Pollen not capable of growing a pollen tube would be sterile (Piffanelli *et al.*, 1998). Some of the T_3 seeds from the co-suppression lines when plated on selection medium did not germinate, indicating that perhaps there was no embryo and fertilization did not take place as the pollen tubes were incapable of growing. Upon revisiting the images taken of the seeds in Figure 2-30, it is evident that some of the seeds in the co-suppression lines appear to be empty and in fact do not contain embryos.

Strong antisense down-regulation of DHS has been shown to interfere with flower and fruit development, a finding that was interpreted as reflecting reduced capacity for hypusination of eIF5A (Wang *et al.*, 2005). Dresselhaus *et al.* (1999) demonstrated that eIF5A transcripts are stored in unfertilized egg cells of maize. They hypothesized that in this metabolically inactive state the egg prepares for selective mRNA translation that would be quickly prompted after fertilization. That AteIF5A-3 has a role in the female side of fertilization has yet to be determined. It is clear, however, from the present study that AteIF5A-3 affects fruit and seed formation as demonstrated by the increase in seed size and changed silique morphology in AteIF5A-3-up-regulated lines. The superior gynoecium of *Arabidopsis thaliana* has two carpels whose locules are separated by a false septum (Smyth *et al.*, 1990). The siliques of plants over-expressing *AteIF5A-3* that produced the largest seeds had 4 locules and 3 partitions, likely the result of 4 fused carpels rather than 2 as in the wild type. The size of the seeds produced within siliques is determined by maternal gene expression (Kiyosue *et al.*, 1999). The size of the seeds that were produced in the over-expressing *AteIF5A-3* plants proved to be positively correlated with AteIF5A-3 expression. Many of the genes that are expressed during embryogenesis are also expressed at the beginning of germination, which is essentially a continuation of embryogenesis. Genome-wide profiling of stored mRNA in *Arabidopsis thaliana* seeds revealed the presence of

AteIF5A-2 and *AteIF5A-3* transcripts in high abundance (Nakabayashi *et al.*, 2005). Since *AteIF5A-2* expression is constitutive, this finding is no surprise. The presence of *AteIF5A-3* transcripts in the seeds presumably reflects the need for translation of mRNAs required for radicle elongation during germination.

Gene duplications and gene families often encode, or are assumed to encode, proteins with similar or overlapping functions. However, it is apparent from the present study that the *eIF5A* genes of *Arabidopsis thaliana* have different roles in cell death and cell growth. AteIF5A-1 appears to play a role in cell death during xylem development and cotyledon/leaf/flower senescence. *AteIF5A-2* transcript is constitutively expressed, and expression of the cognate protein is up-regulated during pathogen ingress or wounding. AteIF5A-3 is expressed in the elongating meristems of roots, root hairs and pollen associated with the stigma and may be involved in the elongation of these cells. That these proteins have the very specific post-translational modification of hypusination and that eIF5A is the only known protein to contain this modification is indicative of their importance in the regulation of plant development. While the exact function of eIF5A isoforms in plant cells is yet to be elucidated, this study has revealed that regulation of their expression is complex and that they have distinct functions.

Chapter 3: Characterization of Diacylglycerol Acyltransferase 1 (DGAT1) in *Arabidopsis thaliana*[4]

3.1 Introduction

Lipids (*Greek: lipos, fat*) are a structurally diverse group of macromolecules that are preferentially soluble in nonaqueous solvents. They comprise a plethora of fatty acid-containing compounds, including pigments and secondary metabolites. Lipid bilayers are the major barriers defining the perimeter of the cell as well as cell organelles, providing compartmentalization of biochemical and physiological processes. In addition to their structural role, lipids are important metabolic intermediates and products, and also serve as signalling molecules and sources of energy. Each plant cell contains a diverse range of lipids, often associated with different cellular structures, and, in addition, some plant species contain highly specialized lipids.

3.1.1 Lipid classes commonly found in plants

Plants have five general classes of lipid that can be easily separated by thin layer chromatography: polar lipids, diacylglycerols, free fatty acids, triacylglycerols, and steryl and wax esters. Typically, these different types of lipids have distinguishable functions in the cell. The lipids vary in fatty acid saturation and chain length. Plant lipid metabolism is inherently complex due primarily to the cellular compartmentalization of eukaryotic and prokaryotic pathways of lipid synthesis and the extensive intermixing of lipid pools between these compartments.

3.1.2 Most fatty acids are esterified

Fatty acids are carboxylic acids with long-chain hydrocarbon side groups. All fatty acids in plants are synthesized within the plastids (Ohlrogge and Jaworski, 1997). During fatty acid biosynthesis, a repeated sequence of reactions incorporates acetyl moieties of acetyl-CoA onto the growing hydrocarbon chain. The most common fatty acids, which are present in both membranes and storage lipids, are the C_{16} and C_{18} fatty acids that are

[4] Some of the work presented in this chapter has been published in *Plant Physiology* (2002) 129: 1616-1626 with co-authors C. D. Froese and J. E. Thompson

completely saturated or contain up to three double bonds. More than 300 different fatty acids occur in plants (Millar *et al.*, 2000). Fatty acids that cannot be described by usual synthesis algorithms are considered "unusual" (Hellyer *et al.*, 1999). Several unusual fatty acids such as lauric (12:0), erucic (22:1) and ricinoleic acid (18:1-OH) are of substantial commercial importance (Voelker and Kinney, 2001). Less is known about the mechanisms for synthesis and accumulation of unusual fatty acids. Most unusual fatty acids occur exclusively in seed oils and may serve a defence function as some are toxic or indigestible (Badami and Patil, 1981). Free unesterified fatty acids are found in minute amounts in phloem sap (Madey *et al.*, 2002), associated with proteins (Taniguchi, 1999; Somerville *et al.*, 2000) and tend to accumulate during senescence within membranes (Barclay and McKersie, 1994; Thompson *et al.*, 1997; Thompson *et al.*, 1998). Free fatty acids are toxic due to their detergent-like effects on membranes (Thomas, 1984).

Most fatty acids are esterified to glycerol, giving rise to glycerolipids. There are three principal types of glycerolipids in plants: triacylglycerols, phospholipids, and glyceroglycolipids. The latter two are polar lipids and are typically found in membranes. Membrane glycerolipids have fatty acids attached to both the *sn*-1 and *sn*-2 positions of the glycerol backbone and a polar head group attached to the *sn*-3 position. If all three positions on glycerol are esterified with fatty acids, a triacylglycerol structure results that is not suitable for membrane structure as it lacks the amphipathic property of polar lipids.

3.1.2.1 Polar lipids are the main components of membranes

Lipids serve many functions in plants, though the most important function is their role as the major component of biological membranes. The hydrophobic barrier conferred upon membranes by their lipids is critical for life, serving to separate cells from their surroundings and the contents of organelles from the cytoplasm. Polar lipids are amphipathic and have both a hydrophilic head group and hydrophobic fatty acid tails (Somerville *et al.*, 2000). This property allows polar lipids to form bilayers (Singer and Nicolson, 1972). Lipid bilayers prevent the free diffusion of hydrophilic molecules between the cellular organelles as well as in and out of cells. This compartmentalization ensures that only specific molecules are transported in and out of the cell and between compartments through selective, vectorial

transport proteins. There are two main groups of polar lipids in plants: glyceroglycolipids and phospholipids (Ohlrogge and Browse, 1995). The thylakoid membranes of chloroplasts, in which the light reactions of photosynthesis take place, primarily contain glyceroglycolipids. Membranes external to plastids are composed mainly of mixtures of phospholipids.

3.1.2.1.1 Phospholipids of plants

Phospholipids are synthesized by esterification of fatty acids to the two hydroxyl groups of *sn*-glycerol 3-phosphate to produce phosphatidic acid (Ohlrogge and Browse, 1995). The products of fatty acid synthesis in plastids may be incorporated directly into chloroplast glycerolipids or exported to the cytoplasm as CoA esters which are then incorporated into endoplasmic reticulum glycerolipids. The first major product of glycerolipid synthesis is phosphatidic acid (Somerville *et al.*, 2000). Phosphatidic acids formed in the plastids by means of the "prokaryotic pathway" and in the endoplasmic reticulum through the "eukaryotic pathway" differ in fatty acyl composition and position (Millar *et al.*, 2000). The enzymes that perform these acylations have substrate specificity and, consequently, the prokaryotic pathway initially gives rise to glycerolipids with hexadecanoic acid (16:0) at the *sn*-2 position and in most cases oleic acid (18:1) at the *sn*-1 position. By contrast, the glycerolipid products of the eukaryotic pathway are highly enriched in C_{18} fatty acids, and if hexadecanoic acid (16:0) is present it is in the *sn*-1 position (Ohlrogge and Browse, 1995). These fatty acids, once incorporated into glycerolipids, can undergo desaturation by membrane- bound desaturases of the endoplasmic reticulum or plastid (Slabas and Fawcett, 1992). All phospholipids are derived from phosphatidic acid by esterification of a polar head group to the phosphoryl group (Somerville *et al.*, 2000). For example, the phosphatidic acid produced by the endoplasmic reticulum gives rise to phosphatidylcholine, phosphatidylethanolamine, phosphotidylserine and phosphatidylinositol (Ohlrogge and Browse, 1995). The only phospholipid derived from prokaryotic synthesis is phosphatidylglycerol (Somerville *et al.*, 2000).

3.1.2.1.2 Glyceroglycolipids of plants

The eukaryotic pathway is the principal route of glycerolipid synthesis in all nonphotosynthetic tissues as well as in the photosynthetic tissue of higher plants (Doermann and Benning, 2002). The phosphatidic acid produced through the eukaryotic pathway is used for phospholipid synthesis as well as chloroplast glyceroglycolipid synthesis. Plants that employ only the eukaryotic pathway for the synthesis of glyceroglycolipids are termed 18:3 plants, because the fatty acids incorporated in the glyceroglycolipids of these plants contain only linolenic acid (18:3) as the polyunsaturated fatty acid component (Awai *et al.*, 2001). Plants that synthesize glyceroglycolipids from precursors of the eukaryotic pathway utilize the diacylglycerol moiety of phosphatidylcholine released by a phosphatidylcholine phosphatase. The diacylglycerol moiety enters the diacylglycerol pool within the chloroplast envelope, where it is then incorporated into the glyceroglycolipids of the chloroplast (Ohlrogge and Browse, 1995). Some plants, including spinach and *Arabidopsis,* are known as 16:3 plants and depend heavily on the prokaryotic fatty acid synthesis pathway for glyceroglycolipid formation. The glyceroglycolipids of these plants contain the polyunsaturated fatty acids, hexadecatrienoic acid (16:3) and linolenic acid (18:3) (Jarvis *et al.*, 2000).

Glyceroglycolipids have a galactosyl or sulfoquinovosyl head group. The glyceroglycolipids of the chloroplasts include the galactolipids, monogalactosyl diacylglycerol (MGDG), digalactosyl diacylglycerol (DGDG) and the sulfolipid sulfoquinovosyl diacylglycerol (SQD). These unusual lipids are found almost exclusively in the thylakoid membrane except, for example, under conditions of phosphate starvation where DGDG is substituted for phospholipids in extraplastidial membranes such as the plasma membrane (Andersson *et al.*, 2005; Nakamura *et al.*, 2005) and mitochondrial membranes (Jouhet *et al.*, 2004). The thylakoid membrane is the internal photosynthetic membrane of higher plant chloroplasts and is the most abundant membrane found in nature (Lee, 2000). Only about 10% of thylakoid membrane lipid is phospholipid, specifically phosphatidylglycerol, and of the remainder, 50% is MGDG, and 30% DGDG (Harwood and Russell, 1984).

In *Arabidopsis*, the diacylglycerol moieties incorporated into galactolipids are derived from the prokaryotic and eukaryotic pathways in approximately equal proportions (Doermann and Benning, 2002). MGDG is predominantly synthesized from prokaryotic-derived diacylglycerol and is characterized by a high content of hexadecatrienoic acid (16:3) (Miege *et al.*, 1999). In this case, the diacylglycerol moiety is derived from phosphatidic acid, which is cleaved by a plastid phosphatidic acid phosphatase. DGDG is mostly of eukaryotic origin and therefore contains linolenic acid (18:3) rather than hexadecatrienoic acid (16:3). The MGDG and DGDG synthases are localized on the inner and outer envelopes of the chloroplast, and in *Arabidopsis* there are three isoforms of MGDG synthase and two isoforms of DGDG synthase (Froehlich *et al.*, 2001). Since MGDG and DGDG are synthesized in the non-photosynthetic membranes of the chloroplast, they must be transported to the thylakoids. It is thought that the galactolipids synthesized in the outer envelope are transported to the inner envelope by lipid transfer proteins (Sánchez-Fernández *et al.*, 2001). For the transport of MGDG and DGDG from the inner envelope to the thylakoids, a vesicular mechanism has been proposed. For example, in plants that are adapting to low temperatures it has been observed that vesicles formed from the inner envelope appear in the stroma (Kroll *et al.*, 2001). Thus, galactolipids are probably transported in the form of vesicles from their site of synthesis to the thylakoid membranes.

Not only do the galactolipids, MGDG and DGDG, have unique head groups, they are also unusual in that they contain two highly unsaturated fatty acyl chains, typically linolenic acid (18:3), leading to unique packing properties when compared to other membrane lipids. Most other membrane lipids contain one saturated and one unsaturated fatty acid chain. MGDG, although a polar amphipathic lipid, does not spontaneously form bilayers in water (Lee, 2000). This is due to its conical shape. By contrast, phosphatidylcholine has a cylindrical shape and does form bilayers in water. The head group of MGDG is larger than choline, but still smaller than the volume occupied by two polyunsaturated fatty acid chains, thus accounting for its conical shape. Cones do not pack well into planar arrays, preferring to assume curved structures (Lee, 2000). Obviously, biological membranes, which are bilayered, cannot be built from lipids that take on this conformation. However MGDG lies in tight association with chlorophyll a/b protein, which

forces it into a bilayer conformation (Jarvis *et al.*, 2000). DGDG has a larger head group than MGDG that occupies a volume comparable to the girth of the two polyunsaturated fatty acids and thus, like phosphatidylcholine, is cylindrical in shape. The different shape of thylakoid lipids together with their association with proteins enables the stacked arrangement of the grana. Stacking leads to a very precise distribution of the components of photosynthesis within the plane of the thylakoid membrane. Specifically, photosystem I is highly enriched in the stromal thylakoid membranes, and photosystem II is concentrated in the stacked thylakoid membranes (Lee, 2000). MGDG, presumably because of its conical shape, is essential for thylakoid stacking (Jarvis *et al.*, 2000).

3.1.2.2 Triacylglycerols are storage lipids

The fats and oils that occur in plants and animals consist largely of triacylglycerols, which are also referred to as triglycerides or neutral fats (Somerville *et al.*, 2000). These non-polar, water-insoluble substances are fatty acid tri-esters of glycerol. Plant oils are usually richer in unsaturated fatty acids than are animal fats, as the lower melting points of oils imply. While animals use fats for energy storage, plants use them mainly for carbon storage. On a mass basis, the ATP yield from catabolism to carbon dioxide and water is approximately twice as high for triacylglycerols as for carbohydrates. In cases where a compact seed is advantageous for facilitating dispersal, the carbon and energy required for seed germination are stored in the form of triacylglycerols rather than starch. Plant triacylglycerols are mainly found in seeds and pollen, though most tissues are capable of synthesizing small amounts of triacylglycerol (Hobbs *et al.*, 1999).

3.1.2.2.1 Enzymes that catalyze triacylglycerol synthesis

Triacylglycerol formation can either be acyl-CoA dependent or acyl-CoA independent. One gene family known to be involved in acyl-CoA independent triacylglycerol synthesis is that encoding phospholipid: diacylglycerol acyltransferase (PDAT). This enzyme catalyzes triacylglycerol formation using phospholipids such as phosphatidylcholine or phosphatidylethanolamine as acyl donors for diacylglycerol esterification (Banas *et al.*, 2000). PDAT activity has been reported in sunflower, castor

bean, *Crepis plaestina* and yeast microsomes (Dahlqvist *et al.*, 2000; Oelkers *et al.*, 2000). The physiological function of PDAT is yet to be determined, but it is speculated to be involved in the esterification of unusual fatty acids in oilseeds (Banas *et al.*, 2000) and to play a role in regulating the fatty acid composition of membrane lipids (Dahlqvist *et al.*, 2000). PDAT is not the foremost enzyme for triacylglycerol synthesis in seed-oil deposition. In fact, knockout lines of PDAT in *Arabidopsis* have essentially the same seed fatty acid content and composition as wild type plants (Mhaske *et al.*, 2005).

Enzymes that are the major contributors to seed triacylglycerol formation are unique to the Kennedy pathway in which diacylglycerol and acyl-CoA are substrates. There are two gene families known to encode enzymes that mediate triacylglycerol formation through this "classic" pathway, DGAT1 and DGAT2. The first DGAT gene to be cloned, DGAT1, has high sequence similarity to sterol acyltransferase (Cases *et al.*, 1998). DGAT2 was first found in the oleaginous fungus, *Morteriella ramanniana* (Cases *et al.*, 2001; Lardizabal *et al.*, 2001). DGAT2 genes have no sequence similarity to DGAT1, but appear to be ubiquitous in fungi, plants and mammals. In humans, there are several DGAT2 isoforms and only one DGAT1 isoform. These families of triacylglycerol- synthesizing enzymes have been characterized in humans as a target for potential therapeutics for obesity (Chen and Farese, 2000). In yet another alternative mechanism for triacylglycerol synthesis in animals and plants, diacylglycerol-diacylglycerol-transacylase mediates its formation using diacylglycerol as an acyl donor and acceptor, although no gene coding such a transacylase has been identified yet (Stobart *et al.*, 1997). That there are four enzymes mediating triacylglycerol formation raises the possibility that they contribute to the accumulation of triacylglycerol at different stages of plant development and possibly in different cellular compartments.

Diacylglycerol acyltransferase (DGAT; EC 2.3.1.20) mediates the final acylation step in the synthesis of triacylglycerol from diacylglycerol. DGAT1 is present in most plant organs, including leaves, petals, fruits, anthers and developing seeds (Hobbs *et al.*, 1999; Zou *et al.*, 1999). Early plant DGAT research was largely limited to studies of activity profiles in homogenates or of membranes isolated from various tissues including developing seeds and

microspore-derived embryos (Martin and Wilson, 1984; Wilson and Kwanyuan, 1986; Ichihara *et al.*, 1988; Sakaki *et al.*, 1990; Sakaki *et al.*, 1990; Stobart *et al.*, 1997). These early studies included partial purification of DGAT from cotyledons of germinating soybean seeds (Kwanyuen and Wilson, 1986), microsomal membranes of developing safflower seeds (Stobart *et al.*, 1997) and ozone-treated spinach leaves (Martin and Wilson, 1984). A DGAT1 gene was first cloned from mouse, and homologous DGAT1 genes have since been cloned from *Arabidopsis* and other plants. There is only one DGAT1 gene in *Arabidopsis,* and mutants of DGAT1 have demonstrated that this gene contributes significantly to triacylglycerol synthesis in developing seeds (Katavic *et al.*, 1995; Zou *et al.*, 1999; Jako *et al.*, 2001).

The *Arabidopsis thaliana* DGAT1 gene (At2g19450) is found on chromosome II, approximately 17.5±3cM from the *sti* locus and 8±2cM from the *cp2* locus (Zou *et al.*, 1999). It has been established that the *Arabidopsis* expressed sequence tag (EST) clone E6B2T7 corresponds to the DGAT1 gene, and the full-length cDNA for DGAT1 (approximately 2.0kb) has been sequenced (Hobbs *et al.*, 1999). An EMS-induced DGAT1 *Arabidopsis* mutant has been shown to have lower seed oil deposition (Zou *et al.*, 1999) as well as altered triacylglycerol fatty acid composition. Specifically, the triacylglycerol of mutant seeds (AS11) in comparison to that of wild-type seeds has reduced eicosenoic acid (20:1), reduced oleic acid (18:1) and enhanced linolenic acid (18:3) (Katavic *et al.*, 1995). AS11 seeds also accumulate diacylglycerol, a precursor to triacylglycerol, indicating that the reduction in triacylglycerol synthesis was not due to a lack of substrate. The mutant phenotype was rescued by transformation with DGAT1 expressed in the sense orientation driven by a seed specific promoter, confirming that it was attributable to malfunctioning DGAT1 (Jako *et al.*, 2001). Several studies, including over-expression of DGAT1, have demonstrated that there is a correlation between DGAT1 expression levels and seed oil content suggesting that DGAT1 catalyzes the rate-limiting step in triacylglycerol biosynthesis (Ichihara *et al.*, 1988; Zou *et al.*, 1999; Bouvier-Nave *et al.*, 2000; Jako *et al.*, 2001).

3.1.3 Lipid bodies in plants

Triacylglycerols are usually packaged into lipid- and protein-containing particles termed lipid bodies. Most triacylglycerol-containing lipid bodies have similar morphologies, where the triacylglycerol is localized in the central portion of the particle and is surrounded by a monolayer of phospholipids associated with a stabilizing protein. Plants have different types of lipid bodies including the oil bodies of seeds and plastoglobuli of the chloroplasts.

3.1.3.1 Seed oil bodies

In seeds, triacylglycerol is synthesized within the membranes of the endoplasmic reticulum and subsequently released into the cytosol as oil bodies (Huang, 1992). True oilseeds can accumulate oil bodies as one of their major storage reserves in amounts of 20 to 70% of the total seed weight (Murphy, 2001). The storage triacylglycerol is localized in the interior of the oil body, and the surfaces of the oil bodies are coated with a monolayer of phospholipids. In oil bodies of desiccation tolerant seeds, the phospholipid monolayer is associated with a protein termed oleosin (Huang, 1996). The acyl chains of the phospholipid monolayer and the central hydrophobic domain of oleosin are embedded in the triacylglycerol interior of the oil body (Murphy, 1993). Oleosin is a small structural protein that is thought to prevent coalescence of oil bodies during seed rehydration (Hills *et al.*, 1993) and may act as a platform for triacylglycerol lipases (Huang, 1996). Also, the greater surface area to volume ratio that oleosin-containing lipid bodies maintain may facilitate efficient breakdown of the storage lipid within (Napier *et al.*, 1996). Certain oleogenic fruits that lack stabilizing proteins such as oleosins have very large oil globules that are not metabolized (Giannoulia *et al.*, 2000).

That oil bodies originate from the endoplasmic reticulum is consistent with the finding that enzymes of triacylglycerol synthesis, including DGAT, are present in microsomal membrane fractions, which are known to contain vesicles of endoplasmic reticulum (Kwanyuen and Wilson, 1986). In addition, triacylglycerol can be synthesized *in vitro* in the presence of microsomes isolated from developing seeds (Lacey *et al.*, 1999). Oil bodies are formed during the final stages of seed development when the storage triacylglycerol accumulates. They form from endoplasmic reticulum, where localized

accumulation of triacylglycerol within the monolayers of the endoplasmic reticulum occurs (Lacey *et al.*, 1999). That is, triacylglycerol tends to accumulate at its site of synthesis, rather than equilibrate with the bulk pool of membrane lipids (Murphy, 2001). The oleosins associated with oil bodies are synthesized in association with the endoplasmic reticulum and are co-translationally inserted into the membrane (Hills *et al.*, 1993). The physical forces resulting from the accumulation of triacylglycerol within the membrane bilayer cause the oil body to bud into the cytosol (Napier *et al.*, 1996), taking some of the endoplasmic reticulum phospholipids as a half-unit membrane as well as the membrane associated oleosins. Oil bodies have never been reported in the lumen of endoplasmic reticulum, indicating that the release of these particles is vectorial. Lipid particles in animal cells are similarly formed (Brindley and Hubscher, 1965; Murphy, 2001).

Although triacylglycerol formation in seeds is believed to occur in the endoplasmic reticulum, there have been several reports indicating that purified chloroplast envelope membranes from leaves are also capable of synthesizing this storage lipid (Siebertz *et al.*, 1979; Martin and Wilson, 1983, 1984). Moreover, triacylglycerol is known to be present in plastoglobuli, which are lipid bodies localized in the stroma of chloroplasts (Martin and Wilson, 1984). DGAT is unique to the triacylglycerol biosynthetic pathway (Bao and Ohlrogge, 1999) and the finding that different types of membranes are capable of synthesizing triacylglycerol suggests that DGAT may have more than one subcellular localization.

3.1.3.2 Chloroplastic lipid bodies

Plastids are maternally inherited organelles that serve to distinguish plant cells from animal cells. All plastids, be they chloroplasts, etioplasts, chromoplasts or amyloplasts, originate from proplastids, which have little or no internal structure (Bauer *et al.*, 2000). While plastids are capable of synthesizing many of their own proteins, the majority of chloroplast proteins are encoded by the nuclear genome and synthesized as precursors in the cytosol. Chloroplasts are the chlorophyll-containing plastids of leaves. Leaf plastids undergo a sequence of structural changes during development to form these photosynthetic organelles. Once they are fully developed, chloroplasts are very complex and contain six subcellular

compartments, namely the outer envelope membrane, the inner envelope membrane, the intermembrane space, the stroma, the thylakoid membranes and the thylakoid lumen. Chloroplasts typify healthy leaf tissues, and as the leaf tissues age and begin to senesce, the chloroplast changes through a precise process of degradation leading to the development of organelles termed gerontoplasts (Sitte *et al.*, 1980). Chlorophyll degradation, a hallmark of leaf senescence, is a symptom of the transition of chloroplasts to gerontoplasts. This conversion is reversible in the leaves of many species (Gan and Amasino, 1995; Novikova *et al.*, 1999) and is controlled by nuclear gene expression (Matile, 1992).

Plastids contain lipid particles, and the best studied of these are the plastoglobuli. Plastoglobuli are similar in structure to other lipid bodies and vary in their size and numbers depending on the species of plant as well as the developmental stage. The size and number of plastoglobuli increases during senescence. Thus, fully developed gerontoplasts consist of a still intact envelope surrounding a number of large plastoglobuli. However, plastoglobuli are also present in the chloroplasts of young healthy leaves. The contents of young plastoglobuli and those of older leaves differ in composition, and it has been suggested that plastoglobuli in chloroplasts of young leaves may serve as a source of reserve components for thylakoid formation (Sarafis, 1998). Plastoglobuli have been reported to contain proteins, polar lipids, pigments and neutral lipids including triacylglycerol (Steinmuller and Tevini, 1985; Sarafis, 1998), implying that chloroplasts contain the required acyltransferases and lipid-body-stabilizing proteins for their formation. Some reports on plastoglobuli composition, however, contradict other reports, and thus it has been suggested that there are in fact two distinguishable populations of particles. Some plastoglobuli particles have been reported to contain photosynthetic protein catabolites (Ghosh *et al.*, 1994) and cytochrome *f* (Smith *et al.*, 2000), and it has been proposed that these particles may be involved in thylakoid membrane turnover in healthy leaves.

During leaf senescence, both the number and the size of plastoglobuli increase dramatically as the thylakoid membranes are dismantled (Thomas, 1982; Matile, 1992). Clearly, these plastid lipid bodies are serving as temporary stores for the neutral lipid breakdown products of the photosynthetic membranes. The contents of the plastoglobuli are

apparently salvaged by the parent plant before leaf abscission (Steinmuller and Tevini, 1985), but the mechanisms underlying this remain to be elucidated. During leaf senescence, there are ultrastructural changes to chloroplasts that include swelling of thylakoids and an increase in size and abundance of plastoglobuli (Barton, 1966; Meier and Lichtenthaler, 1982; Kolodziejek *et al.*, 2003). It is thought that the degradation of the thylakoid membranes is responsible for the increase in plastoglobuli. The ultrastructural changes within chloroplasts are correlated with changes in the level of pigments (Kolodziejek *et al.*, 2003), specifically the decline in chlorophyll. The ultrastructural changes of chloroplasts during senescence are reminiscent of changes caused by different environmental agents that induce oxidative stress (Mostowska, 1999). For example, there is also an increase in plastoglobuli abundance during oxidative stress leading to premature senescence. Cell membranes are one of the first targets of plant stress (Levitt, 1972). The maintenance and/or breakdown of membranes under stress may be an important strategy for tolerance. Even algae grown under sub-optimal conditions are known to accumulate triacylglycerol within their chloroplasts (Cohen *et al.*, 2000). The appearance of large and abundant plastoglobuli in stressed leaves is coincident with the catabolism of polar lipids, especially MGDG (El-Hafid *et al.*, 1989; Sahsah *et al.*, 1998; Kaniuga *et al.*, 1999).

As is the case for oil bodies, it is thought that there is a protein involved in prevention of coalescence of plastoglobuli. An abundant protein termed the plastid lipid-associated protein (PAP) has been reported to bind to the boundary of plastoglobuli in chromoplasts and other plastids of capsicum (Pozueta-Romero *et al.*, 1997). Another older name for PAP is fibrillin (Deruere *et al.*, 1994). PAP-related proteins appear to be a part of a well-conserved group expressed both in dicotyledonous and monocotyledonous plants. PAP is present in most plastid types and is associated with the lipid bodies of plastids (Ting *et al.*, 1998). When PAP from pepper was over-expressed in tobacco, there was a change in both the number and distribution of plastoglobuli (Rey *et al.*, 2000). Specifically, there were more plastoglobuli in both the chloroplasts and chromoplasts of the transgenic plants, and the plastoglobuli, rather than being separate, had formed clusters. Interestingly these PAP-over-expressing plants also exhibited enhanced growth during high light stress (Rey *et al.*, 2000).

3.1.4 Lipases

Enzymes that de-esterify fatty acids from complex lipids are termed lipases. They are hydrolytic enzymes found in all forms of life (Bishop, 1971). They are involved in many aspects of the cell function including mobilization of storage lipid, catabolism of membrane lipids during senescence and stress, and release of fatty acids that are important in cell-signalling cascades. Lipases are classified by the substrate they catabolize. Many lipases contain a 10 amino acid consensus sequence, [LIV]-X-[LIVAFY]-[LIAMVST]-G-[HYWV]-S-X-G-[GSTAC], termed the lipase consensus sequence (Derewenda and Derewenda, 1991). Some lipases are non-specific and can cleave fatty acids from a variety of substrates including phospholipids, wax esters and triacylglycerols (Beisson *et al.*, 2000). True lipases are defined as enzymes that attack triacylglycerols at an oil-water interface, and they are also known as triacylglycerol acyl hydrolases (Galliard, 1980). Other lipases like galactolipases and some phospholipases belong to the group of enzymes termed lipolytic acyl hydrolases (Galliard, 1980). These latter two lipases utilize polar membrane lipids rather than triacylglycerols as substrates.

3.1.4.1 Phospholipases

Phospholipids are glycerolipids with two esterified fatty acids at the *sn*-1 and *sn*-2 positions with a phosphate and associated polar head group at the *sn*-3 position (Somerville *et al.*, 2000). Not only are phospholipids the structural basis of cellular membranes, they are also precursors for the generation of cellular regulators. Hydrolysis of phospholipids by phospholipases is often the first step in generating lipid and lipid-derived messengers. Phospholipids can be hydrolyzed by phospholipases, which are classified on the basis of their point of attack.

Phospholipase D, which forms phosphatidic acid, is the best characterized phospholipase, and there are several isoforms of this enzyme in *Arabidopsis* (Wang, 2000). There are reports that phospholipase D plays a role in senescence (Ryu and Wang, 1995; Wang, 2000). During senescence, membranes lose structural integrity due to a loss of membrane phospholipids and a relative increase in free fatty acids and sterols (Thompson, 1988). It appears that phospholipase D has several subcellular localizations and that it is

involved in the release of signalling molecules during wounding and senescence (Fan *et al.*, 1999; Wang, 2000). Phospholipase C releases diacylglycerol, a known cellular signalling molecule. Diacylglycerol is known to activate kinases, specifically protein kinase C, and thus several downstream operations (Munnik *et al.*, 1998). Phospholipase A_2, catalyzes de-esterification of the fatty acid in the *sn*-2 position of phospholipids. Certain isozymes of phospholipase A_2 are known to release the fatty acid, linolenic acid (18:3), leading to the formation of jasmonic acid and related signalling molecules (Wang, 2001). Thus phospholipase A_2 initiates the octadecanoid pathway, which in turn regulates such cellular processes as wounding and the defence response.

3.1.4.2 Galactolipases

Galactolipases de-esterify fatty acid moieties from galactolipids and have been assayed in senescing leaves and even partially purified from senescing leaves of several species of plants (Anderson *et al.*, 1974; Gemel and Kaniuga, 1987; O'Sullivan *et al.*, 1987; El-Hafid *et al.*, 1989; Kaniuga *et al.*, 1999). Galactolipase activity increases during senescence and under conditions of environmental stress (Sastry and Kates, 1964; Anderson *et al.*, 1974; O'Sullivan *et al.*, 1987; El-Hafid *et al.*, 1989; Engelmann-Sylvestre *et al.*, 1989; Kaniuga *et al.*, 1999; Kim *et al.*, 2001; Matos *et al.*, 2001). Galactolipase appears to be associated with the stromal surface of thylakoid membranes (O'Sullivan *et al.*, 1987) and exhibits autocatalytic activation attributable to the detergent-like action of linolenic acid (18:3) released by its action on galactolipids (Galliard, 1971). However, cloning of the genes encoding galactolipases and full characterization of their function in plant development and senescence has yet to be accomplished.

3.1.4.3 Triacylglycerol lipases

The initial step in the conversion of stored lipid to carbohydrate is the breakdown of triacylglycerols stored in the oil bodies by lipases. The mobilization of seed lipid occurs during imbibition and germination. The initial imbibition of water leads to cell expansion and release of the new seedling from the seed coat. Triacylglycerols stored in the seed lipid bodies are hydrolyzed to glycerol and fatty acids. This is followed by β-oxidation of the

fatty acids to produce acetyl-CoA. The fatty acids are oxidized in a type of peroxisome termed glyoxysomes (DeBellis and Nishimura, 1991). Glyoxysomes are capable of metabolizing acetyl-CoA to succinate, which is transported to the mitochondrion where it is converted first to oxaloacetate and then to malate. The process ends in the cytosol where malate is converted to glucose through gluconeogenesis, and then to sucrose or other phloem mobile sugars (Graham *et al.*, 1990). In many plants, triacylglycerols also appear to serve as precursors for the rapid synthesis of membrane phospholipids to support pollen tube growth (Murphy, 2001).

Triacylglycerol lipase de-esterifies the fatty acids at each of the *sn* positions of triacylglycerol (Somerville *et al.*, 2000). Lipid bodies from fully dehydrated seeds tend to be resistant to lipase attack (Murphy, 1993). In castor bean endosperm, the triacylglycerol lipase is associated with the oil body phospholipid monolayer (Ory *et al.*, 1960; Ory, 1969). Oil bodies of corn (Lin *et al.*, 1983; Lin and Huang, 1984) and cotton (Smaoui and Cherif, 2000) also exhibit lipase activity, but in peanut (Jacks *et al.*, 1967) and soybean (Lin *et al.*, 1982), triacylglycerol lipase activity is present instead in the glyoxysomes. During the breakdown of lipids, oil bodies and glyoxysomes are generally in close physical association. Triacylglycerol lipase activity is thought to be influenced by oil body oleosins, which harbour a putative lipase attachment site. Oleosins also maintain a high surface area to volume ratio, which increases the accessibility of the stored triacylglycerol molecules to lipases (Napier *et al.*, 1996).

Despite the massive scale of lipolysis in germinating oil seeds, the triacylglycerol lipases responsible have yet to be completely characterized. Studies of lipase activity in germinating seedlings indicate that physiologically active lipase is soluble and co-isolates with both membranes and lipid bodies (Lin *et al.*, 1983). The lipase must associate with lipid bodies in order to access its triacylglycerol substrate, but it seems likely that lipolysis occurs in association with a site where the catabolized products are further utilized, for example glyoxysomes (Lin *et al.*, 1982) or the endoplasmic reticulum (Antonian, 1988). A putative triacylglycerol lipase has been cloned and characterized in our lab (Padham, 2002). This triacylglycerol lipase appears to be multifunctional and very important for plant growth and

development. For example, its suppression in transgenic plants resulted stunted growth which was partially rescued by the addition of sucrose during germination (Padham, 2002). This suggests that it is involved in mobilization of seed triacylglycerol. However, this lipase is also present in chloroplasts and increases in abundance in senescing leaves (Padham, 2002).

3.1.5 The role of lipid bodies and lipid metabolizing enzymes during development in plants

The presence of lipid bodies in different plant tissues together with their formation at specific stages of development and following episodes of environmental stress implies that enzymes involved in the synthesis and catabolism of lipids play an important role in development and the response of plants to stress. Support for this contention includes the finding that down-regulation of a triacylglycerol lipase delays seedling establishment and results in stunted growth (Padham, 2002). Also, plants that carry mutations in an MGDG synthase gene have compromised photosynthesis (Jarvis *et al.*, 2000). As well, suppression of SAG101, as senescence-associated lipolytic acyl hydrolase, has been shown to delay leaf senescence, whereas over-expression of the same gene resulted in precocious leaf senescence (He and Gan, 2002).

The present study demonstrates that DGAT1 is up-regulated during senescence of *Arabidopsis* leaves in a manner that is temporally correlated with increased levels of thylakoid fatty acids in triacylglycerol. The chloroplast is the first organelle of mesophyll cells to be affected by senescence, and the onset of chloroplast senescence appears to be initiated by nuclear-encoded proteins (Matile, 1992). Recruitment of membrane carbon from senescing leaves, particularly senescing chloroplasts, to growing parts of the plant is a key feature of leaf senescence, and it involves de-esterification of thylakoid lipids and conversion of the resultant free fatty acids to phloem-mobile sucrose (Matile, 1992). De-esterification of thylakoid lipids appears to be mediated by one or more senescence-induced galactolipases (Engelmann-Sylvestre *et al.*, 1989). The results of the present study indicate that formation of triacylglycerol may be an intermediate step in this mobilization of membrane lipid carbon to phloem-mobile sucrose during leaf senescence.

3.2 Materials and Methods

3.2.1 *In silico* analysis of *Arabidopsis thaliana* DGAT1

3.2.1.1 DGAT1 sequence from *Arabidopsis thaliana*

A search was performed for the sequence of *Arabidopsis thaliana* DGAT at the Entrez Homepage (http://www.ncbi.nlm.nih.gov/gquery/gquery.fcgi). DGAT1 (At2g19450) is not the annotated gene name. However, the corresponding protein has since been described as DGAT1 (Lu *et al.*, 2003). By following the links to the mRNA, protein or genomic sequence, the respective sequences were obtained and aligned manually (Figure 3-1). Also, a region 2 kilobases upstream of the DGAT1 start codon (ATG) was used for the promoter analysis.

3.2.1.2 Detection of putative signalling sequences in DGAT1 protein

Several online programs for plant protein signalling sequences were used for the detection of putative signalling sequences in the DGAT1 amino acid sequence (AAK96671). Programs used for this purpose were ScanProsite (http://au.expasy.org/prosite/), PSORT version 6.4 (http://psort.nibb.ac.jp/), TargetP (http://www.cbs.dtu.dk/services/TargetP/), ChloroP (http://www.cbs.dtu.dk/services/ChloroP/) and Predotar (http://genoplante-info.infobiogen.fr/predotar/predotar.html).

3.2.1.3 Alignment of DGAT1 sequences from different plant species

The *Arabidopsis thaliana* DGAT1 protein sequence (AAK96671) was submitted into the protein-protein BLAST (blastp) search engine (http://www.ncbi.nlm.nih.gov/BLAST/) to find DGAT1 annotated for other plant species. Sequences for six representative oil-producing plant species were chosen and aligned using DIALIGN available at http://bibiserv.techfak. uni-bielefeld.de/dialign with the threshold set to zero and N=5 (Morgenstern, 1999).

Figure 3-1: Alignment of the DGAT1 gene with the DGAT1 protein sequence

The 17 exons are underlined, with the 15 introns unformatted in between. The EST clone E6B2T7 used for Northern blot analysis is indicated in yellow highlight and includes part of the 3'UTR and part of the coding sequence. The C-terminal peptide that was used for the production of polyclonal antibodies is highlighted in blue.

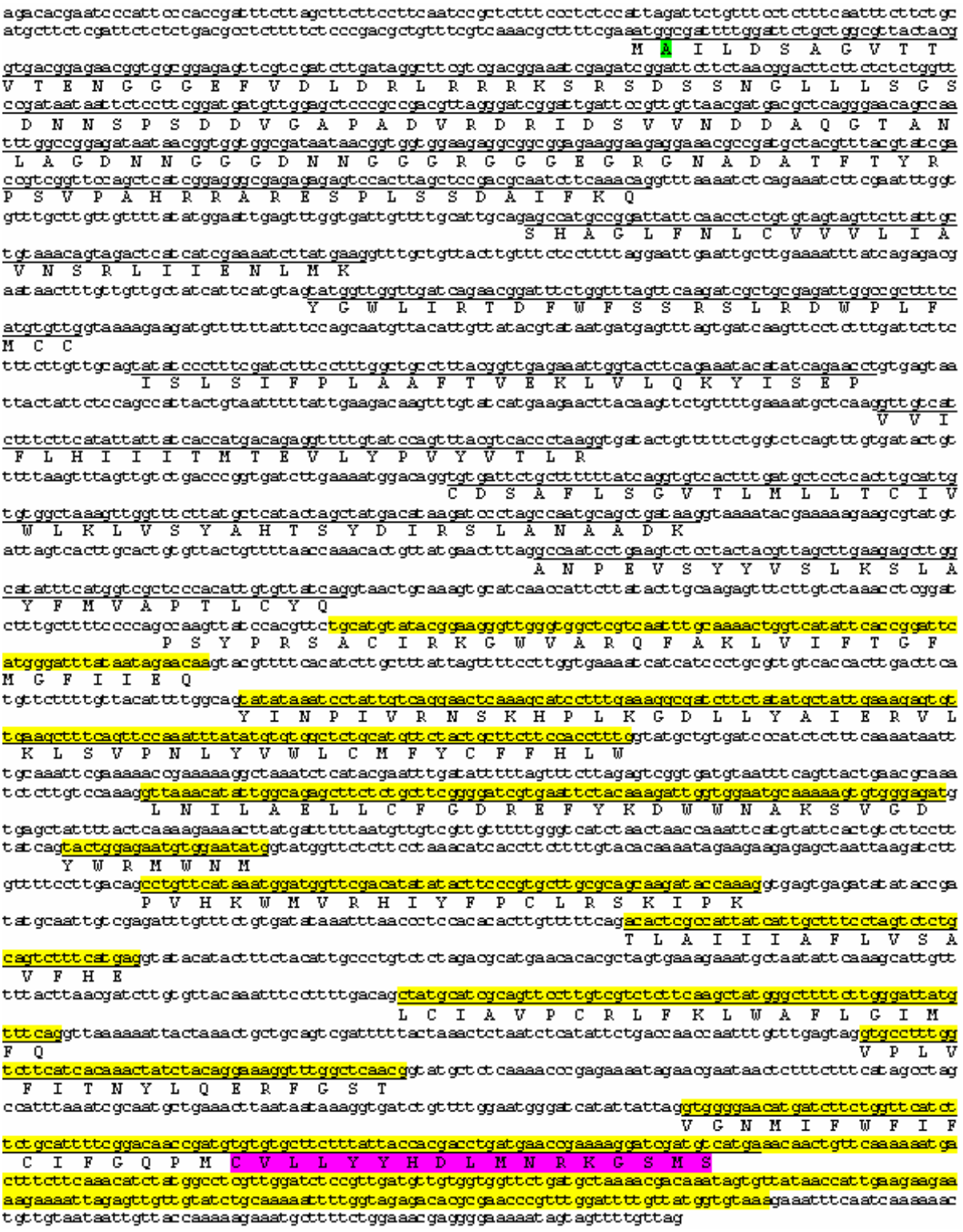

3.2.1.4 Analysis of putative *cis*-acting elements of the DGAT1 promoter

Putative *cis*-acting elements of the DGAT1 promoter were identified using the PLACE (Plant *Cis*-acting Regulatory DNA Elements) program (http://www.dna.affrc.go.jp/PLACE/). A segment of genomic DNA, upstream of the DGAT1 start codon (ATG), 2 kilobases long was submitted to the PLACE Signal Scan Search. A table summarizing some of the putative *cis*-acting elements identified by PLACE was compiled.

3.2.2 Plant material

Seeds of *Arabidopsis thaliana*, ecotype Columbia, were grown in Promix BX soil (Premier Brands, Brampton, Ontario, Canada) in 6-inch pots. Freshly seeded pots were maintained at 4°C for 2 days and then transferred to a growth chamber operating at 22°C with 16-h light/8-h dark cycles. Lighting at 150 μmol radiation $m^{-2} \cdot s^{-1}$ was provided by cool-white fluorescent bulbs. Rosette leaves were harvested after 2, 3, 4, 5, and 6-weeks of growth. Roots, stems, cauline leaves, flowers and siliques were collected from 6-week-old plants. Harvested tissues were either used immediately or frozen in liquid nitrogen and stored at -80°C until analyzed.

3.2.3 RNA analysis

3.2.3.1 RNA isolation and fractionation

Total RNA for Northern blot analysis was isolated from *Arabidopsis thaliana* rosette leaves according to standard protocol (Davis *et al.*, 1986). The plant tissue was ground to a fine powder in liquid nitrogen with a mortar and pestle. The powder was added directly to 10-20mL GIT buffer (4M guanidine isothiocyanate, 25mM sodium acetate, pH 6.0, 0.84mL 2-mercaptoethanol/100mL GIT buffer) in a 50mL Falcon tube and mixed well. The GIT buffer/plant tissue mixture was filtered through Miracloth and layered onto a 10mL cushion of cesium chloride in 35mL disposable polyallomer ultraclear centrifuge tubes. The tubes were balanced and loaded onto a SW28 Ti ultracentrifuge rotor and centrifuged overnight (~16 hours) at 90000 *g* in a Beckman Ultracentrifuge at a maximum temperature of

10°C. The RNA pellet at the bottom of the tube was rinsed briefly with cold 70% ethanol and resuspended in resuspension buffer (0.5M sodium acetate, pH 5.2). The RNA was then either ethanol- precipitated directly or extracted with phenol: chloroform: isoamyl alcohol (25:24:1) before ethanol precipitation. Ethanol precipitation was carried out at -80°C for at least 2 hours. The RNA precipitate was centrifuged into a pellet in a microcentrifuge at maximum speed at 4°C. The resulting pellet was washed in 70% ethanol, dried and resuspended in DEPC-treated water, the volume of which depended on the size of the RNA pellet. RNA quantity and quality were measured with a spectrophotometer. An adjusted OD_{260}, which gave a more accurate RNA quantity, was calculated using the formula: $OD_{260adjusted} = OD_{260} - |OD_{240} - OD_{280}| - OD_{320}$. RNA was aliquoted into 10µg amounts and stored at -80°C.

3.2.3.2 Northern blotting

Purified RNA was fractionated on a 1% agarose formaldehyde denaturing gel (1% agarose, 9% formaldehyde, in 1X MOPS [20mM MOPS, 5mM sodium acetate, 1mM EDTA, pH 7.0]) and transferred to nylon membranes (Hybond-N+, Amersham Biosciences, UK). Briefly, the quantified RNA was mixed with 20µL Ross Hardison solution (60% formamide, 20% formaldehyde, 0.8% bromophenol blue in 1X MOPS), and 0.5µL ethidium bromide (0.5µL/µL). The RNA was heated to 65°C for 5 minutes and immediately placed on ice to cool before loading onto the 1% agarose formaldehyde denaturing gel submerged in cooled 1X MOPS. Electrophoresis was performed at 210V for 10 minutes, forcing the sample into the gel, then continued at 75V for 1.5-2 hours. The RNA was transferred to nylon membrane through upward capillary action, with 10X SSC buffer (1.5M sodium chloride, 0.15M sodium citrate – $2H_2O$, pH 7.0) overnight (Davis *et al.*, 1986). The transferred RNA was cross-linked with UV and photographed for a loading control. Immobilized RNA was pre-hybridized for 2 hours in a pre-hybridization solution (40% formamide, 6X SSC, 1X Denhart's solution, 0.5% SDS, 2mg denatured salmon sperm DNA) at 42°C in the hybridization oven. During the pre-hybridization, the radio-labelled probe was synthesized using DGAT1 EST clone, E6B2T7 (Arabidopsis Biological Resource Center, OH, USA; highlighted in yellow in Figure 3-1). E6B2T7 was labelled with [α-^{32}P]-dCTP using a

random primer kit (Boehringer Mannheim) and passed through a Sephadex G-50 column to remove any unincorporated [α-^{32}P]-dCTP. The prehybridization solution was removed and the membranes were hybridized with denatured 1x10^6 cpm/mL DGAT1 probe overnight at 42^{o}C. The hybridized membranes were washed twice in 2X SSC (0.3M sodium chloride, 0.03M sodium citrate, pH 7.0) containing 0.1% SDS at 42^{o}C for 15 minutes and twice in 1X SSC containing 0.1% SDS at 42^{o}C for 30 minutes. Hybridization was visualized by autoradiography after an overnight exposure at -80^{o}C.

3.2.4 Protein analysis

3.2.4.1 Antibody production

Antibodies were raised in a rabbit against a synthetic DGAT1 peptide (CVLLYYHDLMNRKGSMS; highlighted in blue in Figure 2-1), which corresponds to the C-terminus of the native protein. This 17 amino acid sequence was chosen because of its hydrophilicity, antigenicity, and its uniqueness. The peptide was synthesized in the laboratory of Dr. G. Lajoie (Department of Chemistry, University of Waterloo). The carrier protein, Keyhole Limpet Hemocyanin (Sigma), was conjugated to the N-terminal cysteine of the peptide using *m*-maleimidobenzoyl-*N*-hydroxysuccinimide ester (MBS) according to Drenckhahn *et al.* (1993) and Collawn and Patterson (1999). Briefly, dissolved KLH (10mg/mL in water) was mixed dropwise with MBS dissolved in dimethylformamide (DMF-MBS; 10mg/mL) while stirred with a mini stir bar at room temperature for 30 minutes. The MBS-KLH complex was added slowly to a Sephadex 25 column to separate the activated MBS-KLH from the free MBS. Fractions of 15 drops were collected in glass test tubes and were analyzed for their A_{280} using a spectrophotometer. The fractions with the activated MBS-KLH, identified as a peak in absorbance, were pooled together and adjusted to pH 7.4. In a screw-cap vial, 1 mg DGAT1 peptide was added to 1 mg of MBS-KLH. The tube was sealed under nitrogen and rotated gently at room temperature for 3 hours. The resulting DGAT1-KLH conjugate was dialyzed twice against 3 litres of PBS at 4^{o}C for 3-4 hours.

Antibodies were raised in a rabbit housed in the animal care facility in the Department of Biology according to the University of Waterloo's Animal Care Standard

Operating Procedures. The initial immunization was performed with the DGAT1-KLH complex emulsified in Freund's complete adjuvant (mixed 1:1; Sigma). The rabbit was injected three more times at two-week intervals with the linked peptide in Freund's incomplete adjuvant (mixed 1:1; Sigma). Two weeks after the final injection, the rabbit was exsanguinated, and the serum was collected.

Antibodies were column-purified using SulphoLink Coupling Gel (Pierce) as described by the manufacturer. The SulfoLink Gel was brought to room temperature before making a 1mL packed column, which was equilibrated with 6 column volumes of equilibration buffer (50mM Tris, 5mM EDTA-Na, pH 8.5). The peptide (~1mg) was dissolved in 1mL equilibration buffer and incubated in the column for 15 minutes with mixing and 30 minutes without mixing, all at room temperature. The excess buffer was drained, and the column was washed with 3 column volumes of equilibration buffer. The A_{280} was monitored during the washes to determine coupling efficiency. The non-specific binding sites left on the gel were filled by incubating the column with a 50mM cysteine solution in equilibration buffer (1mL solution was added per 2mL column volume) for 15 minutes with mixing and 30 minutes without mixing. The column was washed with 16 column volumes of 1M sodium chloride and 16 volumes of degassed 0.05% sodium azide in PBS and stored overnight, upright at 4^{o}C. After the column and reagents were all brought to room temperature, the column was washed with 3 column volumes of PBS to remove the sodium azide. The serum collected from the final bleed was added directly (1mL at a time) to the column and allowed to incubate at room temperature for 1 hour. In between serum additions (3 in total), the column was washed with 8 column volumes of PBS. The purified antibody was eluted by applying 5 column volumes of elution buffer (0.1M glycine, pH 2.8). Fractions of about 1mL were collected and neutralized by adding 50µl of 1M Tris, pH 9.5. Elution was monitored by A_{280}, and the fractions with a high reading were pooled and dialyzed overnight against 3 litres of PBS. The purified antibody was aliquoted and stored at -20^{o}C. The titre of the purified antibody was determined using some of the remaining peptide. The DGAT1 antibody was used at a dilution of 1:500 for Western blotting and 1:50 for confocal microscopy.

Antibodies were also raised against cytochrome P450-cinnamate-4-hydroxylase fusion protein by Lily Lu (Lu, 1999) and cytochrome *f* peptide by Dr. Matthew Smith (Smith *et al.*, 2000).

Polyclonal antibodies against formate dehydrogenase were generously provided by Dr. Catherine Colas des Francs-Small (Université Paris-Sud, Orsay Cedex, France).

3.2.4.2 Protein extractions

3.2.4.2.1 Protein extraction from intact tissues

Rosette leaves, stem, cauline leaves, root, flower and silique tissues were homogenized (0.5g/mL) in buffer (50mM EPPS, pH 7.4, 0.25M sorbitol, 10mM EDTA, 2mM EGTA, 1mM DTT, 10mM amino-*n*-caproic acid, 1mM PMSF, 1mM benzamine, 1mM chymostatin) in a mortar and pestle. The homogenates were filtered through Miracloth, and protein was quantified according to (Ghosh *et al.*, 1988) using bovine serum albumin as a standard. Briefly, samples were diluted in 4X SDS loading buffer (200mM Tris, 40% [v/v] glycerol, 8% [w/v] SDS, 20% [v/v] 2-mercaptothanol, 0.5% [w/v] bromophenol blue) and dotted on Whatman 3M blotting paper (2μL per dot). After the dots dried, they were stained in Coomassie brilliant blue stain (50% [v/v] methanol, 12.5% [v/v] acetic acid, 0.1% [w/v] Coomassie brilliant blue R250) for 1 hour and destained in several changes of 40% (v/v) methanol and 10% (v/v) acetic acid to remove background stain. Protein concentration was determined by densitometry using a series of BSA standard spots on the same blots as a comparison. The dried dotted Whatman paper was scanned into a computer using an HP 3200 Scanjet and the integrated volume of each dot measured using ImageQuant software.

3.2.4.2.2 Isolation of chloroplasts and chloroplastic fractions

Intact, physiologically active chloroplasts were purified from 4.5-week-old *Arabidopsis thaliana* rosettes (Kunst, 1998). Briefly (Figure 2-2), 20g of leaves from plants dark-treated for 24 hours were floated on ice-water for 30 minutes, blotted dry and homogenized with a Sorvall Omni-mixer in 200mL of homogenization buffer (0.45 M sorbitol, 20mM tricine-KOH, pH8.4, 10mM EDTA, 10mM sodium bicarbonate) and a drop

Figure 3-2: Isolation of intact chloroplasts and chloroplastic fractions

Chloroplasts were isolated from 4.5-week old rosette leaves. The isolated chloroplasts were lysed to release the stroma from the membrane fractions. The proteins of intact chloroplasts, stroma fraction and the membrane fractions were all separated by SDS-PAGE for Western blotting. Intact chloroplasts were also assayed for cytochrome *c* oxidase to ensure no mitochondrion contamination. HB = homogenization buffer, RB= resuspension buffer and LB = lysis buffer.

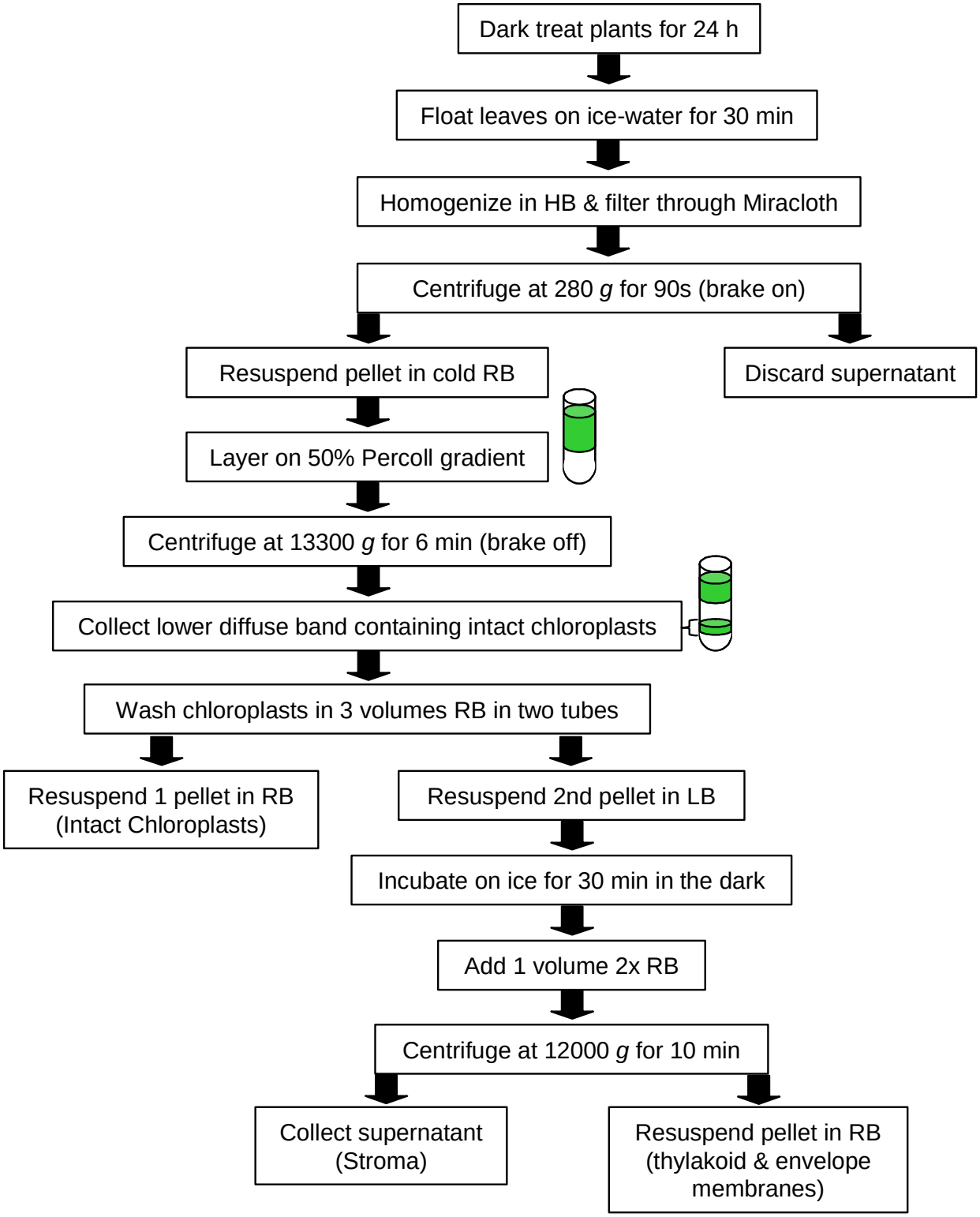
Dark treat plants for 24 h
Float leaves on ice-water for 30 min
Homogenize in HB & filter through Miracloth
Centrifuge at 280 g for 90s (brake on)
Resuspend pellet in cold RB
Discard supernatant
Layer on 50% Percoll gradient
Centrifuge at 13300 g for 6 min (brake off)
Collect lower diffuse band containing intact chloroplasts
Wash chloroplasts in 3 volumes RB in two tubes
Resuspend 1 pellet in RB (Intact Chloroplasts)
Resuspend 2nd pellet in LB
Incubate on ice for 30 min in the dark
Add 1 volume 2x RB
Centrifuge at 12000 g for 10 min
Collect supernatant (Stroma)
Resuspend pellet in RB (thylakoid & envelope membranes)

of antifoam (Sigma). The homogenate was filtered through Miracloth into a beaker on ice. The filtered homogenate was then centrifuged in a Sorvall SS-34 rotor at 280 *g* for 90 seconds with the brake on. The pellets were resuspended gently with a soft brush in 1mL of ice-cold resuspension buffer (0.3M sorbitol, 20mM tricine-KOH, pH7.6, 5mM magnesium chloride, 2.5mM EDTA). This suspension was layered on a Percoll gradient and centrifuged in a Sorvall HB-4 rotor at 13300 *g* for 6 minutes with the brake off. The lower diffuse band comprising intact chloroplasts was collected with a glass pipette, washed once in three volumes of resuspension buffer (in two tubes). Of the resulting pellets, one was resuspended in 1mL of resuspension buffer and the second was lysed as described below to obtain the chloroplastic fractions (stroma and membranes).

Chloroplast membranes were obtained as described by Ghosh *et al.* (1994). Gradient-purified chloroplasts were pelleted and lysed in 1mL of lysis buffer (10mM tricine, pH 7.6, containing 5mM magnesium chloride) on ice in the dark for 30 minutes. At the end of this period, 1mL of 2X resuspension buffer was added, and the chloroplast membranes (a composite of envelope membranes and thylakoids) were pelleted by centrifugation at maximum speed for 10 minutes in a microcentrifuge at 4^{o}C. The supernatant was collected as the stroma, which was centrifuged again at maximum speed for 10 minutes in a microcentrifuge at 4^{o}C to pellet any membrane contaminants. The stroma was concentrated by dehydration to one third the original volume. The membrane pellet produced by the lysis was washed three times to remove any contaminating stroma by resuspension in 1.5mL of resuspension buffer and centrifugation at maximum speed for 10 minutes in a microcentrifuge at 4^{o}C. The final membrane pellet was resuspended in 0.5mL of resuspension buffer.

The isolated intact chloroplasts and the chloroplastic fractions (stroma and membranes) were diluted in 4X SDS loading buffer. Proteins were quantified as described above. Alternatively, fresh intact chloroplasts were used for cytochrome *c* oxidase enzyme assay immediately.

3.2.4.2.3 Enzyme assay

Cytochrome *c* oxidase was assayed as a marker for mitochondrial inner envelope membrane (Hodges and Leonard, 1974). The assay mixture [100mM KPO_4, pH 6.7, 1mM EDTA, 0.5% (w/v) Tween 80, and 1mM reduced cytochrome *c* (reduced by the addition of a few grains of sodium dithionite)] was freshly prepared before use. The reaction was started by the addition of approximately 50µg of membrane protein (from microsomal membranes or purified chloroplasts) at room temperature. The oxidation of cytochrome *c* was monitored as a change in absorbance at 550nm over a period of 3 minutes.

3.2.4.2.4 Gradient fractionation of microsomes

Microsomal membranes from rosettes and developing siliques were fractionated on a continuous sucrose gradient. For isolation of microsomes, rosette leaves (10g) from 4.5-week-old *Arabidopsis thaliana* plants were homogenized in 100mL buffer (3mM Tris HCl, pH 7.5, 2mM EDTA, 250mM mannitol, 2mM DTT, 1mM PMSF, 5% (w/v) PVP) for 45 seconds in a Sorvall Omnimixer and for an additional minute in a Polytron homogenizer. Developing siliques (5g) from 6-week-old plants were homogenized in 50mL of the same buffer, first in a mortar and pestle with glass beads, then, as for leaves, for 45 seconds in a Sorvall Omnimixer and for an additional minute in a Polytron homogenizer. The homogenates were filtered through four layers of cheesecloth and centrifuged in a Sorvall SS-34 rotor at 8000 *g* for 20 minutes at 4°C. The supernatant was collected and centrifuged at 100000 *g* in a 60Ti rotor in a Beckman Ultracentrifuge for 1 hour at 4°C. The resulting pellets of microsomal membranes were resuspended in 6mL of storage buffer (6mM Tris-HCl, pH 7.5, 10% (w/v) glycerol, 250mM mannitol, 2mM DTT, 1mM PMSF), layered on a continuous sucrose density gradient (10-40% w/v) and centrifuged in a Beckman SW-28 rotor at 70000 *g* for 2 hours at 4°C. Fractions (20 drops/fraction) were collected from the bottom, and 10µl from each fraction was used to determine the sucrose concentration with a hand refractometer (Bausch and Lomb). The fractions were diluted five fold with storage buffer, centrifuged at 100000 *g* on a 60Ti rotor in a Beckman Ultracentrifuge for 1 hour at 4°C and the pellets resuspended in 100µL storage buffer. For Western blots, 15µl of each fraction was mixed with 5µL 4X SDS-loading buffer and fractionated by SDS-PAGE.

3.2.4.3 Protein fractionation

SDS-PAGE was performed on Mini protein Dual Slab cells (BioRad, Mississauga, Ontario) using 1-1.5mm thick 4% acrylamide stacking gel and 10-12% acrylamide separating gels (Laemmli, 1970). The gels were either stained with Coomassie brilliant blue R250 (Fairbanks *et al.*, 1971) or transferred to polyvinyldiene difluoride (PVDF) membranes using the semi-dry transfer method (Trans-Blot® Semi-Dry Electrophoretic Transfer cell, Bio-Rad, Hercules, CA). Specifically, the gels stained with Coomassie brilliant blue R250 were stained for at least one hour in staining buffer (50% methanol, 12.5% acetic acid, 0.1% Coomassie brilliant blue R250) and destained until all background stain was removed in destaining buffer (40% methanol, 10% acetic acid). The gels that were transferred to PVDF membranes were first equilibrated in cold transfer buffer (48mM Tris, 39mM glycine, 0.0375% SDS [w/v], pH 9.2, 20% [v/v] methanol), along with the PVDF membranes (pre-wetted in methanol) and filter papers, for 15 minutes. The membrane was sandwiched with the acrylamide gel, between sheets of filter paper cut to size, in the semi-dry transfer apparatus. Power to the transfer apparatus was provided by a BioRad power supply, which transferred the proteins of the mini-gels for 30 minutes at 15V (current limit was set to 5.5mA/cm^2). After the transfer was complete, the gel was stained as described earlier to check for even loading/transfer of proteins. The membrane was blocked and probed as described below.

3.2.4.4 Western blotting

The PVDF blots were blocked for 30s in 1mg/mL polyvinyl alcohol (Miranda *et al.*, 1993) and for one hour in phosphate-buffered saline containing 0.05% (v/v) Tween 20 (PBS-T) and 5% (w/v) powdered milk. After blocking, the blots were incubated with primary antibody, which was diluted in PBS-T with 1% (w/v) powdered milk (1:500 for DGAT1 purified antibody, cytochrome *f* antibody and cytochrome P450-cinnamate-4-hydroxylase antibody; or 1:250 for the formate dehydrogenase antibody). Blots were then washed 3 times in PBS-T for 10 minutes each before incubation for one hour in PBS-T, 1% (w/v) milk with secondary antibody coupled to alkaline phosphatase and produced in goat against rabbit IgG (1:1000; Chemicon, Temecula, CA). After the secondary antibody incubation, the

membranes were washed once with PBS-T containing 1% Triton-X for 10 minutes, then three times in PBS-T for 10 minutes each. To visualize the bands, membranes were exposed to 10mL alkaline phosphatase reaction buffer (100mM Tris-HCl, pH 9.5, 100mM sodium chloride, 5mM magnesium chloride) and the alkaline phosphatase substrates, nitro blue tetrazolium (NBT; 66µl of 50mg/mL stock in 70% [v/v] dimethylformamide per 10mL reaction) and bromochloroindolyl phosphate (BCIP; 33µl of 50mg/mL stock in dimethylformamide per 10mL reaction; BioRad, Mississauga, ON). The colour reaction was terminated by washing the blots quickly and thoroughly with water. As soon as the blots dried, they were scanned into a computer using an HP 3200 Scanjet.

3.2.5 Lipid analysis

3.2.5.1 Lipid extraction

For lipid analysis, 20g of rosette leaf tissue from 3- or 6-week-old *Arabidopsis thaliana* plants were homogenized in 60mL of buffer (50mM EPPS, pH 7.4, 0.25M sorbitol, 10mM EDTA, 2mM EGTA, 1mM DTT, 10mM amino-*n*-caproic acid, 4% (w/v) PVPP) for 45 seconds in a Sorvall Omnimixer and for an additional minute on a Polytron homogenizer (Figure 3-3). The homogenate was filtered through 4 layers of cheesecloth and centrifuged in a Sorvall SS-34 rotor at 3000 *g* for 10 minutes. The resulting sediment largely consisted of starch since the tissue homogenization was of sufficient intensity to disrupt cell organelles which, if intact, might partially sediment under these conditions of centrifugation. An aliquot of the homogenate supernatant was stored at -20^{o}C for total lipid extraction, while the rest of the homogenate was further centrifuged to collect the microsomal membranes. In order to pellet the microsomal membranes, the homogenate supernatant was centrifuged in a Beckman 60Ti rotor at 100000 *g* for 1 hour. The pellets were resuspended in homogenization buffer and stored at -20^{o}C.

Total lipids were extracted according to Bligh and Dyer (1959). All solvents used were HPLC grade, and work was done under a flow of nitrogen as much as possible to prevent lipid oxidation (Bligh and Dyer, 1959). Internal standards (diheptadecanoyl L-α-phosphatidylcholine, diarachidin, heptadecanoic acid, triheptadecanoic acid, and cholesteryl

Figure 3-3: Lipid extraction, thin layer chromatography and gas chromatography/mass spectrometry sample preparation

Lipids were extracted from homogenate and microsomal membranes of pre-senescent (3-week-old) and senescent (6-week-old) rosette leaves. Total lipids were extracted from each sample as well as the different lipid classes (viz., polar lipids, diacylglycerols, free fatty acids, triacylglycerols, and steryl and wax esters) that were resolved by thin-layer chromatography. Fatty acids from each fraction and lipid class were transmethylated for GCMS analysis.

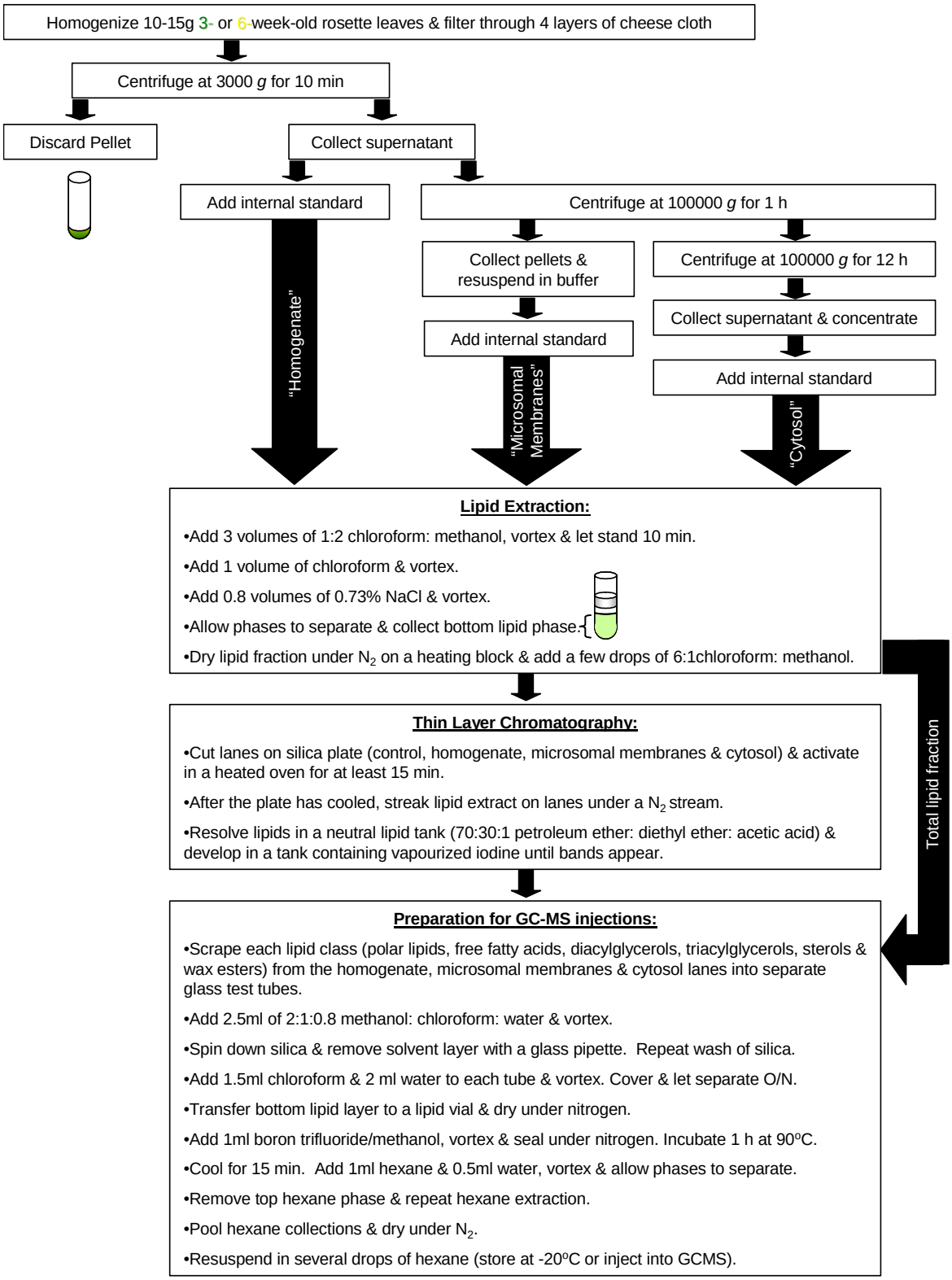
Homogenize 10-15g 3- or 6-week-old rosette leaves & filter through 4 layers of cheese cloth
Centrifuge at 3000 g for 10 min
Discard Pellet
Collect supernatant
Add internal standard
Centrifuge at 100000 g for 1 h
Collect pellets & resuspend in buffer
Add internal standard
Centrifuge at 100000 g for 12 h
Collect supernatant & concentrate
Add internal standard
"Homogenate"
"Microsomal Membranes"
"Cytosol"
Lipid Extraction:
•Add 3 volumes of 1:2 chloroform: methanol, vortex & let stand 10 min.
•Add 1 volume of chloroform & vortex.
•Add 0.8 volumes of 0.73% NaCl & vortex.
•Allow phases to separate & collect bottom lipid phase.
•Dry lipid fraction under N2 on a heating block & add a few drops of 6:1chloroform: methanol.
Total lipid fraction
Thin Layer Chromatography:
•Cut lanes on silica plate (control, homogenate, microsomal membranes & cytosol) & activate in a heated oven for at least 15 min.
•After the plate has cooled, streak lipid extract on lanes under a N2 stream.
•Resolve lipids in a neutral lipid tank (70:30:1 petroleum ether: diethyl ether: acetic acid) & develop in a tank containing vapourized iodine until bands appear.
Preparation for GC-MS injections:
•Scrape each lipid class (polar lipids, free fatty acids, diacylglycerols, triacylglycerols, sterols & wax esters) from the homogenate, microsomal membranes & cytosol lanes into separate glass test tubes.
•Add 2.5ml of 2:1:0.8 methanol: chloroform: water & vortex.
•Spin down silica & remove solvent layer with a glass pipette. Repeat wash of silica.
•Add 1.5ml chloroform & 2 ml water to each tube & vortex. Cover & let separate O/N.
•Transfer bottom lipid layer to a lipid vial & dry under nitrogen.
•Add 1ml boron trifluoride/methanol, vortex & seal under nitrogen. Incubate 1 h at 90°C.
•Cool for 15 min. Add 1ml hexane & 0.5ml water, vortex & allow phases to separate.
•Remove top hexane phase & repeat hexane extraction.
•Pool hexane collections & dry under N2.
•Resuspend in several drops of hexane (store at -20°C or inject into GCMS).

arachidate) were added to the homogenate and microsomal membrane fraction prior to extraction. These five standard lipid classes contained the unusual fatty acids heptadecanoic acid (17:0) or eicosanoic acid (20:0). The amount of internal standard added to each sample was based on an estimation of lipid content. All glassware used for lipid extractions was cleaned with Decon detergent (BDH Inc., Toronto, Ontario) to minimize sources of lipid contamination. Three volumes of chloroform:methanol (1:2) were added to each sample, vortexed vigorously and allowed to stand for 10 minutes before another volume of chloroform was added and vortexed vigorously. In order to separate the lipid soluble fraction from the aqueous soluble fraction, 0.8 volumes of 0.73% sodium chloride was added and vortexed. The tubes were then covered with saran wrap, and the suspension was allowed to separate into three phases. The top phase was the aqueous phase, the middle phase was a white proteineacous phase and the bottom phase was the lipid (chloroform) phase. The bottom layer was removed with a glass Pasteur pipette by bubbling down through the first two phases before drawing up the lipid phase. The lipid phase was dried down in spectrometry grade lipid vials under a stream of nitrogen in a heating block. A few drops of chloroform:methanol (6:1) were added to each of the extracted lipids, and the vials were sealed under nitrogen. An aliquot of total lipids was taken from each sample (homogenate and microsomal membranes), and the remaining lipids were used for thin layer chromatography fractionation. Extracted lipids were stored at -20^{o}C.

3.2.5.2 Thin Layer Chromatography (TLC)

Lipid extracts were fractionated by thin layer chromatography (Yao *et al.*, 1991), against authentic unsaturated lipid standards (dileoyl L-α-phosphatidylethanolamine, dilinolenin, linolenic acid, trilenolein, cholesteryl arachidonate). The silica plates (SIL G-25, 0.25mm silica gel layer, Macherey-Nagel, Germany) were formatted into three lanes; one for the standards and one for each sample, and were activated in a drying oven for at least 15 minutes and cooled in a dry tank.

The lipid extracts from homogenate and microsomal membranes were streaked under a stream of nitrogen gas onto the lanes of the silica plate. The lipids were resolved in a non-polar lipid tank (70mL petroleum ether, 30mL diethyl ether, 1mL acetic acid and a sheet

of filter paper to facilitate the buffer to wick up and fill the tank with vapour), prepared an hour before needed. The plate was removed from the non-polar lipid tank when the solvent front almost reached the top of the plate. The bands corresponding to the separated lipid classes were visualized after being exposed to vapourized iodine in a developing tank. The iodine reacts with the double bonds of the unsaturated fatty acids, resulting in the appearance of yellowish-brown bands. The developed plate was scanned into a computer using an HP 3200 Scanjet, and the lipid classes were marked off with a pencil. The silica corresponding to each lipid class (viz., polar lipids, diacylglycerols, free fatty acids, triacylglycerols, and steryl and wax esters) within each sample (homogenate and microsomal membranes) was scraped off with clean razor blades. The lipids were extracted from the silica in glass test tubes with the addition of 2.5mL of methanol: chloroform: water (2:1:0.8), vortexing and slow centrifugation on a tabletop centrifuge to separate the silica and lipid phases. The lipid phase was removed to a clean test tube with a glass pipette. The silica was washed again with the methanol: chloroform: water mixture and the collected lipid phase was removed and added to the previous fraction collected. To further purify the lipid extract, 1.5mL chloroform and 2mL of water were added to each tube, vortexed and left to separate into a top aqueous phase and bottom lipid phase. The bottom phase was collected into a spectrometry grade lipid vial and dried under nitrogen. These samples were either prepared immediately for gas chromatography mass spectrometry analysis or stored at -20^{o}C in chloroform: methanol (6:1).

3.2.5.3 Gas Chromatography Mass Spectrometry (GCMS) analysis

Fatty acids of the separated lipid fractions were transmethylated (Morrison and Smith, 1964) and the resultant fatty acid methyl esters were quantified by gas chromatography-mass spectrometry (GCMS) (HP-5890 series II gas chromatograph equipped with a DB Wax column (30 x 0.25mm ID, 0.25μm film [JandW Scientific]) and a mass detector [HP-5970] with a scan range of m/z 35-150 operating at 0.16sec/scan). Transmethylation breaks the ester bond of the fatty acid moiety to its backbone and replaces it with a methyl group, giving rise to a fatty acid methyl ester, and this was performed by the addition of 1mL boron tri-fluoride methanol to dried lipid samples. The samples were sealed

under nitrogen, vortexed and incubated in a 90°C water bath for one hour. After the lipid samples were cooled to room temperature, the fatty acid methyl esters were extracted by the addition of 1mL of hexane and 0.5mL of water to each vial, and vortexed. The upper non-polar phase was collected into a clean lipid vial. The lower aqueous phase was washed twice with 1mL hexane to reduce fatty acid loss. The upper phases were pooled together and dried under a continuous stream of nitrogen. The dried fatty acids were then resuspended in several drops of hexane, sealed under nitrogen and stored at -20°C until GCMS injection.

Fatty acid content as well as the identity of fatty acid species present in the lipid extracts were analyzed using GCMS. The temperature program was optimized for the separation of a commercially-available mixture of 37 fatty acid methyl ester standards (Product No. L 9405, Sigma Chemical, St. Louis, MO). The oven temperature was initially held at 80°C for 5 minutes and then increased at 10°C per min to 100°C (held for 10 minutes), 160°C (held for 20 minutes) and finally 220°C (held for 51 minutes). The resulting peaks on the chromatographs were integrated using MS ChemStation data analysis software (HP G1034C), and the identity of each fatty acid species was verified using the NIST/EPA/NIH Mass Spectral Library (HP, version 1.1a, Standard Reference Database 1A). The fatty acid methyl esters were quantified against the internal standards (heptadecanoic acid methyl ester [17:0] and arachidic acid methyl ester [20:0]) added prior to lipid extraction.

3.2.6 Microscopy

3.2.6.1 Electron microscopy

Segments of tissue (~2mm^2) cut from the centre of the first leaf pair from 3- and 6-week-old *Arabidopsis thaliana* plants were vacuum-infiltrated with 0.02 M sodium phosphate buffer (pH 7.2) and fixed in 4% glutaraldehyde in 0.02 M sodium phosphate buffer (pH 7.2) overnight at 4°C. The samples were then washed 4 times in 0.02 M phosphate buffer (pH 7.2), post-fixed in 1% osmium tetroxide in 0.02 M phosphate buffer (pH 7.2) for 2 hours at 4°C and washed 4 times in water for 30 minutes. They were then dehydrated in a graded series of acetone, washed 4 times in 100% acetone for 30 minutes and

embedded in Epon-Araldite. Ultrathin sections (70-90nm) were stained in lead citrate and uranyl acetate and examined with a Philips CM 10 electron microscope operating at 60kV.

3.2.6.2 Confocal microscopy

Leaf discs (~4mm in diameter) were cut from the centre portion of the first leaf pairs of 4- to 6-week old leaves. Alternatively, developing seeds (embryos) were collected at varying stages of development and treated as described below for leaf tissue. The samples were immediately vacuum-infiltrated with 4% paraformaldehyde in phosphate buffered saline (PBS) for 10 minutes, then stored at 4^{o}C until stained. The disks and embryos were washed with PBS twice for 30 minutes at room temperature to remove the fixative and once with 1% Triton X in PBS for 15 minutes to permeablize the tissue. The fixed and permeablized tissues were then gently rocked overnight at room temperature with purified primary antibody against either DGAT1 (1:50) or the chloroplastic triacylglycerol lipase (AAD24845; 1:50) in 1% BSA in PBS. The tissues were washed twice in PBS, for 30 minutes each, at room temperature before incubation with the goat anti-rabbit secondary antibody conjugated to FITC [Sigma; 1:100 in 1% BSA (w/v) in PBS] for two hours in the dark. The samples were washed two times for 30 minutes each in PBS and then were mounted on slides in 70% glycerol. Number 1.5 cover slips were used for optimal visualization by confocal microscopy. The samples were observed using a Zeiss LSM 510 confocal laser scanning microscope attached to an axiovert-inverted microscope.

3.3 Results

3.3.1 DGAT1 is a highly conserved protein in plants

The protein (AAK96671), mRNA (AY054480) and genomic (AC005917) sequences for DGAT1 from *Arabidopsis thaliana* (At2g19450) were obtained from the Entrez Homepage. These sequences have been described elsewhere as DGAT1 (Lardizabal *et al.*, 2001; Lu *et al.*, 2003), and are more similar to sterol acyltransferase than to any of the other enzymes involved in triacylglycerol synthesis (Lardizabal *et al.*, 2001). The full length cDNA of DGAT1 is 1988bp long, containing an open reading frame of 1563bp encoding a protein of 520 amino acids. DGAT1 from *Arabidopsis* (At2g19450) is found on chromosome II, approximately 17.5±3cM from the *sti* locus and 8±2cM from the *cp2* locus (Zou *et al.*, 1999). The DGAT1 protein sequence from *Arabidopsis* (AAK96671) was used to perform a BLASTp search for annotated DGAT1 sequences in other species. While the DGAT1 protein sequence from humans (BAC66170) was about 38% identical, the identity shared between *Arabidopsis* and other plant species, especially other eudicots, was up to 85%. Six of the annotated species from GenBank were chosen for sequence alignment with *Arabidopsis* DGAT1 (Figure 3-4). These plant species were chosen as representative oil producing eudicots, in which oil is the major form of carbon storage found either in seeds or fruits. These six sequences and the *Arabidopsis* DGAT1 sequence were submitted to the DIALIGN program with the threshold set to zero and N=5 (Morgenstern, 1999). The identical amino acids in the alignment (Figure 3-4) are indicated in yellow highlight. *Brassica napus* (canola) is 85% identical to *Arabidopsis.* The species *Topaeolum majus* (nasturtium), *Ricinus communis* (castor bean), and *Olea europaea* (olive) are all 69% identical to *Arabidopsis*, and *Perilla frutescens* (beefsteak mint) and *Nicotiana tabacum* (tobacco) are 65% and 67% identical to *Arabidopsis,* respectively. Most of the identity is found within the conserved MBOAT domain (Membrane Bound O-Acyl Transferase) indicated by the red box (Figure 3-4). Not only is most of the identity found in this region, even where there are some differences in sequence there is still a high level of similarity as indicated by the double row of stars below the sequence. All plant DGAT1s

Figure 3-4: Alignment of DGAT1 for seven oil-producing plant species

Protein alignment of DGAT1 from *Arabidopsis thaliana*, *Brassica napus*, *Tropaeolum majus*, *Ricinus communis*, *Olea europaea*, *Perilla frutescens*, and *Nicotiana tabacum*. All of these plant species are eudicots and produce oil as the major form of carbon storage in either their seeds or fruits. These DGAT1s are members of the MBOAT (Membrane Bound O-Acyl Transferase) family, characterized by a conserved domain indicated by the red box. The active site (HKW-X-X-RH-X-Y-X-P) for DGAT1 is underlined within the MBOAT. Identical aligned amino acid sequences found in all 7 species are indicated in yellow highlight. A double row of stars indicates the regions of high similarity as determined by DIALIGN (Morgenstern, 1999), and a single row of stars indicates regions of lower similarity. Capital letters denote aligned amino acids and lower case letters denote residues that do not align, and have no similarity.

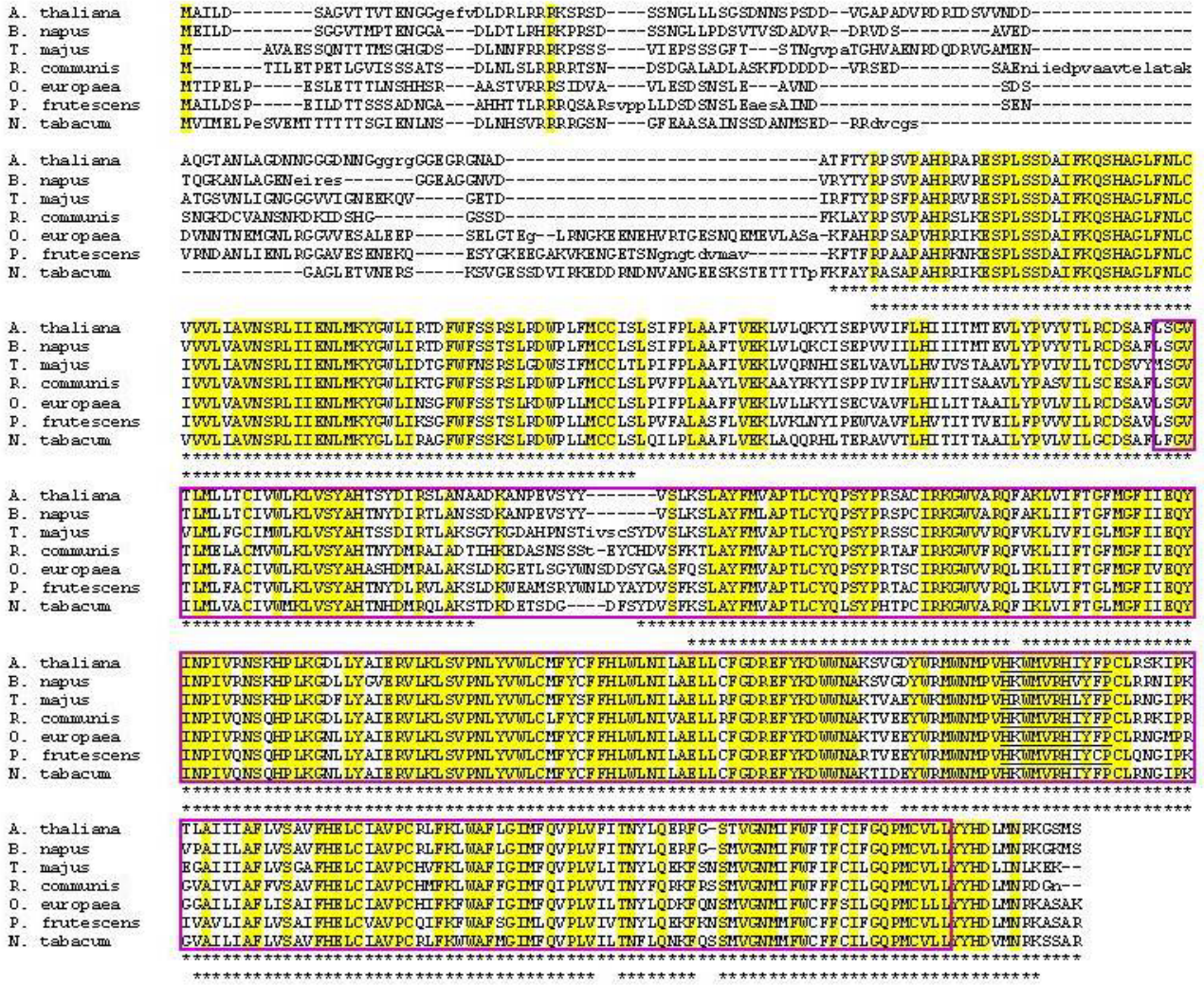
A. thaliana
B. napus
T. majus
R. communis
O. europaea
P. frutescens
N. tabacum

are divergent in the N-terminus and residues 243-268 (Milcamps *et al.*, 2005). The underlined active site HKW-X-X-RH-X-Y-X-P for DGAT1 (Figure 3-4) is also found within the MBOAT domain (Zou *et al.*, 1999).

3.3.2 DGAT1 is an integral membrane protein with many hydrophobic regions

DGAT1 is a membrane bound protein with many transmembrane domains. A Kyte and Doolittle hydrophobicity plot suggests that the protein contains 8 or 9 membrane spanning domains (Figure 3-5A). The regions that have a hydropathy score above zero represent the hydrophobic regions of the amino acid sequence, where regions above a hydropathy score of about 2 signify extremely hydrophobic regions, designating that region as a strong candidate for a transmembrane domain (Kyte and Doolittle, 1982). Several other transmembrane prediction programs available at www.expasy.org also predict 8 or 9 membrane spanning domains. There is currently no crystal structure for DGAT1, but others have also reported that there are likely 9 membrane spanning domains (Hobbs *et al.*, 1999; Bouvier-Nave *et al.*, 2000; Weselake *et al.*, 2004). Figures 3-5B and Figure 3-5C illustrate the putative membrane orientations of DGAT1 if it had 8 or 9 membrane spanning domains, respectively. The N-terminus is predicted to be cytosolic, and this has been confirmed in canola through the use of polyclonal antibodies against the N-terminus (Weselake *et al.*, 2004). DGAT1 may also form tetramers, though this conformation is not necessary for enzyme activity (Cheng *et al.*, 2001).

3.3.3 DGAT1 is expressed in most organs of *Arabidopsis thaliana* and has a multi-element promoter

The extent to which DGAT1 is expressed in different organs of *Arabidopsis thaliana* plants was assessed by Western-blot analysis (Figure 3-6). Total protein from roots, stems, cauline leaves, flowers and siliques was collected from 6-week-old plants, fractionated by SDS-PAGE and blotted on PVDF membranes. At this stage of development, the roots were a mixture of developed and growing structures, the stems and cauline leaves were still growing and developing, the flowers were a mixture of senescing and pre-senescent inflorescences, and the siliques were developing but had not yet reached maturity.

Figure 3-5: DGAT1 hydropathy plot and putative transmembrane spanning domains

A. A Kyte and Doolittle hydropathy plot of *Arabidopsis* DGAT1. The hydropathy score is indicated on the ordinate, where the positive numbers indicate the hydrophobic regions and the negative numbers designate the hydrophilic regions (Kyte and Doolittle, 1982). The window position is indicated on the abscissa and corresponds to the amino acids in the DGAT1 sequence. The hydropathy score of zero is indicated by the black line, and the putative transmembrane domains are indicated at the top of the graph. The domain numbers in red are the most likely transmembrane domains, where domain 5, indicated in blue, falls just below the threshold of 2 for a transmembrane domain and could be a hydrophobic domain that is not transmembrane. The C-terminus peptide that was used for antibody production, identified by the blue box, is in the hydrophilic range of hydropathy score. **B.** Diagram illustrating the putative membrane topology for *Arabidopsis* DGAT1 with 8 transmembrane helices. Domain 5 is just below the threshold of highly hydrophobic composition as shown in A and could be part of the cytosolic face of DGAT1. **C.** Diagram illustrating the putative membrane topology for *Arabidopsis* DGAT1 with 9 transmembrane helices. This is probably the most likely scenario. The C-terminus peptide corresponding to the sequence used for antibody production is indicated as a blue line in both B. and C.

A.

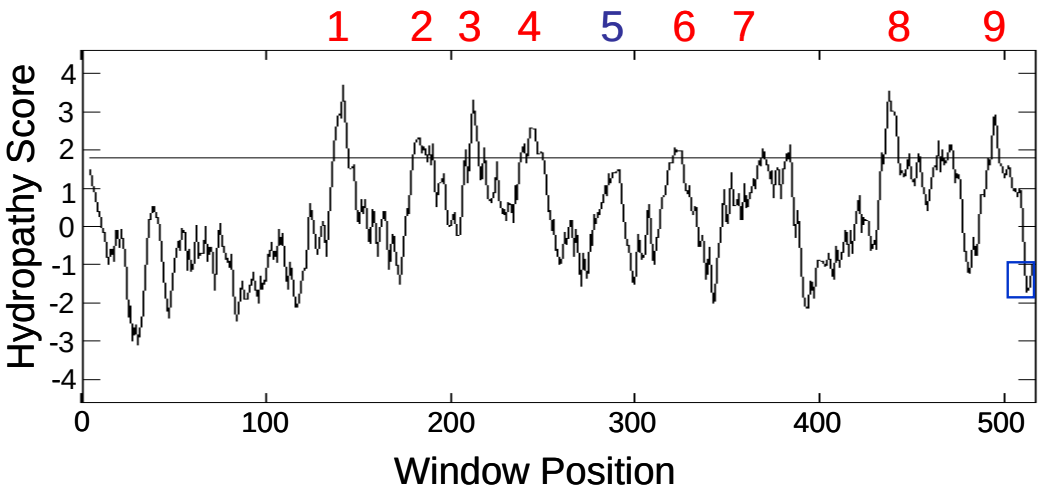
1 2 3 4 5 6 7 8 9
Hydropathy Score
4
3
2
1
0
-1
-2
-3
-4
0
100
200
300
400
500
Window Position

B.

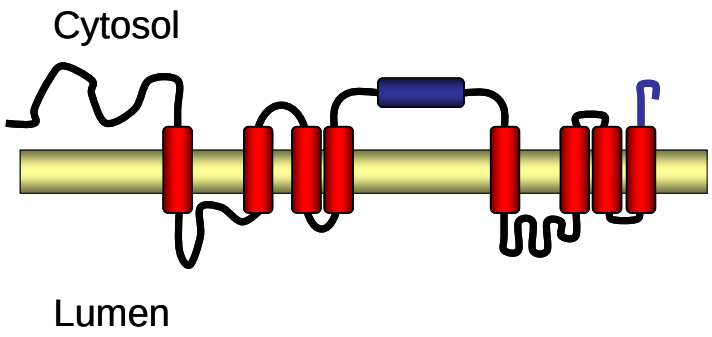
Cytosol
Lumen

C.

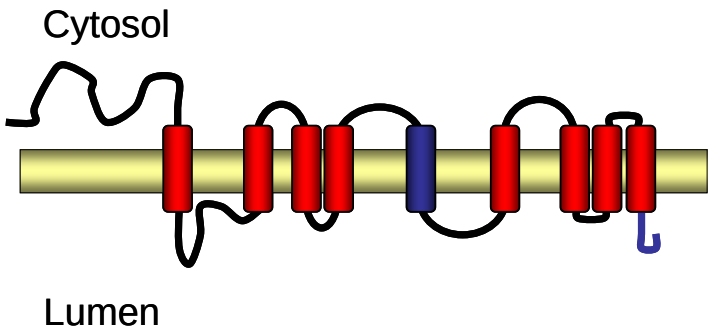
Cytosol
Lumen

Figure 3-6: DGAT1 expression in various organs of *Arabidopsis thaliana*

A. Western blot probed with antibody raised against a synthetic peptide of DGAT1. R=Roots, ST=stem, L=cauline leaf, FL=flowers, and SIL=siliques. The apparent molecular mass of the immunodetected polypeptide is indicated in kilodaltons. **B.** SDS-PAGE stained with Coomassie Brilliant Blue. Lanes are as in A, and the molecular mass markers are indicated on the left. Each lane contained 10μg of protein, and the lanes were confirmed to be equally loaded by densitometry.

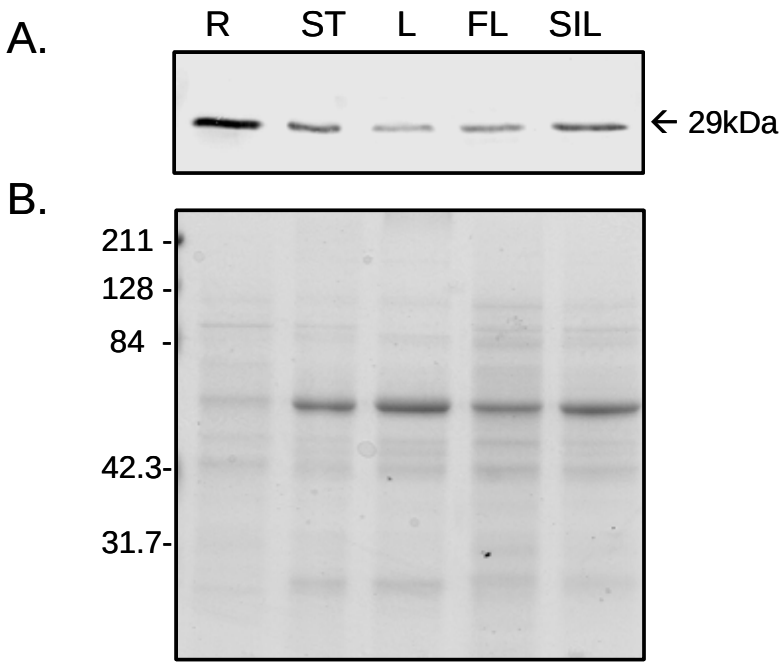
A.
R
ST
L
FL
SIL
← 29kDa
B.
211 -
128 -
84 -
42.3-
31.7-

The blots were probed with polyclonal antibodies raised against a synthetic peptide corresponding to the last 17 amino acids of the C terminus of DGAT1. Probing the blots with DGAT1 antibody revealed that the protein is present in all of these organs, although it is most abundant in roots and siliques and least abundant in cauline leaves (Figure 3-6). The expected size of DGAT1 protein is 59kDa, though others have detected it at 51kDa (Hobbs *et al.*, 1999; Bouvier-Nave *et al.*, 2000; Hobbs and Hills, 2000; Lu *et al.*, 2003). The polypeptide that was routinely detected in the Western blots probed with purified DGAT1 antibody in this study was only 29kDa in size (Figure 3-6) and is presumably a proteolytic catabolite of the native protein. This was observed throughout most experiments, though a band at 51kDa was also detectable in certain circumstances (see Results section 3.3.8).

Since DGAT1 was detectable in various organs in *Arabidopsis thaliana*, it is presumably regulated by a complex promoter. The promoter region of the genomic counterpart of DGAT1 was analyzed for the presence of *cis*-acting elements. To achieve this, a 2 kilobase genomic sequence upstream from the start codon (ATG) was entered into the PLACE program. PLACE is a database of motifs found in plant *cis*-acting regulatory DNA elements, all from previously published reports. In addition to the motifs originally reported, their variations in other genes or in other plant species reported later are also compiled (Higo *et al.*, 1999). Some of the motifs identified during the promoter analysis of DGAT1 are illustrated in alphabetical order in Table 3-1. It should be noted that these motif sites are only putative. Several motifs that were predicted by PLACE were not included in this table due to their unknown role in *Arabidopsis* or their short length (short sequences are more likely to occur randomly). Regardless, a wide range of putative regulatory DNA elements was identified in the promoter region of DGAT1, signifying that DGAT1 has a multi-element promoter and consistent with the finding that DGAT1 protein is expressed in many different organs of *Arabidopsis thaliana* (Figure 3-6).

It was not surprising to see motifs involved in seed-specific expression (-300 ELEMENT, CANBNAPA, MYB1AT, and MYCCONSENSUSAT), since *Arabidopsis* is an oil- seed plant, where oil consists mostly of triacylglycerol, and DGAT1 is involved in the final acylation of triacylglycerol synthesis. Another well characterized tissue for

Table 3-1: Putative *cis*-acting elements predicted in the DGAT1 promoter region by PLACE

Factor or Site Name	Location & Strand (bp upstream of ATG)	Signal Sequence	Description/Keywords	References
-10PEHVPSED	912(+), 466(-), 1928(-)	TATTCT	Plastid genes; Circadian rhythms; Light regulation	(Thum *et al.*, 2001)
-300ELEMENT	1069(+), 526(-), 1193(-)	TGHAAARK	Seed specific; Endosperm	(Colot *et al.*, 1987; Kreis *et al.*, 1986)
ASF1MOTIFCAMV	45(+), 259(+), 17(-)	TGACG	Found in promoters of genes regulated by auxin or salicylic acid; Stress; Disease resistance	(Despres *et al.*, 2003; Katagiri *et al.*, 1989; Redman *et al.*, 2002; Terzaghi and Cashmore, 1995)
BOXIINTPATPB	468(+), 574(+), 1424(+), 174(-), 910(-), 1199(-), 1880(-)	ATAGAA	Conserved in nonconsensus type II promoters of plastid genes	(Kapoor and Sugiura, 1999)
ARR1AT	94(+), 1129(+), 1150(+), 1650(+), 266(-), 1502(-), 1684(-), 1965(-)	AGATT	Response regulator in Arabidopsis; Involved in cytokinin response	(Ross *et al.*, 2004; Sakai *et al.*, 2000)
CANBNAPA	288(+)	CNAACAC	Storage genes in seeds	(Ellerstrom *et al.*, 1996)
ERELEE4	719(+), 1720(+), 1050(-)	AWRRCAAA	Ethylene responsive element; Senescence associated genes	(Itzhaki *et al.*, 1994)
GT1GMSCAM4	298(+), 651(+), 845(+), 1068(+), 1602(+), 1554(+), 222(-), 525(-), 1883(-)	GAAAAA	GT-1 motif; Pathogen and salt induced gene expression; Light regulation	(Park *et al.*, 2004)
IBOX	965(-)	GATAAG	Light regulation	(Donald and Cashmore, 1990)
IBOXCORE	566(+), 1369(+), 1418(+), 964(-), 1111(-), 1946(-), 1993(-)	GATAA	Light regulation	(Terzaghi and Cashmore, 1995)
LTRECOREATCOR15	29(+), 1075(-), 1227(-), 1249(-)	CCGAC	Low temperature responsive element; Cold, drought, ABA	(Kim *et al.*, 2002)
MYB1AT	334(+), 1274(+), 1731(-)	AAACCA	Found in promoters of dehydration-responsive genes; ABA, stress, seed	(Abe *et al.*, 2003)
MYB2AT	877(-)	TAACTG	Water stress	(Urao *et al.*, 1993)
MYCCONSENSUSAT	441(+/-), 520(+/-), 1539(+/-), 1678(+/-), 1735(+/-)	CANNTG	Dehydration-responsive genes; Cold; Seed; Stress; ABA	(Abe *et al.*, 2003; Chinnusamy *et al.*, 2003; Chinnusamy *et al.*, 2004)
POLLEN1LELAT52	192(+), 299(+), 652(+), 846(+), 893(+), 1569(+), 1955(+), 35(-), 73(-), 136(-), 175(-), 215(-), 634(-), 688(-), 1200(-), 1881(-)	AGAAA	Pollen specific activation	(Bate and Twell, 1998)
WBOXATNPR1	424(+), 612(+), 784(+), 803(+), 1296(+), 1627(+), 16(-), 625(-), 816(-), 1279(-)	TTGAC	Recognized by salicylic acid (SA)-induced WRKY DNA binding proteins; Disease resistance	(Chen *et al.*, 2002; Yu *et al.*, 2001)

triacylglycerol synthesis is pollen (Lu *et al.*, 2003), and a pollen-specific element also appears as a putative element in the DGAT1 promoter (POLLEN1LELAT52). Elements that are responsive to water stress, ABA, cold or dehydration (LTRECOREATCOR15, MYB1AT, MYB2AT and MYCCONSENSUSAT) could also be part of the seed-specific compilation of *cis*-acting elements. Another group of putative motifs are those governed by circadian rhythms and light (-10PEHVPSED, GT1GMSCAM4, IBOX, and IBOXCORE). Since several of these putative motifs are present in the DGAT1 promoter, it appears that light may have an influence on the expression of the DGAT1 gene. Two motifs on the DGAT1 promoter are also implicated as appearing in plastid genes (-10PEHVPSED and BOXIINTPATPB). Many plastid proteins are nuclear encoded, and many are regulated by light. Some putative elements in the DGAT1 promoter are involved in stresses other than those associated with seed development, including salt stress (GT1GMSCAM4), pathogenesis (ASF1MOTIFCAMV, GT1GMSCAM4, and WBOXATNPR1) and salicylic acid –induced stress (ASF1MOTIFCAMV, and WBOXATNPR1).

Most of the putative motifs listed in Table 3-1 are influenced at least in part by growth regulators. Water stress is an inducer of ABA, which can increase tolerance to water stress by the induction of ABA responsive genes. The cognate proteins of many ABA responsive genes increase tolerance to water stress by protecting against, or repairing, osmotic stress-induced damage. ABA is also an important growth regulator involved in the induction of seed dormancy. Putative ABA responsive elements (LTRECOREATCOR15, MYB1AT, and MYCCONSENSUSAT) are present in the DGAT1 promoter sequence. Another growth regulator with a putative response element (ARR1AT) in the DGAT1 promoter sequence is cytokinin. Cytokinin is involved in maintaining the integrity of chloroplasts, and induces chloroplast-associated gene expression. The presence of the cytokinin response element in the DGAT1 promoter is consistent with the presence of other putative *cis*-acting elements involved in light regulation and plastid expression. The antagonist to the physiological effects of cytokinin is ethylene, another important growth regulator. A putative response element for ethylene, (ERELEE4), is also predicted in the DGAT1 promoter sequence. Ethylene is an inducer of senescence, which is a developmental

phase leading to death of tissues. Leaf senescence is often studied in *Arabidopsis thaliana* as it is a co-ordinated, reproducible event in its lifecycle.

3.3.4 DGAT1 is expressed at low levels constitutively and is up-regulated at the onset of senescence in *Arabidopsis thaliana* rosettes

Changes in the levels of DGAT1 transcript and its cognate protein during development and senescence of *Arabidopsis thaliana* rosette leaves were examined by Northern- and Western- blot analysis, respectively. Photographs of *Arabidopsis* rosettes harvested from 2- through 6-week-old plants are illustrated in Figure 1-1. At 2-weeks of age, the rosette leaves are still small and juvenile, but they increase in number and enlarge substantially between 2 and 4-weeks of age. By week 5, leaf senescence has engaged, and at week 6 the older leaves are visibly yellow reflecting significant depletion of chlorophyll as senescence progresses.

The DGAT1 EST clone, E6B2T7, was used as a probe for Northern analysis. The sequence corresponding to E6B2T7 is highlighted in Figure 3-1. DGAT1 transcript was detectable in total RNA preparations from all ages of rosette leaves, indicating that there is a basal level of constitutive DGAT1 expression at the transcript level (Figure 3-7). However, the abundance of DGAT1 mRNA changed during leaf development. Specifically, levels were lowest for 2-week-old plants, higher for 3- and 4-week-old plants and then increased again reaching very high levels in the visibly yellow leaves of the 6-week-old plants (Figure 3-7). Similar changes in the abundance of DGAT1 protein in rosette leaves were evident (Figure 3-8). The protein was present in low amounts in the leaves from 2-, 3- and 4-week-old plants, and then increased sharply through weeks 5 and 6, coincident with the onset of senescence.

3.3.5 Increased abundance of triacylglycerols in senescent (6-week-old) rosette leaves relative to pre-senescent (3-week-old) rosette leaves of *Arabidopsis thaliana*

DGAT1 catalyzes the final acylation, and is thought to be the rate-limiting step, in triacylglycerol synthesis (Ichihara *et al.*, 1988). Accordingly, the finding that DGAT1

Figure 3-7: Northern blot of DGAT1 during development and senescence of *Arabidopsis thaliana* rosette leaves

A. Northern blot of total RNA isolated from rosette leaves of 2- through 6-week-old *Arabidopsis* plants. The blot was hybridized with the *Arabidopsis* EST clone E6B2T7. Each lane contained 10μg of RNA. Lanes correspond to age in weeks of the rosette leaves. The apparent size of the detected band is indicated on the right. **B.** Ethidium bromide detection of fractionated RNA after transfer to a nylon membrane to show equal loading. Lanes are as in A.

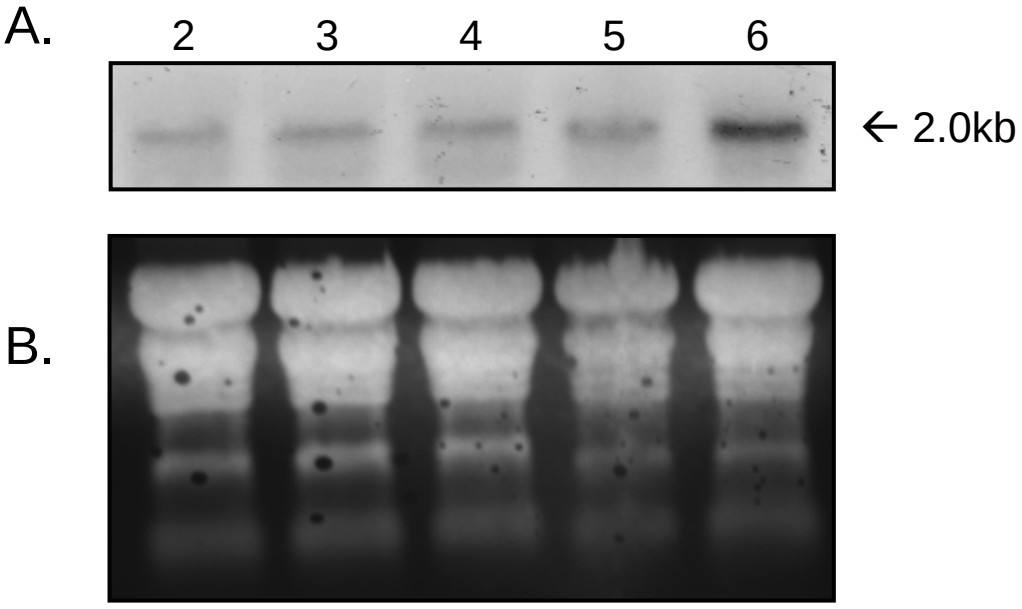
A.
2
3
4
5
6
← 2.0kb
B.

Figure 3-8: Western blot of DGAT1 during development and senescence of *Arabidopsis thaliana* rosette leaves

A. Western blot of DGAT1 in total protein isolated from the rosette leaves of 2- through 6-week-old *Arabidopsis* plants. Each lane contained 10μg of protein. The blot was probed with antibody raised against a synthetic peptide of DGAT1 and visualized by a colorimetric reaction. The apparent molecular mass of the immunodetected polypeptide is indicated in kilodaltons. **B.** SDS-PAGE stained with Coomassie Brilliant Blue. Molecular mass markers are indicated on the left. Lanes correspond to the age in weeks of the rosette leaves.

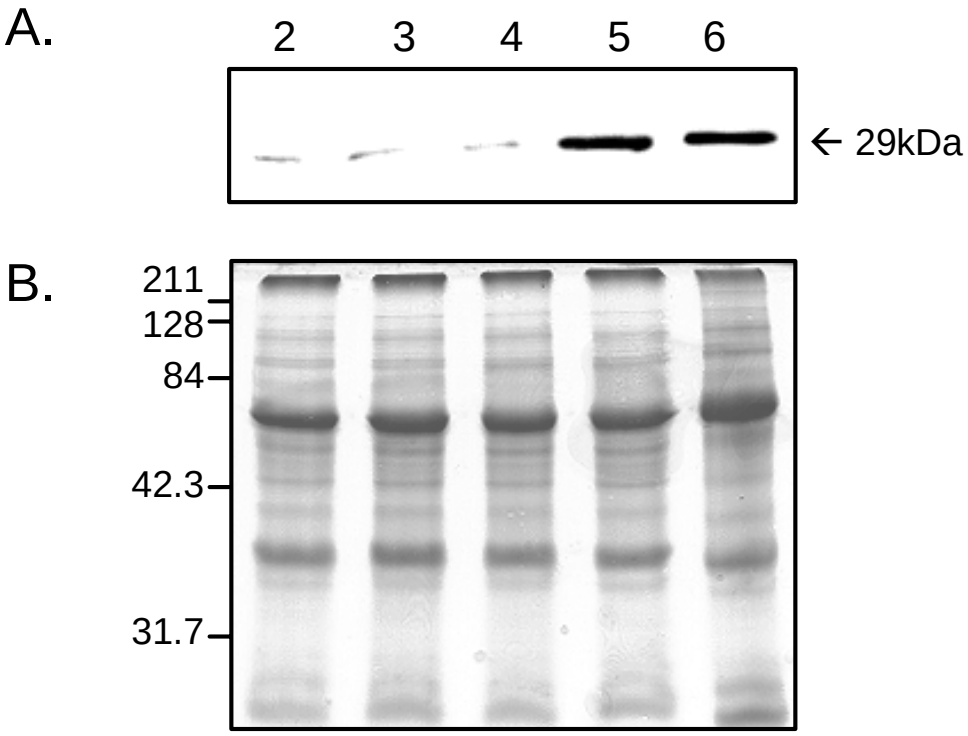
A.
2
3
4
5
6
← 29kDa
B.
211
128
84
42.3
31.7

transcript and cognate protein increase in parallel in senescing rosette leaves of *Arabidopsis* raised the possibility that there would be a parallel increase in triacylglycerol. To test this, the lipid content and composition of rosette leaves that were pre-senescent (3-weeks-old) were compared to the lipid content and composition of senescent (6-week-old) rosette leaves.

Five distinct classes of lipid, viz., polar lipid, diacylglycerols, free fatty acids, triacylglycerols and a mixture of steryl and wax esters were discernible in thin layer chromatograms of total homogenate lipid and microsomal membrane lipid isolated from the rosette leaves of 3- and 6-week-old plants (Figure 3-9). Lipid extracts from homogenates contain total leaf lipid, and those from microsomal membranes contain lipid associated with organellar membranes, for example endoplasmic reticulum and chloroplast membranes, that form microsomes during homogenization (Cao and Huang, 1986; Stobart *et al.*, 1986). The rosette leaves of 3-week-old plants are still growing and maturing and have not yet initiated senescence, whereas the rosette leaves of 6-week-old plants are visibly chlorotic and have initiated senescence. Likewise, the levels of DGAT1 transcript and protein are low in pre-senescent (3-week-old) rosette leaves, and greatly induced in the senescent (6-week-old) rosette leaves.

Several pigments co-resolved with the polar lipid, diacylglycerols, and steryl and wax esters in the homogenate and microsomal membrane fractions of the pre-senescent (3-week-old) rosette leaves (Figure 3-9A). These pigments were present to a much lesser extent in lipids extracted from the senescent (6-week-old) rosette leaves (Figure 3-9B) than the lipids extracted from the pre-senescent (3-week-old) rosette leaves (Figure 3-9A). It should be noted that the lanes on the thin layer chromatograms were not loaded with equal amounts of lipid. Fractionated lipids were scraped from the plates under a stream of nitrogen with a clean razor for each of the lipid classes. The lipids were re-extracted from the silica scraped from the plates and transmethylated to release fatty acid methyl esters in preparation for GCMS injection. A total lipid aliquot removed from each sample prior to TLC separation was also transmethylated in preparation for GCMS injection. These comprised the total lipid samples for the homogenate and microsomal membranes from pre-senescent (3-week-old) and senescent (6-week-old) rosette leaves.

Figure 3-9: Thin Layer Chromatograms (TLC) showing resolved lipid classes for pre-senescent (3-week-old) and senescent (6-week-old) rosette leaves, stained with iodine vapour

Representative TLC plates for lipids extracted from **A.** Pre-senescent (3-week-old) rosette leaves; and **B.** Senescent (6-week-old) rosette leaves. The lipids were resolved using a non-polar solvent mixture and identified using a standard (S) mixture of known lipid classes. For each age of tissue, total lipids extracted from homogenate (H) and microsomal membranes (M) were chromatographed. The TLC plates were stained with iodine vapour until yellowish-brown bands were apparent. Five distinct lipid classes were observed in each lane: PL=polar lipids, DAG=diacylglycerols, FFA=free fatty acids, TAG=triacylglycerols, SWE=steryl and wax esters. The lanes were not equally loaded. The black lines separating the lipid classes delineate the regions scraped for the collection of each lipid class within each sample lane.

A.

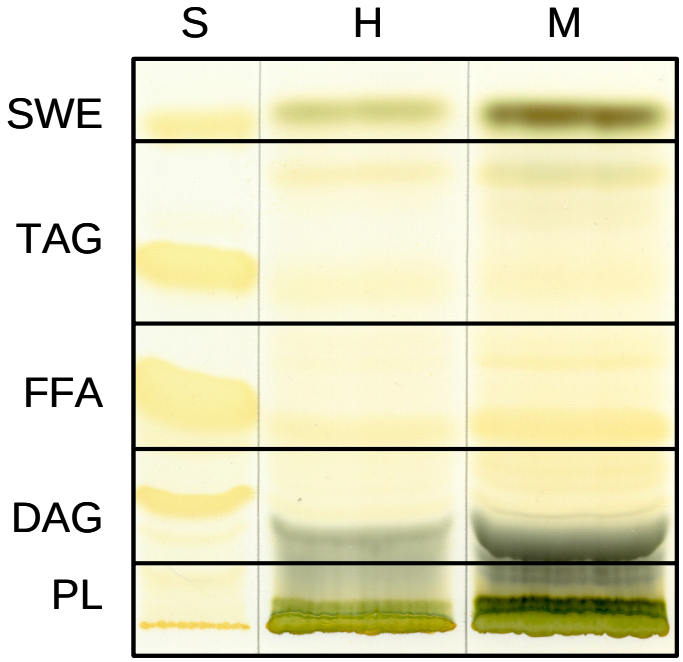

B.

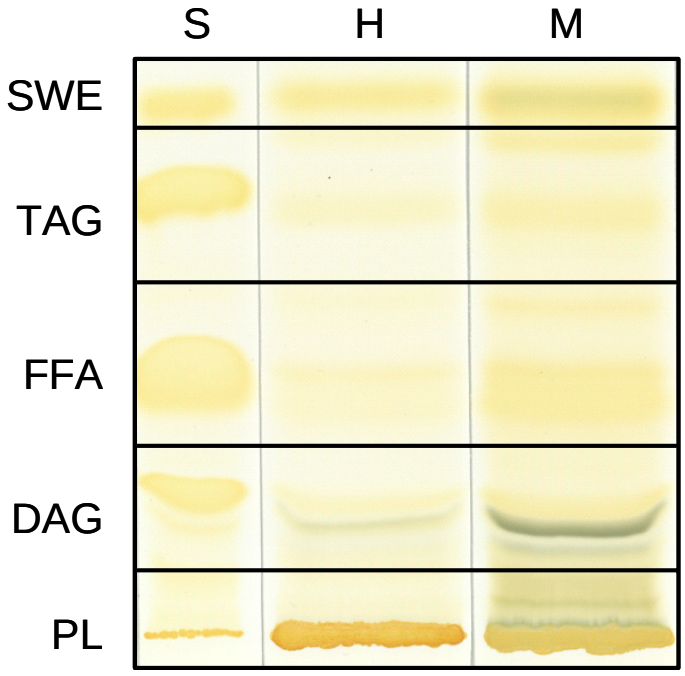

The levels of the different types of lipid were quantified in terms of their fatty acid equivalents and proved to be quite different for homogenate and microsomal membranes isolated from pre-senescent (3-week-old) and senescent (6-week-old) rosette leaves (Figure 3-10 and Figure 3-11). For the homogenate and microsomal membrane fractions of pre-senescent (3-week-old) rosette leaves, polar lipids comprised 84.76 ± 1.34% and 77.82 ± 2.50% of the total lipid respectively (Figure 3-10 and Figure 3-11). By comparison, for the homogenate and microsomal membranes of senescent (6-week-old) rosette leaves, polar lipids represented only 53.03 ± 5.45% (p=0.020) and 52.10 ± 2.54% (p=0.001), respectively, of the total lipid (Figure 3-10 and Figure 3-11).

This reduction in polar lipids was largely accounted for by a corresponding increase in triacylglycerol and steryl and wax esters (Figure 3-10 and Figure 3-11). For example, levels of triacylglycerol in the homogenate increased from 2.02 ± 0.12% of the total lipid for pre-senescent (3-week-old) leaves to 12.33 ± 2.20% (p=0.039) for senescent (6-week-old) leaves (Figure 3-10 and Figure 3-11). In absolute terms, levels of triacylglycerol in the homogenate increased from 0.34 ± 0.01μg/g fresh weight for pre-senescent (3-week-old) leaves to 4.48 ± 0.38 μg/g fresh weight for senescent (6-week-old) leaves, which is a 13-fold increase in triacylglycerol (p=0.008). Similarly, steryl and wax esters which comprise a mere 1.22 ± 0.14% of the total lipid pool for homogenates of pre-senescent (3-week-old) rosette leaves increased to 16.40 ± 3.59% (p=0.049) of the total lipid pool in senescent (6-week-old) leaves (Figure 3-10 and Figure 3-11). In absolute terms, steryl and wax esters increased from 0.21 ± 0.03 μg/g fresh weight in the pre-senescent (3-week-old) leaves to 6.70 ± 2.55 μg/g fresh weights for senescent (6-week-old) leaves. Although this difference is large and clearly represents a trend, it is not significant at the 95% level according to the student's t-test, which generated a p-value of 0.124. The enhancement in triacylglycerols and steryl and wax esters was also evident in the microsomal membranes where they increased by 4.2- and 5.3-fold respectively, between the pre-senescent (3-week-old) and senescent (6-week-old) leaves (Figure 3-10 and Figure 3-11). There was also a significant 2.2-fold increase in free fatty acids in the microsomal membranes of senescent (6-week-old) rosettes compared to the microsomal membranes of pre-senescent (3-week-old) rosettes (p=0.004) (Figure 3-10).

Figure 3-10: Relative levels of lipid classes expressed as a percentage of the total lipid pool

Relative levels of lipid classes in homogenate and microsomal membranes were quantified in terms of their fatty acid equivalents for pre-senescent (3-weeks-old) and senescent (6-week-old) rosette leaves. There were significant changes in the relative levels of polar lipids (PL), triacylglycerol (TAG) and steryl and wax esters (SWE) between pre-senescent (3-week-old) and senescent (6-week-old) rosette leaves for homogenate and microsomal membranes. DAG= diacylglycerols, FFA=free fatty acids.

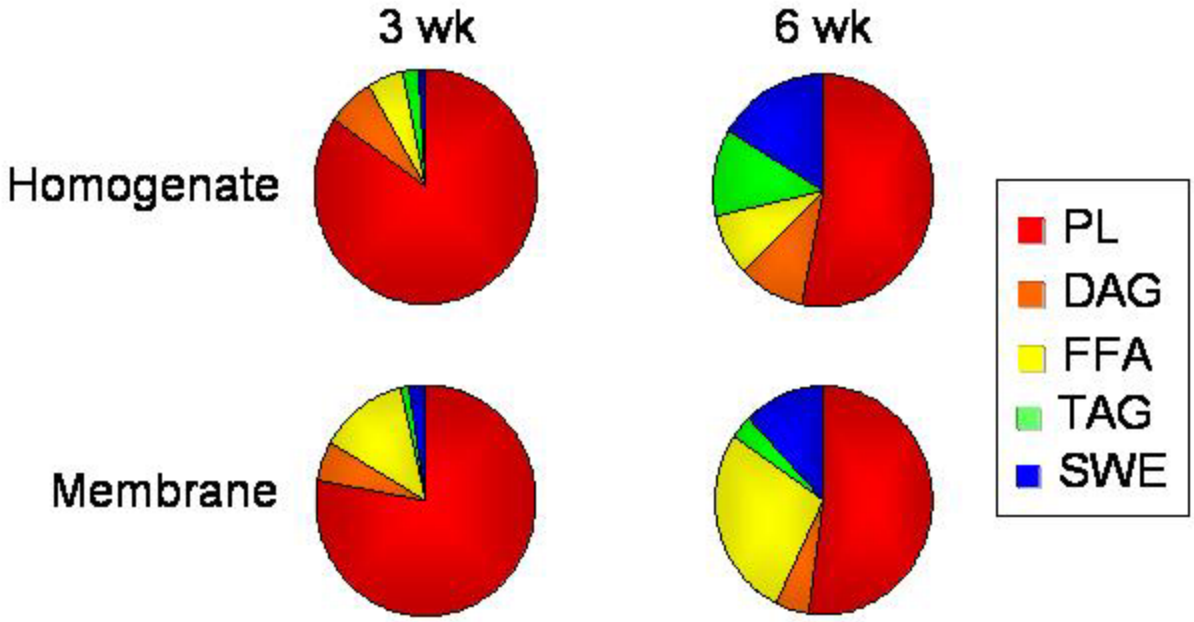
3 wk
6 wk
Homogenate
Membrane
PL
DAG
FFA
TAG
SWE

Figure 3-11: Relative levels of lipid classes expressed as a percentage of the total lipid pool for homogenate and microsomal membranes

Relative levels of lipids were quantified in terms of their fatty acid equivalents. The top panel illustrates the decline in polar lipids (PL) in senescent (6-week-old) rosette leaves (■) compared to the pre-senescent (3-week-old) rosette leaves (■). The middle and bottom panels show the increase in triacylglycerols (TAG) and steryl and wax esters (SWE), respectively, in senescent (6-week-old) rosette leaves (■) compared to the pre-senescent (3-week-old) rosette leaves (■).

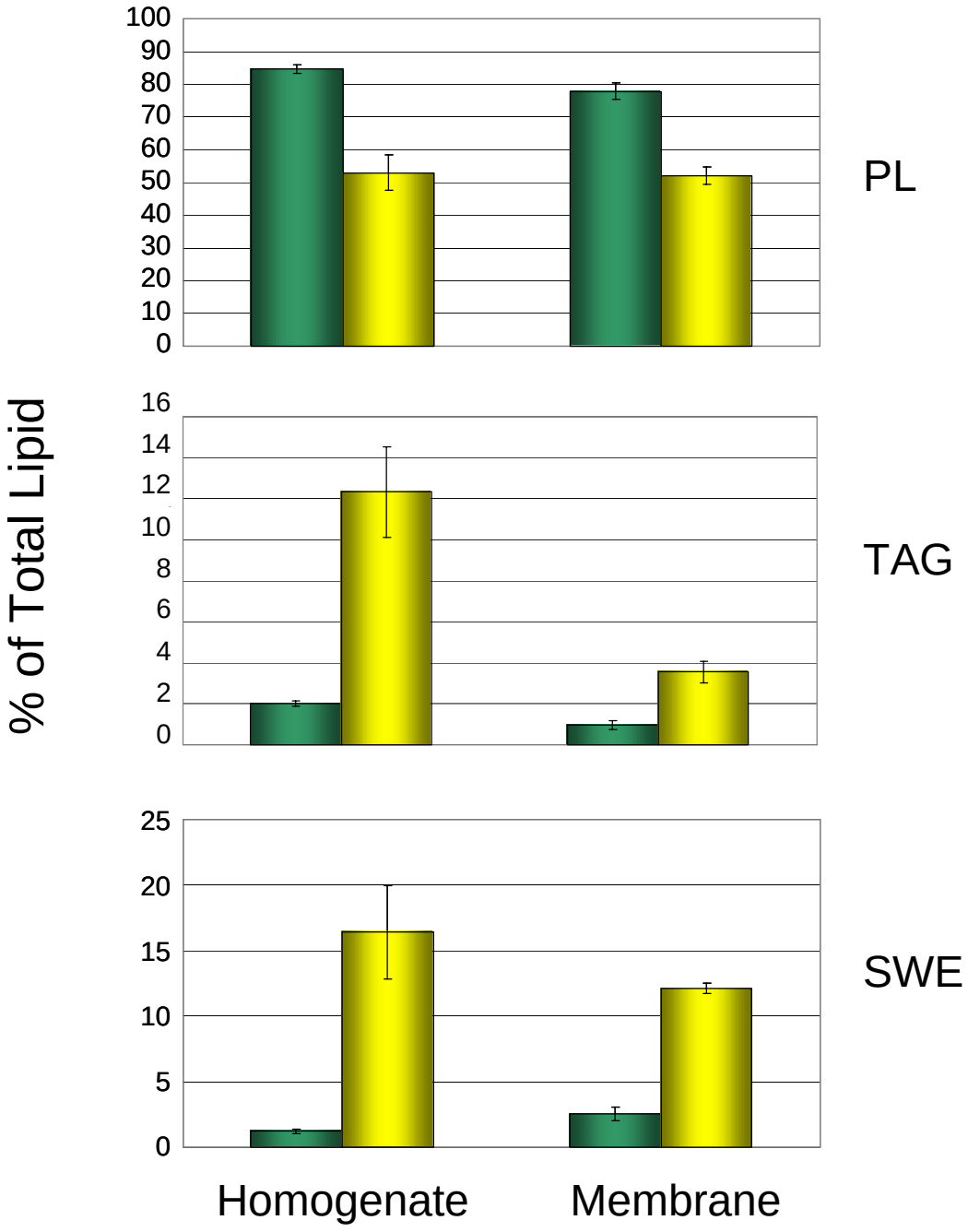
% of Total Lipid
100
90
80
70
60
50
40
30
20
10
0
PL
16
14
12
10
8
6
4
2
0
TAG
25
20
15
10
5
0
SWE
Homogenate
Membrane

However, there was no significant change in the contribution that diacylglycerols made to the total leaf lipid pool between 3- and 6-weeks of age (homogenate p=0.190, microsomal membrane p=0.313).

3.3.6 Fatty acid composition of homogenates and microsomal membranes isolated from pre-senescent (3-week-old) and senescent (6-week-old) rosette leaves

The fatty acid compositions of homogenates and microsomal membranes isolated from pre-senescent (3-week-old) and senescent (6-week-old) leaves were analyzed by GCMS. Levels of individual fatty acids were expressed as a percentage of the total fatty acid content. The fatty acid profiles of the pre-senescent (3-week-old) and senescent (6-week-old) rosette homogenates showed only a few differences in composition (Figure 3-12, top panel). The predominant fatty acids in homogenate total lipid extracts for both the pre-senescent (3-week-old) and senescent (6-week-old) rosette leaves were hexadecanoic acid (16:0), linoleic acid (18:2) and linolenic acid (18:3). Those that differed significantly between homogenates of pre-senescent (3-week-old) and senescent (6-week-old) rosette leaves were myristic acid (14:0; p=0.050), oleic acid (18:1; p=0.011), linoleic acid (18:2; p=0.002), tetracosanoic acid (24:0; p=0.016) and hexacosanoic acid (26:0; p=0.008). The fatty acid profiles of total lipid from isolated microsomal membranes of pre-senescent (3-week-old) and senescent (6-week-old) rosette leaves also featured only small differences (Figure 3-12, lower panel). Again the predominant fatty acids for both the pre-senescent (3-week-old) and senescent (6-week-old) rosette leaves were hexadecanoic acid (16:0), linoleic acid (18:2) and linolenic acid (18:3). The microsomal membrane fatty acids that differed significantly between pre-senescent (3-week-old) and senescent (6-week-old) rosette leaves were lauric acid (12:0; p=0.003), myristic acid (14:0; p=0.011), hexadecenoic acid (16:1; p=0.009), linoleic acid (18:2; p=0.009), tricosanoic acid (23:0; p=0.006), tetracosanoic acid (24:0; p=0.026) and octacosanoic acid (28:0; p=0.029).

In homogenates of pre-senescent (3-week-old) rosette leaves, the major triacylglycerol fatty acids proved to be hexadecanoic acid (16:0), stearic acid (18:0), and erucic acid (22:1; Figure 3-13 bottom panel). By contrast, in the homogenate of senescing

Figure 3-12: Fatty acid profiles of total lipid extracts from homogenates and microsomal membranes isolated from pre-senescent (3-week-old) and senescent (6-week-old) rosette leaves

Levels of individual fatty acids are expressed as a percentage of the total fatty acids. Total lipids were extracted from homogenates (top panel) and microsomal membranes (lower panel) isolated from pre-senescent (3-week-old) rosette leaves (■) and senescent (6-week-old) rosette leaves (■).12:0=lauric acid, 14:0= myristic acid, 15:0= pentadecanoic acid, 16:0= hexadecanoic acid, 16:1= hexadecenoic acid, 16:3= hexadecatrienoic acid, 18:0= stearic acid, 18:1= oleic acid, 18:2= linoleic acid, 18:3= linolenic acid, 22:0= docosanoic acid, 22:1= docosenoic acid, 23:0= tricosanoic acid, 24:0= tetracosanoic acid, 25:0= pentacosanoic acid, 26:0= hexacosanoic acid, 28:0= octacosanoic acid.

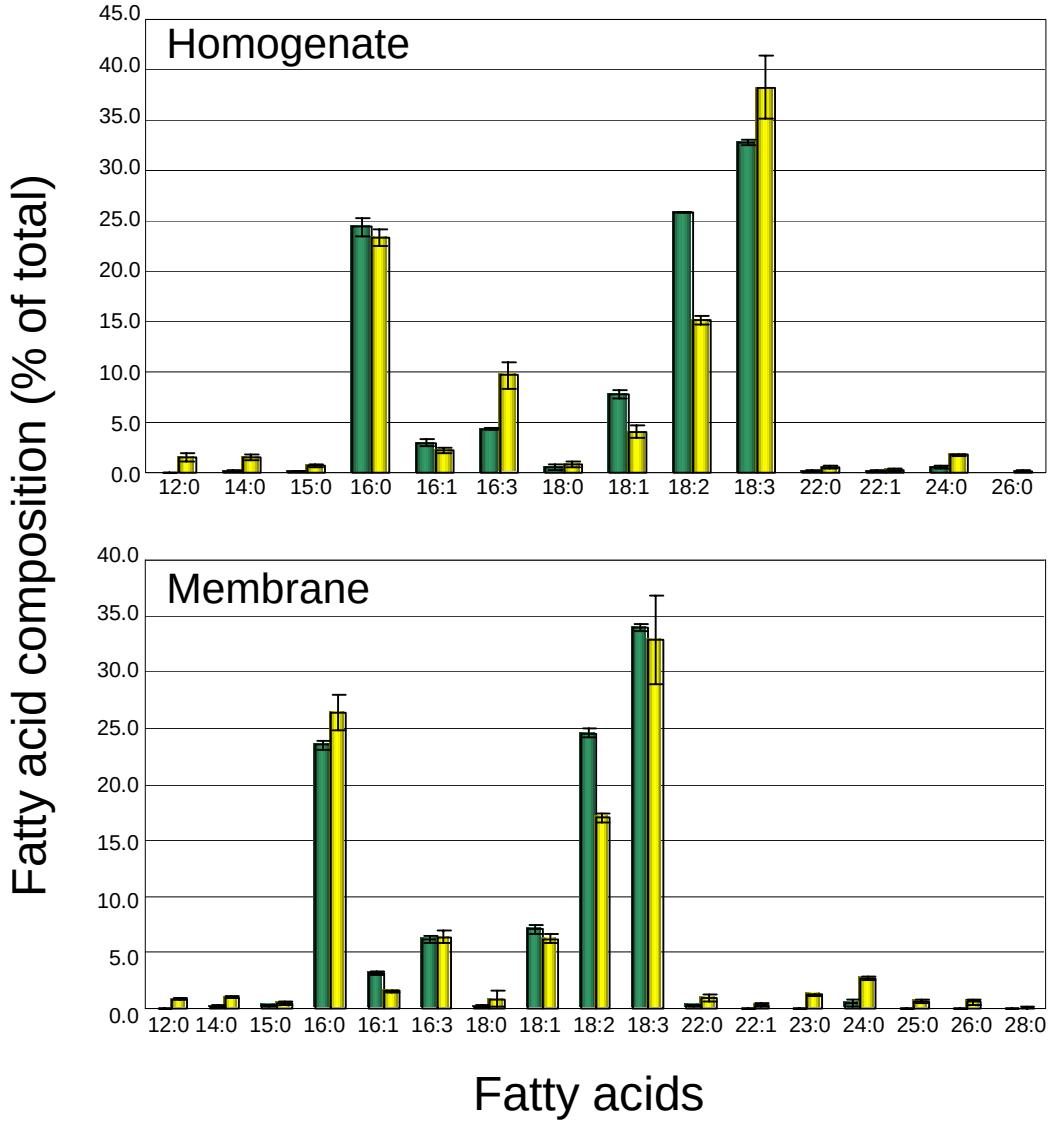
Homogenate
Membrane
Fatty acid composition (% of total)
Fatty acids
45.0
40.0
35.0
30.0
25.0
20.0
15.0
10.0
5.0
0.0
12:0
14:0
15:0
16:0
16:1
16:3
18:0
18:1
18:2
18:3
22:0
22:1
24:0
26:0
23:0
25:0
28:0

(6-week-old) rosette leaves, the dominant triacylglycerol fatty acids included hexadecanoic acid (16:0), as for young leaves, as well as hexadecatrienoic acid (16:3), linoleic acid (18:2) and linolenic acid (18:3) (Figure 3-13, bottom panel). Linolenic acid (18:3) and hexadecatrienoic acid (16:3), which are normally associated with the galactolipids of chloroplast membranes (Awai *et al.*, 2001), collectively accounted for 45.03% ± 2.07% of the total triacylglycerol fatty acid complement in homogenates of 6-week-old senescing leaves, and were not detectable in the triacylglycerol fraction of homogenates for pre-senescent 3-week-old leaves (Figure 3-15 top panel). Thus, the triacylglycerol in the older leaves would appear to be formed at least in part from fatty acids originating from chloroplast membranes. Further to this, levels of linolenic acid (18:3) and hexadecatrienoic acid (16:3) in other lipid classes were also significantly increased between homogenates of senescent (6-week-old) rosette leaves and pre-senescent (3-week-old) rosette leaves. For example, for the free fatty acid and steryl and wax ester fractions they comprised 12.89%±1.17 and 51.25% ± 0.004, respectively, of the total fatty acid complement for 6-week-old senescing leaves and were not detectable in these fractions from 3-week-old pre-senescent leaves (Figure 3-15, top panel).

In the microsomal membranes of pre-senescent (3-week-old) leaves, the major triacylglycerol fatty acids included palmitic acid (16:0), stearic acid (18:0), erucic acid (22:1) as well as oleic acid (18:1) (Figure 3-14, bottom panel). However, the microsomal membrane triacylglycerol fraction from senescent 6-week-old leaves contained not only oleic acid (18:1), but also hexadecanoic acid (16:0), hexadecatrienoic acid (16:3), linoleic acid (18:2) and linolenic acid (18:3) as the major fatty acid constituents (Figure 3-14, bottom panel). Moreover, as was seen for the homogenates hexadecatrienoic acid (16:3) and linolenic acid (18:3) were not detectable in the triacylglycerol fraction of pre-senescent (3-week-old) rosette leaves, but comprised 34.61% ± 1.62% of the total microsomal membrane triacylglycerol fatty acid complement in the senescent (6-week-old) rosette leaves (Figure 3-15, middle panel).

Unlike triacylglycerol, the fatty acid composition for the polar lipids remained relatively unchanged as senescence was engaged in the rosette leaves (Figure 3-13, top

Figure 3-13: Fatty acid composition of polar lipids and triacylglycerols in the homogenate of pre-senescent (3-week-old) and senescent (6-week-old) rosette leaves

Levels of individual fatty acids in polar lipids (PL; upper panel) and triacylglycerol (TAG; lower panel) are expressed as a percentage of the total corresponding fatty acid pool. Pre-senescent 3-week-old rosette leaves (■), senescent 6-week-old rosette leaves (■). 12:0=lauric acid, 14:0= myristic acid, 15:0= pentadecanoic acid, 16:0= hexadecanoic acid, 16:1= hexadecenoic acid, 16:2= hexadecadienoic acid, 16:3= hexadecatrienoic acid, 18:0= stearic acid, 18:1= oleic acid, 18:2= linoleic acid, 18:3= linolenic acid, 22:0= docosanoic acid, 22:1= erucic/ docosenoic acid, 23:0= tricosanoic acid, 24:0= tetracosanoic acid, 24:1= tetracosenoic acid, 25:0= pentacosanoic acid, 26:0= hexacosanoic acid.

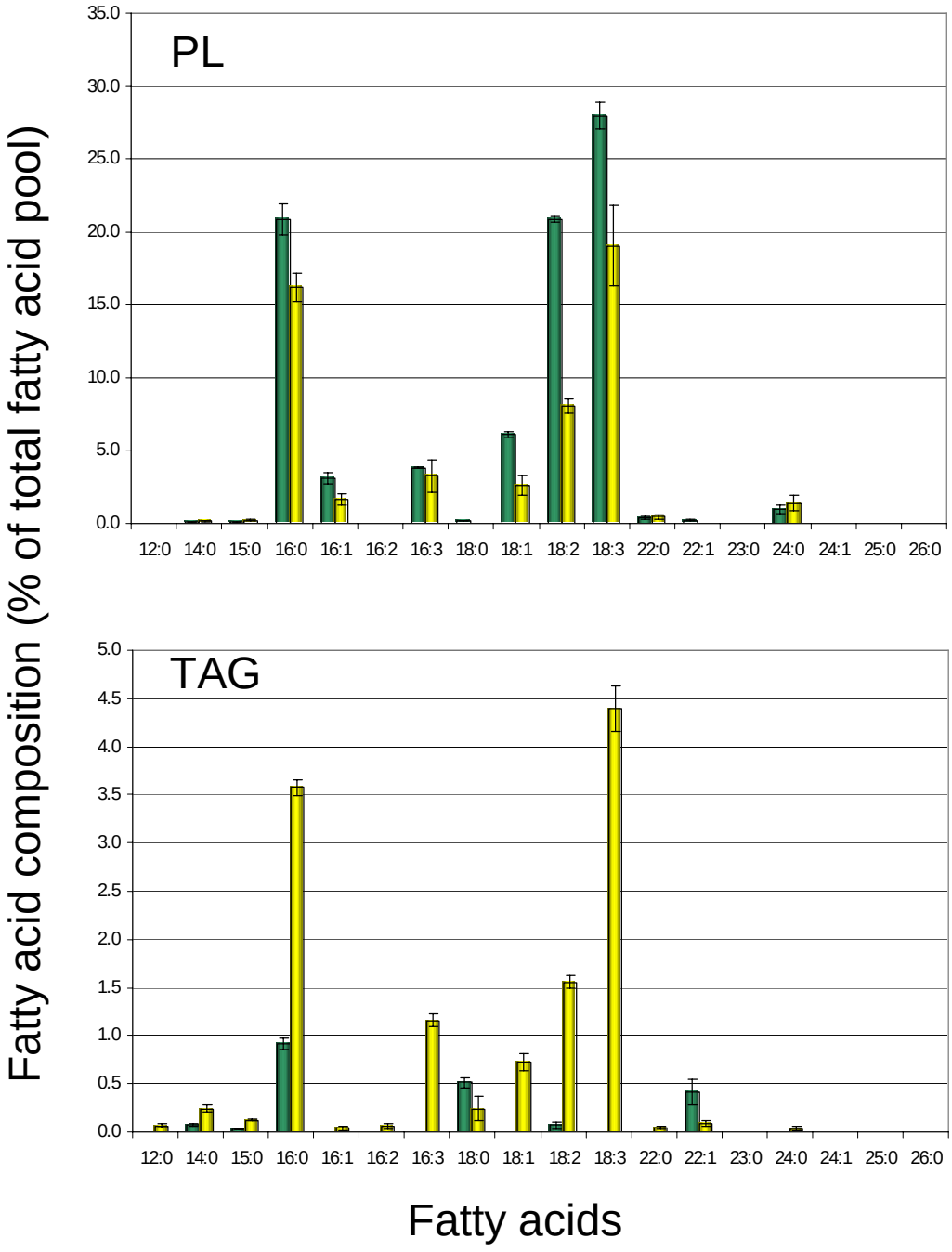
PL
TAG
Fatty acid composition (% of total fatty acid pool)
Fatty acids
35.0
30.0
25.0
20.0
15.0
10.0
5.0
0.0
4.5
4.0
3.5
3.0
2.5
2.0
1.5
1.0
0.5
12:0
14:0
15:0
16:0
16:1
16:2
16:3
18:0
18:1
18:2
18:3
22:0
22:1
23:0
24:0
24:1
25:0
26:0

Figure 3-14: Fatty acid composition of polar lipids and triacylglycerols in microsomal membranes of pre-senescent (3-week-old) and senescent (6-week-old) rosette leaves

Levels of individual fatty acids in polar lipids (PL; upper panel) and triacylglycerol (TAG; lower panel) are expressed as a percentage of the total corresponding fatty acid pool. Pre-senescent 3-week-old rosette leaves (■), senescent 6-week-old rosette leaves (■). 12:0=lauric acid, 14:0= myristic acid, 15:0= pentadecanoic acid, 16:0= hexadecanoic acid, 16:1= hexadecenoic acid, 16:2= hexadecadienoic acid, 16:3= hexadecatrienoic acid, 18:0= stearic acid, 18:1= oleic acid, 18:2= linoleic acid, 18:3= linolenic acid, 22:0= docosanoic acid, 22:1= erucic/ docosenoic acid, 23:0= tricosanoic acid, 24:0= tetracosanoic acid, 24:1= tetracosenoic acid, 25:0= pentacosanoic acid, 26:0= hexacosanoic acid.

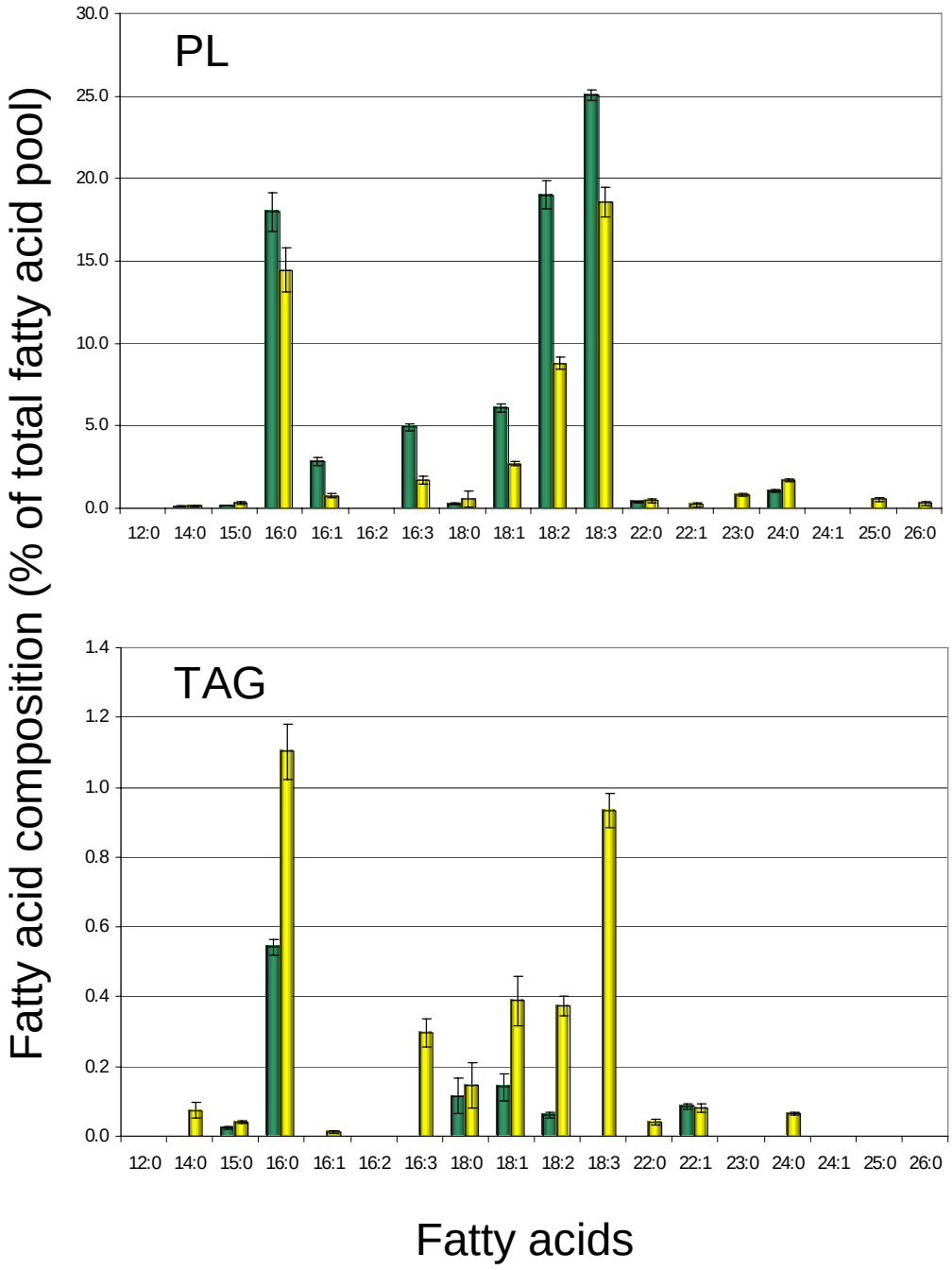
PL
TAG
Fatty acid composition (% of total fatty acid pool)
Fatty acids
30.0
25.0
20.0
15.0
10.0
5.0
0.0
1.4
1.2
1.0
0.8
0.6
0.4
0.2
0.0
12:0 14:0 15:0 16:0 16:1 16:2 16:3 18:0 18:1 18:2 18:3 22:0 22:1 23:0 24:0 24:1 25:0 26:0

panel). The major fatty acids associated with the polar lipids of the homogenate proved to be hexadecanoic acid (16:0) and two polyunsaturated fatty acids, linoleic acid (18:2) and linolenic acid (18:3). These collectively accounted for 82.22% ± 0.59% of the total polar lipid fatty acid complement in the homogenates of pre-senescent (3-week-old) rosette leaves and 81.59% ± 5.80% of the total polar lipid fatty acid complement in senescent (6-week-old) rosette leaves. The predominant fatty acids in the microsomal membrane polar lipids were again hexadecanoic acid (16:0), linoleic acid (18:2) and linolenic acid (18:3; Figure 3-14, top panel). Interestingly, however, there was a significant reduction in hexadecatrienoic acid (16:3) in the polar lipids of microsomal membranes from senescent (6-week-old) rosette leaves in comparison with pre-senescent (3-week-old) rosette leaves (p=0.014). This may at least in part account for the appearance of hexadecatrienoic acid (16:3) in the triacylglycerol fraction of microsomal membranes isolated from senescent (6-week-old) rosette leaves (Figure 3-14, bottom panel). For young and senescing leaves, linolenic acid (18:3) was the dominant fatty acid in the polar lipid fraction (Figure 3-14, top panel). Inasmuch as linolenic acid (18:3) is the major fatty acid of galactolipids, this indicates, as expected, that galactolipids are a substantial component of the polar lipid isolate. The presence of hexadecatrienoic acid (16:3) in the polar lipid fraction also signifies the presence of galactolipids, for this fatty acid is uniquely chloroplastic in 16:3 plants such as *Arabidopsis thaliana* (Awai *et al.*, 2001). However, it is the appearance of hexadecatrienoic acid (16:3) in the free fatty acid, diacylglycerol, triacylglycerol and steryl and wax ester lipid classes that is particularly interesting (Figure 3-15).

In the homogenates for pre-senescent (3-week-old) rosette leaves, hexadecatrienoic acid (16:3) was only found in the polar lipid fraction (Table 3-2). The same proved to be true for the microsomal membrane fraction from pre-senescent (3-week-old) rosettes with the exception of a very small amount of hexadecatrienoic acid (16:3) in the free fatty acid fraction accounting for only 0.92% ± 0.47% of the total fatty acid pool (Table 3-2). However, there is a significant increase in hexadecatrienoic acid (16:3), particularly in triacylglycerol and steryl and wax esters of both homogenate and microsomal membrane fractions and in the free fatty acid complement of homogenate, for senescent (6-week-old)

Figure 3-15: Levels of the chloroplastic fatty acids, hexadecatrienoic acid (16:3) and linolenic acid (18:3), in different lipid classes extracted from homogenates and microsomal membranes isolated from pre-senescent (3-week-old) rosette leaves and senescent (6-week-old) rosette leaves

The sums of the chloroplastic fatty acids, hexadecatrienoic acid (16:3) and linolenic acid (18:3), are expressed as a percentage of the total fatty acid pool for each of the lipid classes extracted from homogenates (top panel) and microsomal membranes (lower panel) isolated from pre-senescent (3-week-old) rosette leaves (■) and senescent (6-week-old) rosette leaves (■). PL=polar lipid, DAG=diacylglycerols, FFA=free fatty acids, TAG=triacylglycerols, SWE=steryl and wax esters.

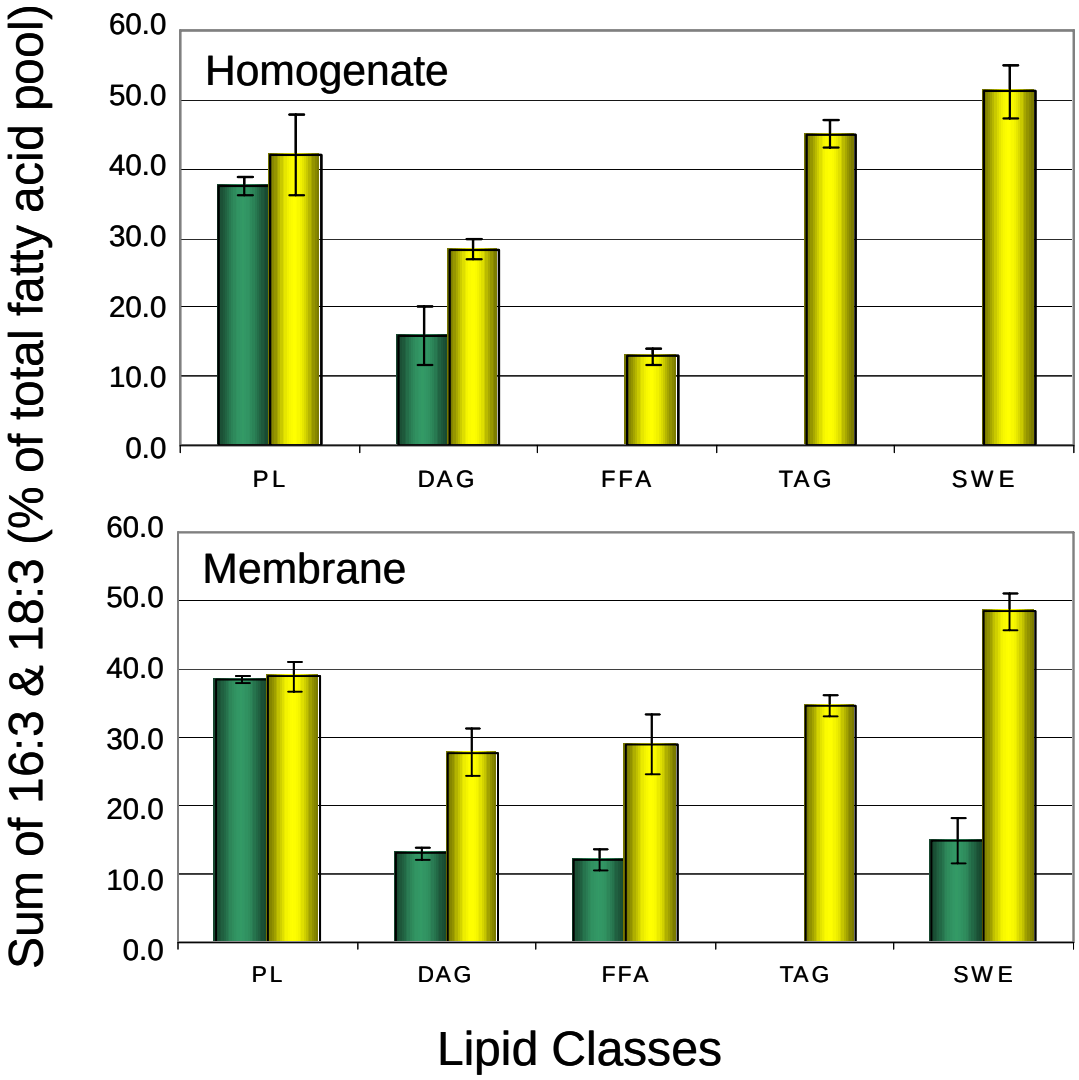
Sum of 16:3 & 18:3 (% of total fatty acid pool)
Homogenate
Membrane
60.0
50.0
40.0
30.0
20.0
10.0
0.0
PL
DAG
FFA
TAG
SWE
Lipid Classes

Table 3-2: Hexadecatrienoic acid (16:3) in isolated lipid classes expressed as a percentage of the total fatty acid complement for homogenate and microsomal membranes of pre-senescent (3-week-old) and senescent (6-week-old) rosette leaves

	Homogenate		Microsomal Membrane	
	3wk	**6wk**	**3wk**	**6wk**
Polar lipid	4.51±0.12	6.16±2.53	6.32±0.28	3.24±0.53*
Diacylglycerol	0.00±0.00	2.96±0.55*	0.00±0.00	2.22±0.97
Free fatty acids	0.00±0.00	3.14±0.40*	0.92±0.47	6.75±1.32
Triacylglycerol	0.00±0.00	9.39±0.70*	0.00±0.00	8.30±1.40*
Steryl and Wax esters	0.00±0.00	26.38±0.01*	0.00±0.00	12.61±0.95*

* Indicates values that are significantly different between pre-senescent (3-week-old) and senescent (6-week-old) samples. $p<0.05$; $n=3$.

leaves (Table 3-2). It can be assumed that the hexadecatrienoic acid in these fractions of senescent (6-week-old) leaves originated from chloroplast polar lipids.

3.3.7 Chloroplast origin of triacylglycerol in senescent rosettes

The finding that triacylglycerol from senescing rosette leaves of 6-week-old plants contains high levels of fatty acids derived from chloroplastic membranes suggests that the newly synthesized triacylglycerol is formed within chloroplasts. This contention is additionally supported by electron microscopic observations indicating greatly increased abundance and size of plastoglobuli in the chloroplasts of senescent (6-week-old) rosette leaves in comparison with those of pre-senescent (3-week-old) rosette leaves (Figure 3-16). Plastoglobuli are known to contain triacylglycerol and are thought to be formed coincident with the dismantling of thylakoid membranes in senescing chloroplasts (Matile, 1992). That DGAT1, the protein mediating the terminal step in triacylglycerol synthesis, is associated with chloroplasts was confirmed by Western-blot analysis (Figure 3-17). Chloroplasts were isolated from 4.5-week-old rosette *Arabidopsis* leaves and subfractionated into membranes, a composite of thylakoid and envelope membranes, and stroma. Immunoblots of chloroplasts and their purified subfractions probed with the DGAT1 peptide antibody revealed that the protein is present in intact chloroplasts, and enriched in the purified chloroplast membrane fraction, but is not detectable in stroma (Figure 3-17).

The purity of the isolated chloroplasts was confirmed by Western-blot analysis (Figure 3-18) using antiserum for formate dehydrogenase, a marker for mitochondria (Frans-Small *et al.*, 1993), cytochrome P_{450}-cinnamate-4-hydroxylase, a marker for endoplasmic reticulum (Young and Beevers, 1976),and cytochrome *f*, a marker for thylakoids (Smith *et al.*, 2000). Formate dehydrogenase, cytochrome P_{450}-cinnamate-4-hydroxylase and cytochrome *f* were all detectable in immunoblots of microsomal membranes. The presence of cytochrome P_{450}-cinnamate-4-hydroxylase and cytochrome *f* in microsomes is in keeping with the fact that this fraction comprises small vesicles formed during tissue homogenization from all cellular membranes, including endoplasmic reticulum and thylakoids. Formate dehydrogenase is a mitochondrial matrix enzyme which would be released into the cytosol during homogenization (Frans-Small *et al.*, 1993), and its presence in the microsomal

Figure 3-16: Electron micrographs of chloroplasts in the mesophyll of a typical pre-senescent (3-week-old) and senescent (6-week-old) rosette leaf

A. A young (3-week-old) rosette leaf chloroplast. **B.** A senescing (6-week-old) rosette leaf chloroplast. S=starch granule; W=cell wall; P=plastoglobuli. Bar=1μm.

A.

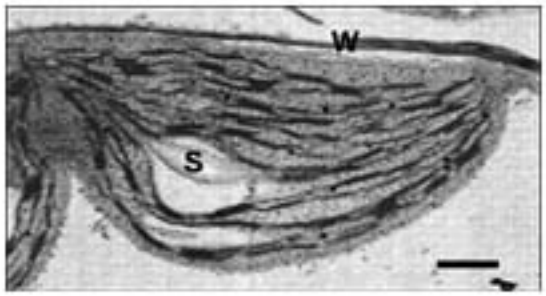

B.

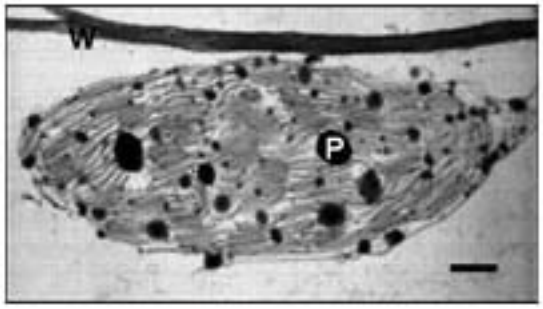

Figure 3-17: Western blot analysis of DGAT1 localization in intact chloroplasts and chloroplastic fractions isolated from 4.5-week-old rosette leaves

A. Western blot probed with antibody raised against a peptide of DGAT1. I=Intact chloroplasts; M=Chloroplastic membranes; S=Stroma. The apparent molecular mass of the immunodetected polypeptide is indicated in kilodaltons. **B.** Corresponding SDS-PAGE. Each lane contained 5μg of protein, and the gel was stained with Coomassie Brilliant Blue. The molecular masses of the marker are indicated on the left. Only the large 55kDa subunit of Rubisco is evident in Figure 2-17 inasmuch as the small 14kD subunit ran off the end of the gel under the conditions of electrophoresis deployed.

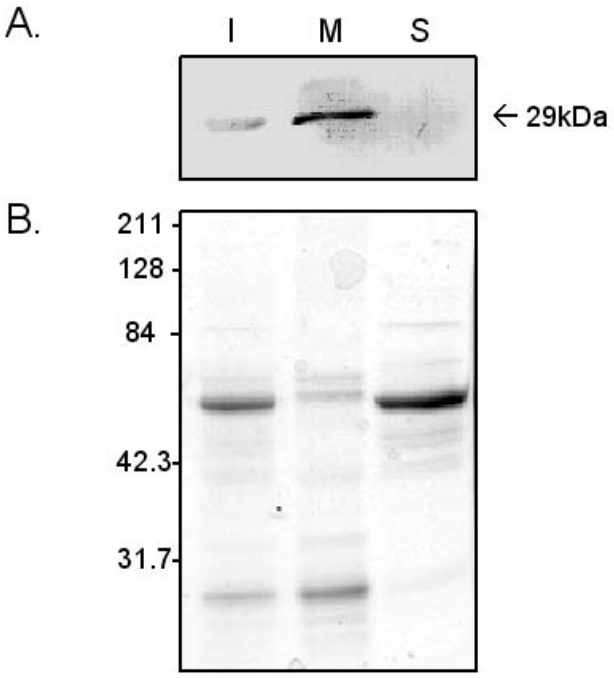
A.
I
M
S
← 29kDa
B.
211
128
84
42.3
31.7

Figure 3-18: Western blot analysis of purified chloroplasts and microsomal membranes isolated from the rosette leaves of 4.5-week-old *Arabidopsis thaliana* plants.

Each lane was loaded with 5μg of protein. MM=microsomal membranes; IC=intact chloroplasts. The blots were probed with polyclonal antibodies against cytochrome P_{450}-cinnamate-4-hydroxylase (C4H, top panel), formate dehydrogenase (FDH, middle panel), and cytochrome *f* (Cyt f, bottom panel).

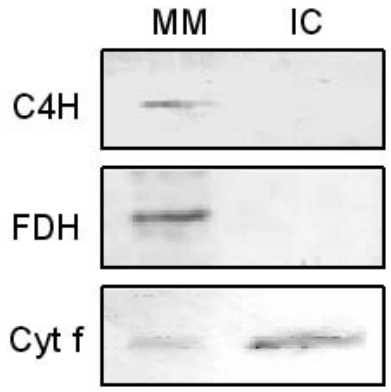
MM
IC
C4H
FDH
Cyt f

fraction reflects the fact that cytosol is occluded within microsomal vesicles as they are formed. Because formate dehydrogenase is a mitochondrial matrix enzyme and would not reveal the presence of mitochondrial membrane vesicles in the intact chloroplast fraction, levels of cytochrome *c* oxidase activity, a marker enzyme for mitochondrial inner membrane (Hodges and Leonard, 1974), were measured in the microsomal membranes and intact chloroplasts. The specific activity of cytochrome *c* oxidase in the intact chloroplast fraction was only 1/25 of that for microsomal membranes, indicating that the purified chloroplast fraction is also essentially free of mitochondrial membrane. That the cytochrome *c* oxidase activity was low in the purified chloroplasts, and there was no detectable cytochrome P_{450}-cinnamate-4-hydroxylase or formate dehydrogenase in Western blots of the purified chloroplasts, indicates that this fraction is essentially free of intact mitochondria and endoplasmic reticulum. Only cytochrome *f* was detectable in intact chloroplasts (Figure 3-18). A further indication of the purity of the intact chloroplast fraction is the fact that cytochrome *f*, a marker for thylakoid membranes, is highly enriched in intact chloroplasts relative to microsomal membranes in immunoblots of the two fractions loaded with constant protein (Figure 3-18). A similar enrichment in DGAT1 expression was seen in chloroplast membranes relative to intact chloroplasts (Figure 3-17).

3.3.8 DGAT1 is targeted to the chloroplast in leaves and to the endoplasmic reticulum in developing siliques

The enzymatic activity of DGAT1 is known to be associated with endoplasmic reticulum in oilseeds and to be a rate-limiting step in seed-filling of oil seeds including *Arabidopsis thaliana* (Cases *et al.*, 1998). The findings that the DGAT1 protein is present in chloroplastic fractions of rosette leaves and that triacylglycerol accumulated during senescence also contains chloroplastic fatty acids, raises the questions of how DGAT1 protein is targeted and what kinds of post-translational modifications it undergoes. To assess this, several protein-targeting programs and pattern-identifying programs identified in the Materials and Methods section were employed. Scan Prosite is a database of protein families and domains. It portrays biologically significant sites, patterns and profiles that enable association of a given protein sequence with known protein families. Prosite identified

several putative phosphorylation sites, N-myristoylation sites as well as a leucine zipper domain in *Arabidopsis* DGAT1. Relevant to this is the finding that DGAT1 in the adipose tissue of rat has been shown to be inactivated through phosphorylation mediated by a protein tyrosine kinase (Lau and Rodriguez, 1996). Prosite only predicted one such site on *Arabidopsis thaliana* DGAT1; however it also predicted another 5 protein kinase C phosphorylation sites and 7 casein kinase II phosphorylation sites. It is likely, therefore, that the activity or the dimerization of DGAT1 is regulated by phosphorylation.

DGAT1 from *Arabidopsis thaliana* was identified as a member of the MBOAT family by BLASTp (see section 3.3.1). Many membrane-associated proteins are N-myristoylated, especially those that exhibit protein-protein interaction regulated by protein phosphorylation, calmodulin binding and membrane phospholipids (Taniguchi, 1999). Prosite predicted 10 putative N-myristoylation sites for *Arabidopsis* DGAT1, though only some of these are plausible as several lack an N-terminal glycine achieved through cleavage of the protein. The most plausible site predicted is at Gly83, where the N-myristoylation predicted site is GGgdNN. If DGAT1 were cleaved at this site and myristoylated, the resulting molecular weight would be approximately 51kDa, the size that was observed in certain samples by the author in this thesis (see Figure 3-19) as well as others (Hobbs *et al.*, 1999; Bouvier-Nave *et al.*, 2000; Hobbs and Hills, 2000; Lu *et al.*, 2003).

Lastly, the leucine zipper domains that were predicted for *Arabidopsis* DGAT1 by Prosite are within the N-terminus, specifically within the transmembrane spanning domains 3 and 4 (Figure 3-5). Leucine zippers are involved in dimerization of proteins, which seems also to be suggested by the putative post-translational modifications of DGAT1 predicted by Prosite. It has been demonstrated that the N-terminus of DGAT1 is involved in the formation of tetramers of the human homologue (Cheng *et al.*, 2001), though the mechanism is unknown. It is likely that dimerization or tetramerization of DGAT1 is facilitated by several post-translational modifications.

Inasmuch as DGAT1 appears to be targeted to the chloroplasts of leaves and is known to be targeted to the endoplasmic reticulum in seeds, several online programs were employed to identify putative targeting sequences within the DGAT1 amino acid sequence.

pSORT is a targeting prediction program that has specific plant-protein targeting sequence coded into its pattern recognition database. There was no predicted N-terminal signal sequence for organellar targeting in *Arabidopsis* DGAT1 protein, but pSORT did predict 8 transmembrane helices (see section 3.3.2). Although there were no predicted N-terminal signal sequences in DGAT1, the second amino acid is alanine, which is a requirement for chloroplast-targeted proteins. TargetP, ChloroP and Predatar also predicted no targeting sequences within the DGAT1 protein. However, these programs only use approximately the first 130 amino acids in a sequence, and it has been established that not all targeting sequences are terminal or for that matter cleaved (Woolhead *et al.*, 2000). Also, not only did these programs not recognize a chloroplast targeting sequence in *Arabidopsis* DGAT1, they did not recognize an endoplasmic reticulum targeting sequence either though it is well established that DGAT1 is associated with the endoplasmic reticulum of developing seeds (Kamisaka and Nakahara, 1996; Cases *et al.*, 1998; Bao and Ohlrogge, 1999; Zou *et al.*, 1999).

To ensure that the antibodies used to identify chloroplast DGAT1 were detecting the same DGAT1 that is associated with the endoplasmic reticulum of developing seeds, Western blots were performed on microsomal membranes isolated from developing siliques (Figure 3-19). The microsomal membranes were fractionated by centrifugation through a linear sucrose gradient. Each fraction collected was fractionated by SDS-PAGE and probed with a cytochrome P_{450}-cinnamate-4-hydroxylase antibody as a marker for endoplasmic reticulum, and with DGAT1 antibody. Western-blot analysis of sequentially removed fractions revealed a parallel distribution of cytochrome P_{450}-cinnamate-4-hydroxylase and DGAT1 along the sucrose gradient fractions (Figure 3-19). In these experiments, both the native DGAT1 protein at 51kDa and a 29kDa proteolytic catabolite of the native protein were detectable. When microsomal membranes from rosette leaves of 4.5-week-old plants were similarly fractionated and analyzed by Western blotting (Figure 3-20), DGAT1 was not detectable in gradient fractions containing cytochrome P_{450}-cinnamate-4-hydroxylase, but rather the fractions that contained cytochrome *f*, a marker for thylakoid membranes. This parallel distribution of DGAT1 and a chloroplastic marker in leaves further substantiates the contention that, in leaves, DGAT1 is associated with chloroplast membranes and is consistent

Figure 3-19: Sucrose gradient fractionation of microsomal membranes isolated from developing siliques

A. Sucrose concentration in consecutive fractions of the gradient after centrifugation. **B.** Western blot analysis of fractionated microsomes isolated from developing siliques of *Arabidopsis* plants. The fractions were probed for cytochrome P_{450}-cinnamate-4-hydroxylase (C4H) and DGAT1. The lanes were loaded with equal volumes of the fractions from the sucrose gradient. Lanes 3 through 12 and lanes 13 through 24 were separate gels run concurrently on the same electrophoresis apparatus. Apparent molecular masses of the immunodetected polypeptides are indicated in kilodaltons.

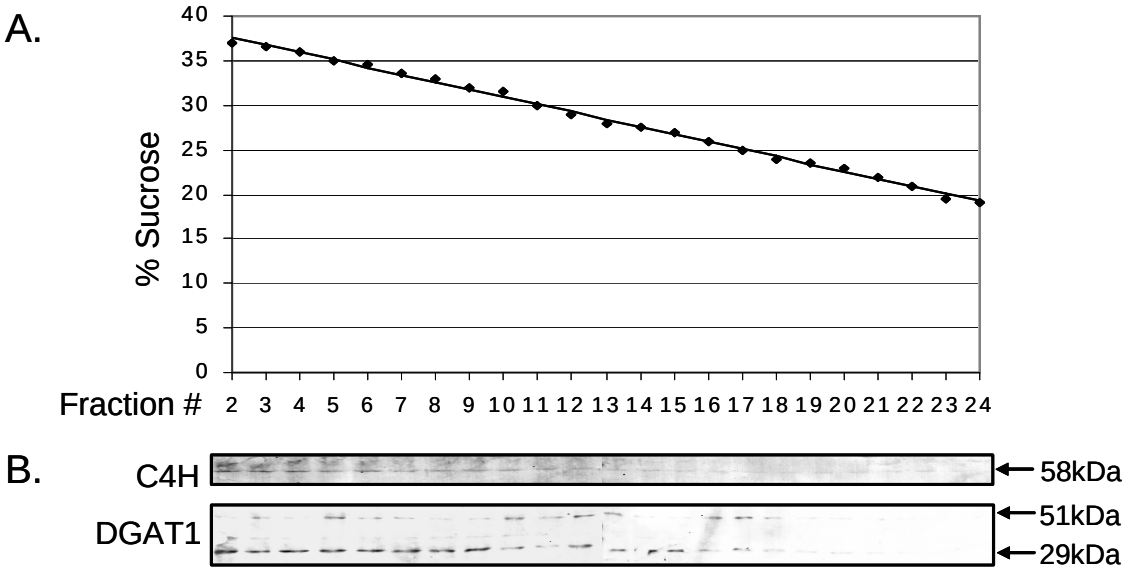
A.
% Sucrose
0
5
10
15
20
25
30
35
40
Fraction #
2 3 4 5 6 7 8 9 10 11 12 13 14 15 16 17 18 19 20 21 22 23 24
B.
C4H
DGAT1
58kDa
51kDa
29kDa

Figure 3-20: Sucrose gradient fractionation of microsomal membranes isolated from 4.5-week old leaves

A. Sucrose concentration in consecutive fractions of the gradient after centrifugation. **B.** Western blot analysis of fractionated microsomes isolated from 4.5-week-old *Arabidopsis* rosette leaves. The fractions were probed for cytochrome P_{450}-cinnamate-4-hydroxylase (C4H), DGAT1 and cytochrome *f* (cyt f). The lanes were loaded with equal volumes of the fractions from the sucrose gradient. Lanes 1 through 10 and lanes 11 through 20 were separate gels run concurrently on the same electrophoresis apparatus. Apparent molecular masses of the immunodetected polypeptides are indicated in kilodaltons.

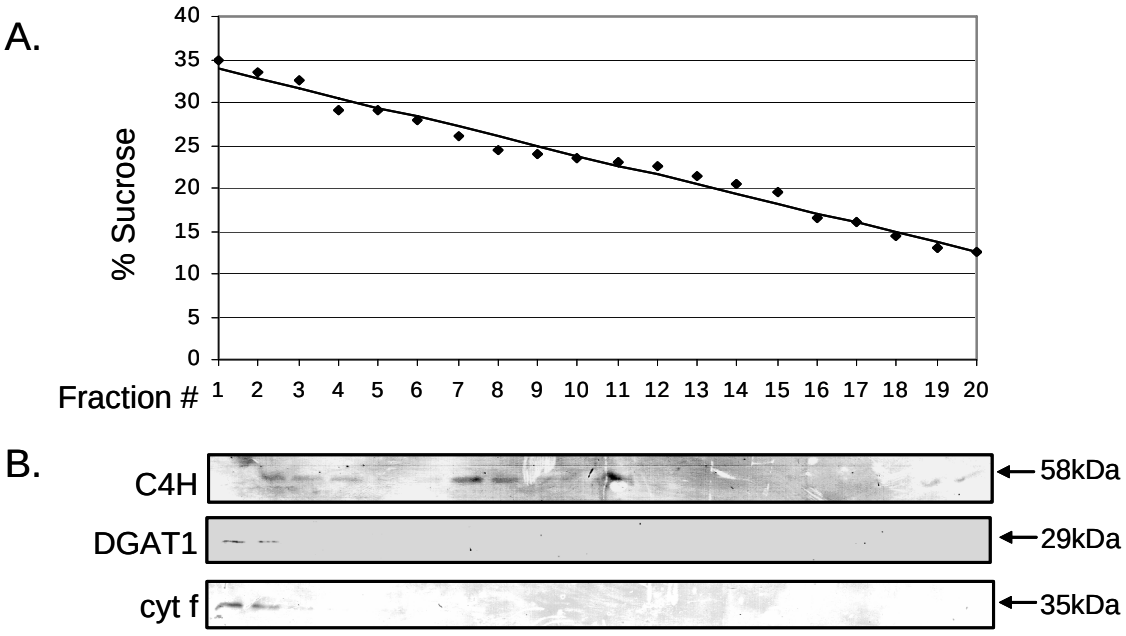
A.
% Sucrose
40
35
30
25
20
15
10
5
0
Fraction #
1 2 3 4 5 6 7 8 9 10 11 12 13 14 15 16 17 18 19 20
B.
C4H
58kDa
DGAT1
29kDa
cyt f
35kDa

with the finding that triacylglycerol accumulated in senescing leaves contains chloroplast-specific fatty acids.

To further verify these findings, confocal microscopy was performed on developing embryos dissected from immature siliques and senescing leaf tissue from 5-week-old leaves (Figures 3-21A and Figure 3-21B, respectively). The confocal data confirmed the presence of DGAT1 on the endoplasmic reticulum of cells within a developing embryo. The label appeared to be associated with wispy membranes around the central vacuole of the cells (Figure 3-21A left image). The embryos also exhibited autofluorescence of chlorophyll, which is a component of the thylakoid membranes (central image Figure 3-21A). It is accepted that some photosynthesis occurs during embryogenesis, which is thought to be essential during seed filling to produce the required reducing energy for oil synthesis (Hills, 2004). DGAT1 label was also seen to a lesser degree in these small chloroplasts of the developing embryos (Figure 3-21A right image).

In senescing leaves, DGAT1 proved to be associated with the membranes, including the envelope and the thylakoids, of the chloroplast (Figure 3-21B). Though previous studies have demonstrated DGAT activity to be associated with the outer envelope membrane of spinach chloroplasts (Martin and Wilson, 1983, 1984), these assays were performed on disrupted young chloroplasts and in a different species. The DGAT1 label exhibited on the thylakoids of *Arabidopsis* is quite strong (Figure 3-21B), and overlaps almost exactly with the chlorophyll autofluorescence (Figure 3-21B center and right images).DGAT1 label also appears to label the envelope membranes, which do not autofluoresce, as shown by a green halo around the autofluorescing thylakoids in the merged image (Figure 3-21B right image).

3.3.9 The expression of DGAT1 is coincident with the expression of a chloroplastic triacylglycerol lipase

It has been demonstrated that DGAT1 is up-regulated at the transcript and protein levels during senescence and is associated with the chloroplasts of rosette leaves. The triacylglycerol population that accumulates within senescing leaves includes fatty acids that are typically chloroplastic and are likely catabolites released during degradation of thylakoid

Figure 3-21: Confocal microscopy of DGAT1 expression in developing embryos and senescing leaves and of triacylglycerol lipase expression in senescing leaves

A. DGAT1 labelled with FITC is expressed on the ER of developing embryos. **B.** DGAT1 labelled with FITC labels the membranes of chloroplasts in senescing rosette leaf tissue. **C.** Chloroplastic triacylglycerol lipase labelled with FITC colocalizes with the plastoglobuli within the chloroplasts. All size bars=5μm. All images are 3D renderings of 5 serial optical sections and pseudocoloured. The cells and chloroplasts that are shown in Figure 3-21A are much smaller than the cells and chloroplasts of the mesophyll of a mature leaf shown in Figure 3-21B. This is typical of cells that have not yet expanded or become involved in "professional" photosynthesis.

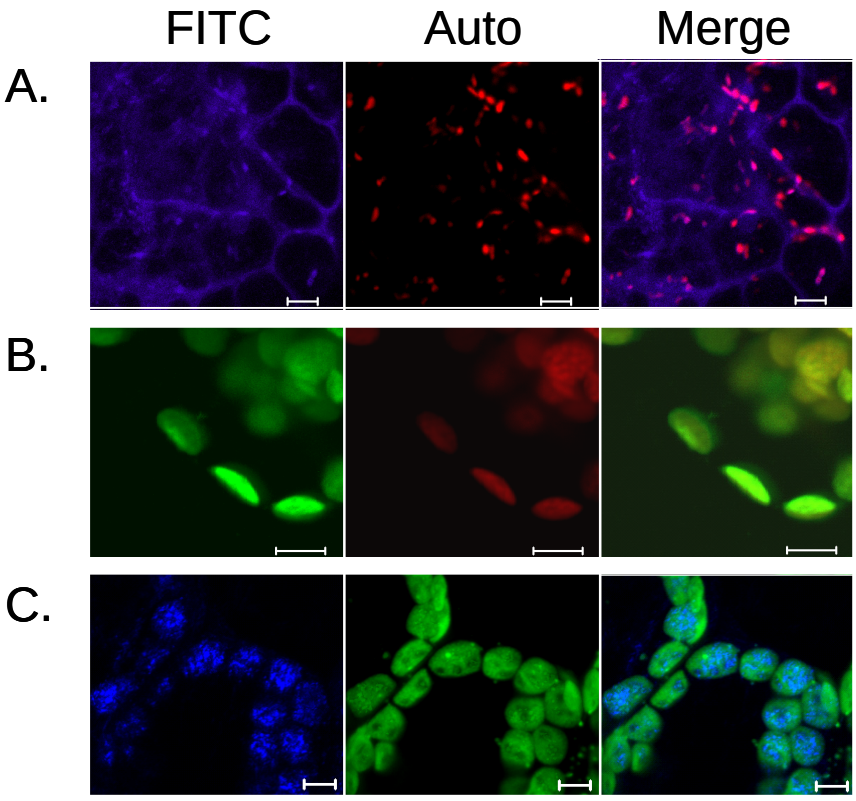
FITC
Auto
Merge
A.
B.
C.

membranes. If the plastoglobuli do in fact contain the triacylglycerol that is accumulated during senescence through the catabolism of the photosynthetic membranes, there must be a remobilization of the carbon stored in the triacylglycerol to translocate these nutrients to the developing seeds (Himelblau and Amasino, 2001). For this, a triacylglycerol lipase that is up-regulated during senescence would be necessary. In fact such a lipase has been identified and characterized in our laboratory (Padham, 2002). This triacylglycerol lipase is up-regulated during leaf senescence, is enriched in chloroplastic fractions, specifically in the stromal fraction, and is essential for plant survival. In the present study, the expression of this triacylglycerol lipase was visualized using confocal microscopy and was seen to be associated with the plastoglobuli within the stroma of chloroplasts (Figure 3-21C). That triacylglycerol lipase and DGAT1 are both localized in chloroplasts (Figure 3-21B and Figure 3-21C), indicates these two enzymes may act in concert to mobilize the lipids of senescing thylakoid membranes.

3.4 Discussion

Senescence is a highly controlled sequence of events induced by changes in gene expression that ultimately leads to the death of cells, tissues or organs (Thompson *et al.*, 1998). It occurs naturally at the end of the life span of an organ or, in the case of monocarpic senescence, the whole plant (Pic *et al.*, 2002). Senescence can be induced prematurely by a variety of environmental stresses, such as drought and pathogenesis (Woo *et al.*, 2001). Though senescence has been described as a type of programmed cell death, it is unique in that there is an intricately regulated recruitment of nutrients from the senescing parts of the plant and their translocation to other tissues that are still developing and growing. Leaf senescence is the most studied form of senescence and, especially at the molecular level, has been extensively examined in *Arabidopsis thaliana*. One of the earliest manifestations of leaf senescence is depletion of chlorophyll reflecting the functional decline and dismantling of thylakoid membranes. Loss of chlorophyll during foliar senescence is coupled to nutrient mobilization and resorption from leaf cells (Ougham *et al.*, 2005). It has been demonstrated that leaf senescence in *Arabidopsis* engenders extensive translocation of nutrients from the senescing leaves to the developing seeds (Himelblau and Amasino, 2001). However, how the senescing leaf remains functional during this massive mobilization remains to be determined.

In the present study, it was established that there is a temporal correlation between the increase in abundance and size of plastoglobuli and an increase in triacylglycerol synthesis in senescing rosette leaves of *Arabidopsis*. Specifically, triacylglycerols were 13-fold more abundant in the homogenates of senescent (6-week-old) rosette leaves than in pre-senescent (3-week-old) rosette leaves. Concurrently, the plastoglobuli were highly abundant in the electron micrographs of chloroplasts in senescent (6-week-old) leaves and sparsely present in those of the younger pre-senescent (3-week-old) leaves. This temporal relationship and the knowledge that triacylglycerol is a major component of plastoglobuli (Steinmuller and Tevini, 1985) suggest that the incremental triacylglycerol in senescing leaves is predominately in plastoglobuli. Indeed, microsomal membrane triacylglycerol, which would not include plastogobular triacylglycerol, was only 4-fold higher for senescent

(6-week-old) than for pre-senescent (3-week-old) leaves. The microsomal membrane fractions were isolated after severe homogenization of leaves, which releases plastoglobuli from chloroplasts into the cytosol, and at the high centrifugation speeds required to isolate microsomes, plastoglobuli float to the top (Smith *et al.*, 2000). Additionally, the fatty acid composition of triacylglycerol in senescent (6-week-old) leaves was unlike that of younger pre-senescent (3-week-old) leaves. The triacylglycerol of senescing leaves contained high levels of chloroplastic fatty acids, specifically hexadecatrienoic acid (16:3) and linolenic acid (18:3). These two fatty acids collectively comprised 45.03% of the total fatty acid complement of triacylglycerol from senescing leaves and were not detectable in the triacylglycerol from the younger leaves. Hexadecatrienoic acid (16:3) is only found in galactolipids, and although linolenic acid is present to a limited extent in phospholipids, it is the most abundant fatty acid of galactolipids (Miquel *et al.*, 1998). It is known that free fatty acids, specifically linolenic acid (18:3) and hexadecatrienoic acid (16:3), stimulate galactolipid:galactolipid galactosyltransferase, which catalyzes the conversion of MGDG to diacylglycerol (Sakaki *et al.*, 1990) a substrate for triacylglycerol synthesis. These findings collectively indicate that the enhanced triacylglycerol in senescing leaves is largely formed from thylakoid fatty acids released during galactolipid catabolism, and that the triacylglycerol is stored in plastoglobuli.

The strong temporal correlation between the increase in abundance of plastoglobuli in senescing leaves and enhanced levels of triacylglycerol is consistent with the finding that there is also up-regulation of DGAT1 transcript as well as its cognate protein. DGAT1 is a highly conserved protein in plants that catalyzes the terminal step in the pathway for triacylglycerol synthesis, one in which a fatty acid is added through an ester linkage to the *sn*-3 carbon of diacylglycerol (Hobbs and Hills, 2000). It is the only enzyme in this pathway unique to triacylglycerol synthesis (Bao and Ohlrogge, 1999) and has been shown to be rate-limiting (Jako *et al.*, 2001). Northern blots indicated that the transcript for DGAT1 is expressed constitutively during leaf expansion but increases sharply at the onset of senescence at 5-weeks of age. The Northern blots of total RNA were probed with E6B2T7, an EST clone that has been annotated as DGAT1. The reported size of *Arabidopsis* DGAT1 mRNA is 2kb (Hobbs *et al.*, 1999), and this is the size of the RNA detected on the Northern

blots. A corresponding increase in DGAT1 protein was discerned by immunoblotting with antibodies raised against a synthetic peptide corresponding to the C-terminus of the protein. Interestingly, it has been reported for developing seeds of castor bean that the expression of DGAT mRNA and protein are not correlated indicating that RcDGAT is post-transcriptionally regulated (He *et al.*, 2004). However, in senescing *Arabidopsis* leaves the increase in DGAT1 protein was only slightly delayed compared to the increase in transcript.

The expected size of *Arabidopsis* DGAT1 protein is 59kDa, though others have reported bands at 51kDa on Western blots probed with DGAT1 antibody (Hobbs *et al.*, 1999). In the present study, the polypeptide typically detected in leaves of *Arabidopsis* by Western blotting was only 29kDa in size. However, in some blots the native ~51kDa DGAT1 protein as well as the smaller 29 kDa catabolite were both detectable, especially for protein extracts from developing silique microsomal membranes. This suggests that the 29kDa polypeptide is a proteolytic catabolite of the native DGAT1 protein, formed during protein extraction and/or tissue fractionation despite the presence of protease inhibitors. This contention is further supported by the fact that the peptide corresponding to the last 17 amino acids of the DGAT1 protein, which were used to generate the DGAT1 antibodies, showed no significant alignments other than to DGAT1 of *Arabidopsis thaliana* and *Brassica napus*, a close relative of *Arabidopsis,* when interrogated by BLAST. Also, the native 51kDa DGAT1 protein was clearly discernible in immunoblots of separated protein extracted from UV treated leaves of *Brassica napus* probed with the *Arabidopsis* antibody. Further to this, the amino acid sequences for DGAT1 of *Brassica napus* and *Arabidopsis* are 85% identical over the length of the protein, and 16/17 amino acids were identical for the peptide used to generate the antiserum.

That DGAT1 is present in chloroplasts isolated from *Arabidopsis* leaves further supports the proposal that the triacylglycerol accumulated in senescing rosette leaves is synthesized in the chloroplasts. In light of this, DGAT1 might be expected to have a consensus chloroplast targeting sequence. This is not the case, but as noted previously (Bauer *et al.*, 2001), this does not preclude a chloroplastic localization. Western blots of chloroplast subfractions revealed that DGAT1 is present in intact chloroplasts and enriched in chloroplastic membranes. The chloroplast membrane fraction includes the chloroplast

envelope and thylakoid membranes. DGAT1 protein was not, however, detected in the stromal fraction in the present study, further supporting the contention that it is membrane-associated (Ichihara *et al.*, 1988; Lacey *et al.*, 1999; Bouvier-Nave *et al.*, 2000). These findings are also consistent with DGAT activity assays reported by Martin and Wilson (1984). Measurements of DGAT activity in chloroplast subfractions from spinach showed activity in the membranes of the chloroplast, especially in the envelope membrane fraction, with some activity in the thylakoid membranes as well (Martin and Wilson, 1984). This along with the fact that chloroplasts also have pools of acyl-CoA and diacylglycerol (Harwood and Stumpf, 1972; Betrams and Heinz, 1976; Sanchez and Mancha, 1981; Shimakata and Stumpf, 1982), which serve as substrates for DGAT1, indicates that chloroplasts are indeed capable of synthesizing triacylglycerol. Chloroplast envelopes have the capacity to assemble many types of lipids and also contain lipid-metabolizing enzymes (Siebertz *et al.*, 1979). When envelope membranes and thylakoids were isolated and their lipids analyzed, there were surprisingly high levels of diacylglycerol in chloroplast envelopes and only trace amounts in thylakoids (Siebertz *et al.*, 1979). Moreover, both diacylglycerol and triacylglycerol fractions of chloroplast envelopes contained high proportions of hexadecatrienoic acid (16:3) and linolenic acid (18:3) (Siebertz *et al.*, 1979).

Although DGAT1 is detectable in chloroplasts, many studies have only focused on its localization with the endoplasmic reticulum in seeds (Little *et al.*, 1994; Katavic *et al.*, 1995; Focks and Benning, 1998; Bao and Ohlrogge, 1999; Zou *et al.*, 1999). However, it is apparent from the present study that DGAT1 protein is expressed in most organs of *Arabidopsis thaliana,* indicating that most tissues are thus capable of producing triacylglycerol. Not surprisingly, roots proved to have high levels of DGAT1 protein expression. A mutation in a single gene (termed PICKLE) in *Arabidopsis* results in a massive accumulation of storage lipids, oleosins and proteins in the roots of affected plants (Henderson *et al.*, 2004). This demonstrates the ease with which root cells can be induced to express seed-like characteristics, including the formation of oleosins and lipid bodies. Though DGAT1 transcript levels within the various organs of *Arabidopsis* were not determined in the present study, others have reported that DGAT1 mRNA is detectable in most organs as well (Hobbs *et al.*, 1999; Lu *et al.*, 2003). This highly distributed nature of

DGAT1 localization implies that it is regulated by a complex promoter, consisting of many different elements. Lu *et al.* (2003) demonstrated this for plants expressing a GUS - DGAT1 promoter construct. GUS expression was evident in developing seeds, pollen, growing seedlings, root tips and was induced by glucose. However, only low levels were observed in leaves. It is unclear why DGAT1 is highly expressed during seed germination, where lipolytic activity is dominant. One possible explanation is that there is separate subcellular compartmentalization of the synthetic and hydrolytic mechanisms associated with triacylglycerol metabolism in germinating cotyledons (Wilson and Kwanyuan, 1986).

There have been reports that the most active triacylglycerol biosynthetic fraction of plant cells is microsomal membranes, which are normally equated with endoplasmic reticulum (Cao and Huang, 1986; Stobart *et al.*, 1986). However, the microsomal fraction is made up of a mixture of membrane vesicles, many of which are derived from endoplasmic reticulum, but some also originate from plasmalemma, Golgi and membranes of other organelles such as the plastid envelope (Cao and Huang, 1986; Herman, 1987). In keeping with its association with the endoplasmic reticulum in seeds, DGAT1 was immunologically detectable in protein blots of microsomal membranes isolated from developing seeds of *Arabidopsis* in the present study. However, it was not evident in Western blots of microsomal membranes corresponding to endoplasmic reticulum from rosette leaves, possibly because it is not an abundant protein in leaf endoplasmic reticulum or is only targeted to the chloroplasts in leaves.

Plastoglobuli have often been compared to oil bodies, the triacylglycerol-containing storage particles in seeds (Murphy, 2001). Not only do they both store triacylglycerol, but plastoglobuli contain fibrillin, which is analogous to oleosin, a structural protein associated with oil bodies (Pozueta-Romero *et al.*, 1997; Kessler *et al.*, 1999; Rey *et al.*, 2000). These structural proteins are thought to prevent coalescence of particles, whether they be plastoglobuli or oil bodies (Huang, 1996; Rey *et al.*, 2000). Rey *et al.* (2000) produced transgenic plants in which fibrillin was over-expressed. These plants exhibited an increased abundance of plastoglobuli, even in young tissue, demonstrating that the availability of fibrillin regulates the formation of plastoglobuli in much the same way that oleosin regulates oil body formation (Huang, 1992).

The data presented in this thesis are consistent with the view that plastoglobuli are formed within chloroplast membranes through the action of DGAT1 and released from the membrane surface into a hydrophilic compartment. Oil bodies are thought to be formed in a similar manner from endoplasmic reticulum membrane (Napier *et al.*, 1996). Late in senescence plastoglobuli shrink, presumably because of the action of a senescence induced triacylglycerol lipase (Matile, 1992). It is apparent from immunolocalization analyses conducted in the present study that DGAT1 protein is associated with chloroplastic membranes and that there is a coincident up-regulated expression of a senescence induced triacylglycerol lipase in plastoglobuli. Furthermore, like DGAT1 (Lu *et al.*, 2003) this lipase is also upregulated in developing *Arabidopsis* seedlings (Padham, 2002). Moreover, suppression of this lipase in transgenic plants resulted in stunted growth, reduced seed production, and an increased abundance of plastoglobuli in chloroplasts even before senescence is initiated (Padham *et al.*, submitted 2006). These observations were interpreted as indicating that this triacylglycerol lipase is essential for mobilizing the triacylglycerol carbon temporarily stored in plastoglobuli. Thus, DGAT1 and the triacylglycerol lipase perform pivotal roles in the recruitment and mobilization of carbon in the chloroplast.

Previous studies have demonstrated that there is a concurrent decrease in galactolipids and phospholipids and an increase in triacylglycerol synthesis during ozone stress (Sakaki *et al.*, 1990; Sakaki *et al.*, 1990). Similarly, drought-stressed cotton leaves exhibit a significant decline in polar lipids and a parallel increase in triacylglycerol (El-Hafid *et al.*, 1989). Chloroplasts in drought-stressed leaves have an increased surface area and also appear to have a high number of tight associations with peroxisomes and mitochondria (Zellnig *et al.*, 2004). Sakaki *et al.*1990 have proposed that the activation of triacylglycerol synthesis in ozone-treated leaves functions to sequester fatty acids de-esterified from galactolipids in response to ozone stress. By analogy, the senescence-related up-regulation of DGAT1 and subsequent synthesis of triacylglycerol may serve to temporarily sequester galactolipid fatty acids released during chloroplast senescence and thus be an intermediate step in the conversion of thylakoid fatty acid to energy or phloem-mobile sucrose by peroxisomes with the help of mitochondria. Plants are incredible recyclers and do so by employing senescence and death for resource allocation (Thomas *et al.*, 2003). Trienoic fatty

acids, including hexadecatrienoic acid (16:3) and linolenic acid (18:3), are dominant fatty acid species in plant membrane lipids. They are crucial for the adaptation of plants to abiotic stresses, especially temperature. They are also involved in the production of reactive oxygen species during the hypersensitive response to pathogen ingression, resulting in programmed cell death and disease resistance. These fatty acids thus appear to play an important role in the regulation of plant defence responses (Yaeno *et al.*, 2004) and, when released during the developmental stage of senescence, need to be sequestered into triacylglycerol. Besides its involvement in signalling, free linolenic acid (18:3), containing three double bonds, is highly susceptible to free radical attack. Thus 18:3 is likely a substrate in the peroxidation reaction resulting in the formation of hydroperoxides. Also, free fatty acids can act as fusogens, promoting membrane fusion. These would render the membrane non-functional. Therefore, as these fatty acids are released by galactolipases during senescence, in order for the membrane to remain functional, they need to be sequestered, and this appears to be achieved by their incorporation into neutral lipids such as triacylglycerols and steryl and wax esters.

The chloroplast is the first organelle to show symptoms of senescence in mesophyll cells. Specifically the thylakoid membranes are dismantled while leaving the chloroplast envelope intact until the very late stages of senescence (Peoples *et al.*, 1980). The thylakoid membranes are the most abundant membrane in nature (Lee, 2000), thus constituting a rich source of carbon and nitrogen equivalents. These nutrients are mobilized during leaf senescence and are transported through the phloem to developing structures of the plant. The thylakoid membranes are largely comprised of the galactolipids, monogalactosyldiacylglycerol (MGDG) and digalactosyldiaclyglycerol (DGDG). In fact, together they comprise approximately 80% of the total lipid content of the thylakoids. As the chloroplasts senesce, the galactolipids are catabolized by senescence-induced galactolipases (O'Sullivan *et al.*, 1987). Indeed, there appears to be no galactolipase activity involved in galactolipid turnover, and degradation of MGDG and DGDG is specific to senescence or stress-induced senescence (O'Sullivan and Dalling, 1989). Perturbed or destabilized membrane bilayers, such as those containing free fatty acids, are more susceptible to further degradation by lipases (Barclay and McKersie, 1994). The contention that free fatty acids

released by galactolipases during senescence are stored temporarily is supported by the finding that both DGAT1 and triacylglycerol lipase are up-regulated in senescing leaves. A proposed model illustrating the fate of thylakoid fatty acids during senescence is illustrated in Figure 3-22. Basically, the fatty acids that are released by galactolipases appear to be sequestered into triacylglycerol within the thylakoid membrane by DGAT1, and the triacylglycerol is in turn released into the stroma within plastoglobuli, which bleb from the thylakoid membrane surface. This results in an increase in plastoglobuli number and size during senescence. Although the precise role of plastoglobuli has not been elucidated, it is assumed based on their increase in size during thylakoid degradation, that they temporarily store thylakoid lipid metabolites, especially those liberated during leaf senescence (Sprey and Lichtenthaler, 1966; Lichtenthaler, 1969; Lichtenthaler and Weinert, 1970). It is proposed here that triacylglycerols within the plastoglobuli are metabolized by a plastid triacylglycerol lipase. It has also been proposed that plastoglobuli are extruded through the chloroplast envelope membranes into the cytosol where they become associated with glyoxysomes (Guiamet *et al.*, 1999). This would enable the fatty acid equivalents of plastoglobular triacylglycerol to be metabolized by β-oxidation for energy production or gluconeogenesis leading to sucrose formation. The conversion of leaf peroxisomes to glyoxysomes as senescence is initiated and the correlative up-regulation of the key glyoxylate cycle enzymes, malate synthase and isocitrate lyase, is established (DeBellis *et al.*, 1990; DeBellis and Nishimura, 1991). The fatty acids of thylakoid lipids are thus fuel for the senescence process as well as a source of carbon for the synthesis of phloem-mobile sucrose. During leaf senescence, even when the parenchyma cells become completely inactive, the vein system and particularly the phloem are completely functional, losing viability only late in senescence (Bieleski, 1995).

It is clear that leaf senescence is a highly regulated and highly co-ordinated event. The role of DGAT1 during senescence may seem counterintuitive in that it is synthesizing molecules rather than catabolizing molecules during a developmental stage that has been often described as shift to catabolism. Though DGAT1 may play an important role in controlling the catabolism of thylakoid lipids and preventing senescing cells from losing

.

Figure 3-22: Proposed roles of DGAT1, galactolipase and plastid triacylglycerol lipase in senescing chloroplasts

As chloroplasts within the mesophyll differentiate into gerontoplasts, a major effort is made to salvage nitrogen and carbon stored in proteins and lipids, respectively. Digalactosyl diacylglycerol (DGDG) and monogalactosyl diacylglycerol (MGDG) are the key lipid components of thylakoids. Thylakoid membranes are depicted as flattish discs stacked together in chloroplasts, and as senescence progresses they become less tightly packed and become swollen. Senescence-up-regulated galactolipases act on both MGDG and DGDG to release fatty acids from the *sn*-1 and *sn*-2 positions. DGDG can also be initially converted to MGDG through the action of a senescence-specific α-galactosidase. The free fatty acids that are released by galactolipase action would be toxic to the membranes and cause further uncontrolled catabolism. It has been demonstrated that photosynthesis persists during the early stages of senescence, and thus the thylakoid membranes must remain intact as catabolism of galactolipids occurs. It is proposed in this thesis that through the action of DGAT1 localized in the chloroplast, the free fatty acids are temporarily sequestered into triacylglycerol until they are further mobilized by triacylglycerol lipase. This second catabolic step releases fatty acids in a controlled manner and feeds them directly into the glyoxysome where they are catabolized by β-oxidation for energy or are remobilized through the glyoxylate cycle and gluconeogenesis to produce phloem-mobile sucrose.

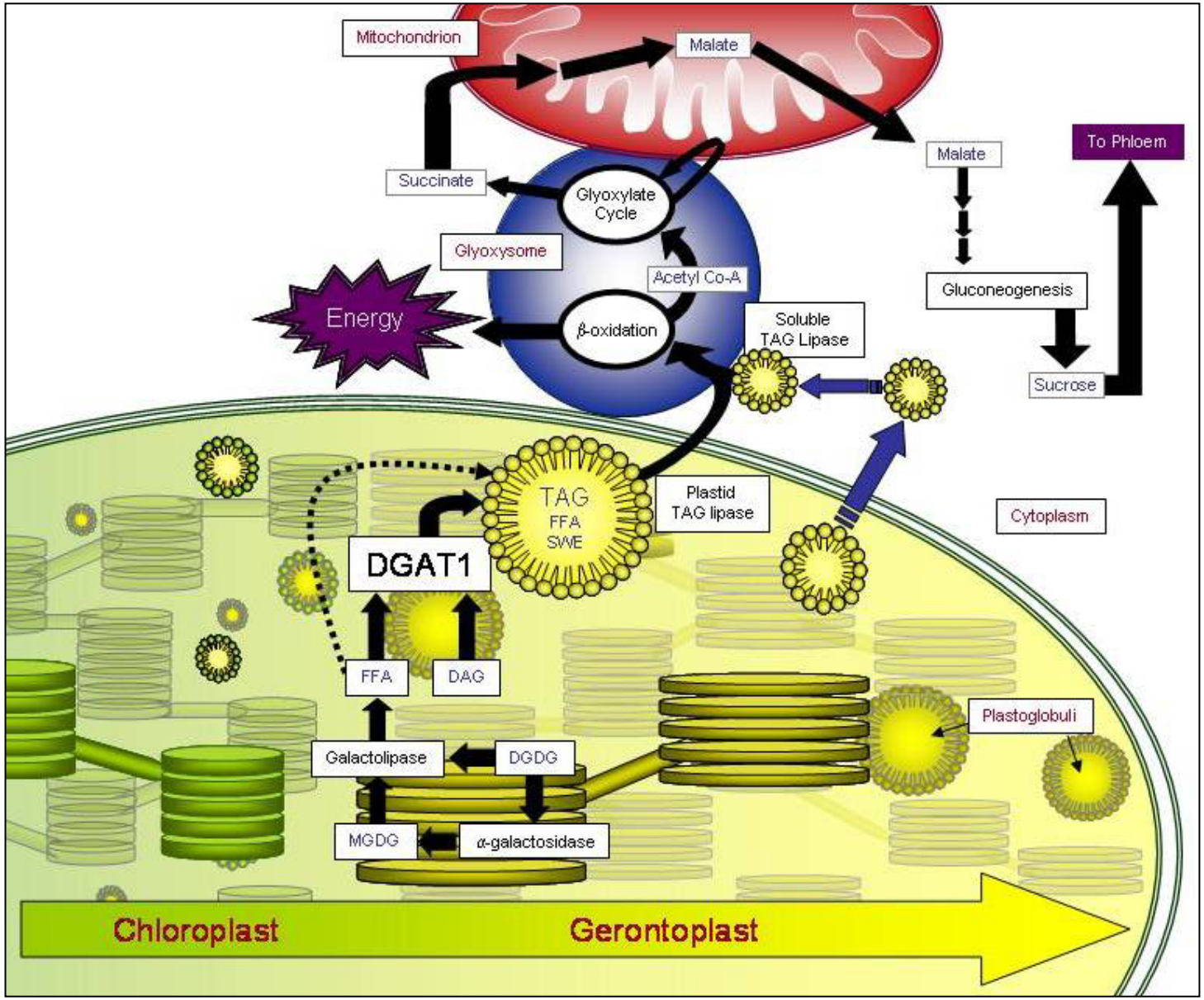
Mitochondrion
Malate
Malate
To Phloem
Succinate
Glyoxylate Cycle
Glyoxysome
Acetyl Co-A
Energy
β-oxidation
Soluble TAG Lipase
Gluconeogenesis
Sucrose
TAG
FFA
SWE
Plastid TAG lipase
Cytoplasm
DGAT1
FFA
DAG
Plastoglobuli
Galactolipase
DGDG
MGDG
α-galactosidase
Chloroplast
Gerontoplast

control over nutrient recruitment, this role may not be essential or may have redundant counterparts. For example, the reduction in DGAT1 activity in mutants does not appear to have any effect on the appearance of the plant, but rather only an effect on the seed oil content (Zou *et al.*, 1999). It is thought that senescence proceeds through several parallel pathways (He *et al.*, 2001). Accepting the notion that senescence is essential for the overall fitness of the plant, the strategy of having redundant pathways would be advantageous in the context of ensuring the fidelity of the senescence process. Thus the model proposed in this chapter may not be the only way that carbon stores in the chloroplasts are degraded during senescence.

Chapter 4: General Discussion

An understanding of fundamental aspects of plant biology is essential for the advancement of agriculture, especially in the context of using transgenic technology to enhance agronomically important traits. The model plant, *Arabidopsis thaliana*, has been used extensively for these types of studies, in part because its genome is fully sequenced and also because it has a short life cycle. Moreover, *Arabidopsis* is closely related to canola, a major agronomic crop. The need for other model systems for the purpose of crop enhancement is clear, however, and this is the underlying basis for ongoing efforts to sequence the genomes of major crop plants such as maize and rice.

A major objective of bioengineering and breeding programs for crop plants is to increase yield. Yield is a complex trait that involves many developmental processes, including organogenesis, morphogenesis, growth and differentiation. Yield increases can be obtained indirectly through increasing tolerance or resistance to pests and other stressors. Other more direct approaches for increasing yield include enhancing growth and modifying the structure of the plant to better suit current farming practices. While only small improvements have been made through breeding programs, bioengineering holds in prospect being able to greatly improve yield because of the ability to modulate the expression of individual genes (Camp, 2005).

Crop losses to insect herbivory are in the order of 10-20% of total yield (Ferry *et al.*, 2004), so it is not surprising that some of the first commercially available genetically modified crop plants included corn and cotton plants expressing Bt toxin from *Bacillus thuringiensis,* which confers insect resistance. While these transgenic plants express an exogenous gene obtained from bacteria, endogenous plant genes are also being studied for protection against herbivory and pathogenesis. Plants invoke resistance mechanisms to achieve protection from herbivory and pathogenesis. Both of these stresses induce aquired resistance, first locally in the area of pathogen ingress or wound, then systemically throughout the plant. Several toxic or repellent molecules are produced by plants in response to wounding or pathogen ingress, including proteinase inhibitors (Gatehouse, 2002) and green leaf volatiles (Pare and Tumlinson, 1999). In addition, the up-regulation of

pathogenesis-related (PR) proteins at the site of pathogen ingression leads to systemic acquired resistance. Increased resistance to pests is often equated to increased yield, which may be indirect as a consequence of reduced plant death or direct through an increase in plant growth. For example, the constitutive over-expression of maize PR-1 in tobacco resulted in improved growth and increased seed yield (Murillo *et al.*, 2003). The enhanced growth appeared to reflect in part a role for PR-1 in increasing symplastic sucrose transport.

Down-regulation of AteIF5A-2 by antisense has been shown to abrogate the development of disease induced by the bacterial pathogen, *Pseudomonas syringae* (Gatsukovich, 2004). *Pseudomonas syringae* is a facultative necrotroph that is initially a biotrophic pathogen, but then induces plant host cells to die as it enters into its necrotrophic phase and causes disease (Katagiri *et al.*, 2002). The down-regulation of AteIF5A-2 reduced programmed cell death induced by the pathogen. Interestingly, although AteIF5A-2 appears to be involved in the regulation of programmed cell death induced by wounding or disease, it is not required for the induction of systemic acquired resistance (Gatsukovich *et al.*, submitted 2006). Over-expression of AteIF5A-2 in the present study resulted in decreased fecundity and decreased plant size, traits that are not desirable in terms of yield. However, down-regulation or knock-out of the wounding/pathogenesis responsive eIF5A in crop plants may lead to increased disease resistance and a decrease in yield losses due to pathogenesis.

Programmed cell death also occurs during developmental senescence and post-harvest senescence. Loss of quality of fruits and vegetables after harvest is manifested by rapid deterioration in appearance, flavour and nutrient value. Post-harvest senescence accounts for major losses in food crops. Some of the molecular targets for reducing post-harvest senescence and increasing shelf life of produce include proteins involved in ethylene biosynthesis (Eze *et al.*, 1986; Park *et al.*, 1992) and lipid catabolism (Page *et al.*, 2001; Lo *et al.*, 2004). It was demonstrated by Wang *et al.* (2005) that down-regulation of DHS in tomato fruit using antisense technology significantly delayed post-harvest fruit softening. Strong constitutive down-regulation of DHS, however, also had deleterious consequences, such as pollen sterility and delayed development (Wang *et al.,* 2005). By reducing DHS or the eIF5A isoform involved specifically in senescence selectively in harvestable organs, these deleterious effects can be reduced. For example, leaf specific reduction of DHS led to

a delay in leaf senescence by at least a week without deleterious pleiotropic effects (Jamal, 2004), indicating that organ-specific down-regulation of this gene may be better suited for applications in agriculture. Since AteIF5A-1 is involved in developmental programmed cell death, such as xylogenesis, it would be imperative to down-regulate it in an organ-specific manner.

Plant architecture is determined by cell division and cell elongation. Accordingly, increased growth through manipulation of the cell-cycle or cell elongation has been studied with the ultimate goal of increasing organ size (Camp, 2005). The cell-cycle machinery is highly conserved across eukaryotic kingdoms. An interesting upstream regulator of cell division is ARGOS, where the over-expression of ARGOS in *Arabidopsis* resulted in a direct increase in leaf size (Hu *et al.*, 2003). Over-expression of expansins, which are involved in elongation, in soybean stimulated an increase in root elongation, but there were problems with the aerial portions of the plant with respect to cellular organization in the leaves (Rochange *et al.*, 2001). The expression of expansins perhaps would benefit the plant more if the transgene expression was in the roots only. The regulation of elongation in plants is finely tuned, and appears to be tightly linked to the level of gene expression. This was apparent, for example, in the present study when *AteIF5A-3* was over-expressed in *Arabidopsis*. The more highly over-expressed the protein was, the larger the seeds became. Since over-expression of *AteIF5A-3* appeared to have an effect on development, tissue-specific over-expression of *AteIF5A-3* may have better results for increasing yield. For example, flower and fruit specific over-expression of AteIF5A-3 may lead to the same large seed phenotype without the changes in plant body form such as changes in leaf shape and phyllotaxy that were observed when the gene was constitutively over-expressed. Increased seed size is a beneficial trait for oilseed plants, as there is a smaller surface area to volume ratio, making oil extraction more efficient.

In summary, members of gene families tend to be lumped together, without specific functions of each member being teased out. The eIF5A gene family in *Arabidopsis thaliana* is highly conserved, but individual members of this gene family exhibit different temporal and spatial expression patterns and appear to have distinct functions.

Increase in yield not only pertains to increase in biomass. Specific products of plants, such as seed oil, are also of interest in respect of improving agriculture. The selective over-expression of diacylglycerol acyltransferase 1 (DGAT1) in seeds has been shown to increase the seed oil content and seed weight of *Arabidopsis thaliana* (Jako *et al.*, 2001). While constitutive DGAT1 over-expression has not been explored, in light of the present study it may offer some surprising advantages. That DGAT1 is the limiting step in triacylglycerol formation is well documented (Ichihara *et al.*, 1988; Bao and Ohlrogge, 1999). The presence of DGAT1 associated with the chloroplasts of leaves and the concurrent increase in plastoglobuli demonstrated in the present study led to the hypothesis that DGAT1 sequesters free fatty acids removed from the thylakoid membrane by lipases dismantling the chloroplasts during senescence. The ability of DGAT1 to temporarily sequester free fatty acids in an inert form is especially important during times of stress and senescence. Thus, constitutive over-expression of DGAT1 might lead to increased chloroplast health through the sequestering of free fatty acids throughout development and especially during episodes of stress and senescence. Furthermore, mutants deficient in DGAT1 display increased sensitivity to various treatments including the application of exogenous abscisic acid and osmotic stress during germination and seedling development (Lu and Hills, 2002). It is clear, therefore, that DGAT1 is an important target for enhancement of agricultural traits.

Chapter 5: Literature Cited

Abbruzzese A, Park MH, Folk JE (1986) Deoxyhypusine hydroxylase from rat testis: partial purification and characterization. Journal of Biological Chemistry **261:** 3085-3089

Abbruzzese A, Park MH, Folk JE (1986) Indirect assays for deoxyhypusine hydroxylase using dual-label ratio changes and oxidative release of radioactivity. Analytical Biochemistry **154:** 664-670

Abramovitch RB, Martin GB (2004) Strategies used by bacterial pathogens to suppress plant defenses. Current Opinion in Plant Biology **7:** 356-364

Anderson MM, McCarty RE, Zimmer EA (1974) The role of galactolipids in spinach chloroplast lamellar membranes: I. Partial purification of a bean leaf galactolipid lipase and its action on subchloroplast particles. Plant Physiology **53:** 699-704

Andersson MX, Larsson KE, Tjellstrom H, Liljenberg C, Sandelius AS (2005) Phosphate-limited oat. The Journal of Biological Chemistry **280:** 27578-27586

Andrus L, Szabo P, Grady RW, Hanauske AR, Huima-Byron T, Slowinska B, Zagulska S, Hanauske-Abel HM (1998) Antiretroviral effects of deoxyhypusyl hydroxylase inhibitors: A hypusine-dependent host cell mechanism for replication of human immunodeficiency virus type 1 (HIV-1). Biochemical Pharmacology **55:** 1807-1818

Antonian E (1988) Recent advances in the purification, characterization and structure determination of lipases. Lipids **23:** 1101-1106

Aoki H, Dekany K, Adams SL, Ganoza MC (1997) The gene encoding the elongation factor P protein is essential for viability and is required for protein synthesis. Journal of Biological Chemistry **272:** 32254-32259

Apelbaum A, Canellakis ZN, Appelwhite PB, Kaur-Sawhney R, Galston AW (1988) Binding of spermidine to a unique protein in thin-layer tobacco tissue culture. Plant Physiology **88:** 996-998

Awai K, Marechal E, Block MA, Brun D, Masuda T, Shimada H, Takamiya K-I, Ohta H, Joyard J (2001) Two types of MGDG synthase genes, found widely in both 16:3 and 18:3 plants, differentially mediate galactolipid synthesis in photosynthetic and nonphotosynthetic tissues in *Arabidopsis thaliana*. Proceedings of the National Academy of Science U.S.A **98:** 10960-10965

Badami RC, Patil KB (1981) Structure and occurrence of unusual fatty acids in minor seed oils. Progress in Lipid Research **19:** 119-153

Banas A, Dahlqvist A, Stahl U, Lenman M, Stymne S (2000) The involvement of phospholipid:diacylglycerol acyltransferases in triacylglycerol production. Biochemical Society Transactions **28:** 703-705

Bao X, Ohlrogge J (1999) Supply of fatty acid is one limiting factor in the accumulation of triacylglycerol in developing embryos. Plant Physiology **120:** 1057-1062

Barclay KD, McKersie BD (1994) Peroxidation reactions in plant membranes: Effects of free fatty acids. Lipids **29:** 877-882

Bartig D, Lemkemeier K, Frank J, Lottspeich F, Klink F (1992) The archaebacterial hypusine-containing protein. Structural features suggest common ancestry with eukaryotic translation initiation factor 5A. European Journal of Biochemistry **204:** 751-758

Barton R (1966) Fine structure of mesophyll cells in senescencing leaves of *Phaseolus*. Planta **71:** 314-325

Bauer J, Chen K, Hiltbunner A, Wehrli E, Eugster M, Schnell D, Kessler F (2000) The major protein import receptor of plastids is essential for chloroplast biogenesis. Nature **403:** 203-207

Bauer J, Hiltbunner A, Kessler F (2001) Molecular biology of chloroplast biogenesis: gene expression, protein import and intraorganellar sorting. Cellular and Molecular Life Sciences **58:** 420-433

Beers EP, McDowell JM (2001) Regulation and execution of programmed cell death in response to pathogen, stress and developmental cues. Current Opinion in Plant Biology **4:** 561-567

Beisson F, Arondel V, Verger R (2000) Assaying *Arabidopsis* lipase activity. Biochemical Society Transactions **28:** 773-775

Beninati S, Ferraro G, Abbruzzese A (1990) Catalytic properties of deoxyhypusine hydroxylase. Italian Journal of Biochemistry **39:** 183A-185A

Beninati S, Gentile V, Caraglia M, Lentini A, Tagliaferri P, Abbruzzese A (1998) Tissue transglutaminase expression affects hypusine metabolism in BALB/c 3T3 cells. FEBS Letters **437:** 34-38

Bentsink L, Koornneef M (2002) Seed dormancy and germination. *In* The Arabidopsis Book. American Society of Plant Biologists, pp 1-18

Bergeron RJ, Weimar WR, Muller R, Zimmerman CO, McCosar BH, Yao H, Smith RE (1998) Effect of polyamine analogues on hypusine content in JURKAT T-cells. Journal of Medical Chemistry **41:** 3901-3908

Betrams M, Heinz E (1976) Experiments on enzymatic acylation of *sn*-glycerol 3-phosphate with enzyme preparations from pea and spinach leaves. Planta **132:** 161-168

Bevec D, Hauber J (1997) Eukaryotic initiation factor 5A activity and HIV-1 Rev function. Biological Signals **6:** 124-133

Bevec D, Klier H, Holter W, Tschachler E, Valent P, Lottspeich F, Baumruker T, Hauber J (1994) Induced gene expression of the hypusine-containing protein

eukaryotic initiation factor 5A in activated human T lymphocytes. Proceedings of the National Academy of Science U.S.A **91:** 10829-10833

Bevec DH, Jaksche M, Oft T, Wohl M, Himmelspach A, Pacher M, Schebesta K, Koettnitz M, Dobrovnik R, Csonga F, Lottspeich F, Hauber J (1996) Inhibition of HIV-1 replication in lymphocytes by mutants of the Rev cofactor eIF-5A. Science **271:** 1858-1860

Bieleski RL (1995) Onset of phloem export from senescent petals of daylily. Plant Physiology **109:** 557-565

Birnbaum K, Shasha DE, Wang JY, Jung JW, Lambert GM, Galbraith DW, Benfey PN (2003) A Gene Expression Map of the *Arabidopsis* Root. Science **302:** 1956-1960

Bishop DG (1971) Lipid Metabolism. *In* AR Johnson, JB Davenport, eds, Biochemistry and Methodology of Lipids. John Wiley & Sons Inc., Toronto, pp 425-455

Blanc G, Barakat A, Guyot R, Cooke R, Delseny M (2000) Extensive duplication and reshuffling in the *Arabidopsis* genome. The Plant Cell **12:** 1093-1101

Bleecker AB, Patterson SE (1997) Last exit: Senescence, abscission and meristem arrest in *Arabidopsis*. The Plant Cell **9:** 1169-1179

Bligh EG, Dyer WJ (1959) A rapid method of total lipid extraction and purification. Candian Journal of Biochemistry and Physiology **37:** 911-917

Boone AN, Hopkins MT, Taylor CA, Thompson JE (2004) siRNA against eukaryotic translation initiation factor 5A reduces TNF- secretion in PBMCs and modulates IFN signaling in macrophages. *In* International Cytokine Society Meeting, San Juan, Puerto Rico

Bouvier-Nave P, Benveniste P, Oelkers P, Sturley SL, Schaller H (2000) Expression in yeast and tobacco of plant cDNAs encoding acyl CoA:diacylglycerol acyltransferase. European Journal of Biochemistry **267:** 85-96

Bowman J, ed (1994) Arabidopsis: An atlas of morphology and development. Springer-Verlag New York, Inc., New York

Boyes DC, Zayed AM, Ascenzi R, McCaskill AJ, Hoffman NE, Davis KR, Goerlach J (2001) Growth stage-based phenotypic analysis of *Arabidopsis*: A model for high throughput functional genomics in plants. The Plant Cell **13:** 1499-1510

Bradley D, Ratcliffe O, Vincent C, Carpenter R, Coen E (1997) Inflorescence commitment and architecture in *Arabidopsis*. Science **275:** 80-83

Brindley D, Hubscher G (1965) The intracellular distribution of the enzymes catalyzing the biosynthesis of glycerides in the intestinal mucosa. Biochimica et Biophysica Acta **106:** 495-509

Buchanan-Wollaston V (1997) The molecular biology of leaf senescence. Journal of Experimental Biology **48:** 181-199

Bucher M, Brunner S, Zimmermann P, Zardi GI, Amrhein N, Willmitzer L, Riesmeier JW (2002) The expression of an extensin-like protein correlates with cellular tip growth in tomato. Plant Physiology **128:** 911-923

Byers TL, Lakanen JR, Coward JK, Pegg AE (1994) The role of hypusine depletion in cytostasis induced by S-adenosyl-L-methionine decarboxylase inhibition: new evidence provided by 1-methylspermidine and 1,12-dimethylspermine. Biochemistry Journal **303:** 363-368

Byers TL, Wiest L, Wechter RS, Pegg AE (1993) Effects of chronic 5'-([(Z)-4-amino-2-butenyl]methylamino)-5'-deoxy- adenosine (AbeAdo) treatment on polyamine and eIF-5A metabolism in AbeAdo-sensitive and -resistant L1210 murine leukaemia cells. Biochemistry Journal **290:** 115-121

Camp WV (2005) Yield enhancement genes: seeds for growth. Current Opinion in Biotechnology **16:** 147-153

Campbell LH, Borg KT, Haines JK, Moon RT, Schoenberg DR, Arrigo SJ (1994) Human immunodeficiency virus type 1 Rev is required in vivo for binding of poly(A)-binding protein to Rev-dependent RNAs. Journal of Virology **68:** 5433-5438

Cao Y-Z, Huang HC (1986) Diacylglycerol acyltransferase in maturing oil seeds of maize and other species. Plant Physiology **82:** 813-820

Caraglia M, Marra M, Giuberti G, D'Alessandro AM, Baldi A, Tassone P, Venuta S, Tagliaferri P, Abbruzzese A (2003) The eukaryotic initiation factor 5A is involved in the regulation of proliferation and apoptosis induced by interferon-alpha and EGF in human cancer cells. Journal of Biochemistry (Tokyo) **133:** 757-765

Caraglia M, Marra M, Giuberti G, D'Alessandro AM, Budillon A, Prete Sd, Lentini A, Beninati S, Abbruzzese A (2001) The role of eukaryotic initiation factor 5A in the control of cell proliferation and apoptosis. Amino Acids **20:** 91-104

Caraglia M, Tagliaferri P, Budillon A, Abbruzzese A (1999) Post-translational modifications of eukaryotic initiation factor-5A (eIF-5A) as a new target for anti-cancer therapy. Advanced Experimental Medical Biology **472:** 187-198

Cases S, Smith SJ, Zheng Y-W, Myers HM, Lear SR, Sande E, Novak S, Collins C, Welch CB, Lusis AJ, Erickson SK, Jr. RVF (1998) Identification of a gene encoding an acyl Co-A:diaclyglycerol acyltransferase, a key enzyme in triacylglycerol synthesis. Proceeding of the National Academy of Science U.S.A. **95:** 13018-13023

Cases S, Stone S, Zhou P, Yen E, Tow B, Lardizabal KD, Voelker T, Jr. RVF (2001) Cloning of DGAT2, a second mammalian diacylglycerol acyltransferase, and related family members. Journal of Biological Chemistry **276:** 38870-38876

Chamot D, Kuhlemeier C (1992) Differential expression of genes encoding the hypusine-containing translation initiation factor, eIF-5A, in tobacco. Nucleic Acids Research **20:** 665-669

Chan KL, New D, Ghandhi S, Wong F, Lam CM, Wong JT (2002) Transcript levels of the eukaryotic translation initiation factor 5A gene peak at early G(1) phase of the cell cycle in the dinoflagellate *Crypthecodinium cohnii*. Applied Environmental Microbiology **68:** 2278-2284

Charrier B, Champion A, Henry Y, Kreis M (2002) Expression profiling of the whole *Arabidopsis* shaggy-like kinase multigene family by real-time reverse transcriptase-polymerase chain reaction. Plant Physiology **130:** 577-590

Chatterjee I, Gross SR, Kinzy TG, Chen KY (2006) Rapid depletion of mutant eukaryotic initiation factor 5A at restrictive temperature reveals connections to actin cytoskeleton and cell cycle progression. Molecular Genetics and Genomics **12:** 1-13

Chattopadhyay MK, Tabor CW, Tabor H (2003) Spermidine but not spermine is essential for hypusine biosynthesis and growth of *Saccharomyces cerevisiae*: Spermine is converted to spermidine in vivo by the FMS1-amine oxidase. Proceedings of the National Academy of Science U.S.A **100:** 13869-13974

Chen G, Gharib TG, Thomas DG, Huang CC, Misek DE, Kuick RD, Giordano TJ, Iannettoni MD, Orringer MB, Hanash SM, Beer DG (2003) Proteomic analysis of eIF-5A in lung adenocarcinomas. Proteomics **3:** 496-504

Chen HC, Farese RV (2000) DGAT and triglyceride synthesis: A new target for obesity treatment? Trends in Cardiovascular Medicine **10:** 188-192

Chen ZP, Chen KY (1997) Dramatic attenuation of hypusine formation on eukaryotic initiation factor 5A during senescence of IMR-90 human diploid fibroblasts. Journal of Cell Physiology **170:** 248-254

Chen ZP, Yan YP, Ding QJ, Knapp S, Potenza JA, Schugar HJ, Chen KY (1996) Effects of inhibitors of deoxyhypusine synthase on the differentiation of mouse neuroblastoma and erythroleukemia cells. Cancer Letters **105:** 233-239

Cheng D, Meegalla RL, He B, Cromley DA, Billheimer JT, Young PR (2001) Human acyl-CoA: diacylglycerol acyltransferase is a tetrameric protein. Biochemical Journal **359:** 707-714

Cheong YH, Chang H-S, Gupta R, Wang X, Zhu T, Luan S (2002) Transcriptional profiling reveals novel interactions between wounding, pathogen, abiotic stress, and hormonal responses in *Arabidopsis*. Plant Physiology **129:** 661-677

Chou W-C, Huang Y-W, Tsay W-S, Chiang T-Y, Huang D-D, Huang H-J (2004) Expression of genes encoding the rice translation initiation factor, eIF5A, is involved in developmental and environmental responses. Physiologia Plantarum **121:** 50-57

Chow K-S, Lim SM, Han K-H (2003) Characterisation of a family of eIF-5A cDNAs from *Hevea brasiliensis*. Journal of Rubber Research **6:** 107-120

Chung SI, Park MH, Folk JE, Lewis MS (1991) Eukaryotic initiation factor 5A: the molecular form of the hypusine-containing protein from human erythrocytes. Biochimica et Biophysica Acta **1076:** 448-451

Clemens MJ, Bommer U-A (1999) Translational control: The cancer connection. International Journal of Biochemistry and Cell Biology **31:** 1-23

Clement PMJ, Hanauske-Abel HM, Wolff EC, Kleinman HK, Park MH (2002) The antifungal drug ciclopirox inhibits deoxyhypusine and proline hydroxylation, endothelial cell growth and angiogenesis in vitro. International Journal of Cancer **100:** 491-498

Clement PMJ, Henderson CA, Jenkins ZA, Smit-McBride Z, Wolff EC, Hersey JWB, Park MH, Johansson HE (2003) Identification and characterization of eukarytic initiation factor 5A-2. European Journal of Biochemistry **270:** 4254-4263

Clough SJ, Bent AF (1998) Floral dip: a simplified method for *Agrobacterium*-mediated transformation of *Arabidopsis thaliana*. The Plant Journal **16:** 735-743

Cohen SS (1998) A Guide to the Polyamines. Oxford University Press, Oxford

Cohen Z, Khozin-Goldberg I, Adlerstein D, Bigogno C (2000) The role of triacylglycerol as a reservoir of polyunsaturated fatty acids for the rapid production of chloroplastic lipids in certain microalgae. Biochemical Society Transactions **28:** 740-743

Cooper HL, Park MH, Folk JE (1982) Posttranslational formation of hypusine in a single major protein occurs generally in growing cells and is associated with activation of lymphocyte growth. Cell **29:** 791-797

Cooper HL, Park MH, Folk JE, Safer B, Braverman R (1983) Identification of the hypusine-containing protein hy+ as translation initiation factor eIF-4D. Proceedings of the National Academy of Science U.S.A **80:** 1854-1857

Cracchiolo BM, Heller DS, Clement PMJ, Wolff EC, Park M-H, Hanauske-Abel HM (2004) Eukaryotic initiation factor 5A-1 (eIF5A-1) as a diagnostic marker for aberrant proliferation in intraepithelial neoplasia of the vulva. Gynecologic Oncology **94:** 217-222

Csonga R, Ettmayer P, Auer M, Eckerskorn C, Eder J, Klier H (1996) Evaluation of the metal ion requirement of the human deoxyhypusine hydroxylase from HeLa cells using a novel enzyme assay. FEBS Letters **380:** 209-214

Dahlqvist A, Stahl U, Lenman M, Banas A, Lee M, Sndager L, Ronne H, Stymne S (2000) Phospholipid:diacylglycerol acyltransferase: An enzyme that catalyzes the

acyl-CoA-independent formation of triacylglycerol in yeast and plants. Proceedings of the National Academy of Science U.S.A **97:** 6487-6492

Davis LG, Dibner MD, Battey JB (1986) Preparation and analysis of RNA from eukaryotic cells. *In* Basic methods in molecular biology. Elsevier Science Publishing Co., Inc., New York, pp 130-156

DeBellis L, Nishimura M (1991) Development of enzymes of hte glyoxylate cycle during senescence of pumpkin cotyledons. Plant Cell Physiology **32:** 555-561

DeBellis L, Nishimura M (1991) Development of enzymes of the glyoxylate cycle during senescence of pumpkin cotyledons. Plant Cell Physiology **32:** 555-561

DeBellis L, Picciarelli P, Pistelli L, Alpi A (1990) Localization of glyoxylate-cycle marker enzymes in peroxisomes of senescent leaves and green cotyledons. Planta **180:** 435-439

Derewenda ZS, Derewenda U (1991) Relationships among serive hydrolase: evidence for a common structural motif in triacylglyceride lipases and esterases. Biochemical and Cell Biology **69:** 842-851

Deruere J, Roemer S, d'Harlingue A, Backhaus RA, Kuntz M, Camara B (1994) Fibril assembly and carotenoid overaccumulation in chromoplasts: a model for supramolecular lipoprotein structures. Plant Cell **6:** 119-133

Dietrich RA, Delaney TP, Uknes SJ, Ward ER, Ryals JA, Dangl JL (1994) Arabidopsis mutants simulating disease resistance response. Cell **77:** 565-577

Dinneny JR, Yanofsky MF (2004) Drawing lines and borders: how the dehiscent fruit of *Arabidopsis* is patterned. BioEssays **27:** 42-49

Doermann P, Benning C (2002) Galactolipids rule in seed plants. Trends in Plant Science **7:** 112-118

Dou QP, Chen KY (1989) The hypusine-containing proteins identified by metabolic labelling in chick embryo fibroblasts. Journal of the Chinese Chemistry Society **36:** 443-450

Dresselhaus T, Cordts S, Lorz H (1999) A transcript encoding translation initiation factor eIF-5A is stored in unfertilized egg cells of maize. Plant Molecular Biology **39:** 1063-1071

Duckett CM, Oparka KJ, Prior DAM, Dolan L, Roberts K (1994) Dye-coupling in the root epidermis of *Arabidopsis* is progressively reduced during development. Development **120:** 3247-3255

Duguay J (2004) Characterization of deoxyhypusine synthase and eukaryotic translation initiation factor 5A1 expression during growth and senescence in Arabidopsis thaliana. MSc. University of Waterloo, Waterloo

Edlund AF, Swanson R, Preuss D (2004) Pollen and stigma structure and function: The role of diversity in pollination. The Plant Cell **16:** S84-S97

Elfgang C, Rosorius O, Hofer L, Jaksche H, Hauber J, Bevec D (1999) Evidence for specific nucleocytoplasmic transport pathways used by leucine-rich nuclear export signals. Proceedings of the National Academy of Science U.S.A **96:** 6229-6234

El-Hafid L, Thi ATP, Zuily-Fodil Y, Silva JVd (1989) Enzymatic breakdown of polar lipids in cotton leaves under water stress. I. Degradation of monogalactosyl-diacylglycerol. Plant Physiology and Biochemistry **27:** 495-502

Engelmann-Sylvestre I, Bureau J-M, Tremolieres A, Paulin A (1989) Changes in membrane phospholipids and galactolipids during the senescence of cut carnations. Connection with ethylenic rise. Plant Physiology and Biochemistry **27:** 931-937

Eze JMO, Mayak S, Thompson JE, Dumbroff EB (1986) Senescence in cut carnation flowers: Temporal and physiological relationship among water status, ethylene, abscisic acid and membrane permeability. Physiologia Plantarum **68:** 323-328

Facchiano AM, Stiuso P, Chiusano ML, Caraglia M, Giuberti G, Marra M, Abbruzzese A, Colonna G (2001) Homology modelling of the human eukaryotic initiation factor 5A (eIF-5A). Protein Engineering **14:** 881-890

Fairbanks G, Steck TL, Wallach DFH (1971) Coomassie blue R250 used in isopropanolacetic acid. Biochemistry **10:** 2606-2618

Fan L, Zheng S, Cui D, Wang X (1999) Subcellular distribution and tissue expression of phospholipase Dα, Dβ, and Dγ in Arabidopsis. Plant Physiology **119:** 1371-1378

Fedoroff NV (2002) RNA-binding proteins in plants: the tip of an iceberg? Current Opinion in Plant Biology **5:** 452-459

Ferry N, Edwards MG, Gatehouse JA, Gatehouse AMR (2004) Plant-insect interactions: molecular approaches to insect resistance. Current Opinion in Biotechnology **15:** 155-161

Focks N, Benning C (1998) *wrinkled1*: A novel, low-seed-oil mutant of *Arabidopsis* with a deficiency in the seed-specific regulation of carbohydrate metabolism. Plant Physiology **118:** 91-101

Frans-Small CCd, Ambard-Bretteville F, Small ID, Remy R (1993) Identification of a major soluble protein in mitochondria from nonphotosynthetic tissues as NAD-dependent formate dehydrogenase. Plant Physiology **102:** 1171-1802

Froehlich JE, Benning C, Dormann P (2001) The digalactosyldiacylglycerol (DGDG) synthase DGD1 is inserted into the outer envelope membrane of chloroplasts in a manner independent of the general import pathway and does not depend on direct

interaction with monogalactosyldiacylglycerol synthase for DGDG biosynthesis. The Journal of Biological Chemistry **276:** 31806-31812

Fukuda H, Komamine A (1983) Changes in the synthesis of RNA and protein during tracheary element differentiation in single cells isolated from the mesophyll of *Zinnia elegans*. Plant Cell Physiology **24:** 603-614

Galliard T (1971) Enzymatic deacylation of lipids in plants. The effects of free fatty acids on the hydrolysis of phospholipids by the lipolytic acyl hydrolase of potato tubers. European Journal of Biochemistry **21:** 90-98

Galliard T (1980) Degradation of acyl lipids: hydrolytic and oxidative enzymes. *In* PK Stumpf, ed, The Biochemistry of Plants, Vol 4. Academic Press, New York, pp 85-116

Gan S, Amasino RM (1995) Inhibition of leaf senescence by autoregulated production of cytokinin. Science **270:** 1986-1988

Gatehouse JA (2002) Plant resistance towards insect herbivores: a dynamic interaction. New Phytologist **156:** 145-169

Gatsukovich Y (2004) Characterization of eukaryotic translation initiation factor 5A-2 (eIF5A-2) in *Arabidopsis thaliana*: Effects of wounding and pathogen attack. MSc. University of Waterloo, Waterloo

Gatsukovich Y, Hopkins MT, Perry G, McNamara LM, Wang TW, Thompson JE (submitted 2006) eIF5A regulates cell death in *Arabidopsis* induced by *Pseudomonas syringae* infection.

Gemel J, Kaniuga Z (1987) Comparison of galactolipase activity and free fatty acid levels in chloroplasts of chill-sensitive and chill-resistant plants. European Journal of Biochemistry **166:** 229-233

Gerner EW, Mamont PS, Bernhardt A, Siat M (1986) Post-translational modification of the protein-synthesis initiation factor eIF-4D by spermidine in rat hepatoma cells. Biochemistry Journal **239:** 379-386

Ghosh S, Gepstein S, Heikkila JJ, Dumbroff EB (1988) Use of a scanning densitometer or an ELISA plate reader for measurement of nanogram amounts of protein in crude extracts from biological tissues. Analytical Biochemistry **169:** 227-233

Ghosh S, Hudak KA, Dumbroff EB, Thompson JE (1994) Release of photosynthetic protein catabolites by blebbing from thylakoids. Plant Physiology **106:** 1547-1553

Giannoulia K, Haralampidis K, Poghosyan Z, Murphy DJ, Hatzopoulous P (2000) Differential expression of diacylglycerol acyltransferase (DGAT) genes in olive tissues. Biochemical Society Transactions **28:** 695-697

Gilmour SJ, Artus NN, Thomashow MF (1992) cDNA sequence analysis and expression of two cold-regulated genes of *Arabidopsis thaliana*. Plant Molecular Biology **18:** 13-21

Glick BR, Ganoza MC (1975) Identification of a soluble protein that stimulates peptide bond synthesis. Proceedings of the National Academy of Science U.S.A **72:** 4257-4260

Gorczyca W, Tuziak T, Kram A, Melamed MR, Darzynkiewicz Z (1994) Detection of apoptosis-associated DNA strand breaks in fine-needle aspiration biopsies by in situ end labeling of fragmented DNA. Cytometry **15:** 169–175

Gordon ED, Mora R, Meredith SC, Lee C, Lindquist SL (1987) Eukaryotic initiation factor 4D, the hypusine-containing protein, is conserved among eukaryotes. Journal of Biochemistry **262:** 16585-16589

Goyns MH (1982) The role of polyamines in animal cell physiology. Journal of Theoretical Biology **97:** 577-589

Graham IA, Smith LM, Leaver CJ, Smith SM (1990) Developmental regulation of expression of the malate synthase gene in transgenic plants. Plant Molecular Biology **15:** 539-549

Grbic V, Bleecker AB (1995) Ethylene regulates the timing of leaf senescence in *Arabidopsis*. The Plant Journal **8:** 595-602

Greenberg JT (1996) Programmed cell death: A way of life for plants. Proceedings of the National Academy of Science U.S.A **93:** 12094-12097

Greenberg JT (1997) Programmed cell death in plant-pathogen interactions. Annual Review in Plant Physiology and Plant Molecular Biology **48:** 525-545

Greenberg JT, Yao N (2004) The role and regulation of programmed cell death in plant-pathogen interactions. Cellular Microbiology **6:** 201-211

Guan XY, Sham JS, Tang TC, Fang Y, Huo KK, Yang JM (2001) Isolation of a novel candidate oncogene within a frequently amplified region at 3q26 in ovarian cancer. Cancer Research **61:** 3806-3809

Guiamet JJ, Pichersky E, Nooden LD (1999) Mass exodus from senescing soybean chloroplasts. Plant Cell Physiology **40:** 986-992

Han CU, Lee CH, Jang KS, Choi GJ, Lim HK, Kim J-C, Ahn S-N, Choi JE, Cha JS, Kim HT, Cho KY, Lee S-W (2004) Identification of rice genes induced in a rice blast-resistant mutant. Molecules and Cells **17:** 462-468

Hanauske-Abel HM, Park MH, Hanauske AR, Popowicz AM, Lalande M, Folk JE (1994) Inhibition of the G1-S transition of the cell cycle by inhibitors of deoxyhypusine hydroxylation. Biochim Biophys Acta **1221:** 115-124

Hanauske-Abel HM, Slowinska B, Zagulska S, Wilson RC, Staiano-Coico L, Hanauske AR, McCaffrey T, Szabo P (1995) Detection of a sub-set of polysomal mRNAs

associated with modulation of hypusine formation at the G1-S boundary. Proposal of a role for eIF-5A in onset of DNA replication. FEBS Letters **366:** 92-98

Harwood JL, Russell NJ (1984) Lipids in Plants and Microbes. George Allen & Unwin, London

Harwood JL, Stumpf PK (1972) Fat metabolism in higher plants: XLIX. Fatty acid biosynthesis by subcellular fractions of higher plants. Lipids **7:** 8-19

He X, Chen GQ, Lin JT, McKeon TA (2004) Regulation of diacylglycerol acyltransferase in developing seeds of castor. Lipids **39:** 865-871

He Y, Gan S (2002) A gene encoding an acyl hydrolase is involved in leaf senescence in *Arabidopsis*. The Plant Cell **14:** 805-815

He Y, Tang W, Swain JD, Green AL, Jack TP, Gan S (2001) Networking senescence-regulating pathways by using *Arabidopsis* enhancer trap lines. Plant Physiology **126:** 707-716

Heath MC (2000) Hypersensitive response-related death. Plant Molecular Biology **44:** 321-334

Hellyer SA, Chandler IC, Bosley JA (1999) Can the fatty acid selectivity of plant lipases be predicted from the composition of the seed triglyceride? Biochimica et Biophysica Acta **1440:** 215-224

Henderson BR, Percipalle P (1997) Interactions between HIV Rev and nuclear import and export factors: the Rev nuclear localisation signal mediates specific binding to human importin-beta. Journal of Molecular Biology **274:** 693-707

Henderson JT, Li HC, Rider SD, Mordhorst AP, Romero-Severson J, Cheng JC, Robey J, Sung ZR, deVries SC, Ogas J (2004) PICKLE acts throughout the plant to repress expression of embryonic traits and may play a role in gibberellin-dependent responses. Plant Physiology **134:** 995-1005

Herman EM (1987) Immunogold-localization and synthesis of an oil-body membrane protein in developing soybean seeds. Planta **172:** 336-345

Hershey JWB, Miyamoto S (2000) Translational control and cancer. *In* N Sonenberg, JWB Hershey, MB Mathews, eds, Translational control of gene expression. Cold Spring Harbor Laboratory Press, Cold Spring Harbor, NY, pp 637-654

Higo K, Ugawa Y, Iwamoto M, Korenaga T (1999) Plant cis-acting regulatory DNA elements (PLACE) database. Nucleic Acids Research **27:** 297-300

Hills MH, Watson MD, Murphy DJ (1993) Targeting of oleosin to the oil bodies of oilseed rape (*Brassica napus* L.). Planta **189:** 24-29

Hills MJ (2004) Control of storage-product synthesis in seeds. Current Opinion in Plant Biology **7:** 302-308

Himelblau E, Amasino RM (2001) Nutrients mobilized from leaves of *Arabidopsis thaliana* during leaf senescence. Journal of Plant Physiology **158:** 1317-1323

Hobbs DH, Hills MJ (2000) Expression and characterization of diacylglycerol acyltransferase from *Arabidopsis thaliana* in insect cell cultures. Biochemical Society Transactions **28:** 687-695

Hobbs DH, Lu C, Hills MJ (1999) Cloning of a cDNA encoding diacylglycerol acyltransferase from *Arabidopsis thaliana* and its functional expression. FEBS Letters **452:** 145-149

Hodges TK, Leonard RT (1974) Purification of a plasma membrane-bound adenosine triphosphatase from plant roots. *In* S Fleischer, L Packer, eds, Methods in Enzymology, Vol 32. Academic Press, New York, NY, pp 392-446

Hu Y, Xie Q, Chua N-H (2003) The Arabidopsis auxin-inducible gene ARGOS controls lateral organ size. The Plant Cell **15:** 1951-1961

Huang AHC (1992) Oil bodies and oleosins in seeds. Annual Reviews in Plant Physiology and Plant Molecular Biology **43:** 177-200

Huang AHC (1996) Oleosins and oil bodies in seeds and other organs. Plant Physiology **110:** 1055-1061

Ichihara K, Takahashi T, Fujii S (1988) Diacylglycerol acyltransferase in maturing safflower seeds: its influences on the fatty acid composition of triacylglycerol and on the rate of triacylglycerol synthesis. Biochimica et Biophysica Acta **958:** 125-129

Igarashi K, Kashiwagi K (2000) Polyamines: mysterious modulators of cellular function. Biochemical and Biophysical Research Communications **271:** 559-564

Itzhaki H, Maxson JM, Woodson WR (1994) An ethylene-responsive enhancer element is involved in the senescence-related expression of the carnation glutathione-S-transferase (GST1) gene. Proceedings of the National Academy of Science U.S.A **91:** 8925-8929

Jacks TJ, Yatsu LY, Altschul AM (1967) Isolation and characterization of peanut spherosomes. Plant Physiology **42:** 585-597

Jager SMd, Maughan S, Dewitte W, Scofield S, Murray JAH (2005) The developmental context of cell-cycle control in plants. Seminars in Cell and Developmental Biology **16:** 385-396

Jako C, Kumar A, Wei Y, Zou J, Barton DL, Giblin EM, Covello PS, Taylor DC (2001) Seed-specific over-expression of an *Arabidopsis* cDNA encoding a diacylglycerol acyltransferase enhances seed oil content and seed weight. Plant Physiology **126:** 861-874

Jakus J, Wolff EC, Park MH, Folk JE (1993) Features of the spermidine-binding site of deoxyhypusine synthase as derived from inhibition studies. The Journal of Biological Chemistry **268:** 13151-13159

Jamal S (2004) Delaying leaf senescence in *Arabidopsis thaliana* by tissue-specific antisense suppression of deoxyhypusine synthase. MSc. University of Waterloo, Waterloo

Jannsson BPM, Malandrin L, Johansson HE (2000) Cell cycle arrest in archea by the hypusination inhibitor N-guanyl-1,7-diaminoheptane. Journal of Bacteriology **182:** 1158-1161

Jao DL, Chen KY (2005) Tandem affinity purification revealed the hypusine-dependent binding of eukaryotic initiation factor 5A to the translating 80S ribosomal complex. Journal of Cellular Biochemistry **Epub ahead of printing**

Jao DL-E, Chen KY (2002) Subcellular localization of the hypusine-containing eukaryotic initiation factor 5A by immunofluorescent staining and green fluorescent protein tagging. Journal of Cellular Biochemistry **86:** 590-600

Jarvis P, Doermann P, Peto CA, Lutes J, Benning C, Chory J (2000) Galactolipid deficiency and abnormal chloroplast development in the *Arabidopsis MGD synthase 1* mutant. Proceedings of the National Academy of Science U.S.A **97:** 8175-8179

Jin BF, He K, Wang HX, Wang J, Zhou T, Lan Y, Hu MR, Wei KH, Yang SC, Shen BF, Zhang XM (2003) Proteomic analysis of ubiquitin-proteasome effects: insight into the function of eukaryotic initiation factor 5A. Oncogene **22:** 4819-4830

Joao HC, Csonga R, Klier H, Koettnitz K, Auer M, Eder J (1995) The polypeptide chain of eukaryotic initiation factor 5A occurs in two distinct conformations in the absence of the hypusine modification. Biochemistry **34:** 14703-14711

Joe YA, Wolff EC, Park MH (1995) Cloning and expression of human deoxyhypusine synthase cDNA. The Journal of Biological Chemistry **270:** 22386-22392

Jouhet J, Marechal E, Baldan B, Bligny R, Joyard J, Block MA (2004) Phosphate deprivation induces transfer of DGDG galactolipid from chloroplast to mitochondria. Journal of Cell Biology **167:** 863-874

Kamisaka Y, Nakahara T (1996) Activation of detergent-solubilized diacylglycerol acyltransferase by anionic phospholipids. Journal of Biochemistry **119:** 520-523

Kang HA, Hershey JW (1994) Effect of initiation factor eIF-5A depletion on protein synthesis and proliferation of *Saccharomyces cerevisiae*. Journal of Biological Chemistry **269:** 3934-3940

Kang HA, Schwelberger HG, Hershey JW (1993) Translation initiation factor eIF-5A, the hypusine-containing protein, is phosphorylated on serine in *Saccharomyces cerevisiae*. Journal of Biological Chemistry **268:** 14750-14756

Kaniuga Z, Saczynska V, Miskiewicz E, Garstka M (1999) Degradation of leaf polar lipids during chilling and post-chilling rewarming of *Zea mays* genotypes reflects differences in their response to chilling stress. The role of galactolipase. Acta Physiologiae Plantarum **21:** 45-56

Katagiri F, Thilmony R, He SY (2002) The *Arabidopsis thaliana-Pseudomonas syringae* interaction. *In* CR Somerville, EM Meyerowitz, eds, The Arabidopsis Book. American Society of Plant Biologists, Rockville, pp 1-35

Katavic V, Reed DW, Taylor DC, Giblin EM, Barton DL, Zou J, MacKenzie SL, Covello PS, Kunst L (1995) Alteration of seed fatty acid composition by an ethyl methanesulfonate-induced mutation in *Arabidopsis thaliana* affecting diacylglycerol acyltransferase activity. Plant Physiology **108:** 399-409

Kemper WM, Berry KW, Merrick WC (1976) Purification and properties of rabbit reticulocyte protein synthesis initiation factors M2Balpha and M2Bbeta. Journal of Biological Chemistry **251:** 5551-5557

Kerstetter RA, Poethig RS (1998) The specification of leaf identity during shoot development. Annual Review in Cell Development Biology **14:** 373-398

Kessler F, Schnell D, Blobel G (1999) Identification of proteins associated with plastoglobules isolated from pea (*Pisum sativum* L.) chloroplasts. Planta **108:** 107-113

Kim KK, Hung LW, Yokota H, Kim R, Kim SH (1998) Crystal structures of eukaryotic translation initiation factor 5A from *Methanococcus jannaschii* at 1.8 A resolution. Proceedings of the National Academy of Science U.S.A **95:** 10419-10424

Kim M-J, Oh J-M, Cheon S-H, Cheong T-K, Lee S-H, Choi E-O, Lee HG, Park CS, Park KH (2001) Thermal intactivation kinetics and application of phospho- and galactolipid-degrading enzymes for evaluation of quality changes in frozen vegetables. Journal of Agriculture and Food Chemistry **49:** 2241-2248

Kiyosue T, Ohad N, Yadegari R, Hannon M, Dinneny J, Wells D, Katz A, Margossian L, Harada JJ, Goldberg RB, Fischer RL (1999) Control of fertilization-independent endosperm development by the MEDEA polycomb gene in *Arabidopsis*. Proceedings of the National Academy of Science U.S.A **96:** 4186-4191

Kolodziejek I, Koziol J, Waleza M, Mostowska A (2003) Ultrastructure of mesophyll cells and pigment content in senescing leaves of maize and barley. Journal of Plant Growth Regulation **22:** 217-227

Koorneef M, Karssen CM (1994) Seed dormancy and germination. *In* EM Meyerowitz, CR Somerville, eds, Arabidopsis. Cold Spring Harbor Laboratory Press, Cold Spring Harbor, New York, pp 313-334

Korves TM, Bergelson J (2003) A developmental response to pathogen infection in *Arabidopsis*. Plant Physiology **133:** 339-347

Kroll D, Meierhoff K, Bechtold N, Kinoshita M, Westphal S, Vothknecht UC, Soll J, Westhoff P (2001) VIPP1, a nuclear gene of *Arabidopsis thaliana* essential for thylakoid membrane formation. Proceedings of the National Academy of Science U.S.A **98:** 4238-4242

Kruse M, Rosorius O, Kratzer F, Bevec D, Kuhnt C, Steinkasserer A, Schuler G, Hauber J (2000) Inhibition of CD83 cell surface expression during dendritic cell maturation by interference with nuclear export of CD83 mRNA. Journal of Experimental Medicine **191:** 1581-1590

Kunst L (1998) Preparation of physiologically active chloroplasts from *Arabidopsis*. *In* JM Martinez-Zapater, J Salinas, eds, Methods in Molecular Biology: *Arabidopsis* Protocols. Humana Press, Totowa, NJ, pp 43-48

Kushner SR (1978) An improved method for transformation of *E. coli* with ColE1-derived plasmids. *In* HB Boyer, S Nicosia, eds, Genetic Engineering. Elsevier/North-Holland, Amsterdam, pp 17-23

Kwanyuen P, Wilson RF (1986) Isolation and purification of diacylglycerol acyltransferase from germinating soybean cotyledons. Biochimica et Biophysica Acta **877:** 238-245

Kyrpides NC, Woese CR (1998) Universally conserved translation initiation factors. Proceedings of the National Academy of Science U.S.A **95:** 224-228

Kyte J, Doolittle RF (1982) A simple method for displaying the hydropathic character of a protein. Journal of Molecular Biology **157:** 105-132

Lacey DJ, Beaudoin F, Dempsey CE, Shewry PR, Napier JA (1999) The accumulation of triacylglycerols within the endoplasmic reticulum of developing seeds of *Helianthus annuus*. The Plant Journal **17:** 397-405

Laemmli UK (1970) Cleavage of structural proteins during the assembly of the head of bacteriophage T4. Nature **277:** 680-685

Lantin S, O'Brien M, Matton DP (1999) Pollination, wounding and jasmonate treatments induce the expression of a developmentally regulated pistil dioxygenase at a distance, in the ovary, in the wild potato *Solanum chacoense* Bitt. Plant Molecular Biology **41:** 371-386

Lardizabal KD, Mai JT, Wagner NW, Wyrick A, Voelker T, Hawkins DJ (2001) DGAT2: A new diacylglycerol acyltransferase gene family: purification, cloning, and expression in insect cells of two polypeptides from *Mortierella ramanniana* with diacylglycerol acyltransferase activity. Journal of Biological Chemistry **279:** 38862-38869

Lau TE, Rodriguez MA (1996) A protein tyrosine kinase associated with the ATP-dependent inactivation of adipose diacylglycerol acyltransferase. Lipids **31:** 277-283

Lee AG (2000) Membrane lipids: It's only a phase. Current Biology **10:** R377-R380

Lee D, Ahn J, Song S, Choi Y, Lee J (2003) Expression of an expansin gene is correlated with root elongation in soybean. Plant Physiology **131:** 985-997

Lee S, Roberts AW (2004) Tracheary element differentiation is correlated with inhibition of cell expansion in xylogenic mesophyll suspension cultures. Plant Physiology and Biochemistry **42:** 43-48

Lee Y, Kim HK, Park HE, Park MH, Joe YA (2002) Effect of N1-guanyl-1,7-diaminoheptane, an inhibitor of deoxyhypusine synthase, on endothelial cell growth, differentiation and apoptosis. Molecular and Cellular Biochemistry **237:** 69-76

Lee YB, Joe YA, Wolff EC, Dimitriadis EK, Park MH (1999) Complex formation between deoxyhypusine synthase and its protein substrate, the eukaryotic translation initiation factor 5A (eIF5A) precursor. Biochemistry Journal **340:** 273-281

Lee YB, Park MH, Folk JE (1995) Diamine and triamine analogs and derivatives as inhibitors of deoxyhypusine synthase: synthesis and biological activity. Journal of Medical Chemistry **38:** 3053-3061

Levitt J (1972) Responses of Plants to Environmental Stresses. Academic Press, New York, NY

Li A-L, Li H-Y, Jin B-F, Ye Q-N, Zhou T, Yu X-D, Pan X, Man J-H, He K, Yu M, Hu M-R, Wang J, Yang S-C, Shen B-F, Zhang X-M (2004) A novel eIF5A complex functions as a regulator of p53 and p53-dependent apoptosis. The Journal of Biological Chemistry **279:** 49251-49258

Liao D-I, Wolff EC, Park MH, Davies DR (1998) Crystal structure of the NAD complex of human deoxyhypusine synthase: an enzyme with a ball-and-chain mechanism for blocking the active site. Structure **6:** 23-32

Lim PO, Woo HR, Nam HG (2003) Molecular genetics of leaf senescence in *Arabidopsis*. Trends in Plant Science **8:** 272-278

Lin Y-H, Huang AHC (1984) Purification and initial characterization of lipase from the scutella of corn seedlings. Plant Physiology **76:** 719-722

Lin YH, Moreau RA, Huang AHC (1982) Involvement of glyoxysomal lipase in the hydrolysis of storage triacylglycerols in the cotyledons of soybean seedlings. Plant Physiology **70:** 108-112

Lin Y-H, Wimer LT, Huang AHC (1983) Lipase in the lipid bodies of corn scutella during seedling growth. Plant Physiology **73:** 460-463

Lipowsky G, Bischoff FR, Schwarzmaier P, Kraft R, Kostka S, Hartmann E, Kutay U, Gorlich D (2000) Exportin 4: a mediator of a novel nuclear export pathway in higher eukaryotes. Embo Journal **19:** 4362-4371

Little D, Weselake R, Pomeroy K, Furukawa-Stoffer T, Bagu J (1994) Solubilization and characterization of diacylglycerol acyltransferase from microspore-derived cultures of oilseed rape. Biochemical Journal **304:** 951-958

Liu YP, Nemeroff M, Yan YP, Chen KY (1997) Interaction of eukaryotic initiation factor 5A with the human immunodeficiency virus type 1 Rev response element RNA and U6 snRNA requires deoxyhypusine or hypusine modification. Biological Signals **6:** 166-174

Liu Z, Duguay J, Ma F, Wang TW, Tshin R, Hopkins MT, Nowack L, Thompson JE (submitted 2006) eIF-5A1 is a Positive Regulator of Xylem Development in Arabidopsis. The Plant Cell

Lo M, Taylor C, Wang L, Nowack L, Wang T-W, Thompson JE (2004) Characterization of an ultraviolet B-induced lipase in Arabidopsis. Plant Physiology **135:** 947-958

Lu C, Hills MJ (2002) Arabidopsis mutants deficient in diacylglycerol acyltransferase display increased sensitivity to abscisic acids, sugars, and osmotic stress during germination and seedling development. Plant Physiology **129:** 1352-1358

Lu CL, Noyer SBd, Hobbs DH, Kang J, Wen Y, Krachtus D, Hills MJ (2003) Expression pattern of diacylglycerol acyltransferase-1, and enzyme involved in triacylglycerol biosynthesis, in *Arabidopsis thaliana*. Plant Molecular Biology **52:** 31-41

Lu J, Chen ZP, Yan YP, Knapp S, Schugar H, Chen KY (2000) Aminohexanoic hydroxamate is a potent inducer of the differentiation of mouse neuroblastoma cells. Cancer Letters **160:** 59-66

Lu LD (1999) Use of antibodies raised against recombinant fusion proteins to study protein turnover in the endoplasmic reticulum. M.Sc. University of Waterloo, Waterloo

Madey E, Nowack LM, Thompson JE (2002) Isolation and characterization of lipid in phloem sap of canola. Planta **214:** 625-634

Maleck K, Dietrich RA (1999) Defense on multiple fronts: How do plants cope with diverse enemies? Trends in Plant Science **4:** 215-219

Martin BA, Wilson RF (1983) Properties of diacylglycerol acyltransferase from spinach leaves. Lipids **18:** 1-6

Martin BA, Wilson RF (1984) Subcellular localization of triacylglycerol synthesis in spinach leaves. Lipids **19:** 117-121

Martinex-Zapater JM, Coupland G, Dean C, Koornneef M (1994) The transition to flowering in *Arabidopsis*. *In* EM Meyerowitz, CR Somerville, eds, Arabidopsis. Cold Spring Harobor Laboratory Press, Cold Spring Harbor, NY, pp 403-434

Mathur J (2005) Conservation of boundary extension mechanisms between plants and animals. The Journal of Cell Biology **168:** 679-682

Matile P (1992) Chloroplast senescence. *In* NR Baker, and H. Thomas, ed, Crop Photosynthesis: Spatial and Temporal Determinants. Elsevier Science Publishers B.V., pp 413-440

Matos AR, d'Arcy-Lameta A, Franca M, Petres S, Edelman L, Kader J-C, Zuily-Fodil Y, Pham-Thi AT (2001) A novel patatin-like gene stimulated by drought stress encodes a galactolipid acyl hydrolase. FEBS Letters **491:** 188-192

McCabe MS, Garratt LC, Schepers F, Jordi WJRM, Stoopen GM, Davelaar E, Rhijn JHAv, Power JB, Davey MR (2001) Effects of P_{SAG12}-IPT gene expression on development and senescence in transgenic lettuce. Plant Physiology **127:** 505-516

McCaffrey TA, Pomerantz KB, Sanborn TA, Spokojny AM, Du B, Park MH, Folk JE, Lamberg A, Kivirikko KI, Falcone DJ, *al. e* (1995) Specific inhibition of eIF-5A and collagen hydroxylation by a single agent. Antiproliferative and fibrosuppressive effects on smooth muscle cells from human coronary arteries. Journal of Clinical Investigations **95:** 446-455

McCarty DR (1995) Genetic control and integration of maturation and germination pathways in seed development. Annual Reviews in Plant Physiology and Plant Molecular Biology **46:** 71-93

Mehta AM, Saftner RA, Mehta RA, Davies PJ (1994) Identification of posttranslationally modified 18-kilodalton protein from rice as eukaryotic translation initiation factor 5A. Plant Physiology **106:** 1413-1419

Mehta AM, Saftner RA, Schaeffer GW, Mattoo AK (1991) Translational modification of an 18 kilodalton polypeptide by spermidine in rice cell suspension cultures. Plant Physiology **95:** 1294-1297

Meier D, Lichtenthaler HK (1982) Special senescence stages in chloroplast ultrastructure of radish seedlings induced by the photosystem II-herbicide bentazon. Protoplasma **110:** 138-142

Mhaske V, Beldjilali K, Ohlrogge J, Pollard M (2005) Isolation and characterization of an *Arabidopsis thaliana* knockout line for phospholipid: diacylglycerol transacylase gene (At5g13640). Plant Physiology and Biochemistry **43:** 413-417

Miege C, Maréchal E, Shimojima M, Awai K, Block MA, Ohta H, Takamiya K, Douce R, Joyard J (1999) Biochemical and topological properties of type A MGDG synthase, a spinach chloroplast envelope enzyme catalyzing the synthesis of both prokaryotic and eukaryotic MGDG. European Journal of Biochemistry **265**

Milcamps A, Tumaney AW, Paddock T, Pan DA, Ohlrogge J, Pollard M (2005) Isolation of a gene encoding a 1,2-diacylglycerol-*sn*-acetyl-CoA acetyltransferase from developing seeds of *Euonymus alatus*. The Journal of Biological Chemistry **280:** 5370-5377

Millar AA, Smith MA, Kunst L (2000) All fatty acids are not equal: discrimination in plant membrane lipids. Trends in Plant Science **5:** 95-101

Miquel M, Cassagne C, Browse J (1998) A new class of *Arabidopsis* mutants with reduced hexadecatrienoic acid fatty acid levels. Plant Physiology **117:** 923-930

Miranda PV, Brandelli A, Tezon JG (1993) Instantaneous blocking for immunoblots. Analytical Biochemistry **209:** 376-377

Morgenstern B (1999) DIALIGN 2: Improvement of the segment-to-segment approach to multiple sequence alignment. Bioinformatics **15:** 211-218

Morrison WR, Smith LM (1964) Preparation of fatty acid methyl esters and dimethylacetals from lipids with boron tri-fluoride methanol. Journal of Lipid Research **5:** 600-608

Mostowska A (1999) Response of chloroplast structure to photodynamic herbicides and high oxygen. Zeitung Naturforsch **54c:** 621-628

Munnik T, Irvine RF, Musgrave A (1998) Phospholipid signalling in plants. Biochimica et Biophysica Acta **1389:** 222-272

Murashige T, Skoog F (1962) A revised medium for rapid growth and bioassays with tobacco tissue cultures. Physiologia Plantarum **15:** 473-497

Murillo I, Roca R, Bortolotti C, Segundo B (2003) Engineering photoassimilate partitioning in tobacco plants improves growth and productivity and provides pathogen resistance. Plant Journal **36:** 330-341

Murphey RJ, Gerner EW (1987) Hypusine formation in protein by a two-step process in cell lysates. Journal of Biological Chemistry **262:** 15033-15036

Murphy D (2001) The biogenesis and functions of lipid bodies in animals, plants and microorganisms. Progress in Lipid Research **40:** 325-438

Murphy DJ (1993) Structure, function and biogenesis of storage lipid bodies and oleosins in plants. Progress in Lipid Research **32:** 247-280

Mussgnug JH, Wobbe L, Elles I, Claus C, Hamilton M, Fink A, Kahmann U, Kapazoglou A, Mullineaux CW, Hippler M, Nickelsen J, Nixon PJ, Kruse O (2005) NAB1 Is an RNA Binding Protein Involved in the Light-Regulated Differential Expression of the Light-Harvesting Antenna of Chlamydomonas reinhardtii. The Plant Cell **17:** 3409-3421

Nakabayashi K, Okamoto M, Koshiba T, Kamiya Y, Nambara E (2005) Genome-wide profiling of stored mRNA in *Arabidopsis thaliana* seed germination: epigenetic and genetic regulation of transciption in seed. The Plant Journal **41:** 697-709

Nakamura Y, Awai K, Masuda T, Yoshioka Y, Takamiya K, Ohta H (2005) A novel phosphatidylcholine-hydrolyzing phospholipase C induced by phosphate starvation in *Arabidopsis*. The Journal of Biological Chemistry **280:** 7469-7476

Napier JA, Stobart AK, Shewry PR (1996) The structure and biogenesis of plant oil bodies: the role of the ER membrane and the oleosin class of proteins. Plant Molecular Biology **31:** 945-956

Ning S-B, Wang L, Song Y-C (2002) Identification of programmed cell death *in situ* in individual plant cells *in vivo* using a chromosome preparation technique. Journal of Experimental Botany **53:** 651-658

Nishimura K, Murozumi K, Shirahata A, Park MH, Kashiwagi K, Igarashi K (2005) Independent roles of eIF5A and polyamines in cell proliferation. Biochemical Journal **385:** 779-785

Nooden LD (1988) The phenomenon of senescence and aging. *In* LD Nooden, AC Leopold, eds, Senescence and Aging in Plants. Acedemic Press, pp 1-50

Nooden LD, Penney JP (2001) Correlative controls of senescence and plant death in *Arabidopsis thaliana* (Brassicaceae). Journal of Experimental Botany **52:** 2151-5159

Notredame C, Higgins DG, Heringa J (2000) T-Coffee: A novel method for fast and accurate multiple sequence alignment. Journal of Molecular Biology **302:** 205-217

Novikova GV, Moshkov IE, Smith AR, Kulaeva ON, Hall MA (1999) The effect of ethylene and cytokinin on guanosine 5`-triphosphate binding and protein phosphorylation in leaves of *Arabidopsis thaliana*. Planta **208:** 239-246

Ober D, Harms R, Witte L, Hartmann T (2003) Molecular evolution by change of function. Alkaloid-specific homospermidine synthase retained all properties of deoxyhypusine synthase except binding the eIF5A precursor protein. Journal of Biological Chemistry **278:** 12805-12812

Ober D, Hartmann T (1999) Deoxyhypusine synthase from tobacco. The Journal of Biological Chemistry **274:** 32040-32047

Oelkers P, Tinkelenberg A, Erdeniz N, Cromley D, Billheimer JT, .Sturley SL (2000) A lecithin cholesterol acyltransferase-like gene mediates diaclyglycerol esterification in yeast. Journal of Biological Chemistry **275:** 15609-15612

Ohlrogge J, Browse J (1995) Lipid biosynthesis. The Plant Cell **7:** 957-970

Ohlrogge JB, Jaworski JG (1997) Regulation of fatty acid synthesis. Annual Review in Plant Physiology and Plant Molecular Biology **48:** 109-136

Ohno CK, Reddy GV, Heisler MGB, Meyerowitz EM (2003) The *Arabidopsis* JAGGED gene encodes a zinc finger protein that promotes leaf tissue development. Development **131:** 1111-1122

Orozco-Cardenas M, Ryan CA (1999) Hydrogen peroxide is generated systemically in plant leaves by wounding and systemin via the octadecanoid pathway. Proceedings of the National Academy of Science U.S.A **96:** 6553-6557

Ory RL (1969) Acid lipase of the castor bean. Lipids **4:** 177-185

Ory RL, Angelo AJS, Altschul AM (1960) Castor bean lipase: action on its endogenous substrates. Journal of Lipid Research **1:** 208-213

Orzaez D, Blay R, Granell A (1999) Programme of senescence in petals and carpels of *Pisum sativum* L. flowers and its control by ethylene. Planta **208:** 220-226

O'Sullivan JN, Dalling MJ (1989) Investigation of galactolipid turnover in mature primary leaves of wheat (*Triticum aestivum* L.). Journal of Plant Physiology **134:** 338-344

O'Sullivan JN, Warwick NWM, Dalling MJ (1987) A galactolipase activity associated with the thylakoids of wheat leaves (Triticum aestivum L.). Journal of Plant Physiology **131:** 393-404

Ougham HJ, Morris P, Thomas H (2005) The colors of autumn leaves as symptoms of cellular recycling and defenses against environmental stresses. Current Topics in Developmental Biology **66:** 135-160

Padham AK (2002) Isolation and characterization of a plastid lipase from *Arabidopsis thaliana*. Master of Science. University of Waterloo, Waterloo

Padham AK, Hopkins MT, Wang TW, Nowack LM, Lo M, Smith MD, Taylor CA, Thompson JE (submitted 2006) Characterization of a putative chloroplast lipase from Arabidopsis. Plant Physiology

Page T, Griffiths G, Buchanan-Wollaston V (2001) Molecular and biochemical characterization of postharvest senescence in broccoli. Plant Physiology **125:** 718-727

Pare PW, Tumlinson JH (1999) Plant volatiles as a defense against insect herbivores. Plant Physiology **121:** 325-332

Park JH, Aravind L, Wolff EC, Kaevel J, Kim YS, Park MH (2006) Molecular cloning, expression, and structural prediction of deoxyhypusine hydroxylase: a HEAT-repeat-containing metalloenxyme. Proceedings of the National Academy of Science U.S.A **103:** 51-56

Park KY, Drory A, Woodson WR (1992) Molecular cloning of an 1-aminocyclopropane-1-carboxylate synthase from senescing carnation flower petals. Plant Molecular Biology **18:** 377-386

Park MH (1988) The identification of an eukaryotic initiation factor 4D precursor in spermidine-depleted Chinese hamster ovary cells. Journal of Biological Chemistry **263:** 7447-7449

Park MH, Cooper HL, Folk JE (1981) Identification of hypusine, an unusual amino acid, in a protein from human lymphocytes and of spermidine as its biosynthetic precursor. Proceedings of the National Academy of Science U.S.A **78:** 2869-2873

Park MH, Cooper HL, Folk JE (1982) The biosynthesis of protein-bound hypusine (N^{ε}-(4-amino-2-hydroxybutyl)lysine). The Journal of Biological Chemistry **257:** 7217-7222

Park MH, Joe YA, Kang KR (1998) Deoxyhypusine synthase activity is essential for cell viability in the yeast *Saccharomyces cerevisiae*. Journal of Biological Chemistry **273:** 1677-1683

Park MH, Lee YB, Joe YA (1997) Hypusine is essential for eukaryotic cell proliferation. Biological Signals **6:** 115-123

Park MH, Liberato DJ, Yergey AL, Folk JE (1984) The biosynthesis of hypusine (N^{ε}-(4-amino-2-hydroxybutyl)lysine). The Journal of Biological Chemistry **259:** 12123-12127

Park MH, Liu TY, Neece SH, Swiggard WJ (1986) Eukaryotic initiation factor 4D. Purification from human red blood cells and the sequence of amino acids around its single hypusine residue. Journal of Biological Chemistry **261:** 14515-14519

Park MH, Wolff EC (1988) Cell-free synthesis of deoxyhypusine. Separation of protein substrate and enzyme and identification of 1,3-diaminopropane as a product of spermidine cleavage. Journal of Biological Chemistry **263:** 15264-15269

Park MH, Wolff EC, Folk JE (1993) Is hypusine essential for eukaryotic cell proliferation? Trends in Biochemical Science **18:** 475-479

Park MH, Wolff EC, Lee YB, Folk JE (1994) Antiproliferative effects of the inhibitors of deoxyhypusine synthase. Journal of Biological Chemistry **269:** 27827-27832

Parker MT, Gerner EW (2002) Polyamine-mediated post-transcriptional regulation of COX-2. Biochimie **84:** 815-819

Pay A, Heberle-Bors E, Hirt H (1991) Isolation and sequence determination of the plant homologue of the eukaryotic initiation factor 4D cDNA from alfalfa, *Medicago sativa*. Plant Molecular Biology **17:** 927-929

Peat TS, Newman J, Waldo GS, Berendzen J, Terwilliger TC (1998) Structure of translation initiation factor 5A from *Pyrobaculum aerophilum* at 1.75 A resolution. Structure **6:** 1207-1214

Peoples MB, Beilharz VC, Waters SP, Simpson RJ, Dalling MJ (1980) Nitrogen redistribution during grain growth in wheat (*Triticum aestivum* L.): II. Chloroplast senescence and the degradation of ribulose-1,5-bisphosphate carboxylase. Planta **149:** 241-251

Pic E, Serve BTdl, Tardieu F, Turc O (2002) Leaf senescence induced by mild water deficit follows the same sequence of macroscopic, biochemical, and molecular events as monocarpic senescence in pea. Plant Physiology **128:** 236-246

Piffanelli P, Ross JHE, Murphy DJ (1998) Biogenesis and function of the lipidic structures of pollen grains. Sexual Plant Reproduction **11:** 65-80

Pigliucci M, Schmitt J (1999) Genes affecting phenotypic plasticity in *Arabidopsis*: pleiotropic effects and reproductive fitness of photomorphogenic mutants. Journal of Evolution Biology **12:** 551-562

Pilloff RK, Devadas SK, Enyedi A, Raina R (2002) The *Arabidopsis* gain-of-function mutant *dll1* spontaneously develops lesions mimicking cell death associated with disease. The Plant Journal **30:** 61-70

Pozo Od, Pedley KF, Martin GB (2004) MAPKKKα is a positive regulator of cell death associated with both plant immunity and disease. Embo Journal **23:** 3072-3082

Pozueta-Romero J, Rafia F, Houlné G, Cheniclet C, Carde J-P, Schantz M-L, Schantz R (1997) A ubiquitous plant housekeeping gene, PAP, encodes a major protein component of bell pepper chromoplasts. Plant Physiol **115:** 1185–1194

Razem FA, El-Kereamy A, Abrams SR, Hill RD (2006) The RNA-binding protein FCA is an abscisic acid receptor. Nature **439:** 290-294

Rey P, Gillet B, Roemer S, Eymery F, Massimino J, Peltier G, Kuntz M (2000) Over-expression of a pepper plastid lipid-associated protein in tobacco leads to changes in plastid ultrastructure and plant development upon stress. The Plant Journal **21:** 483-494

Richberg MD, Aviv DH, Dangl JL (1998) Dead cells do tell tales. Current Opinion in Plant Biology **1:** 480-485

Riefler M, Novak O, Strnad M, Schmuelling T (2006) *Arabidopsis* cytokinin receptor mutants reveal functions in shoot growth, leaf senescence, seed size, germination, root development, and cytokinin metabolism. The Plant Cell **18:** 40-54

Rochange SF, Wenzel CL, McQueen-Mason SJ (2001) Impaired growth in transgenic plants over-expressing and expansin isoform. Plant Molecular Biology **46:** 581-589

Rosorius O, Reichart B, Kratzer F, Heger P, Dabauvalle MC, Hauber J (1999) Nuclear pore localization and nucleocytoplasmic transport of eIF-5A: evidence for direct interaction with the export receptor CRM1. Journal of Cell Science **112:** 2369-2380

Ruhl M, Himmelspach M, Bahr GM, Hammerschmid F, Jaksche H, Wolff B, Aschauer H, Farrington GK, Probst H, Bevec D, *al. e* (1993) Eukaryotic initiation factor 5A is a cellular target of the human immunodeficiency virus type 1 Rev activation domain mediating trans-activation. Journal of Cell Biology **123:** 1309-1320

Ruuska SA, Girke T, Benning C, Ohlrogge JB (2002) Contrapuntal networks of gene expression during *Arabidopsis* seed filling. The Plant Cell **14:** 1191-1206

Rylott EL, Hooks MA, Graham IA (2001) Co-ordinate regulation of genes involved in storage lipid mobilization in *Arabidopsis thaliana*. Biochemical Society Transactions **29:** 283-287

Ryu SB, Wang X (1995) Expression of Phospholipase D during Castor Bean Leaf Senescence. Plant Physiology **108:** 713-719

Sahsah Y, Campos P, Gareil M, Zuily-Fodil Y, Pham-Thi AT (1998) Enzymatic degradation of polar lipids in *Vigna unguiculata* leaves and influence of drought stress. Physiologia Plantarum **104:** 577-586

Sakaki T, Kondo N, Yamada M (1990) Free fatty acids regulate two galactosyltransferases in chloroplast envelope membranes isolated from spinach leaves. Plant Physiology **94:** 781-787

Sakaki T, Kondo N, Yamada M (1990) Pathway for the synthesis of triacylglycerols from monogalacotsyldiacylglycerols in ozone-fumigated spinach leaves. Plant Physiology **94:** 773-780

Sakaki T, Saito K, Kawaguchi A, Kondo N, Yamada M (1990) Conversion of monogalactosyldiacylglycerols to triacylglycerols in ozone-fumigated spinach leaves. Plant Physiology **94:** 766-772

Sanchez J, Mancha M (1981) Synthesis of acyl CoAs by isolated spinach chloroplasts in relation to added CoA and ATP. Planta **153:** 519-523

Sánchez-Fernández R, Davies TGE, Coleman JOD, Rea PA (2001) The *Arabidopsis thaliana* ABC protein superfamily, a complete inventory. Journal of Biological Chemistry **276:** 30231-30244

Sarafis V (1998) Chloroplasts: a structural approach. Journal of Plant Physiology **152:** 248-264

Sastry PS, Kates M (1964) Lipid components of leaves: V. Galactolipids, cerebrocides and lecithin of runner-bean Ieaves. Biochemistry **3:** 1280-1287

Schardl CL, Byrd AD, Benzion G, Altschuler MA, Hildebrand DF, Hunt AG (1987) Design and construction of a versatile system for the expression of foreign genes in plants. Gene **61:** 1-11

Schatz O, Oft M, Dascher C, Schebesta M, Rosorius O, Jaksche H, Dobrovnik M, Bevec D, Hauber J (1998) Interaction of the HIV-1 rev cofactor eukaryotic initiation factor 5A with ribosomal protein L5. Proceedings of the National Academy of Science U.S.A **95:** 1607-1612

Scheres B, Benfey P, Dolan L (2002) Root development. *In* CR Somerville, EM Meyerowitz, eds, The Arabidopsis Book. American Society of Plant Biologists, Rockville

Schnier J, Schwelberger HG, Smit-McBride Z, Kang HA, Hershey JW (1991) Translation initiation factor 5A and its hypusine modification are essential for cell viability in the yeast *Saccharomyces cerevisiae*. Molecular Cell Biology **11:** 3105-3114

Schwelberger HG, Kang HA, Hershey JW (1993) Translation initiation factor eIF-5A expressed from either of two yeast genes or from human cDNA. Functional identity under aerobic and anaerobic conditions. Journal of Biological Chemistry **268:** 14018-14025

Senda K, Ogawa K (2004) Induction of PR-1 accumulation accompanied by runaway cell death in the *lsd1* mutant of *Arabidopsis* is dependent on glutathione levels but independent of the redox state of glutathione. Plant Cell Physiology **45:** 1578-1585

Shi XP, Yin KC, Waxman L (1997) Effects of inhibitors of RNA and protein synthesis on the subcellular distribution of the eukaryotic translation initiation factor, eIF-5A, and the HIV-1 Rev protein. Biological Signals **6:** 143-149

Shi XP, Yin KC, Zimolo ZA, Stern AM, Waxman L (1996) The subcellular distribution of eukaryotic translation initiation factor, eIF-5A, in cultured cells. Experimental Cell Research **225:** 348-356

Shi ZP, Yin KC, Ahern J, Davis LJ, Stern AM, Waxman L (1996) Effects of N1-guanyl-1,7-diaminoheptane, an inhibitor of deoxyhypusine synthase, on the growth of tumorigenic cell lines in culture. Biochimica et Biophysica Acta **1310:** 119-126

Shiba T, Mizote H, Kaneko T, Nakajima T, Kakimoto Y (1971) Hypusine, a new amino acid ocurring in bovine brain. Isolation and structural determination. Biochimica et Biophysica Acta **244:** 523-531

Shimakata T, Stumpf PK (1982) Fatty acid synthetase of *Spinacia oleracea* leaves. Plant Physiology **69:** 1257-1262

Siebertz HP, Heinz E, Linscheid M, Joyard J, Douce R (1979) Characterization of lipids from chloroplast envelopes. European Journal of Biochemistry **101:** 429-438

Simpson GG, Gendall AR, Dean C (1999) When to switch to flowering. Annual Review in Cell Development Biology **95**

Singer SJ, Nicolson GL (1972) The fluid mosaic model of the structure of cell membranes. Science **175:** 720-731

Sinha N (1999) Leaf development in angiosperms. Annual Review in Plant Physiology and Plant Molecular Biology **50:** 419-446

Sitte P, Falk H, Liedvogel B (1980) Chromoplasts. *In* F-C Czygan, ed, Pigments in Plants, Ed 2. Gustav Fischer, Stuttgart

Slabas AR, Fawcett T (1992) The biochemistry and molecular biology of plant lipid biosynthesis. Plant Molecular Biology **19:** 169-191

Smaoui A, Cherif A (2000) Changes in molecular species of triacylglycerols in developing cotton seeds under salt stress. Biochemical Society Transactions **28:** 902-905

Smith MD, Licatalosi DD, Thompson JE (2000) Co-association of cytochrome *f* catabolites and plastid-lipid-associated protein with chloroplast lipid particles. Plant Physiology **124:** 211-221

Smit-McBride Z, Schnier J, Kaufman RJ, Hershey JW (1989) Protein synthesis initiation factor eIF-4D. Functional comparison of native and unhypusinated forms of the protein. Journal of Biological Chemistry **264:** 18527-18530

Smyth DR, Bowman JL, Meyerowitz EM (1990) Early flower development in *Arabidopsis*. The Plant Cell **2:** 755-767

Somerville C, Browse J, Jaworski JG, Ohlrogge JB (2000) Lipids. *In* B Buchanan, W. Gruissem, and R. Jones, ed, Biochemistry and Molecular Biology of Plants. American Society of Plant Physiologists, pp 456-527

Sommer M-N, Bevec D, Klebl B, Flicke B, Hoelscher K, Freudenreich T, Hauber I, Hauber J, Mett H (2004) Screening assay for the identification of deoxyhypusine synthase inhibitors. Journal of Biomolecular Screening **9:** 434-438

Steinmuller D, Tevini M (1985) Composition and function of plastoglobuli:II. Lipid composition of leaves and plastoglobuli during beech leaf senescence. Planta **163:** 91-96

Stobart AK, Stymne S, Hoglund S (1986) Safflower microsomes catalyze oil accumulation in vitro: a model system. Planta **169:** 33-37

Stobart K, Mancha M, Lenman M, Dahlqvist A, Stymne S (1997) Triacylglycerols are synthesized and utilized by transacyltion reactions in microsomal preparations of developing safflower (*Cartharmus tinctorius* L.) seeds. Planta **203:** 58-66

Sun K, Hunt K, Hauser BA (2004) Ovule abortion in *Arabidopsis* triggered by stress. Plant Physiology **135:** 2358-2367

Takeuchi K, Nakamura K, Fujimoto M, Kaino S, Kondoh S, Okita K (2002) Heat stress-induced loss of eukaryotic initiation factor 5A (eIF-5A) in a human pancreatic cancer cell line, MIA PaCa-2, analyzed by two-dimensional gel electrophoresis. Electrophoresis **23:** 662-669

Taniguchi H (1999) Protein myristoylation in protein-lipid and protein-protein interactions. Biophysical Chemistry **82:** 129-137

Tatusova TA, Madden TL (1999) Blast 2 sequences - a new tool for comparing protein and nucleotide sequences. FEMS Microbiolgy Letters **174:** 247-250

Taylor CA, Cliche DO, Sun Z, Hopkins MT, Thompson JE (submitted 2006) Eukaryotic translation initiation factor 5A induced apoptosis in colon cancer cells and is imported into the nucleus in response to tumour necrosis factor α signalling. Cell Death and Differentiation

Taylor CA, Senchyna M, Flanagan J, Joyce EM, Cliche DO, Boone AN, Culp-Stewart S, Thompson JE (2004) Role of eIF5A in TNF-α-mediated apoptosis of lamina cribosa cells. Investigative Ophthalmology and Visual Science **45:** 3568-3576

Thomas H (1982) Control of chloroplast demolition during leaf senescence. *In* PF Waring, ed, Plant Growth Substances. Academic Press, London, pp 559-567

Thomas H (1984) Cell senescence and protein metabolism in the photosynthetic tissues of leaves. *In* I Davies, D Sigee, eds, Cell Aging and Cell Death. Cambridge University Press, UK, pp 171-188

Thomas H, Ougham HJ, Wagstaff C, Stead AD (2003) Defining senescence and death. Journal of Experimental Botany **54:** 1127-1132

Thomashow MF (1999) Plant cold acclimation: Freezing tolerance genes and regulatory mechanisms. Annual Reviews of Plant Physiology and Plant Molecular Biology **50:** 571-599

Thompson GM, Cano VSP, Valentini SR (2003) Mapping eIF5A binding sites for Dys1 and Lia1: in vivo evidence for regulation of eIF5A hypusination. FEBS Letters **555**

Thompson JE (1988) The molecular basis for membrane deterioration during senescence. *In* LD Nooden, and A.C. Leopold, ed, Senescence and aging in plants. Academic Press, Inc., San Diego, CA, pp 51-83

Thompson JE, Froese CD, Hong Y, Hudak KA, Smith MD (1997) Membrane deterioration during senescence. Canadian Journal of Botany **75:** 867-879

Thompson JE, Froese CD, Madey E, Smith MD, Hong Y (1998) Lipid metabolism during plant senescence. Progress in Lipid Research **37:** 119-141

Thompson JE, Hopkins MT, Taylor C, Wang T-W (2004) Regulation of senescence by eukaryotic translation initiation factor 5A: implications for plant growth and development. Trends in Plant Science **9:** 174-179

Thompson JE, Mayak S, Shinitzky M, Halevy AH (1982) Acceleration of membrane senescence in cut carnation flowers by treatment with ethylene. Plant Physiology **69:** 859-863

Tienderen PHv, Hammad I, Zwaal FC (1996) Pleiotropic effects of flowering time genes in the annual crucifer *Arabidopsis thaliana* (Brassicaceae). American Journal of Botany **83:** 169-174

Ting JTL, Wu SSH, Ratnayake C, Huang AHC (1998) Constituents of the tapetosomes and elaioplasts in *Brassica campestris* tapetum and their degradation and retention during microsporogenesis. Plant Journal **16:** 541-551

Tome ME, Fiser SM, Payne CM, Gerner EW (1997) Excess putrescine accumulation inhibits the formation of modified eukaryotic initiation factor 5A (eIF-5A) and induces apoptosis. Biochemistry Journal **328:** 847-854

Tome ME, Gerner EW (1996) Hypusine modification in eukaryotic initiation factor 5A in rodent cells selected for resistance to growth inhibition by ornithine decarboxylase-inhibiting drugs. Biochemistry Journal **320:** 55-60

Tome ME, Gerner EW (1997) Cellular eukaryotic initiation factor 5A content as a mediator of polyamine effects on growth and apoptosis. Biological Signals **6:** 150-156

Tshin R (2004) Effects of constitutive suppression of eukaryotic translation initiation factor 5A1 expression during growth and senescence in arabidopsis thaliana. MSc. University of Waterloo, Waterloo

Tsukaya H (2002) Leaf Development. *In* EM Meyerowitz, ed, The Arabidopsis Book. American Society of Plant Biologists, Rockville

Urao T, Yamaguchi-Shinozaki K, Urao S, Shinozaki K (1993) An *Arabidopsis* myb homolog is induced by dehydration stress and its gene product binds to the conserved MYB recognition sequence. The Plant Cell **5:** 1529-1539

Valentini SR, Casolari JM, Oliveira CC, Silver PA, McBride AE (2002) Genetic interactions of yeast eukaryotic translation initiation factor 5A (eIF5A) reveal connections to poly(A)-binding protein and protein kinase C signaling. Genetics **160:** 393-405

Varani G (1998) RNA-protein recognition during RNA processing and maturation. *In* DS Eggleston, CD Prescott, ND Pearson, eds, The Many Faces of RNA. Academic Press, London, pp 67-82

Voelker T, Kinney AJ (2001) Variations in the biosynthesis of seed-storage lipids. Annual Review in Plant Physiology and Plant Molecular Biology **52:** 335-361

Wang H, Li J, Bostock RM, Gilchrist DG (1996) Apoptosis: A functional paradigm for programmed plant cell death induced by a host-selective phytotoxin and invoked during development. The Plant Cell **8:** 375-391

Wang TW, Lu L, Wang D, Thompson JE (2001) Isolation and characterization of senescence-induced cDNAs encoding deoxyhypusine synthase and eucaryotic translation initiation factor 5A from tomato. Journal of Biological Chemistry **276:** 17541-17549

Wang TW, Lu L, Zhang CG, Taylor CA, Thompson JE (2003) Pleiotropic effects of suppressing deoxyhypusine synthase expression in *Arabidopsis thaliana*. Plant Molecular Biology **52:** 1223-1235

Wang TW, Zhang CG, Wu W, Nowack LM, Madey E, Thompson JE (2005) Antisense suppression of deoxyhypusine synthase in tomato delays fruit softening and alters growth and development. Plant Physiology **138:** 1372-1382

Wang X (2000) Multiple forms of phospholipase D in plants: the gene family, catalytic and regulatory properties, and cellular functions. Progress in Lipid Research **39:** 109-149

Wang X (2001) Plant phospholipases. Annual Review in Plant Physiology and Plant Molecular Biology **52:** 211-231

Weselake RJ, Madavji M, Foroud N, Szarka S, Patterson N, Wiehler W, Nykiforuk C, Burton T, Boora P, Mosimann S, Moloney M, Laroche A (2004) Probing the

structure/function of diacylglycerol acyltransferase-1 from *Brassica napus*. *In* 16th International Plant Lipid Symposium, Budapest, Hungary

Whalen MC, Innes RW, Bent AF, Staskawicz BJ (1991) Identification of *Pseudomonas-syringae* pathogens of *Arabidopsis* and bacterial locus determining avirulence on both *Arabidopsis* and soybean. The Plant Cell **3:** 49-59

Wilson RF, Kwanyuan P (1986) Triacylglycerol synthesis and metabolism in germinating soybean cotyledons. Biochimica et Biophysica Acta **877:** 231-237

Wolff EC, Folk JE, Park MH (1997) Enzyme-substrate intermediate formation at lysine 329 of human deoxyhypusine synthase. Journal of Biological Chemistry **272:** 15865-15871

Wolff EC, Kinzy TG, Merrick WC, Park MH (1992) Two isoforms of eIF-5A in chick embryo. Isolation, activity, and comparison of sequences of the hypusine-containing proteins. Journal of Biological Chemistry **267:** 6107-6113

Wolff EC, Lee YB, Chung SI, Folk JE, Park MH (1995) Deoxyhypusine synthase from rat testis: purification and characterization. Journal of Biological Chemistry **270:** 8660-8666

Wolff EC, Park MH, Folk JE (1990) Cleavage of spermidine as the first step in deoxyhypusine synthesis. The role of NAD. Journal of Biological Chemistry **265:** 4793-4799

Woo HR, Chung KM, Park J-H, Oh SA, Ahn T, Hong SH, Jang SK, Nam HG (2001) ORE9, an F-box protein that regulates leaf senescence in *Arabidopsis*. The Plant Cell **13:** 1779-1790

Woolhead C, Bolhuis A, Robinson C (2000) Novel mechanisms for the targeting of proteins into and across chloroplast membranes. Biochemical Society Transactions **28:** 491-494

Xu A, Chen KY (2001) Hypusine is required for a sequence-specific interaction of eukaryotic initiation factor 5A with postsystematic evolution of ligands by exponential enrichment RNA. Journal of Biological Chemistry **276:** 2555-2561

Xu A, Jao DL, Chen KY (2004) Identification of mRNA that binds to eukaryotic initiation factor 5A by affinity co-purification and differential display. Biochemical Journal **384:** 585-590

Xu J, Brearley CA, Lin W-H, Wang Y, Ye R, Mueller-Roeber B, Xu Z-H, Xue H-W (2005) A role of *Arabidopsis* inositol polyphosphate kinase, AtIPK2a, in pollen germination and root growth. Plant Physiology **137:** 94-103

Xu P, Rogers SJ, Roossinck MJ (2004) Expression of antiapoptotic genes bcl-xL and ced-9 in tomato enhances tolerance to viral-induced necrosis and abiotic stress. Proceedings of the National Academy of Science U.S.A **101:** 15805-15810

Yaeno T, Matsuda O, Iba K (2004) Role of chloroplast trienoic fatty acids in plant disease defense responses. The Plant Journal **40:** 931-941

Yamaguchi S, Smith MW, Brown RG, Kamiya Y, Sun T (1998) Phytochrome regulation and differential expression of gibberellin 3β-hydroxylase genes in germinating *Arabidopsis* seeds. Plant Cell **10:** 2115-2126

Yamauchi Y, Ogawa M, Kuwahara A, Hanada A, Kamiya Y, Yamaguchi S (2004) Activation of gibberellin biosynthesis and response pathways by low temperature during imbibition of *Arabidopsis thaliana* seeds. The Plant Cell **16:** 367-378

Yan YP, Tao Y, Chen KY (1996) Molecular cloning and functional expression of human deoxyhypusine synthase cDNA based on expressed sequence tag information. Biochemistry Journal **315:** 429-434

Yang S, Yang H, Grisafi P, Sanchatjate S, Fink GR, Sun Q, Hua J (2006) The BON/CPN gene family represses cell death and promotes cell growth in *Arabidopsis*. The Plant Journal **45:** 166-179

Yao K, Paliyath G, Humphrey RW, Hallett FR, Thompson JE (1991) Identification and characterization of nonsedimentable lipid-protein microvesicles. Proceedings of the National Academy of Science U.S.A. **88:** 2269-2273

Yi SY, Kim J-H, Joung Y-H, Lee S, Kim W-T, Yu SH, Choi D (2004) The pepper transcription factor *CaPF1* confers pathogen and freezing tolerance in *Arabidopsis*. Plant Physiology **136:** 2862-2874

Young O, Beevers H (1976) Mixed function oxidase from germinating castor bean endosperm. Phytochemistry **15:** 379-385

Yu D, Chen C, Chen Z (2001) Evidence for an important role of WRKY DNA binding proteins in the regulation of NPR1 gene expression. The Plant Cell **13:** 1527-1540

Zanelli CF, Valentini SR (2005) Pkc1 acts through Zds1 and Gic1 to suppress growth and cell polarity defects of a yeast eIF5A mutant. Genetics **171:** 1571-1581

Zellnig G, Zechmann B, Perktold A (2004) Morphological and quantitative data of plastids and mitochondria within drought-stressed spinach leaves. Protoplasma **223:** 221-227

Zou J, Wei Y, Jako C, Kumar A, Selvaraj G, Taylor DC (1999) The *Arabidopsis thaliana* TAG1 mutant has a mutation in a diacylglycerol acyltransferase gene. The Plant Journal **19:** 645-653

Appendix A: Statistical calculations for Chapter 3

Table 6-1: Lipid classes expressed as a percentage of the total lipid pool for homogenates of pre-senescent (3-week-old) and senescent (6-week-old) rosette leaves

	% of Total Fatty Acid Pool		Standard Error *		
Lipid Class:	**3 wk**	**6 wk**	**3 wk**	**6 wk**	**P-Values****
Polar lipids	84.76	53.03	1.34	5.45	0.020
Diacylglycerols	6.74	9.63	0.40	1.83	0.190
Free fatty acids	5.26	8.60	1.06	1.45	0.261
Triacylglycerols	2.02	12.33	0.12	2.20	0.039
Steryl/wax esters	1.22	16.40	0.14	3.59	0.049

*n=3

**P-values were calculated using a two-tailed test with α=0.05

Table 6-2: Lipid classes expressed as a percentage of the total lipid pool for microsomal membranes of pre-senescent (3-week-old) and senescent (6-week-old) rosette leaves

	% of Total Fatty Acid Pool		Standard Error *		
Lipid Class:	**3 wk**	**6 wk**	**3 wk**	**6 wk**	**P-Values ****
Polar lipids	77.82	52.10	2.50	2.54	0.001
Diacylglycerols	5.42	5.22	0.91	1.16	0.313
Free fatty acids	13.23	27.02	2.60	1.46	0.004
Triacylglycerols	0.97	3.55	0.20	0.52	0.044
Steryl/wax esters	2.56	12.12	0.55	0.37	0.001

*n=3

**P-values were calculated using a two-tailed test with α=0.05

Table 6-3: Lipid classes expressed as μg lipid/g fresh weight (fwt) in the homogenates of pre-senescent (3-week-old) and senescent (6-week-old) rosette leaves

	μg lipid/g fwt		Standard Error *		
Lipid Class:	**3 wk**	**6 wk**	**3 wk**	**6 wk**	**P-Values ****
Polar lipids	14.48	20.57	1.12	4.60	0.223
Diacylglycerols	1.15	3.53	0.09	0.44	0.025
Free fatty acids	0.92	3.12	0.25	0.18	0.012
Triacylglycerols	0.34	4.48	0.01	0.38	0.008
Steryls/wax esters	0.21	6.70	0.03	2.55	0.124
Total lipid aliquot	41.06	60.67	3.52	6.89	0.123

*n=3

**P-values were calculated using a two-tailed test with α=0.05

Table 6-4: Lipid classes expressed as μg lipid/g fresh weight (fwt) in the microsomal membranes of pre-senescent (3-week-old) and senescent (6-week-old) rosette leaves

	μg lipid/g fwt		Standard Error *		
Lipid Class:	**3 wk**	**6 wk**	**3 wk**	**6 wk**	**P-Values ****
Polar lipids	63.29	33.20	5.21	5.48	0.055
Diacylglycerols	4.47	3.11	1.01	0.49	0.475
Free fatty acids	10.53	17.07	1.65	2.29	0.117
Triacylglycerols	0.77	2.16	0.13	0.08	0.008
Steryl/wax esters	2.04	7.72	0.36	1.21	0.054
Total lipid aliquot	257.54	104.55	19.41	7.55	0.014

*n=3

**P-values were calculated using a two-tailed test with α=0.05

Table 6-5: Fatty acid composition for homogenate total lipid of pre-senescent (3-week-old) and senescent (6-week-old) rosette leaves

	% of Total		Standard Error *		
Fatty acid:	**3 wk**	**6 wk**	**3 wk**	**6 wk**	**P-Values ****
12:0	0.00	1.54	0.00	0.44	0.074
14:0	0.19	1.53	0.04	0.33	0.051
15:0	0.19	0.67	0.01	0.17	0.094
16:0	24.39	23.27	0.85	0.83	0.544
16:1	2.97	2.23	0.36	0.24	0.220
16:3	4.35	9.66	0.12	1.26	0.054
18:0	0.58	0.85	0.28	0.29	0.549
18:1	7.78	4.08	0.39	0.61	0.011
18:2	25.83	15.17	0.05	0.45	0.002
18:3	32.80	38.26	0.28	3.19	0.237
22:0	0.16	0.52	0.06	0.17	0.155
22:1	0.19	0.26	0.03	0.12	0.660
24:0	0.57	1.76	0.19	0.05	0.016
26:0	0.00	0.20	0.00	0.02	0.008

*n=3

**P-values were calculated using a two-tailed test with α=0.05

Table 6-6: Fatty acid composition for total lipids of microsomal membranes of pre-senescent (3-week-old) and senescent (6-week-old) rosette leaves

	% of Total		Standard Error *		
Fatty acid:	**3 wk**	**6 wk**	**3 wk**	**6 wk**	**P-Values ****
12:0	0.00	0.87	0.00	0.05	0.003
14:0	0.21	1.01	0.03	0.07	0.011
15:0	0.27	0.49	0.05	0.18	0.452
16:0	23.51	26.36	0.44	1.56	0.204
16:1	3.18	1.52	0.11	0.11	0.009
16:3	6.18	6.37	0.32	0.58	0.818
18:0	0.22	0.86	0.10	0.75	0.514
18:1	7.04	6.23	0.35	0.43	0.376
18:2	24.56	17.02	0.37	0.35	0.009
18:3	34.06	32.89	0.31	3.92	0.799
22:0	0.26	0.93	0.03	0.31	0.182
22:1	0.04	0.31	0.02	0.19	0.297
23:0	0.00	1.21	0.00	0.09	0.006
24:0	0.49	2.66	0.26	0.11	0.026
25:0	0.00	0.64	0.00	0.17	0.060
26:0	0.00	0.58	0.00	0.24	0.132
28:0	0.00	0.07	0.00	0.01	0.029

*n=3

**P-values were calculated using a two-tailed test with α=0.05

Table 6-7: Fatty acid composition for homogenate polar lipid and triacylglycerol of pre-senescent (3-week-old) and senescent (6-week-old) rosette leaves

	% of Total Fatty Acid Pool		Standard Error *		
Lipid Class and Fatty acid:	**3 wk**	**6 wk**	**3 wk**	**6 wk**	**P-Values ****
Polar lipids					
14:0	0.09	0.15	0.01	0.02	0.174
15:0	0.12	0.22	0.01	0.04	0.114
16:0	20.87	16.18	1.07	0.93	0.125
16:1	3.09	1.64	0.36	0.40	0.125
16:3	3.82	3.27	0.08	1.10	0.678
18:0	0.21	0.00	0.02	0.00	0.011
18:1	6.14	2.62	0.21	0.67	0.042
18:2	20.86	8.06	0.17	0.50	0.001
18:3	27.96	19.03	0.89	2.77	0.133
22:0	0.38	0.47	0.11	0.14	0.574
22:1	0.23	0.00	0.03	0.00	0.021
24:0	0.99	1.38	0.30	0.52	0.594
Triacylglycerol					
12:0	0.00	0.06	0.00	0.02	0.102
14:0	0.08	0.24	0.01	0.03	0.019
15:0	0.03	0.12	0.00	0.01	0.010
16:0	0.91	3.57	0.06	0.08	0.001
16:1	0.00	0.04	0.00	0.02	0.192
16:2	0.00	0.06	0.00	0.03	0.166
16:3	0.00	1.16	0.00	0.07	0.004
18:0	0.51	0.24	0.05	0.13	0.242
18:1	0.00	0.73	0.00	0.10	0.017
18:2	0.07	1.56	0.04	0.07	0.002
18:3	0.00	4.40	0.00	0.24	0.003
22:0	0.00	0.05	0.00	0.02	0.102
22:1	0.42	0.10	0.13	0.04	0.085
24:0	0.00	0.03	0.00	0.02	0.276

*n=3

**P-values were calculated using a two-tailed test with α=0.05

Table 6-8: Fatty acid composition for microsomal membrane polar lipid and triacylglycerol of pre-senescent (3-week-old) and senescent (6-week-old) rosette leaves

	% of Total Fatty Acid Pool		Standard Error *		
Lipid Class and Fatty acid:	**3 wk**	**6 wk**	**3 wk**	**6 wk**	**P-Values ****
Polar lipids					
14:0	0.12	0.13	0.02	0.03	0.864
15:0	0.15	0.35	0.02	0.10	0.157
16:0	17.99	14.47	1.19	1.36	0.136
16:1	2.86	0.76	0.26	0.12	0.009
16:3	4.91	1.67	0.18	0.23	0.014
18:0	0.27	0.58	0.05	0.51	0.625
18:1	6.07	2.71	0.24	0.10	0.003
18:2	19.00	8.78	0.85	0.37	0.013
18:3	25.05	18.57	0.34	0.90	0.034
22:0	0.37	0.47	0.06	0.11	0.318
22:1	0.00	0.23	0.00	0.14	0.240
23:0	0.00	0.84	0.00	0.07	0.007
24:0	1.04	1.70	0.09	0.11	0.071
25:0	0.00	0.53	0.00	0.13	0.057
26:0	0.00	0.31	0.00	0.12	0.124
Triacylglycerol					
14:0	0.00	0.07	0.00	0.02	0.080
15:0	0.02	0.04	0.01	0.01	0.185
16:0	0.54	1.10	0.02	0.08	0.022
16:1	0.00	0.01	0.00	0.00	0.070
16:3	0.00	0.30	0.00	0.04	0.018
18:0	0.11	0.15	0.05	0.06	0.781
18:1	0.14	0.39	0.04	0.07	0.150
18:2	0.06	0.37	0.01	0.03	0.013
18:3	0.00	0.93	0.00	0.05	0.003
22:0	0.00	0.04	0.00	0.01	0.038
22:1	0.09	0.08	0.01	0.01	0.856
24:0	0.00	0.07	0.00	0.00	0.002

*n=3

**P-values were calculated using a two-tailed test with α=0.05

Table 6-9: Levels of hexadecatrienoic acid (16:3) and linolenic acid (18:3) within each lipid class for homogenates of pre-senescent (3-week-old) and senescent (6-week-old) rosette leaves

	% of Total Fatty Acid Pool		Standard Error *		
Lipid Class and Fatty acid:	**3 wk**	**6 wk**	**3 wk**	**6 wk**	**P-Values ****
Polar lipids					
16:3	4.51	6.16	0.12	2.53	0.517
18:3	32.99	35.88	1.28	6.41	0.689
Sum 16:3 and 18:3	37.49	42.04	1.36	5.70	0.513
Diacylglycerol					
16:3	0.00	2.96	0.00	0.55	0.022
18:3	15.81	25.44	4.17	1.07	0.152
Sum 16:3 and 18:3	15.81	28.40	4.17	1.39	0.190
Free fatty acids					
16:3	0.00	3.14	0.00	0.40	0.011
18:3	0.00	9.75	0.00	1.27	0.011
Sum 16:3 and 18:3	0.00	12.89	0.00	1.17	0.005
Triacylglycerol					
16:3	0.00	9.39	0.00	0.70	0.004
18:3	0.00	35.64	0.00	2.34	0.003
Sum 16:3 and 18:3	0.00	45.03	0.00	2.07	0.001
Steryl and wax esters					
16:3	0.00	26.38	0.00	0.01	0.009
18:3	0.00	24.86	0.00	0.01	0.004
Sum 16:3 and 18:3	0.00	51.25	0.00	0.01	0.004

*n=3

**P-values were calculated using a two-tailed test with α=0.05

Table 6-10: Levels of hexadecatrienoic acid (16:3) and linolenic acid (18:3) within each lipid class for microsomal membranes of pre-senescent (3-week-old) and senescent (6-week-old) rosette leaves

	% of Total Fatty Acid Pool		Standard Error *		
Lipid Class and Fatty acid:	**3 wk**	**6 wk**	**3 wk**	**6 wk**	**P-Values ****
Polar lipids					
16:3	6.32	3.24	0.28	0.53	0.041
18:3	32.19	35.64	0.54	2.11	0.247
Sum 16:3 and 18:3	38.50	38.88	0.55	2.12	0.874
Diacylglycerol					
16:3	0.00	2.22	0.00	0.97	0.107
18:3	12.95	25.57	0.80	2.60	0.014
Sum 16:3 and 18:3	12.95	27.80	0.80	3.38	0.021
Free fatty acids					
16:3	0.92	6.75	0.47	1.32	0.057
18:3	11.12	22.22	1.74	3.99	0.129
Sum 16:3 and 18:3	12.04	28.97	1.53	4.30	0.064
Triacylglycerol					
16:3	0.00	8.30	0.00	1.40	0.018
18:3	0.00	26.31	0.00	1.71	0.003
Sum 16:3 and 18:3	0.00	34.61	0.00	1.62	0.001
Steryl and wax esters					
16:3	0.00	12.61	0.00	0.95	0.004
18:3	14.76	35.78	3.33	3.50	0.041
Sum 16:3 and 18:3	14.76	48.40	3.33	2.69	0.015

*n=3

**P-values were calculated using a two-tailed test with α=0.05